น้ำยางธรรมชาติดัดแปรโดยกราฟต์โคพอลิเมอไรเซชันด้วยเมทิลเมทาคริเลตหรือสไตรีน

และไฮโดรจิเนชันโดยใช้ OsHCl(CO)(O$_2$)(PCy$_3$)$_2$ เป็นตัวเร่งปฏิกิริยา

นางสาว สุวดี ก้องพารากุล

วิทยานิพนธ์นี้เป็นส่วนหนึ่งของการศึกษาตามหลักสูตรปริญญาวิทยาศาสตรดุษฎีบัณฑิต

สาขาวิชาเคมีเทคนิค   ภาควิชาเคมีเทคนิค

คณะวิทยาศาสตร์ จุฬาลงกรณ์มหาวิทยาลัย

ปีการศึกษา 2550

MODIFIED NATURAL RUBBER LATEX BY GRAFT COPOLYMERIZATION WITH

METHYL METHACRYLATE OR STYRENE AND HYDROGENATION

USING OsHCl(CO)(O$_2$)(PCy$_3$)$_2$ AS A CATALYST

Miss Suwadee Kongparakul

A Dissertation Submitted in Partial Fulfillment of the Requirements

for the Degree of Doctor of Science Program in Chemical Technology

Department of Chemical Technology

Faculty of Science

Chulalongkorn University

Academic year 2007

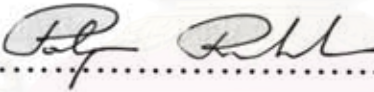|	
Thesis Title	MODIFIED NATURAL RUBBER LATEX BY GRAFT COPOLYMERIZATION WITH METHYL METHACRYLATE OR STYRENE AND HYDROGENATION USING OsHCl(CO)(O$_2$)(PCy$_3$)$_2$ AS A CATALYST
By	Miss Suwadee Kongparakul
Field of Study	Chemical Technology
Thesis Advisor	Professor Pattarapan Prasassarakich, Ph.D.
Thesis Co-advisor	Professor Garry L. Rempel, Ph.D.

Accepted by the Faculty of Science, Chulalongkorn University in Partial Fulfillment of the Requirements for the Doctoral Degree

....Dean of the Faculty of Science

(Professor Supot Hannongbua, Ph.D.)

THESIS COMMITTEE

....Chairman

(Associate Professor Tharapong Vitidsant, Ph.D.)

....Thesis Advisor

(Professor Pattarapan Prasassarakich, Ph.D.)

....Thesis Co-advisor

(Professor Garry L. Rempel, Ph.D.)

....Member

(Professor Suda Kiatkamjornwong, Ph.D.)

....Member

(Associate Professor Somkiat Ngamprasertsith, Ph.D.)

....Member

(Kitikorn Charmondusit, Ph.D.)

สุวดี ก้องพารากุล : น้ำยางธรรมชาติดัดแปรโดยกราฟต์โคพอลิเมอไรเซชันด้วยเมทิลเมทาคริเลตหรือสไตรีนและไฮโดรจิเนชันโดยใช้ OsHCl(CO)(O$_2$)(PCy$_3$)$_2$ เป็นตัวเร่งปฏิกิริยา. (MODIFIED NATURAL RUBBER LATEX BY GRAFT COPOLYMERIZATION WITH METHYL METHACRYLATE OR STYRENE AND HYDROGENATION USING OsHCl(CO)(O$_2$)(PCy$_3$)$_2$ AS A CATALYST) อ. ที่ปรึกษา : ศ.ดร. ภัทรพรรณ ประศาสน์สารกิจ, อ. ที่ปรึกษาร่วม : Prof. Garry L. Rempel, 167 หน้า.

งานวิจัยนี้ศึกษากราฟต์โคพอลิเมอไรเซชันของเมทิลเมทาคริเลตหรือสไตรีนบนยางธรรมชาติโดยใช้คูมีนไฮโดรเปอร์ออกไซด์เป็นตัวริเริ่มแบบรีดอกซ์ กราฟต์โคพอลิเมอร์ที่สังเคราะห์ได้นำมาทำให้บริสุทธิ์และศึกษาลักษณะสมบัติด้วยเทคนิคโปรตอน - นิวเคลียร์แมกเนติกเรโซแนนซ์ ประสิทธิภาพการกราฟต์ขึ้นกับความเข้มข้นของตัวริเริ่ม อัตราส่วนมอนอเมอร์ต่อยางธรรมชาติและอุณหภูมิปฏิกิริยา กราฟต์โคพอลิเมอร์บริสุทธิ์มาทำไฮโดรจิเนชันโดยใช้ OsHCl(CO)(O$_2$)(PCy$_3$)$_2$ เป็นตัวเร่งปฏิกิริยาเอกพันธุ์ ข้อมูลทางจลนพลศาสตร์ของไฮโดรจิเนชันได้จากการบันทึกปริมาณแก๊สไฮโดรเจนที่ถูกใช้ไปเป็นฟังก์ชันกับเวลาจากเครื่องแก๊สอัพเทค ผลการทดลองทางจลนพลศาสตร์แสดงว่าไฮโดรจิเนชันของยางธรรมชาติกราฟต์เป็นปฏิกิริยาอันดับหนึ่งกับความเข้มข้นของตัวเร่งปฏิกิริยา และเป็นปฏิกิริยาอันดับหนึ่งกับ [C=C] สำหรับยางธรรมชาติกราฟต์เมทิลเมทาคริเลตและเป็นปฏิกิริยาอันดับสองกับ [C=C] สำหรับยางธรรมชาติกราฟต์สไตรีน เนื่องจากสิ่งเจือปนเปื้อนในยางธรรมชาติอัตราการเกิดไฮโดรจิเนชันลดลงกับการเพิ่มความเข้มข้นของยางธรรมชาติกราฟต์ ค่าพลังงานกระตุ้นของอัตราการเกิดไฮโดรจิเนชันของยางธรรมชาติกราฟต์เมทิลเมทาคริเลตและยางธรรมชาติกราฟต์สไตรีนมีค่า 70.3 และ 106.5 กิโลจูล/โมล ตามลำดับ การเติมกรดปริมาณน้อยและการเติมพอลิเมทิลเมทาคริเลตหรือพอลิสไตรีนมีผลต่ออัตราการเกิดไฮโดรจิเนชัน งานวิจัยนี้มีการนำยางธรรมชาติกราฟต์ไฮโดรจิเนตใช้เป็นสารเพิ่มความเข้ากันได้ในพอลิเมอร์ผสมของพอลิเมทิลเมทาคริเลตและอีพีดีเอ็มหรือพอลิสไตรีนและอีพีดีเอ็ม นอกจากนี้ได้ศึกษาสมบัติเชิงความร้อน สมบัติเชิงกลและสัณฐานวิทยาของพอลิเมอร์ผสม

ภาควิชา	เคมีเทคนิค	ลายมือชื่อนิสิต.........................
สาขาวิชา	เคมีเทคนิค	ลายมือชื่ออาจารย์ที่ปรึกษา.........................
ปีการศึกษา	2550	ลายมือชื่ออาจารย์ที่ปรึกษาร่วม.........................

4673837723 : MAJOR CHEMICAL TECHNOLOGY

KEY WORD: GRAFT COPOLYMERIZATION / HYDROGENATION / NATURAL RUBBER / HOMOGENEOUS CATALYSIS / OSMIUM

SUWADEE KONGPARAKUL : MODIFIED NATURAL RUBBER LATEX BY GRAFT COPOLYMERIZATION WITH METHYL METHACRYLATE OR STYRENE AND HYDROGENATION USING OsHCl(CO)(O$_2$)(PCy$_3$)$_2$ AS A CATALYST. THESIS ADVISOR : PROF. PATTARAPAN PRASASSARAKICH, THESIS COADVISOR : PROF. GARRY L. REMPEL, 167 pp.

Graft copolymerization of methyl methacrylate or styrene onto natural rubber in latex form has been carried out using cumene hydroperoxide redox initiator. The synthesized graft copolymers were purified and then characterized by proton nuclear magnetic resonance. Grafting efficiency is discussed with respect to the influence of initiator concentration, monomer to rubber ratio and reaction temperature. The purified graft copolymer was then hydrogenated by using a homogeneous osmium complex catalyst, OsHCl(CO)(O$_2$)(PCy$_3$)$_2$. A detailed kinetic investigation of the hydrogenation was carried out by monitoring the amount of hydrogen consumption as a function of reaction time using a gas–uptake apparatus. The kinetic results for the hydrogenation of graft natural rubber indicated that the rate of hydrogenation exhibited a first–order dependence on the catalyst concentration and a first–order dependence on [C=C] for methyl methacrylate grafted natural rubber and a second–order dependence on [C=C] for styrene grafted natural rubber. Due to the presence of impurities within the natural rubber the rate of hydrogenation was found to decrease with increasing polymer concentration. The apparent activation energy for hydrogenation of natural rubber grafted with methyl methacrylate and natural rubber grafted with styrene was found to be 70.3 and 106.5 kJ/mol, respectively. The addition of a small amount of acid and PMMA or PS provided a beneficial effect on the hydrogenation of grafted natural rubber. The hydrogenated grafted natural rubber could be used as a compatibilizer for PMMA/EPDM or PS/EPDM blends. Thermal properties, mechanical properties and morphology of the blends were also investigated.

Department   Chemical Technology   Student's signature...Suwadee Kongparakul...

Field of study   Chemical Techonology   Advisor's signature...

Academic year   2007   Co-advisor's signature...

ACKNOWLEDGEMENTS

CONTENTS

LIST OF TABLES

TABLE   PAGE

LIST OF FIGURES

FIGURE   PAGE

FIGURE   PAGE

FIGURE   PAGE

NOMENCLATURES

CCD Camera	:	Charge Coupled Devices Camera
CHPO	:	Cumene Hydroperoxide
CPIP	:	$cis-1,4-$Polyisoprene
3-CPA	:	3−Chloropropionic acid
DEPT	:	Distortionless Enhancement of Polarization Transfer
DOP	:	Dioctyl Phthalate
DMA	:	Dynamic Mechanical Analysis
DRC	:	Dry Rubber Content
DSC	:	Differential Scanning Calorimetry
E'	:	Storage Modulus
E''	:	Loss Modulus
EDTA	:	Ethylenediamine Tetraacetic Acid
ENR	:	Epoxidized Natural Rubber
EPDM	:	Ethylene − Propylene Copolymer
FTIR	:	Fourier Transform Infrared Spectroscopy
GE	:	Grafting Efficiency
GL	:	Grafting Level
GNR	:	Grafted Natural Rubber
GPC	:	Gel Permeation Chromatography
HANRL	:	High Ammonia Natural Rubber Latex
HGMMA	:	Hydrogenated Grafted Methyl Methacrylate onto Natural Rubber
HGST	:	Hydrogenated Grafted Styrene onto Natural Rubber
HNR	:	Hydrogenated Natural Rubber
HSBR	:	Hydrogenated Styrene − Butadiene Rubber
INT	:	Initiator
Ir	:	Iridium
KOH	:	Potassium Hydroxide
M	:	Monomer
MCB	:	Monochlorobenzene
M_w	:	Weight − Average Molecular Weight

M_n	:	Number – Average Molecular Weight
MMA	:	Methyl Methacrylate
MW	:	Molecular Weight
MWD	:	Molecular Weight Distribution
NBR	:	Acrylonitrile – Butadiene Rubber
NMR	:	Nuclear Magnetic Resonance Spectroscopy
NR	:	Natural Rubber
NRL	:	Natural rubber latex
Os	:	Osmium
PBD	:	Polybutadiene
PCy_3	:	Tricyclohexylphosphine
Pd	:	Palladium
PDI	:	Polydispersity Index
$PiPr_3$	:	Triisopropylphosphine
PI	:	Polyisoprene
PMMA	:	Poly(methyl methacrylate)
PS	:	Polystyrene
PVC	:	Poly(vinyl chloride)
p–TSA	:	p–Toluenesulfonic acid
p–TSH	:	p–Toluenesulphonyl hydrazide
Rh	:	Rhodium
Ru	:	Ruthenium
SA	:	Succinic Acid
SBR	:	Styrene – Butadiene Rubber
SDS	:	Sodium Dodecyl Sulfate
SEM	:	Scanning Electron Microscopy
ST	:	Styrene
T_g	:	Glass Transition Temperature
T_{id}	:	Initial Decomposition Temperature
T_{max}	:	Maximum Decomposition Temperature
TBHPO	:	t–Buthyl Hydroperoxide

CHAPTER I

INTRODUCTION

1.1 Natural Rubber

Natural rubber latex (NRL) is a renewable material produced at a very low cost and is used in large and growing amounts, in the making of tires, carpet lining, diving gear and adhesives. *Hevea brasiliensis*, a tropical tree, is a major source of the world's natural rubber. Thailand has approximately 5 million acres of rubber plantations located mostly in the southern and eastern parts of the country and is the world's largest natural rubber producer followed by Indonesia and Malaysia with these three countries producing around 90% of the world's natural rubber (NR). The statistics of natural rubber exportation is shown in Figure 1.1.
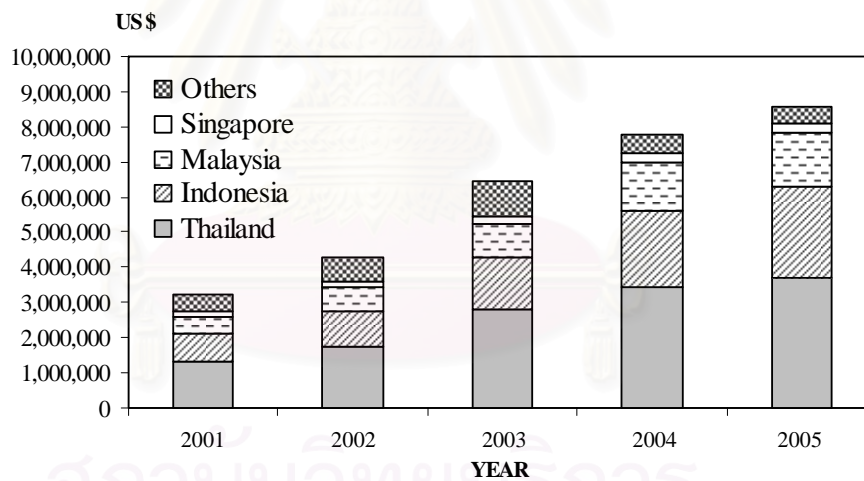
Figure 1.1 Export of product: Natural rubber, balata, gutta−percha, guayule, chicle and similar natural gums, in primary forms (including latex) or in plates, sheets or strip (United Nations Statistics Division) [1].

Natural rubber latex is an aqueous colloidal dispersion stable at high pH (e.g. due to ammonium hydroxide addition) of rubber (*cis*−1,4−polyisoprene), lutoid and Frey − Wyssling particles, with negative zeta potentials assigned to the adsorbed proteins, phospholipids and fatty acid ammonium salts [2]. Many elements are found in the latex films beyond the C, H, O, N, S and P associated with the rubber,

phospholipids and protein. The presence of Ca, Al, Si, Na, Mg, Mn, Cu and Fe in inorganic particles enclosed in the rubber matrix and/or dispersed throughout the rubber phase show that the particles are compatible with rubber through protein accumulation at the particle – rubber interface. Tanaka et al. [3] reported that the rubber chain is composed of an oligopeptide (ω′) followed by two *trans* – isoprene units, a sequence of thousands of *cis* – isoprene units and terminated by a fatty acid ester (α′) group. The chemical structure of natural rubber is shown in Figure 1.2.
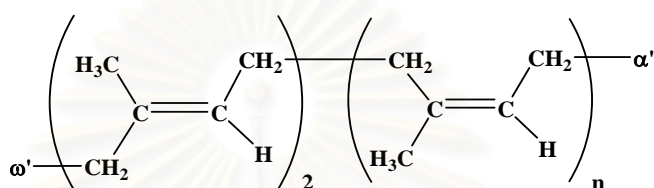
Figure 1.2 Chemical structure of natural rubber [3].

The composition of the fresh latex is rather complex due to its origin and the relative proportions of certain constituents (e.g. proteins and minerals). Fresh latex consists of approximately 25 – 40% dry rubber content (DRC) and 5 – 10% of non-rubber substances. The composition varies according to clones of the rubber tree, age of the rubber tree, and the trapping method. A typical fresh natural rubber latex composition is presented in Table 1.1.

Table 1.1 Typical Fresh Natural Rubber Latex Composition [4].

	% Composition
Total Solids Content	41.5
Dry Rubber Content	36.0
Amino Acids and N–Bases	0.30
Neutral lipids	1.00
Proteins	1.60
Phospholipids	0.60
Inositols–Carbohydrates	1.50
Salts (mainly K, P and Mg)	0.50
Water	58.5

The rubber particles are believed to be covered by some proteins and phospholipids, concerned with the colloidal stability of the natural rubber latex. Phospholipids are strongly adsorbed on the surfaces of the rubber particles, and believed to be intermediate by which the proteins are anchored on the rubber particles as shown in Figure 1.3. The molecular weight (MW) and molecular weight distribution (MWD) of natural rubber showed a great variation depending on the age and clone of rubber trees [5]. Figure 1.4 illustrates MWD curves for seven clones of 25 year old mature trees. Although most heights of the MW peaks appeared in the low molecular weight region, the actual value of the molecular weight showed a great variation depending on the different types of clone rubber trees. The weight-average molecular weight (M_w) showed a variation from 6.8×10^5 to 2.9×10^6 and the number-average molecular weight (M_n) varied from about 1.2×10^5 to 3.2×10^5. The molecular weight distribution (MWD) showed a wide range from 5 to 11. For commercial natural rubber latex production, the rubber latex is a mixture of different clone rubber lattices, therefore the large variation in MW and MWD is reduced.

Natural rubber is often used for vehicle tire and for blending with various synthetic rubbers. Natural rubber exhibits good elasticity and mechanical strength but deteriorates when exposed to sunlight, ozone and oxygen because of poor heat resistance and low resistance to weathering and chemical reagents. Natural rubber is a good eco–material but its overall usage is restricted since it cannot be used for high performance and in high functional materials. Thus, if natural rubber can be improved to have better chemical resistance properties, it might be competitive with synthetic rubbers.
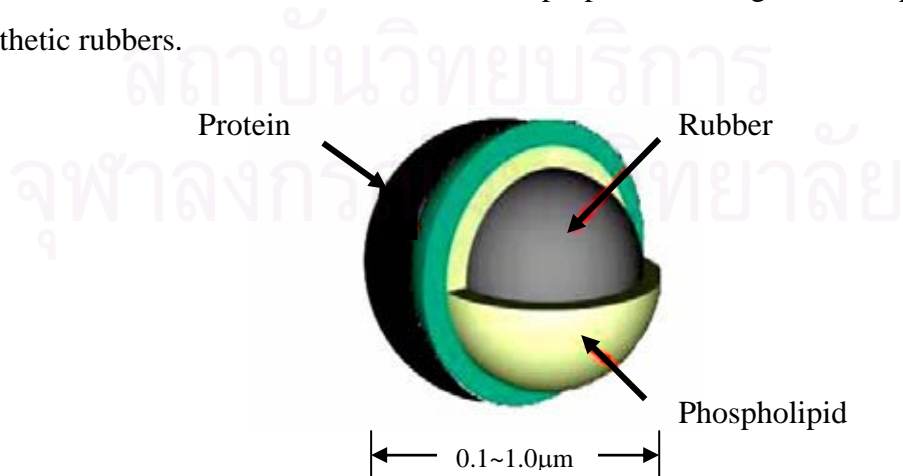
Figure 1.3 Presumed structure of a rubber particle [6].
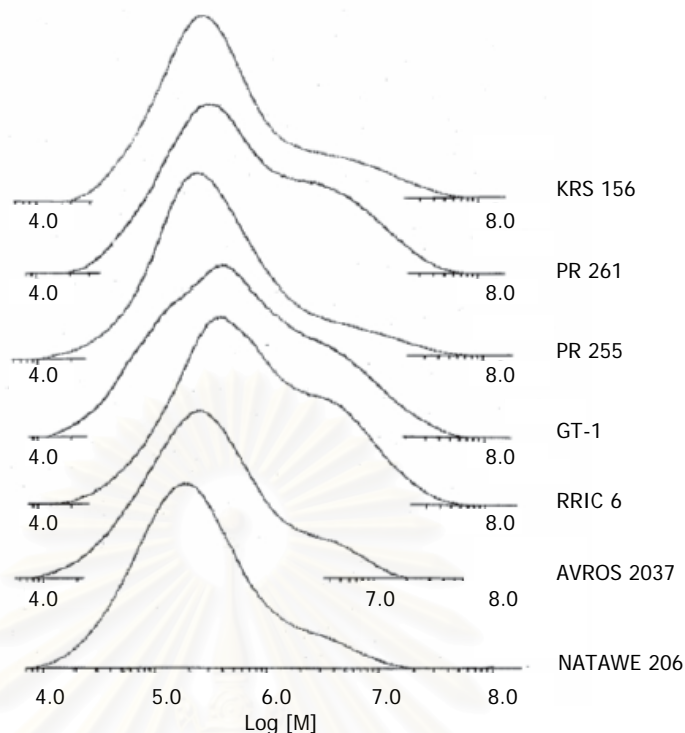
Figure 1.4 Molecular weight and molecular weight distribution of natural rubber
latex from 7 different matured clones, aged 25 years [5].

1.2 Chemical Modification of Unsaturated Polymers

Chemical modification of polymers is a postpolymerization reaction. These reactions may occur on reactive sites dispersed within the polymer main chain. Some of the most important commercial polymers are diene polymers e.g., natural rubber (NR), polyisoprene (PI), polybutadiene (PBD) and styrene butadiene rubber (SBR). Such reactions include chain extensions, cross–linking, graft and block copolymer formation [7, 8]. The reaction may also occur on reactive sites attached directly or via other group/chains bound to the polymer backbone. Reactions of this type include halogenation, sulfonation, hydrolysis, epoxidation, surface, and other miscellaneous reactions of polymers. In both cases, these types of reactions transform existing polymers into those having new and/or improved properties. Of course, there are some aspects (e.g., solubility, viscosity, neighboring–group, conformational sequence, and statistical effects) which are unique to reactions on macromolecular chains [9].

Similar to other olefin molecules, the double bond within the repeating unit of natural rubber can be modified by various chemical reactions. NR has a very uniform microstructure that provides the material with some unique and important characteristics. Application of NR in rubber products gives the product very useful characteristics such as good tensile strength, high resilience, excellent flexibility and impact resistance. However, NR is less resistant to oxidation, ozone, weathering and a wide range of chemicals and solvents, mainly due to the carbon–carbon double bonds (C=C) in the chemical structure of NR. Chemical modification of the unsaturated polymer may be classified according to different criteria. One criterion is the chemical modification of unsaturated polymer due to the various types of chemical reaction on the double bond. The chemical modification of NR can be classified into three main categories [10]:

- Modification by bond rearrangement without introducing new atoms, such as, carbon–carbon cross–linking, cyclization, and *cis, trans*–isomerization.

- Modification by attachment of a new chemical groups through addition or substitution reactions at the olefinic double bonds, such as, chlorinated NR, hydrogenated NR, hydrochlorinated NR and epoxidized NR (ENR).

- Grafting a second polymer onto the NR backbone.

1.3 Graft Copolymerization

The chemical modification of polymers that constitute the polymer backbone contributes to the ultimate properties of polymeric products. For a polymer to be useful, it must be able to function properly in a given application. Graft copolymerization is one of the most useful methods to modify unsaturated polymers to provide desirable properties. Graft copolymers contain a long sequence of one monomer (often referred to as the backbone polymer) with one or more branches (grafts) with a long sequence of a second monomer [11]. In graft copolymerization,

polymer side chains are formed and attached to preformed macromolecules of different chemical composition and usually the side chains are distributed randomly [12]. The essential three approaches for the preparation of graft copolymers are (a) chain transfer to a saturated or unsaturated polymer, (b) activation by photochemical or radiative methods, and (c) introduction and subsequent activation of peroxide and hydroperoxide groups.

There are two general methods for vinyl monomer polymerization: the polymerization of a monomer in the presence of a polymer by the initiation of growth through chain transfer; and polymerization of a monomer in the presence of a polymer containing reactive sites. In both of these methods, the polymerization of a monomer in the presence of polymer results in a mixture of products: (1) the initial homopolymer that did not participate in the reaction; (2) the homopolymer of the fresh monomer; (3) the cross−linked parent homopolymer; and (4) the desired copolymer. The composition of the product mixture will depend on the nature of polymer, monomer, and initiator. In any case, the desired pure product can be obtained by extraction methods.

Block copolymers are linear, but graft copolymers are branched, with the main chain generally consisting of a homopolymer or a random copolymer, while the grafted side chains are composed of either the same or another monomer or several monomers [13]. The numerous ways for the synthesis of graft copolymers can be divided into three categories. The first category (a) belongs to the homo− and copolymerization of macromonomers. For this purpose, macromolecules with only one polymerizable end group are needed. The second pathway (b) is called "grafting from". This means that active sites are generated at the polymer backbone **A** which initiate the polymerization of monomer **B**. The third possibility (c) to prepare graft copolymers is termed "grafting onto". The growing chain **B** attacks the polymer backbone **A** with formation of a long branch. The overall pathways for preparation of graft copolymers are shown in Figure 1.5.

Graft polymerization onto natural rubber has been carried out in solution, solid rubber, and latex phases. However, the grafting in the latex phase is the most economical and practical method, such that previously formed latex particles are grafted in further polymerization steps. Emulsion polymerization is a complex heterogeneous process. There are many formulation components which can be present in a latex formulation, such as monomer, surfactant, initiator, buffer, chain transfer agent and water, all of which may affect the polymerization rate [14]. A typical emulsion system is illustrated in Figure 1.6.

(a)

$+ M_2$

$R\bullet$
(or R- or R+)

(b)

M_1

I   I   I   I

(c)

X   X   X   X

Y   Y   Y   Y
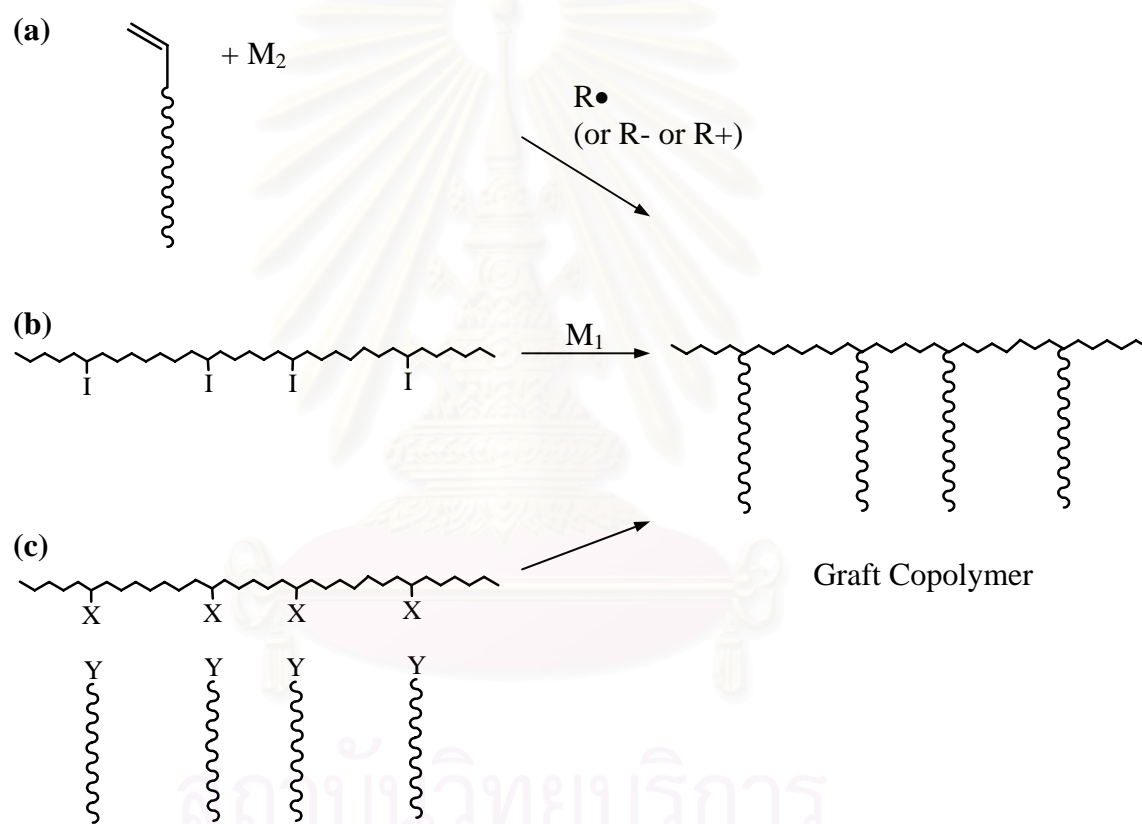
Graft Copolymer

Figure 1.5 Pathways for synthesis of graft copolymers: (a) homo− and copolymerization of macromonomers route, (b) "grafting from" route, (c) "grafting onto" route. (M = monomer, R = radicals, I = azo or peroxo group, X and Y = reactive side groups)
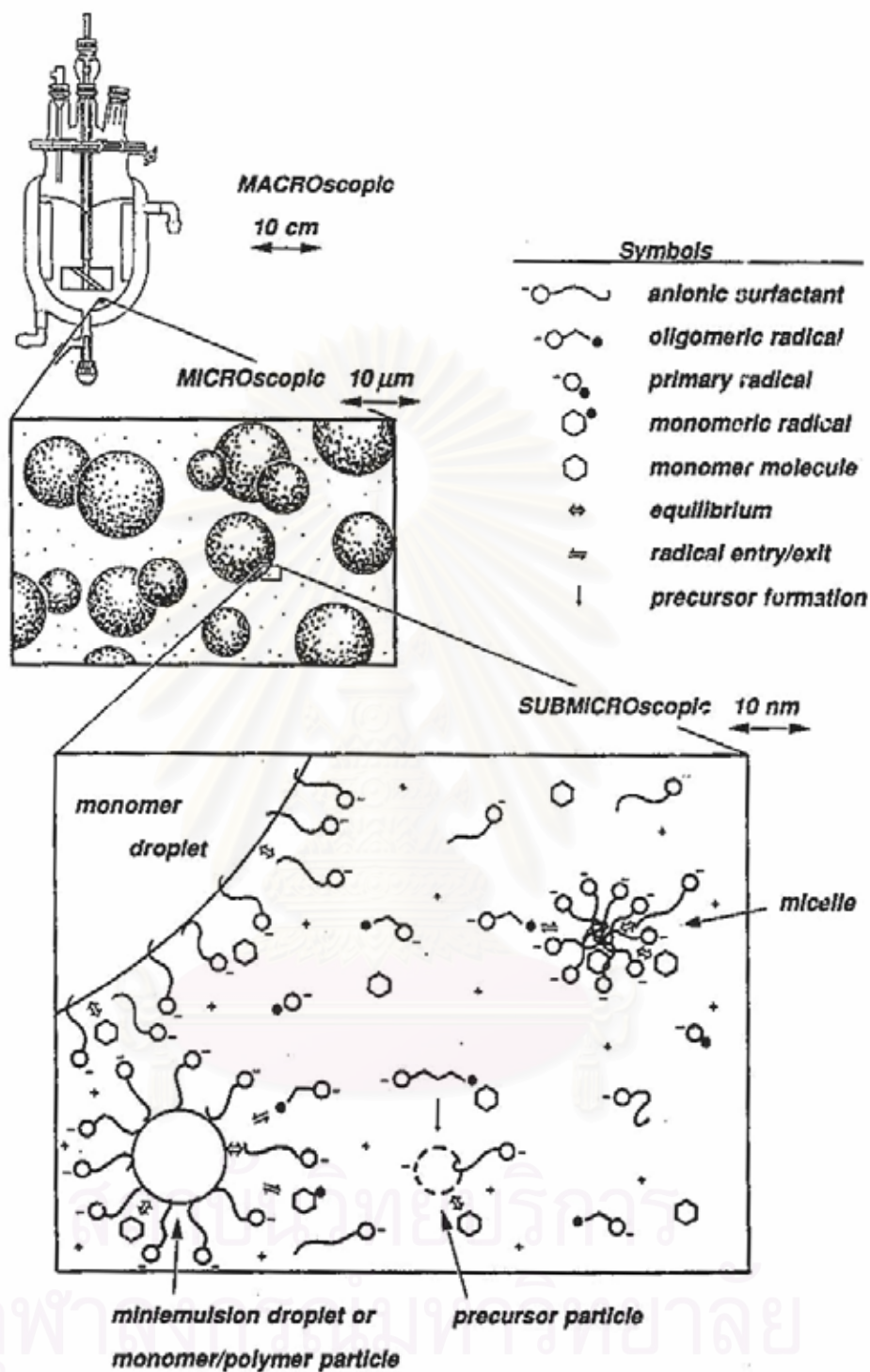
Figure 1.6   Schematic representation of the early stages of emulsion polymerization illustrating three scales of observation: macroscopic, microscopic, and submicron scopes [15].

Graft copolymerization of natural rubber is mostly carried out using vinyl monomers such as methyl methacrylate (MMA) and styrene (ST). The commercial grade of available grafted copolymer of NR is a natural rubber grafted with methyl methacrylate (Heveaplus MG) with two grades: 30% grafted MMA (MG 30) and 49% grafted MMA (MG49). The grafted products have degrees of grafting in the range of 60 − 80% and some free PMMA. Heveaplus MG has superior properties like hardness, modulus, abrasion, electrical resistance and light color. It is used to improve the impact properties of polystyrene, in blends with NR and also as a reinforcing agent. The solution or latex form of Heveaplus MG is used as an adhesive or bonding agent to bond rubber to poly(vinyl chloride) (PVC), leather, textiles and metals [16].

There are many research reports on the modification of natural rubber by grafting reactions in both latex and solution. Most of the commercial processes for grafting monomers onto NR are carried out using emulsion polymerization. Charmondusit et al. [17] studied the graft copolymerization of methyl methacrylate and styrene onto natural rubber using potassium persulfate as an initiator. At optimum conditions, the maximum percentage of monomer conversion was 79.5% and the grafting efficiency was 65.3. The grafted natural rubber product was used as an impact modifier for PVC/grafted NR blend. The impact strength of the PVC blends increased with increasing grafted natural rubber content. The good mechanical properties of PVC were obtained at 10 and 15 phr (part per hundred part of rubber) of the grafted NR product.

Arayapranee et al. [18, 19] studied the graft copolymerization of 50/50 (w/w) styrene/methyl methacrylate mixtures onto natural rubber latex using cumene hydroperoxide/sodium formaldehyde sulfoxylate dihydrate/ethylenediamine tetraacetic acid (EDTA)−chelated Fe^{2+} as a redox initiator. The effects of the process factors such as the amount of initiator, emulsifier, and chain−transfer agent; monomer−to−rubber ratio (M/R); and temperature on the grafting efficiency (GE) and grafting level (GL) were reported. It was found that the formation of graft copolymers occurred on the surface of the latex particles through a chain−transfer process. It was confirmed that the graft copolymerization was a surface − controlled process.

Kochthongrasamee et al. [20] investigated the graft copolymerization of MMA monomer onto natural rubber particles. The graft copolymerization was performed by using three different redox initiator systems: cumene hydroperoxide/tetraethylene petamine (CHPO/TEPA), *tert*−buthyl hydroperoxide /tetraethylene petamine (TBHPO/TEPA), and potassium persulfate/sodium thiosulfate $(K_2S_2O_8)/Na_2S_2O_3$. The graft copolymerization initiated with CHPO/TEPA gave the highest grafting efficiency. A redox initiating system consisting of hydroperoxide and TEPA was effectively used for the emulsion polymerization in the NR latex because it is not sensitive to oxygen, and worked well when ammonia was present.

1.4 Catalytic Hydrogenation in the Presence of $OsHCl(CO)(O_2)(PCy_3)_2$

Hydrogenation is a reaction which involves the addition of hydrogen across the double bonds in unsaturated part of polymer chain. A catalyst and heat must be present to initiate the reaction, which, once started, is exothermic. The structure of the hydrogenated polymer has better resistance to thermal and oxidative degradation. Examples of commercially hydrogenated polymers are hydrogenated styrene−butadiene rubber (HSBR, Kraton) by Shell and hydrogenated acrylonitrile−butadiene rubber (HNBR) by Nippon Zeon Chemicals and Lanxess Inc. These hydrogenated rubbers have excellent high temperature stability and resistance to oxygen, ozone, and ultraviolet radiation, which are far superior to those of the parent rubbers [7].

According to a literature review, the osmium complex $OsHCl(CO)(O_2)(PCy_3)_2$ is an effective catalyst for hydrogenation not only for small olefin molecules, but also an efficient catalyst for diene−based polymer hydrogenation such as acrylonitrile−butadiene rubber (NBR), synthetic *cis*−1,4−polyisoprene (CPIP) and natural rubber (NR). The osmium complex is stable under the reaction conditions since this osmium complex has bulky, strong σ−donor and weak π−acceptor phosphine ligands, PCy_3, with Tolman's cone angle $\geq 160°C$. It exhibits high catalytic activity due to the ease of dissociation of a PCy_3 ligand from an 18−electron complex to produce a 16−electron species. Furthermore previous studies

on polymer hydrogenation catalyzed by $OsHCl(CO)(O_2)(PCy_3)_2$ have shown the robustness and temperature stability of this catalyst [21 – 24].

The osmium complex, $OsHCl(CO)(PR_3)_2$ where R=Cy or i–Pr, has been prepared by Moers [25]. Esteruelas et al. [26, 27] demonstrated that osmium complexes such as $OsHCl(CO)(PR_3)_2$ are active catalysts for olefin hydrogenation. Remarkably, these complexes are more active at industrial conditions than the current generation of Ru, Rh and Pd systems. Figure 1.7 illustrated the chemical reaction pathway to create the Os (II) complex. Complex **1** is a stable five coordinate complex. It is known that the osmium center lies essentially in the basal plane of complex **1**. The other ligands such as O_2, H_2, and –CN can coordinated to the Os metal at the vacant coordination site *trans* to the hydride to give the six–coordinate complexes. The corresponding dioxygen adduct, $OsHCl(CO(O_2)(PR_3)_2$ (**2**) has superior stability as a solid [26, 28]. Complex **1** forms a *trans*–hydridodihydrogen complexes, $OsHCl(\eta^2–H_2)(CO)(L)(PR_3)_2$ (**3**) through the η^2–coordination of H_2. Consistent with the addition reactions described above, dihydrogen coordinates *trans* to the hydride to create the Os (II) complex as shown in Figure 1.7.
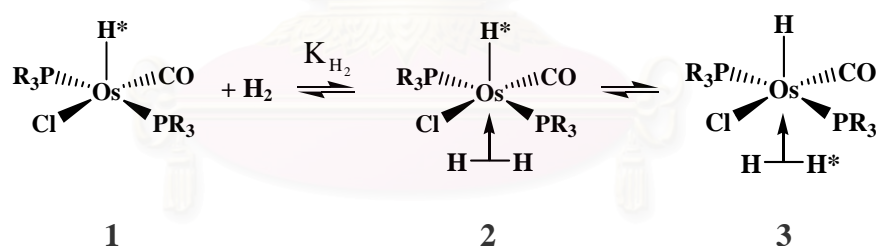
Figure 1.7 Dihydrogen coordinates *trans* to the hydride to create the Os (II) complex [29].

Parent et al. [29] also studied the reactivity of complexes formed by the addition of O_2, H_2 and R'CN to $OsHCl(CO)(PR_3)_2$ (R = Cy or i–Pr). Under 24 bar of hydrogen pressure and a temperature of 65°C, the dioxygen ligand of $OsHCl(CO)(O_2)(PR_3)_2$ **2** is displaced to yield the *trans*–hydridodihydrogen complex (**3**). The coordination of $OsHCl(CO)(R'CN)(PR_3)_2$ to **1** can account for a reduction in catalytic activity associated with increase in NBR copolymer concentration. The phosphine ligands of **1** and **3** exchange with unbound, bulky alkyl phosphines at a rate

that is slow. Moreover, in the presence of excess PCy_3, complex **3** yields the exchange products $OsHCl(\eta^2–H_2)(CO)(i–Pr_3)(PCy_3)$ and **3**.

The osmium complexes, $OsHCl(CO)(O_2)(PR_3)_2$ can be classified into three classes according to the different types of phosphine ligands: (I) bulky monophosphines with Tolman's cone angle $\geq 160°$ such as $PiPr_3$, PCy_3, and PCy_2Ph, (II) smaller monophosphines such as PPh_3 and $P(m–C_6H_4Me)_3$, and (III) diphosphine such as $Ph_2P(CH_2)_3PPh_2(dppp)$. Mao and Rempel [30] studied a series of osmium complexes for the catalytic hydrogenation of acrylonitrile–butadiene copolymers with various ligand types. It was found that the activity of these complexes decreases as follows: class I > class II > class III which is mainly attributed to the ease of dissociation of a ligand from an 18–electron complex to generate a 16–electron species $O_2 > PR_3 > dppp$ in the catalytic hydrogenation reaction. In class I phosphine ligands, their catalytic activities increase in the order: $PCy_2Ph < P^iPr_3 << PCy_3$. This trend does not appear to correlate with the steric effect based on Tolman's cone angles, however, it is in good agreement with the electronic effect, which was evaluated based on the infrared υ_{CO} values of these complexes. The catalytic activity of these complexes increases with the decrease of υ_{CO} values, which is consistent with the increase of the donor power of phosphine ligands. For classes II and III phosphine ligands, a complex containing a bulky, strong σ–donor and weak π–acceptor phosphine is a good catalyst whereas that containing a chelating phosphine ligand would be a poor catalyst. Parent et al. [22] also studied the hydrogenation of NBR rubber in the presence of $OsHCl(CO)(O_2)(PCy_3)_2$. The extent of crosslinking of the NBR copolymer was dependent on the process conditions and could be reduced by using a low catalyst concentration and high hydrogen pressure.

1.5 Catalytic and Non–Catalytic Hydrogenation of *cis*–1,4–Polyisoprene and Natural Rubber

Hydrogenation of *cis*–1,4–polyisoprene (CPIP) in the presence of $OsHCl(CO)(O_2)(PCy_3)_2$ and $[Ir(COD)py(PCy_3)]PF_6$ as catalyst was investigated by Charmondusit et al. [31, 32]. The results of a preliminary study of CPIP hydrogenation showed that $RhCl(PPh_3)_3$ is an efficient catalyst for hydrogenation of

most olefin polymers, but the activity is rather low for hydrogenation of CPIP. However, both the Os and Ir catalysts mentioned above were effective for CPIP hydrogenation with more than 95% degree of hydrogenation being achieved at optimum conditions. The kinetic results indicated that this system had a second–order dependence for the hydrogenation rate of CPIP on hydrogen pressure and then decreased toward a zero–order dependence for hydrogen pressures above 13.8 bar. The hydrogenation was also observed to be first–order with respect to catalyst loading and polymer concentration. The apparent activation energy was found to be 109.32 kJ/mol.

Hydrogenation of natural rubber, the main natural renewable rubber resource, has been of interest over the past few decades. The hydrogenation of natural rubber was both studied in solid form in solvent medium [33] and aqueous latex or emulsion form [34]. The hydrogenation of natural rubber converts the unsaturated structure to a saturated form to provide an ideal alternating ethylene-propylene copolymer (EPDM) which is difficult to prepare by conventional polymerization. Hydrogenated natural rubber (HNR) is more stable against thermal, oxidative, and radiation induced degradation as the thermal stability of NR is improved by converting the weak C=C π bond within NR to the stronger C–H σ bonds [31]. The hydrogenation NR provides the hydrogenated NR (HNR), which has a structure of an alternating copolymer of ethylene and propylene as shown in Figure 1.8.
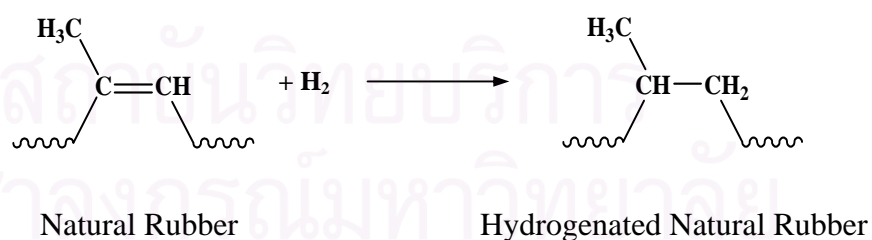
Figure 1.8 Hydrogenation of natural rubber.

Hydrogenation of natural rubber can be achieved using either non−catalytic or catalytic methods. It can be classified into three methods to hydrogenate natural rubber: (i) homogeneous catalysts, (ii) heterogeneous catalysts, and (iii) non−catalytic hydrogenation. The comparison of hydrogenation methods is summarized in Table 1.2.

Table 1.2 Comparison of Hydrogenation Methods [35].

Methods of Hydrogenation	Yield	Side Reaction	Catalyst Poisoning and Removal
Homogeneous hydrogenation	High yield of saturated products can be obtained with hydrogenation up to 100%	Degradation of NR occurs but can be overcome by using Ni catalyst	Ni catalyst is easily poisoned by impurities and difficult to be removed
Heterogeneous hydrogenation	Yields purer products	Degradation does not occur and foreign groups are present	Catalyst can cause poisoning
Non−catalytic hydrogenation	Low level of hydrogenation with < 70% of conversion	Isomerization, attachment of hydrazine fragments (can be minimized with the addition of antioxidant), depolymerization and cyclization occur	No poisoning or catalyst removal issue

Catalytic hydrogenation can be achieved with either heterogeneous or homogeneous catalyst systems. However, the homogeneous catalysts are more favorable than heterogeneous catalysts because of their higher selectivity and absence of microscopic diffusion problems. Moreover, the role of the homogeneous catalyst can be explained and understood at the molecular level [36]. Based on the previous literature, catalytic hydrogenation of natural rubber generally involves the use of a homogeneous catalyst such as $Ru[CH=CH(Ph)]Cl(CO)(PCy_3)_2$, $RhCl(PPh_3)_3$, $[Ir(COD)py(PCy_3)]PF_6$, or $OsHCl(CO(O_2)(PCy_3)_2$.

Tangthongkul et al. [37, 38] reported the hydrogenation of CPIP and NR in the presence of Ru[CH=CH(Ph)]Cl(CO)(PCy$_3$)$_2$. It was found that the presence of impurities and the high molecular weight of NR may reduce the efficiency of the catalyst. The addition of a small amount of acid, that is, p−toluenesulfonic acid (p−TSA), appears to neutralize the poisonous effect of the system. The hydrogenated natural rubber (HNR) resulted in a polymer akin to an alternating ethylene−propylene copolymer. The hydrogenation reaction leads to an increase in the thermal stability of NR without affecting its glass transition temperature (T$_g$).

Hinchiranan et. al [39] studied the catalytic hydrogenation of cis−1,4−polyisoprene (CPIP) and natural rubber using [Ir(COD)py(PCy$_3$)]PF$_6$ as catalyst. The kinetic results for the hydrogenation of both synthetic CPIP and NR indicated that the hydrogenation rate exhibited a first−order dependence on hydrogen pressure and a first to zero−order dependence with respect to the catalyst concentration. It was also suggested that a side reaction such as dimerization of the iridium catalyst might have occurred at a higher catalyst loading. Because of impurities inside the natural rubber, the hydrogenation of NR showed an inverse behavior dependence on the rubber concentration, whereas the hydrogenation rate of synthetic rubber, that is, cis−1,4−polyisoprene, remained constant when the rubber concentration increased. The apparent activation energies for the hydrogenation of synthetic CPIP and NR were evaluated to be 79.8 and 75.6 kJ/mol, respectively.

The hydrogenation of NR using OsHCl(CO)(O$_2$)(PCy$_3$)$_2$ was also investigated in subsequent work [24]. The kinetic results indicated that the hydrogenation rate exhibited a first−order shifted to zero−order dependence on hydrogen at lower hydrogen pressure, which then decreased toward an inverse behavior at pressures higher than 41.4 bar. The hydrogenation was also observed to be first−order with respect to catalyst concentration, and an apparent inverse dependence on rubber concentration was observed due to the impurities in the rubber. The hydrogenation rate was dependent on reaction temperature, and the apparent activation energy over the temperature range of 125 – 145°C was found to be 122.76 kJ/mol. The addition of some acids such as 3−chloropropionic acid (3−CPA) and p−toluenesulfonic acid (p−TSA) showed an effect on the hydrogenation rate of CPIP

and NR hydrogenation. The addition of 3–CPA and *p*–TSA increased the rate of NR hydrogenation, then diminished and leveled off at an optimum acid concentration. The role of acids in the NR hydrogenation may partially be due to the possible neutralization of the impurities in the rubber. The thermal stability of hydrogenated natural rubber (HNR) increased with an increase in the percentage of hydrogenation level. The mechanistic aspects for NR hydrogenation for the Os complex catalyst is illustrated in Figure 1.9.
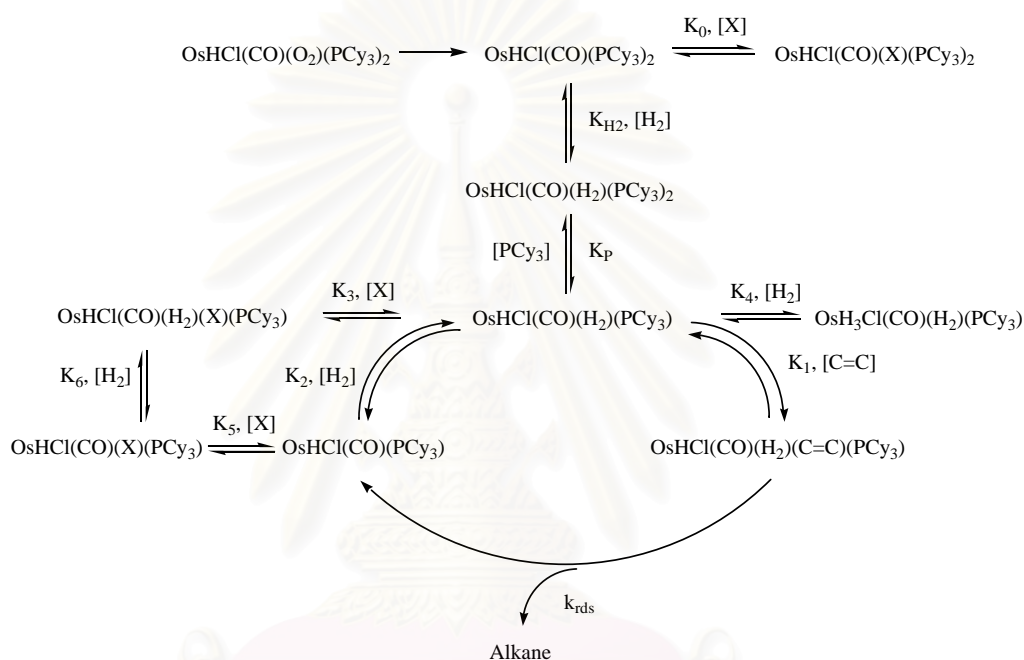
Figure 1.9   Proposed catalytic mechanism for NR hydrogenation in the presence of
OsHCl(CO)(O$_2$)(PCy$_3$)$_2$ [24].

Most hydrogenation reactions employ solutions of rubber as the reaction media. However, natural rubber and certain synthetic elastomers are available in the aqueous latex or emulsion form; thus it would be advantageous to hydrogenate the elastomer in the latex phase. The catalytic hydrogenation by using the homogeneous osmium catalyst, OsHCl(CO)(O$_2$)(PCy$_3$)$_2$, has recently been applied for natural rubber latex (NRL) [23]. From preliminary study of NRL hydrogenation in chlorobenzene by using various catalyst types, it was found that OsHCl(CO(O$_2$)(PCy$_3$)$_2$ is a much more efficient catalyst than [Ir(COD)py(PCy$_3$)]PF$_6$,

Ru[CH=CH(Ph)]Cl(CO)(PCy$_3$)$_2$, and RhCl(PPh$_3$)$_3$ catalysts. From a kinetic investigation of the NRL hydrogenation in the presence of OsHCl(CO)(O$_2$)(PCy$_3$)$_2$, the process showed first−order dependence on the osmium catalyst concentration. The catalytic activity decreased at high rubber concentration, as a result of the high amount of impurities, thus, the hydrogenation showed an inverse order dependence on rubber concentration. The result showed a second−order dependence of the hydrogenation rate on hydrogen pressure and then decreased toward a zero−order dependence for hydrogen pressures above 13.8 bar. A similar result was found for the hydrogenation of synthetic *cis*−1,4−polyisoprene. The hydrogenation rate was dependent on the reaction temperature and an apparent activation energy of 56.79 kJ/mol was found.

The addition of a controlled amount of *p*−TSA demonstrated a beneficial effect on the hydrogenation rate, and 95% hydrogenation was achieved in 3 h at 150°C under a hydrogen pressure of 27.6 bar. The presence of a *p*−toluene sulfonic acid in the hydrogenation process helped to prevent the poisoning of the osmium catalyst by impurities present in the emulsion system. The hydrogenation provides a method to improve the thermal stability of natural rubber without affecting its glass transition temperature. The catalytic cycle for NRL hydrogenation in the presence of OsHCl(CO(O$_2$)(PCy$_3$)$_2$ is shown in Figure 1.10.
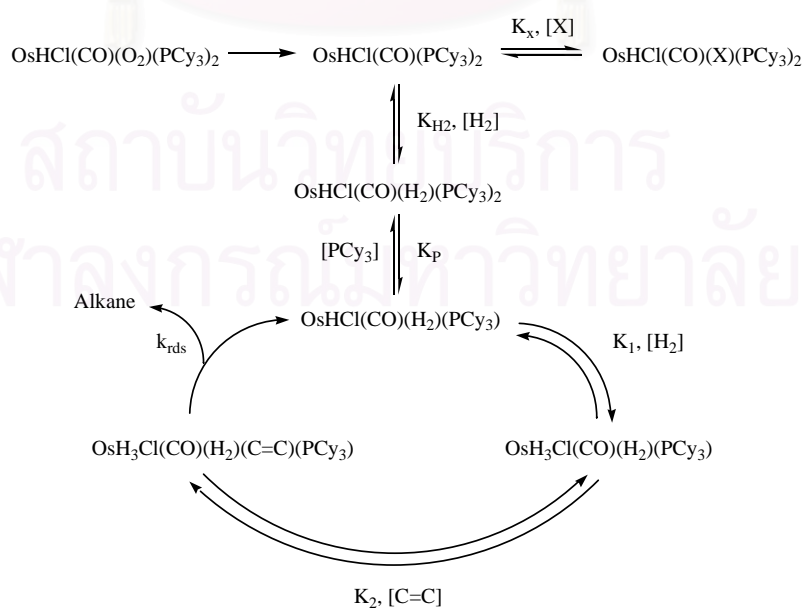
Figure 1.10 Catalytic cycle for NRL hydrogenation [23].

For the non−catalytic hydrogenation of natural rubber, the main method used involves diimide reduction. The overall hydrogenation reaction of the unsaturated polymer latex with diimide can be expressed as follows:

$$N_2H_4 + H_2O_2 + -HC = CH- \quad \rightarrow \quad N_2 + -HC - CH- + 2H_2O \quad (1.1)$$

However, side reactions such as chain scission, cyclization, crosslinking, and gel formation, which is very undesirable, were found [9, 40]. Wideman [41] patented the hydrogenation process for various latex polymers and natural rubber latex hydrogenation was investigated. Diimide, generated in *situ* from *p*−toluenesulphonyl hydrazide (*p*−TSH), has been extensively studied as a source for hydrogenation. It was claimed that 27% hydrogenation of high ammonia natural rubber latex (HANRL) system was achieved at 100°C in 3 h. Samran et al. [42] also studied the hydrogenation of NR and epoxidized NR (ENR) by diimide generated in *situ* from thermal decomposition of *p*−TSH in xylene at 135°C. With an excess of *p*−TSH, a 85 − 95% degree of hydrogenation was achieved. It was also found that the high reaction temperature employed led to polymer chain degradation.

Mahittikul et al. [43] studied the hydrogenation of natural rubber in latex form using diimide generated in *situ*. It was accomplished by thermolysis of *p*−toluenesulfonyl hydrazide (*p*−TSH). The optimum condition of *p*−TSH to double bond mole ratio was 2:1, which achieved > 90 % hydrogenation.   The effect of impurities present in the latex and water was not significant. The diimide hydrogenation method improved the thermal stability of natural rubber latex with out affecting its glass transition temperature. Mahittikul et al. [44] also investigated the hydrogenation of natural rubber latex (NRL) via an other diimide reduction system. This system used hydrazine hydrate/hydrogen peroxide and Cu^{2+} as catalyst. It was found that cupric acetate is a highly active catalyst for the reaction and the addition of a controlled amount of gelatin demonstrated a beneficial effect on the degree of hydrogenation, whereas, sodium dodecyl sulfate (SDS) acted as a stabilizer of the latex particle in the reaction system and reduced the degree of hydrogenation. In the presence of SDS, a longer reaction time and a higher amount of hydrazine hydrate was required for NRL hydrogenation. Gel formation during hydrogenation did not

significantly affect the degree of hydrogenation. Gel inhibitors such as hydroquinone also decreased the degree of hydrogenation.

1.6 Polymer Blending

During the last three decades polymer blends have played a very important role in the commercialization of polymers. The practice of polymer blending is as old as the polymer industry itself with early examples involving natural rubber [45]. Polymer blending products are frequently formulated by blending two or more polymers. The rational for this development involves one or more of the following points: (a) develop new properties, (b) improve properties, (c) reduce material costs, (d) improve processibility, (e) modified polymeric materials, and (f) reuse of plastic scrap. Thus, the recent industrial efforts have been directed towards development of: (i) blends for high performance polymers, (ii) multiphase blends, with several polymers, and/or reinforcements, (iii) reactive processing, (iv) blends with controlled morphology and (v) blends from recycled materials.

There are various kind of polymer blends such as two thermoplastics (plastics blends), two rubbers (rubber blends), a thermoplastics resin filled with an elastomer as the dispersed phase (rubber−modified plastics), or a rubber with a plastic as the disperse phase (polymer−filled elastomer) [46]. Two chemically different polymers often form incompatible blends. The adherence can be compatibilized the immiscible blends, including compatibilization by introduction of a non−reactive graft or block copolymers, non−bonding specific interactions, low molecular weight coupling agents, and reactive polymers [47]. Compatibilized blends are termed "compatible blends" and characterized by the presence of a finely dispersed phase, good adhesion between blend phases, strong resistance to phase coalescence, and technologically desirable properties [48]. Moreover, process can be designed to reduce the interfacial energy and improve the interfacial addition during mixing of the blend components.

Compatibilizers are polymeric analogs of surfactants in that they are interfacially active materials. It is necessary to make a molecule that has sections,

which are miscible with each of the components, and it will be very difficult to find a homopolymer miscible with both of them. Thus, the compatibilizer will need to have chemically different sections or blocks. The schematic of steric suppression of coalescence due to the presence of a copolymer at the interface is illustrated in Figure 1.11.

Broader
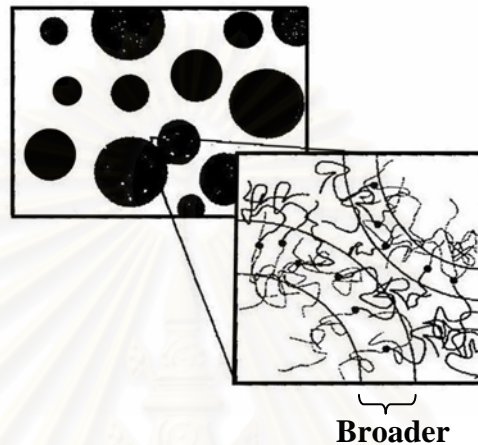
Figure 1.11 Suppression of coalescence. Two drops that have a layer of diblock or graft copolymer at the interface are less likely to coalescence since the copolymer molecules form shells around the drop [49].

Polymer blend is an important consideration since the blending may provide the improvement of mechanical properties as well as processibility. Oommen and Thomas [50] studied the morphology and mechanical properties of natural rubber (NR)/poly(methyl methacrylate) (PMMA) blends as a function of blend ratio and compatibilizer concentration. It was found that addition of compatibilizer reduced the domain size of the dispersed phase followed by a leveling off at higher graft copolymer concentration. Tensile strength, tear strength and the Young's modulus decreased with an increase in NR content. The mechanical properties attained a maximum value at the leveling point, which is an indication of interfacial saturation and the attainment of maximum interfacial adhesion between the homopolymers.

Charmondusit et al. [17] investigated the modification of graft copolymer of methyl methacrylate and styrene onto natural rubber (MMA/ST-*g*-NR). It was used as an impact modifier in PVC. The good mechanical properties of the blend were obtained at 10 and 15 phr of the grafted NR product. Thiraphattaraphun et al. [51] reported the methyl methacrylate-*g*-natural rubber/poly(methyl methacrylate) blends. The mechanical properties and the fracture behavior of the blends were evaluated as a function of the graft copolymer composition and the blend ratio. The tensile strength, tear strength, and hardness increased with an increase in PMMA content. The fracture surface of a tensile specimen examined by scanning electron microscopy (SEM) indicated that the graft copolymer acted as an interfacial agent and gave a good adhesion between the two phases of the compatibilized blend.

Suriyachai et al. [52] studied the graft copolymerization of styrene and glycidyl methacrylate onto natural rubber latex (ST/GMA-*g*-NR) and its application. The grafted natural rubber product could be used as a compatibilizer for natural rubber/PMMA blends. The tensile strength, tear strength, hardness and impact energy of the blends exhibited considerable improvement upon the addition of the grafted natural rubber. Good compatibility of NR/PMMA blends at a ratio of 50/50 and 70/30 was obtained at grafted NR contents of 5 and 10 phr, respectively. The morphology of the blends showed good interfacial adhesion upon the addition of grafted NR.

Most commercial multi–component polymer systems are two–phase blends that provide advantages over the single–phase systems. There is a general agreement that the properties of polymer blends are usually controlled by the properties of the components, morphology of the blends and interaction between components in the blends. The domain size is often used to indicate the extent of compatibility of multiphase polymer systems, i.e., the smaller the domain size, the more compatible are the systems and the better are the mechanical properties. Macosko el al. [53] have performed model experiments in order to investigate the initial stage of mixing at very short times. The primary mode of morphology development at short mixing times appeared to be a shearing of the phases into ribbon or sheet like structures followed by a shear or interfacial tension of these sheets or ribbons into nearly spherical particles, as shown in Figure 1.12. Thus, the dependence

of the dispersed phase size on the mixing time over a wide range of torque ratio was found for the blends.
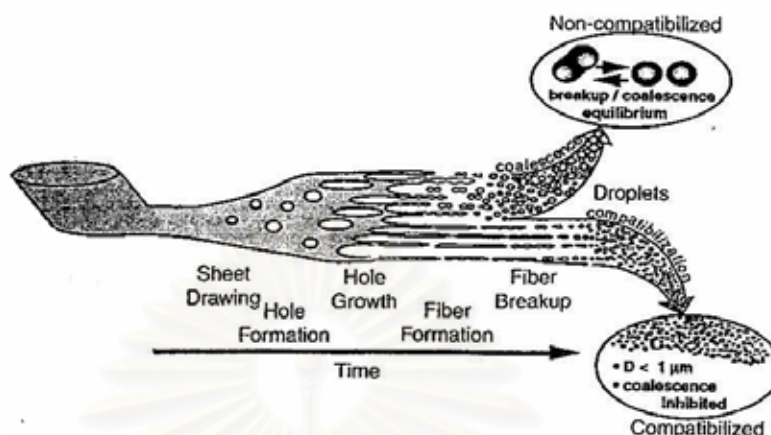
Figure 1.12 Schematic representation of the morphology development in compatibilized and non−compatibilized blends [53].

1.7 Objective and Scope

The chemical modification of natural rubber has been investigated for several years and several works have been carried out. One chemical modification is graft copolymerization. However, grafted natural rubber deteriorates when exposed to sunlight, ozone and oxygen due to the unsaturation of carbon−carbon double bonds in natural rubber backbone. Thus, it is necessary to improve grafted natural rubber to have better chemical resistance properties, so that it might be competitive with synthetic rubbers. This research work will give an overview of two types of modification of NR through a grafting reaction with vinyl monomer and hydrogenation of the grafted natural rubber, respectively. Moreover, the application of modified rubbers was studied with respect to polymer blending. As mentioned above, since numerous graft copolymers have been reported and used as a compatibilizer for polymer blends; the improvement of compatilibilization for thermoplastic/elastomer blends was also studied.

Chapter I provides historic overview of the understanding of natural rubber, graft copolymerization in emulsion stage, hydrogenation of diene−based

polymer and modification of graft copolymer by polymer blending. The experimental information and characterization methods are given in Chapter II. In Chapter III, the experimental method for synthesis the graft copolymer of vinyl monomer onto natural rubber by using cumene hydroperoxide/tetraethylene pentamine as redox initiator is explained. Two vinyl monomers, methyl methacrylate and styrene, were used for the graft copolymerization reaction. The effects of process parameters such as the amount of initiator, monomer to rubber ratio, and reaction temperature on grafting efficiency were investigated.

In Chapters IV and V, the detailed kinetic studies of grafted natural rubber hydrogenation in the presence of $OsHCl(CO)(O_2)(PCy_3)_2$ are discussed. The effects of process variables on the hydrogenation of grafted NR were examined through a statistical analysis and univariate experiments. Univariate experiments were used to study the effect of each parameter on the hydrogenation rate followed by the mechanistic interpretation of each grafted natural rubber hydrogenation based on kinetic data from an automatic gas–uptake apparatus. The hydrogenated rubbers were characterized by FTIR and NMR spectroscopy. Furthermore, the molecular weight and thermal properties (glass transition temperature and degradation temperature) of both grafted natural rubber and hydrogenated grafted natural rubber are presented in Chapter VI. In Chapter VII, the application of hydrogenated grafted natural rubber is explored. The objective of this chapter is to study the compatibility of the hydrogenated MMA-*g*-NR and hydrogenated ST-*g*-NR for improving the compatibility of EPDM/PMMA and EPDM/PS blends. The conclusions and recommendations resulting from this study are summarized in Chapter VIII.

CHAPTER II

EXPERIMENTAL AND CHARACTERIZATION

2.1 Materials

The commercial natural rubber latex (60% dry rubber content) was provided by Thai Rubber Latex Co., Ltd. (Bangkok, Thailand). The overall composition of the natural rubber latex is summarized in Appendix A (Table A−1). Ethylene−propylene rubber (EPDM) of grade Nordel IP 4640 was obtained from Chemical Innovation Co., Ltd. (Bangkok, Thailand). The physical properties of EPDM are summarized in Appendix A (Table A−2). All polymers were used as received. Poly(methyl methacrylate) (PMMA) (M_w ~ 120,000) and polystyrene (M_w ~ 230,000) were purchased from Aldrich Chemical Co. Inc. (Milwaukee, WI, USA). Commercial grade poly(methyl methacrylate) pellets were obtained from Diapolyacrylate Co., Ltd. (Bangkok, Thailand). All information about the polymeric materials is summarized in Appendix A (Table A−3 and Table A−4).

The reagent grade methyl methacrylate monomer (MMA, ~99%) and styrene monomer (ST, ~99%) from Aldrich Chemical Co., Inc. (Milwaukee, WI, USA) were purified by washing with 10% sodium hydroxide solution to remove the inhibitor, followed by deionized water until neutral. The initiator cumene hydroperoxide (CHPO, >88%), tetraethylene pentamine (TEPA) and the emulsifier sodium dodecylsulfate (SDS, ~98%) were obtained from Aldrich Chemical Co., Inc. (Milwaukee, WI, USA) and used as received. Potassium hydroxide and *i*−propanol were obtained from EMD Chemicals Inc. (Darmstadt, Germany) and used as received. Deionized water was used throughout the work.

Reagent grade monochlorobenzene (MCB) was purchased from Fisher Scientific., (Fair Lawn, NJ, USA). 2−Methoxyethanol from Aldrich Chemical Co. Inc. (Milwaukee, WI, USA), toluene, methanol and hexane from EMD Chemicals Inc. (Darmstadt, Germany), tetrahydrofuran from Caledon Laboratories Ltd. (Georgetown,

ON, Canada) were all reagent grade and used as received. 99.99% oxygen–free hydrogen gas for the hydrogenation experiments was supplied by Praxair Inc. (Kitchener, ON, Canada).

$OsHCl(CO)(O_2)(PCy_3)_2$ was prepared according to the procedure outlined in the literature (Esteruelas et al. 1986, 1988). Osmium (III) chloride ($OsCl_3*H_2O$) and tricyclohexylphosphine (PCy_3) were purchased from Strem Chemicals (Newburyport, MA, USA). The *p*–toluenesulfonic acid (*p*–TSA), 3–chloropropionic acid (3–CPA), and succinic acid (SA) were obtained from Aldrich Chemical Co., Inc. (Milwaukee, WI, USA)

2.2 Catalyst Preparation

$OsHCl(CO)(O_2)(PCy_3)_2$ was prepared by refluxing $OsCl_3*H_2O$ (1 g) with tricyclohexylphosphine (5 g) in degassed 2–methoxyethanol (100 mL) in a 500 mL round bottom flask with gas inlet tube under a nitrogen atmosphere for 24 h and then cooled down to room temperature. After cooling, the red–orange crystalline product, $OsHCl(CO)(PCy_3)_2$ was kept under a nitrogen atmosphere until it was dried. $OsHCl(CO)(PCy_3)_2$ was analyzed by NMR spectroscopy and the ^1H and ^{31}P spectra obtained are shown in Figure 2.1: ^1H–NMR (CD_2Cl_2): δ −33.0 (br.), $^{31}P\{^1H\}$–NMR (CD_2Cl_2): δ 37.5 (s). $OsHCl(CO)(O_2)(PCy_3)_2$ was synthesized by exposing a degassed hexane (50 mL) suspension of the species $OsHCl(CO)(PCy_3)_2$ to pure oxygen gas until the white product, $OsHCl(CO)(O_2)(PCy_3)_2$, formed which was then filtered by normal filtration since this osmium complex was air–stable. This oxygen complex was then washed with hexane and dried in vacuum overnight. The NMR and FTIR spectra of the final product are shown in Figure 2.2. (^1H–NMR (CD_2Cl_2): δ −2.99 (t), $^{31}P\{^1H\}$–NMR (CD_2Cl_2): δ 16.63 (s), IR: ν(CO) 1947 cm^{-1}). The spectrum obtained from the ^1H–NMR spectroscopy was showed a triplet, attributed to the metal–hydride peaks at −3.00 ppm, and the peaks for the various cyclohexyl protons of the complex appeared in the region from 2.5 to 0.8 ppm. The integration of the hydride and cyclohexyl protons gave a ratio of approximately 64 to 1 in close accord with the molecular formula.
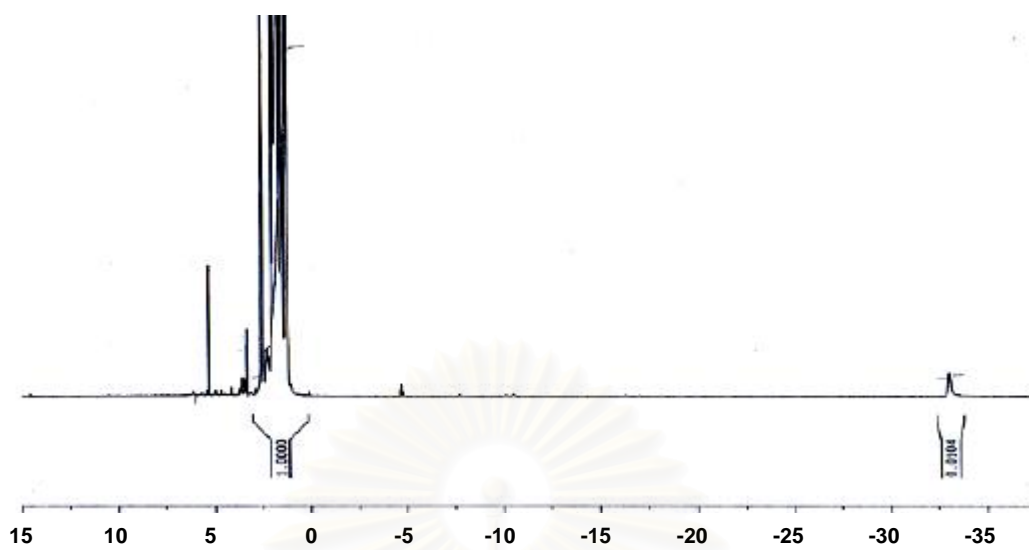
(a) ^{1}H–NMR
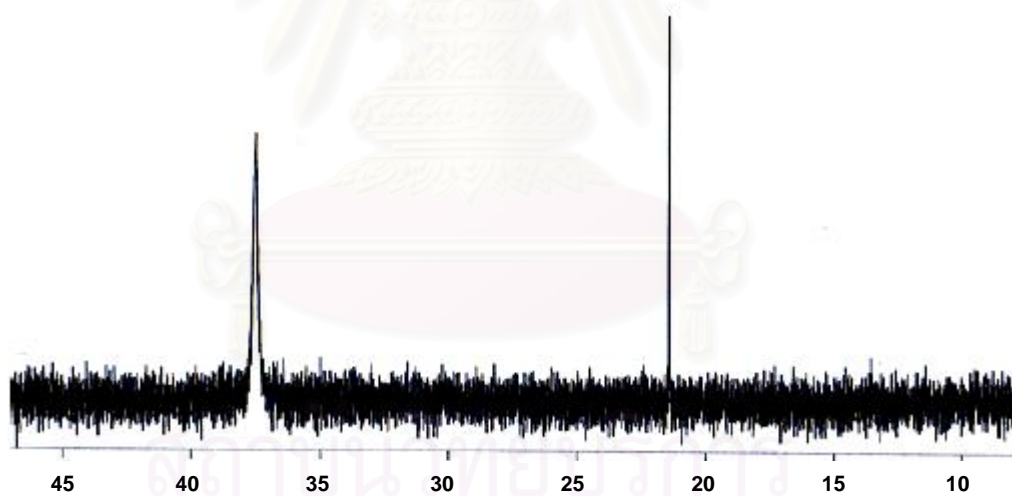
(b) ^{31}P{^{1}H}–NMR

Figure 2.1 ^{1}H–NMR and ^{31}P{^{1}H}–NMR spectra of OsHCl(CO)(PCy$_3$)$_2$.

(a) ^{1}H–NMR

(b) ^{31}P{^{1}H}–NMR

1947.6

(c) FTIR
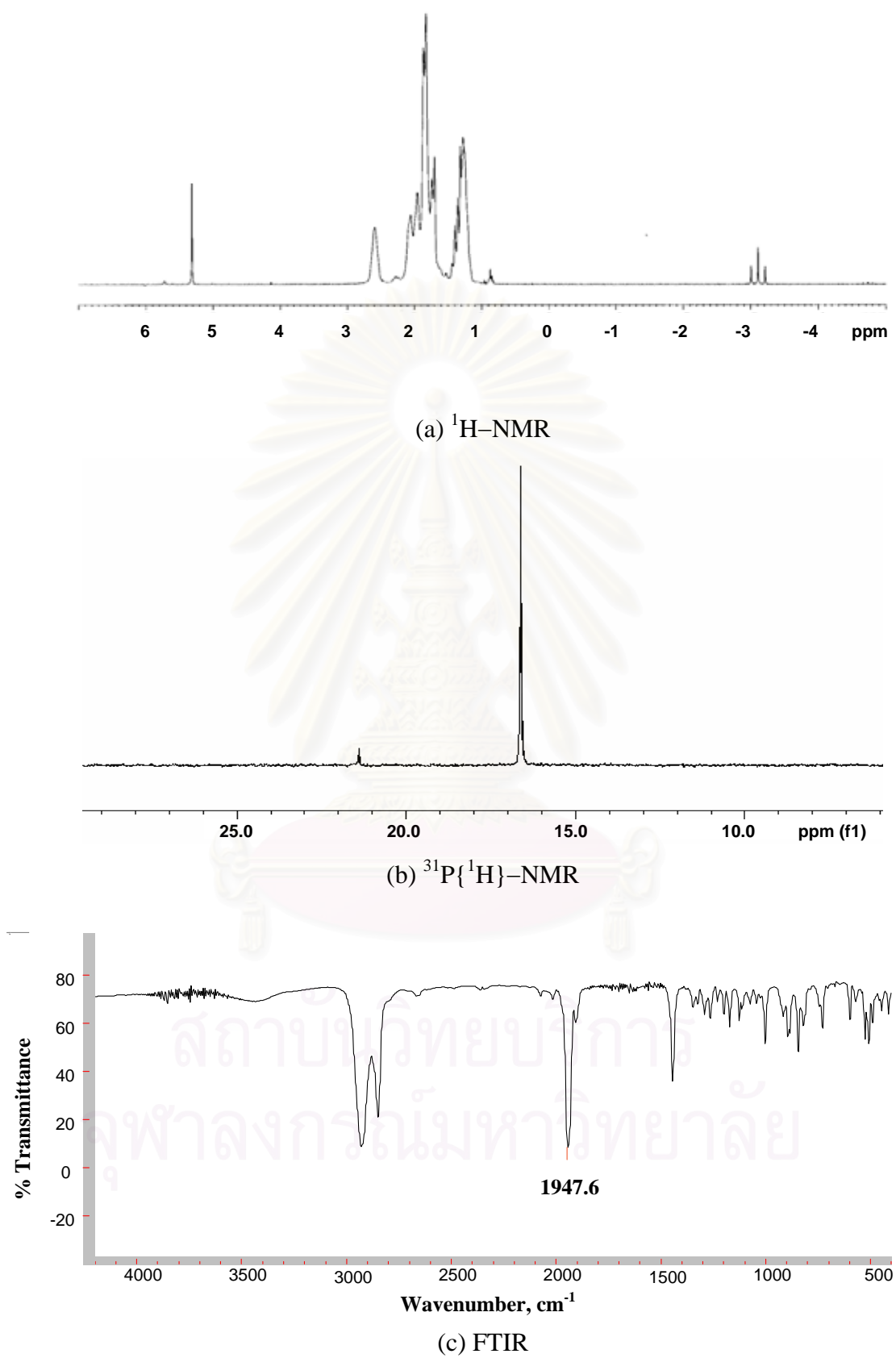
Figure 2.2 ^{1}H–NMR, ^{31}P{^{1}H}–NMR and FTIR spectra of OsHCl(CO)(O$_2$)(PCy$_3$)$_2$.

2.3 Graft Copolymerization of Natural Rubber Latex

The graft copolymerization of natural rubber was carried out in a 500 mL, four−necked round bottom flask, equipped with stirrer, condenser, nitrogen inlet, and thermometer. The NRL (DRC 59.9%) was charged into the flask containing 100 mL deionized water, 10 phr (10 part per 100 part of dry rubber content, by weight) i−propanol as stabilizer, and 1.0 phr SDS as an emulsifier. A potassium hydroxide solution was added to maintain the pH of the latex above 10. Then, the mixture was deoxygenated by purging with nitrogen gas. The 100 phr monomer was fed to the reactor and TEPA was added as an activator agent. The 1.0 phr initiator (CHPO) was then added. The reaction was performed at 50°C for 8 h. The graft copolymer latex was precipitated in 3% v/v of formic acid [18].

The grafted natural rubber was recovered and dried to a constant weight in vacuum. Soxhlet extraction procedures were carried out to assess the amounts of the free NR and graft copolymer in the final product. The free NR was washed out with light petroleum ether (bp. 40 − 60°C) for 24 h. To remove free homopolymer, poly(methyl methacrylate) or polystyrene, the residue was extracted in acetone or methyl ethyl ketone for 24 h, respectively. Weight of both initial samples and the extracted samples were measured for the determination of the graft copolymer and free copolymer contents. The monomer conversion and grafting efficiency were determined by gravimetric calculation. The mole fraction of MMA in the graft NR was also determined from the integrated peak area of the corresponding protons from the ^{1}H−NMR spectra. A typical experimental procedure is shown in Figure 2.3.

The weight difference between the initial sample and the extracted samples is a measure of the grafting properties: the grafting efficiency (GE), free homopolymer, and percentage of free NR were calculated using the following relationships:

$$\text{GE (\%)} \;=\; \frac{\text{Weight of monomers grafted}}{\text{Total weight of monomers polymerized}} \times 100 \qquad (2.1)$$

$$\text{Homopolymer (\%)} = \frac{\text{Weight of free homopolymer}}{\text{Weight of gross polymer}} \times 100 \qquad (2.2)$$

$$\text{Free NR (\%)} = \frac{\text{Weight of free natural rubber}}{\text{Weight of gross polymer}} \times 100 \qquad (2.3)$$

The molar percentage of MMA in the grafted copolymer was also calculated from the integrated peak area of the ^{1}H–NMR spectrum. The peaks at 5.15 ppm are assigned to the olefinic protons content in the NR. The peaks observed at 3.7 ppm are attributed to the methoxy group ($-OCH_3$) of poly(methyl methacrylate) (PMMA). The signals at 6.5 – 7.5 ppm are attributed to the phenyl group of polystyrene (PS). From the different signal areas, the amount of isoprene per proton (S_0), the amount of MMA per proton (S_1) and the amount of styrene per proton (S_2) were calculated using the following equations [54]:

$$\text{MMA (\% mole)} = \left[\frac{S_1/3}{(S_0 + S_1/3)} \right] \times 100 \qquad (2.4)$$

$$\text{ST (\% mole)} = \left[\frac{S_2/5}{(S_0 + S_2/5)} \right] \times 100 \qquad (2.5)$$

where S_0 is the integrated peak area value of the unsaturated olefinic proton, S_1 is integrated peak area value of the methoxy proton of the methyl methacrylate unit, S_2 is integrated peak area value of the styrenic proton of the styrene unit, and MMA or ST is the molar percentage of methyl methacrylate or styrene in the graft copolymer chain.
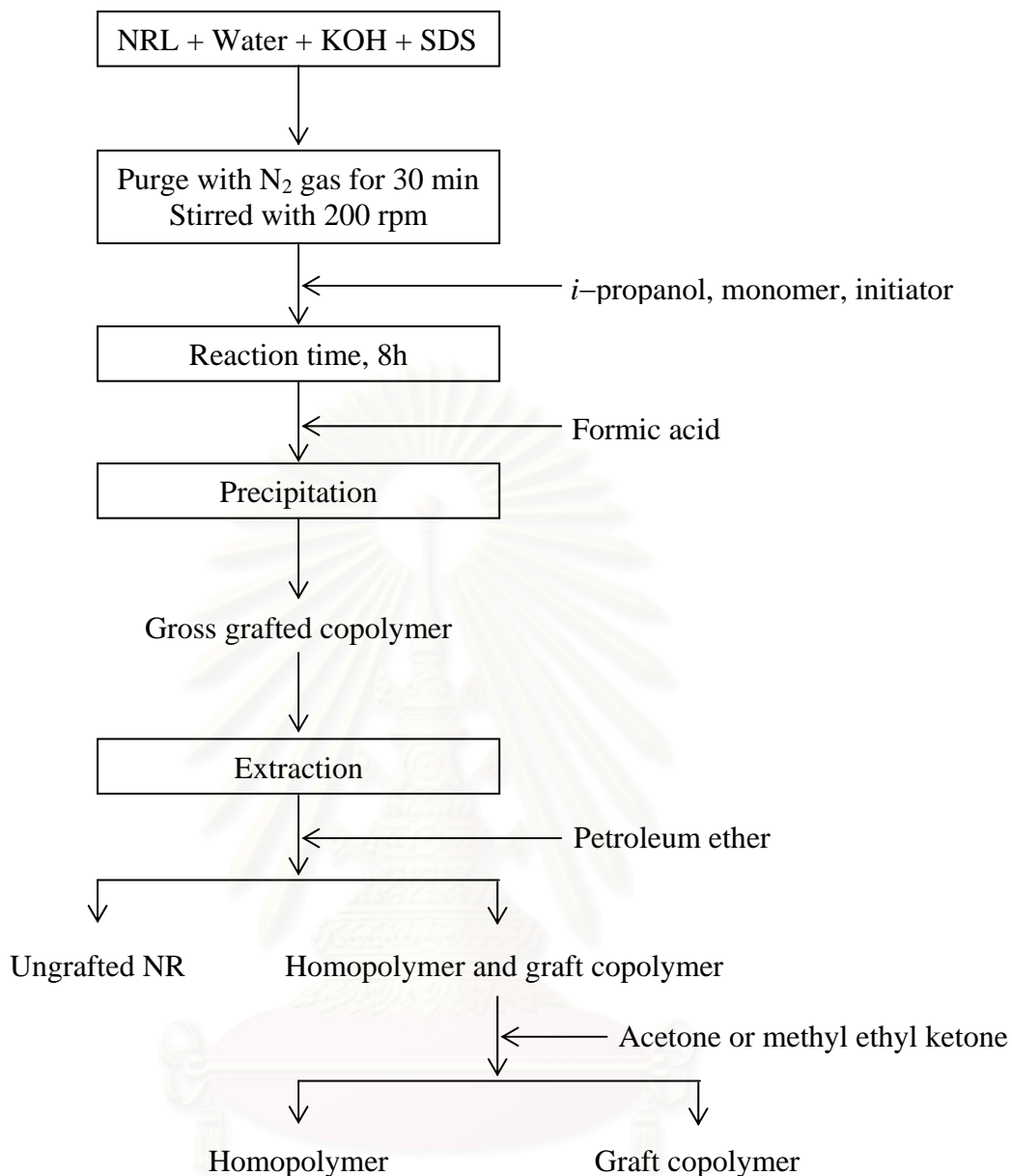
Figure 2.3 The experimental procedure for the grafting reaction.

2.4 Hydrogenation in a Gas−Uptake Apparatus

An automatic gas−uptake apparatus is a reactor facility used to collect experimental kinetic data for the hydrogenation reaction by measuring the amount of hydrogen consumption as a function of time and the reaction temperature of the rubber solution throughout the course of the reaction. The gas−uptake apparatus

utilized in this investigation is a computer controlled batch reactor system that was developed by Mohammadi and Rempel [55]. Reliable kinetics studies for gas consuming catalytic reactions were carried out in the apparatus that was designed to maintain a constant pressure and temperature while monitoring H_2 consumption as a function of real time. Figure 2.4 illustrates the operational schematic of the equipment. A drop in the autoclave pressure relative to the reference bomb RB−1 was detected by the differential pressure transducer (PT−1). This error signal functioned as the input for the control algorithm residing within a personal computer. Via an i/p converter, the PC activated the pneumatic control valve to permit H_2 from the supply cell to recharge the autoclave to the set pressure. This control system maintained the autoclave pressure to less than 0.3 psi below its set point.

PT−2 monitored pressure drop in the supply cell relative to RB−2 and the amount of H_2 consumed during the reaction is an integrated measure of the hydrogenation rate. PT−2 convert the signal to millimoles of H_2 by calibrating its output voltage against the conversion of a known amount of substrate. The technique assumed that a change in pressure was linearly proportional to the H_2 loss from the supply cell. Ideal gas behavior was maintained for H_2 at 1250 psi and 295K.
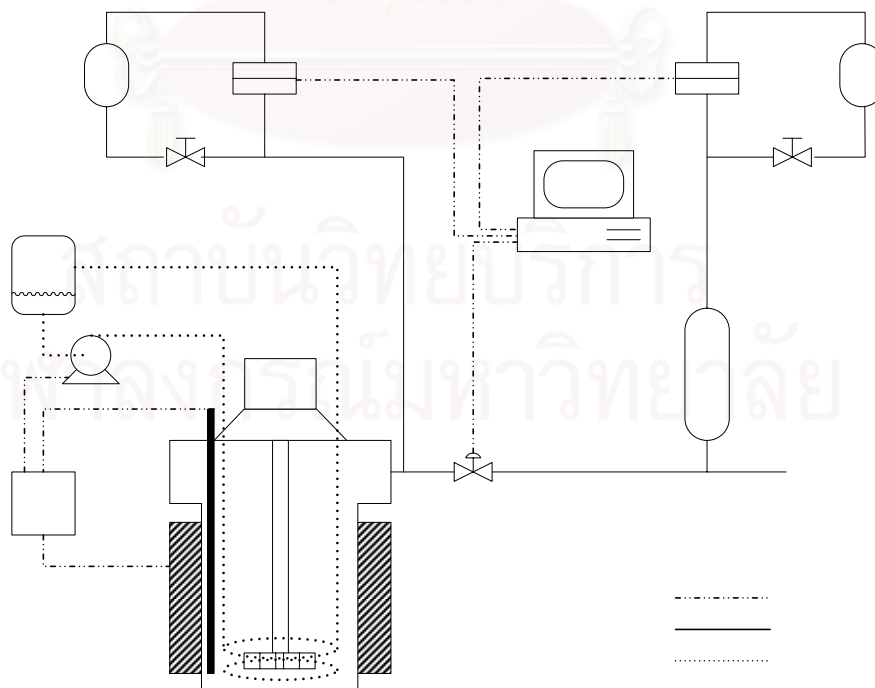
Figure 2.4 Schematic of gas−uptake apparatus.

2.5 Procedure for a Typical of Kinetic Experiment

The kinetic data for the hydrogenation of the graft copolymer in the presence of $OsHCl(CO)(O_2)(PCy_3)_2$ was obtained by measuring the amount of hydrogen consumed as a function of time by using the gas−uptake apparatus. The hydrogenation conditions can be controlled at a constant temperature $\pm 1°C$ and pressure ± 0.02 bar from the target point throughout the reaction. Typically, graft copolymer was prepared by dissolving the desired mass in monochlorobenzene within a 100 mL volumetric flask which was kept in the dark. Then, this rubber mixture was transferred into the autoclave and the flask was rinsed well with 50 mL of monochlorobenzene to provide a total solution volume of 150 mL. The required mass of catalyst was weighed into a small glass bucket and then it was loaded into a catalyst addition chamber on the reactor head. The autoclave, containing the rubber mixture and catalyst bucket, was then assembled.

Due to the sensitivity of the catalyst to air when in solution form, the system was eliminated of air by rigorously purging with hydrogen gas (H_2). Three cycles of charging the reactor with the H_2 at 14 bar and venting were performed without agitation. Then, the agitator was started at 200 rpm and the autoclave was immersed in an ice−water bath until the temperature inside the autoclave dropped to below $10°C$ in order to reduce the vapor pressure of the solvent. Subsequently, the reactor pressure was vented and recharged with H_2 continuously at 14 bar for a ca. 20 min while the agitator speed was changed to 1,200 rpm to ensure that the oxygen in the reactor was completely removed. After that, the ceramic band heater was installed. To achieve the desired reaction conditions, the reactor was pressurized to approximately 80% of the target value of the H_2 pressure and the desired temperature via the temperature controller. The increased in the temperature of the sealed autoclave provided the pressure to reach the set point. Once the system reached the desired conditions, it was allowed a minimum of 45 min to equilibrate.

The H_2 uptake monitoring program employed two user−specified, data logging intervals. The first was of short duration and was designed to monitor the reaction during its initial stages where the reaction rates are the highest. The second

interval was initiated by the operator to avoid the unnecessary collection of data during periods of the slow hydrogenation. Once activated, the program waited one logging interval before starting to record the time, reaction temperature and amount of H_2 consumed. At this point, the reference isolation valves V1 and V2 were closed and the catalyst bucket was dropped. For dispersing the catalyst powder in the rubber solution, the agitator speed was adjusted to 1,200 rpm.

After the reaction of each experiment terminated, the reactor was cooled down to below 50°C using the cooling unit and blowing with air before releasing the pressure of the reactor. Then, the autoclave was disassembled and the hydrogenated product was precipitated with ethanol and dried under vacuum. Then, the residue of the product in the reactor was removed by using toluene. Then, the reactor containing toluene was reassembled and heated at ca. 120°C with 200 rpm of agitation speed. After this rinse, the reactor was blown dry with air before starting the next reaction. The final degree of olefin conversion obtained from gas uptake was confirmed by ^{1}H–NMR spectroscopy.

2.6 Blending of Thermoplastics and Elastomers

The thermoplastic blends were prepared at various ratios of thermoplastics and elastomers by a melt–mixing system. Melt blending of polymers was conducted using an internal mixer, Brabender Plasticoder (HAAKE Polydrive), which had two counter–rotating roller rotors. In this study, the thermoplastics were poly(methyl methacrylate) (PMMA) and polystyrene (PS) and the elastomers were ethylene–propylene rubber (EPDM) and grafted natural rubber (GNR). PMMA/EPDM/GNR and PS/EPDM/GNR were prepared. In all experiments, about 70% of the total available volume was filled with material. The plastic resin was first warmed in the mixing chamber for 3 min without rotation of the rotors. The rubber was incorporated after mixing of the plastic resin for 3 min with a rotor speed of 50 rpm at a mixing temperature of 200°C. The mixing was continued for 7 min after incorporation of the rubber.

2.7 Characterization Methods

2.7.1 Fourier Transform Infrared Spectroscopy Analysis

FTIR spectra were record on Bio–Rad FTS 3000X spectrometer. The samples for FTIR analyses were prepared by dissolving in toluene and casting as thin films on NaCl disks.

2.7.2 Nuclear Magnetic Resonance (NMR) and Degree of Hydrogenation Determination

The monomer content in the grafted product and the final degree of hydrogenation were investigated by NMR spectroscopic analysis. The ^{1}H–NMR, ^{13}C–NMR, and DEPT–135 spectra were obtained by dissolving 0.01g of the rubbers in CDCl$_3$ and recording the spectra using an Advance 300 MHz spectrometer, Bruker.

According to the unsaturation in the grafted natural rubber backbone, the level of hydrogenation was determined by using ^{1}H–NMR spectroscopy. Integration of the spectra was used to determine the amount of characteristic protons of each structure in the grafted natural rubber. For the graft copolymer of methyl methacrylate onto natural rubber and styrene onto natural rubber, the peak area of saturated protons (–CH$_2$– and –CH$_3$) in the range of 0.8 – 2.3 ppm and peak area of unsaturated protons in rubber backbone at 5.2 ppm were measured in order to calculate the degree of hydrogenation using eq. (2.6) and eq. (2.7), respectively.

$$\% \text{ Hydrogenation of MMA-}g\text{-NR} = \left(\frac{A - 5B - 6C}{A - 5B + 3C} \right) \times 100 \qquad (2.6)$$

$$\% \text{ Hydrogenation of ST-}g\text{-NR} = \left(\frac{A - 6B - 2C}{A + 3B - 2C} \right) \times 100 \qquad (2.7)$$

where A is the peak area of saturated protons, B is the peak area of unsaturated protons, and C is the peak area of the functional group proton. An example for the degree of hydrogenation calculation is illustrated in Appendix B.

The data obtained from the automated gas−uptake apparatus consisted of three outputs: reaction time (s), total gas uptake (mmoles), and reaction temperature (°C). The degree of hydrogenation resulting from gas uptake monitoring program was compared with the degree of hydrogenation from [1]H−NMR spectroscopy to confirm the amount of gas uptake.

2.7.3 Gel Permeation Chromatography (GPC)

The molecular weight and molecular weight distribution of grafted NR and hydrogenated grafted NR were obtained using a GPC system which consisted of a Waters 1515 isocratic HPLC pump and Waters 2414 refractive index detector (RID). Breeze software was used for data collection and processing. Three Waters styragel columns (7.8 × 300 mm), HR 3, HR 4, and HR 6, were used for separation at 40°C. HPLC grade tetrahydrofuran (Lab Scan Asia) was used as the mobile phase at a flow rate of 1.0 mL/min. The GPC samples of 0.1% (w/v) rubber solution were filtered through a 0.45 μm pore size filter and then 100 μL of filtered samples were injected into the GPC for analysis. The molecular weights of the samples were obtained from calibration lines using polystyrene standards, having a peak molecular weight (M_p) range of 1.5×10^3 to 6.5×10^6), supplied by Fluka.

2.7.4 Thermogravimetric Analysis (TGA)

Thermogravimetric analysis (TGA) was performed on a Perkin−Elmer Pyris Diamond thermogravimetric/differential thermal analysis instrument. The samples were placed into a platinum pan. The temperature was raised under a nitrogen atmosphere from room temperature to 700°C at a constant heating rate of 10°C/min. The nitrogen gas flow rate was 50 mL/min. The initial decomposition temperature (T_{id}) and the temperature at the maximum of mass−loss rate (T_{max}) were evaluated.

2.7.5 Differential Scanning Calorimetry (DSC)

Differential scanning calorimetry (DSC) of the sample was carried out on a TA Instrument DSC Model 2920. The instrument signal was derived from the temperature difference between the sample and the reference. The sample was cooled to −100°C with liquid nitrogen and then heated to 150°C at a constant rate of 20°C/min. The glass transition temperature (T_g) was calculated from the midpoint of the base−line shift of the DSC thermogram.

2.7.6 Morphological Studies

Morphological studies were carried out using a JEOL scanning electron microscope, model JSM 6400 and operated at a voltage of 15 kV. In order to have sufficient phase contrast in a fractured surface sample before using the microscope, the samples were also subjected to the appropriate chemical treatment during 48 h to selectively dissolve one of the minor phases. Petroleum ether was used to extract EPDM at room temperature. After that, the specimen was coated with gold and the morphology was observed using a scanning electron microscope.

2.7.7 Mechanical Properties

The mechanical properties in terms of tensile strength, impact and hardness of the blended polymer were evaluated. Tensile properties of the blends were determined according to the standard method ASTM D638 using dumbbell shaped specimens, type I. The testing was performed on a Universal Testing Machine (LLOYD Instruments model LR 10K Plus) with a crosshead speed of 50 mm/min. The Charpy impact strength of samples was measured according to the standard testing method ASTM D6110. The impact energy was obtained by the difference of the potential energy of the falling hammer before and after impact. Impact energy per unit breadth of the sample was expressed as the impact strength. The machine used in the present investigation was a Impact Tester (model GOTECH GT−7045). The reported value is the average of five replicates of each property test. The hardness of

the specimens was performed using Rockwell hardness tester 4150 AR following ASTM D785.

The dynamic mechanical properties of the blends were measured on a dynamic mechanical analyzer (NETZSCH DMA 242C) with a liquid nitrogen cooling system. The dual bending mode was used to the temperature range of −75 to +125°C at heating rate of 3°C/min and at a frequency of 1.0 Hz.

CHAPTER III

GRAFT COPOLYMERIZATION OF VINYL MONOMERS ONTO NATURAL RUBBER USING CUMENE HYDROPEROXIDE / TETRAETHYLENE PENTAMINE AS INITIATOR

Graft copolymerization of vinyl monomers onto natural rubber (NR) has been widely studied in recent years. The initiator systems employed include benzoyl peroxide, redox initiator, and radiation systems. Andrews and Turner [56] suggested that the nature of different initiator systems determined primarily the morphological structure of composite NR−based latex particles. The rubber samples used to prepare graft copolymers are solid, solution, or latex phase. Since NR is obtained from *Hevea Brasiliensis* as latex, the most economical way for chemical modification is in latex state. Natural rubber grafted with methyl methacrylate rubber (MG rubber), formed by polymerization of MMA with natural rubber latex (NRL), is a commercially important modified NRL. It has been found useful as a shoe adhesive (trade name: Hevea plus MG).

Most commercial processes for grafting monomers onto NR are based on redox polymerization. The graft copolymerization of MMA onto NR using three different initiator systems has been investigated [20]. The graft copolymerization initiated with cumene hydroperoxide/tetraethylene petamine (CHPO/TEPA) exhibited the highest percentage grafting efficiency when compared with the *t*ert−buthyl hydroperoxide system (TBHPO/TEPA) and the potassium persulfate system ($K_2S_2O_8$). CHPO as the more hydrophobic initiator was more efficient than TBHPO and $K_2S_2O_8$ for grafting a relatively polar monomer onto natural rubber. A redox initiating system consisting of hydroperoxide and TEPA was effectively used for the emulsion polymerization in NR latex because it is not sensitive to oxygen and is effective when ammonia was present.

The purpose of the present work is to study the grafting process of natural rubber with a vinyl monomer such as methyl methacrylate or styrene. The effect of initiator concentration, monomer to rubber ratio and reaction temperature on

the grafting reaction of methyl methacrylate onto natural rubber was studied using two–level factorial design and univariate experiments. The appropriate condition from the univariate experiments was chosen for preparation of the grafted NR.

For the graft copolymerization of styrene onto natural rubber (ST-*g*-NR), the graft copolymerization was carried out under an optimum condition based on a previous literature report [57]. The appropriate grafting condition was as follows: NRL = 50 g, water = 100 mL, [*i*–propanol] = 5.0 phr, [KOH] = 0.5 phr, [SDS] = 1.5 phr, [CHPO] = 1.0 phr, M/R = 1.0 at 50°C for 8 h. The synthesized MMA-*g*-NR and ST-*g*-NR could be hydrogenated in the presence of $OsHCl(CO)(O_2)(PCy_3)_2$ and the results will be presented in Chapter IV and V.

3.1 Experimental Design of Grafting Reaction Univariate Experiments

A 2^3 factorial design experiment was applied to study the main effects and interaction effects of process variables on the grafting efficiency. The low level, coded as (−), and the high level, coded as (+), were defined for each independent variable. Yates's algorithm was applied to calculate the main effects and joint effects on the grafting efficiency derived from the experimental data. Gravimetric calculation was used to determine the grafting efficiency, monomer conversion, and the composition of the gross polymers, such as free rubber, free homopolymer, and graft copolymer. Table 3.1 shows the overall factorial design experimental data. The grafting efficiency ranges from 13.3 to 51.6%, graft copolymers from 5.3 to 62.8%, free copolymers from 14.5 to 29.7%, and free rubber from 11.1 to 69.7%, depending on the process conditions, which will be subsequently discussed in detail.

The Yate's algorithm calculation and the results of the factorial design analysis are shown in Tables 3.2 and 3.3. The results indicated that initiator concentration ([INT]) and T showed a negative influence on the grafting efficiency, whereas monomer to rubber ratio (M/R) exhibited a positive result. This implies that the grafting efficiency increased with an increase in M/R. In contrast, the grafting efficiency decreased with an increase in [INT] and T. The two–factor interactions,

[INT]×M/R, [INT]×T, and M/R×T, and the three−factor interaction, [INT]×M/R×T were not highly significant.

Table 3.1   Results from 2^3 Factorial Design for Graft Copolymerization of Methyl Methacrylate onto Natural Rubber

Experiment	[INT] (phr)	M/R	T (^{o}C)	GE (%)
1	1.0	0.6	50	41.1
2	1.0	0.6	50	43.4
3	2.0	0.6	50	38.7
4	2.0	0.6	50	39.4
5	1.0	1.0	50	51.6
6	1.0	1.0	50	49.0
7	2.0	1.0	50	42.3
8	2.0	1.0	50	43.6
9	1.0	0.6	60	39.1
10	1.0	0.6	60	39.2
11	2.0	0.6	60	35.2
12	2.0	0.6	60	32.6
13	1.0	1.0	60	51.2
14	1.0	1.0	60	47.5
15	2.0	1.0	60	37.9
16	2.0	1.0	60	39.5

Condition: Emulsifier concentration = 1.0 phr and stabilizer concentration = 10 phr

Table 3.2 Yate's Algorithm Calculation of the 2^3 Factorial Experiment

Test	Design Matrix Variables [INT]	M/R	T	GE (%)	(1)	(2)	(3)	Divisor	Estimate	Identification
1	-	-	-	42.24	81.28	174.55	335.65	8	41.96	Average
2	+	-	-	39.03	93.28	161.10	-26.44	4	-6.61	[INT]
3	-	+	-	50.30	73.07	-10.54	26.95	4	6.74	M/R
4	+	+	-	42.97	88.03	-15.90	-9.57	4	-2.39	[INT]×M/R
5	-	-	+	39.15	-3.21	12.00	-13.45	4	-3.36	T
6	+	-	+	33.93	-7.33	14.95	-5.37	4	-1.34	[INT] ×T
7	-	+	+	49.35	-5.22	-4.12	2.96	4	0.74	M/R×T
8	+	+	+	38.67	-10.68	-5.46	-1.34	4	-0.34	[INT] ×M/R×T

[INT] = (-) 1.0 or (+) 2.0 phr; M/R = 0.6 or (+) 1.0; T = (-) 50 or (+) 60°C.

TABLE 3.3   Calculations of Effects and Standard Errors for the 2^3 Factorial Design Experiment

Effect	Estimate	± Standard Error
Average	41.96	± 0.38
Main Effects		
Initiator Concentration, [INT]	-6.61	± 0.75
Monomer to Rubber Ratio, M/R	6.74	± 0.75
Reaction Temperature, T	-3.36	± 0.75
Two-Factor Interaction		
[INT]×M/R	-2.39	± 0.75
[INT]×T	-1.34	± 0.75
M/R×T	0.74	± 0.75
Three-Factor Interaction		
[INT]×M/R×T	-0.34	± 0.75

3.2 Univariate Experiments

Three process parameters, initiator concentrations ([INT]), monomer to rubber ratio (M/R) and reaction temperature (T) were studied in the range of 1.0 to 2.0 phr, 0.6 to 1.0 and 40 to 60°C, respectively. Stabilizer concentration of 10 phr, emulsifier concentration ([SDS]) of 1.0 phr, and CHPO/TEPA ratio of 1.0 were kept constant. The statistical analysis described above provides only information on the significant factors on the grafting reaction. In order to determine how each variables affects the graft copolymerization reaction, the univariate experiments were used to determine their influence on the grafting efficiency. The effect of process parameters on the total conversion, the content of the components of the gross polymer such as free natural rubber, free poly(methyl methacrylate) and grafted natural rubber were investigated. By gravimetric calculation, it was found that the free NR ranges from 11 − 67%, free PMMA from 17 − 30%, grafted NR from 6.5 − 62%, MMA conversion from 26 − 92% and grafting efficiency from 16 − 50% as shown in Table 3.4.

Integration peak areas from ^{1}H−NMR spectroscopy were also used to investigate the mole fraction of MMA in the grafted NR. Table 3.4 also presents the amount of grafted MMA on the NR backbone. The MMA content ranges from 5 − 28 mole % depending on the process parameters. The purification of the graft product by Soxhlet extraction technique could cause degradation of the graft sample, possible additional crosslinking reactions and the possibility of extraction of some polymers grafted onto the NR backbone together with non−grafted molecules. ^{1}H−NMR spectroscopy is a useful method to access the extent of grafting of the copolymers on to the NR backbone. Eventhough the level of grafting MMA was not so high, the results led to a good understanding of the relative mole composition of components in the graft copolymer. The values of the integrated peak areas from such spectra indicate a strong dependence on the amount of monomer present in the graft samples.

Table 3.4 Effect of Process Variables on Grafting Efficiency

Expt.	[INT] (phr)	M/R	T (°C)	Conv. (%)	Free NR (%)	Free PMMA (%)	Graft NR (%)	GE (%)	Grafting MMA[1] (% mol)
1	0.5	1.0	50	40.1	68.6	24.9	6.5	16.4	5.7
2	1.0	1.0	50	78.1	23.7	23.6	52.7	47.9	24.4
3	1.5	1.0	50	86.6	24.9	27.1	48.0	43.2	21.0
4	2.0	1.0	50	92.1	24.2	28.1	47.7	43.0	20.8
5	1.0	0.6	50	84.0	20.2	20.1	59.7	42.2	19.6
6	1.0	0.8	50	86.6	30.5	23.9	45.5	43.3	20.6
7	1.0	1.0	50	85.3	23.7	23.6	52.7	50.3	28.9
8	1.0	1.2	50	87.5	11.1	29.7	59.2	43.5	20.0
9	1.0	1.0	40	26.7	44.2	17.8	38.0	19.6	9.2
10	1.0	1.0	50	85.3	23.7	23.6	52.7	50.3	28.9
11	1.0	1.0	60	50.6	12.9	25.0	62.1	28.2	14.6

[1]Grafting MMA on natural rubber backbone calculated from ^{1}H–NMR results.

3.2.1 Dependence on Initiator Concentration

The effect of the initiator concentration on conversion and grafting efficiency was studied over the range of 0.5 to 2.0 phr for which the M/R ratio (1.0), emulsifier concentration (1.0 phr), stabilizer concentration (10 phr), reaction temperature (50°C), and reaction time (8 h) were kept constant. The results of these experiments are shown in Figure 3.1. The monomer conversion and grafting efficiency increased with an increase of the initiator concentration. From Figure 3.1, the increasing initiator concentrations up to 1.0 phr are accompanied by a significant increase in grafting efficiency. Beyond this concentration, the grafting efficiency decreased markedly. With initiator concentrations of more than 1.0 phr, the excessive radicals react with each other, leading to a faster rate of termination or primary termination. Up to this point, the grafting efficiency does not increase at all.
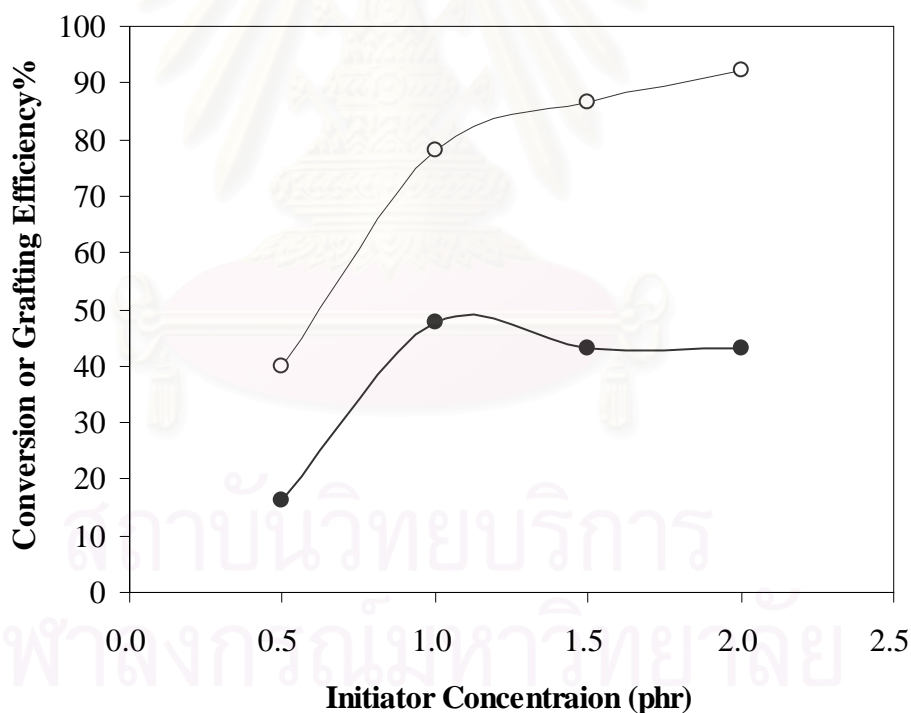
Figure 3.1   Effect of the initiator concentration on percentage conversion (○) and grafting efficiency (●).

3.2.2 Dependence on Monomer−to−Rubber Ratio

The effects of the monomer to rubber ratio (M/R) on the conversion and percentage grafting efficiency were investigated. Experiments were performed at a M/R ratio of 0.6 to 1.2 when the initiator concentration of 1.0 phr, SDS concentration of 1.0 phr, *i*−propanol of 10 phr, and reaction temperature of 50°C, and reaction time of 8 h were kept constant. The conversion increased with an increase in monomer concentration as shown in Figure 3.2. As the monomer concentration increases, the grafting efficiency increased and reached a maximum at a monomer concentration of 100 phr, and thereafter, it decreased. At higher M/R, many reactions probably compete with the grafting reaction. This means that homopolymerization is more pronounced than the graft copolymerization at higher M/R. Therefore, the grafting system with high M/R ratio has a lower surface area at the reaction site, and the rate of homopolymerization determination is more favored than the polymeric radicals transfer rate to NR, thus accounting for reduced grafting efficiency with an increase in the monomer−to−rubber ratio. Similar results were observed by Kochthongrasamee et al. [20], Thiraphattaraphun et al. [51], and Oliveiria et al. [54].
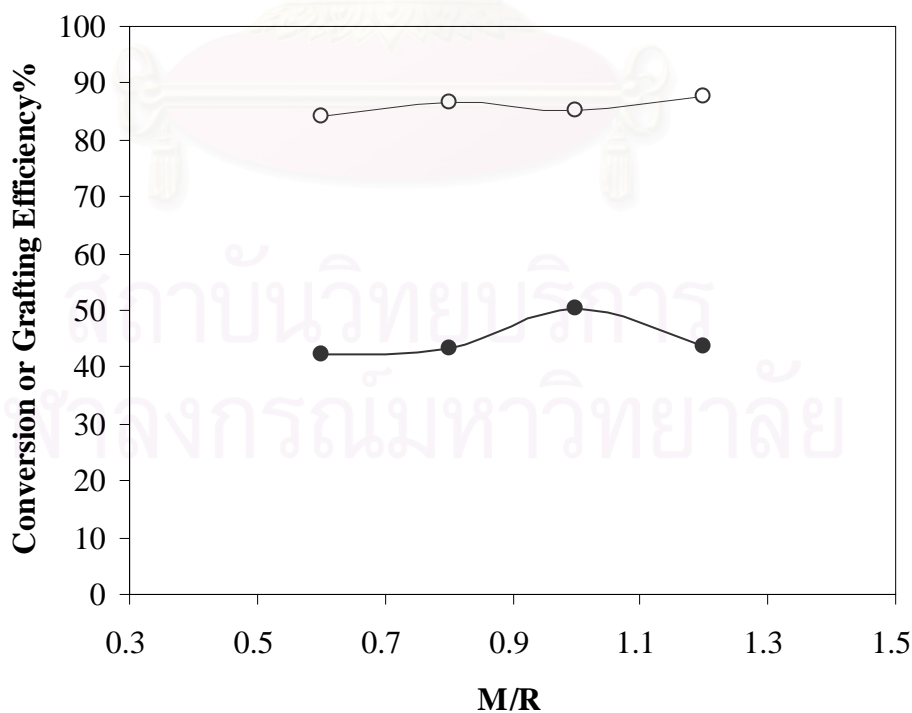
Figure 3.2 Effect of the monomer to rubber ratio on percentage conversion (○) and grafting efficiency (●).

3.2.3 Dependence on Reaction Temperature

The effect of reaction temperature on the graft copolymerization was investigated. The conditions for the graft copolymerization were as follows: M/R ratio of 1.0, initiator concentration of 1.0 phr, reaction temperature of $40 - 60°C$ and a reaction time of 8 h. Over the temperature range of $40 - 50°C$, the polymerization temperature had a positive effect on grafting efficiency and monomer conversion. At a polymerization temperature above 50°C, the grafting efficiency decreased with an increase in reaction temperature. It was believed that the decomposition of the initiator (CHPO) increased with increasing reaction temperature; it caused an increase in both the number of free radicals and the rate of polymerization. The free radicals underwent either recombination or other side reactions such as chain transfer reactions; the initiator efficiency for grafting was thus reduced at higher temperature.
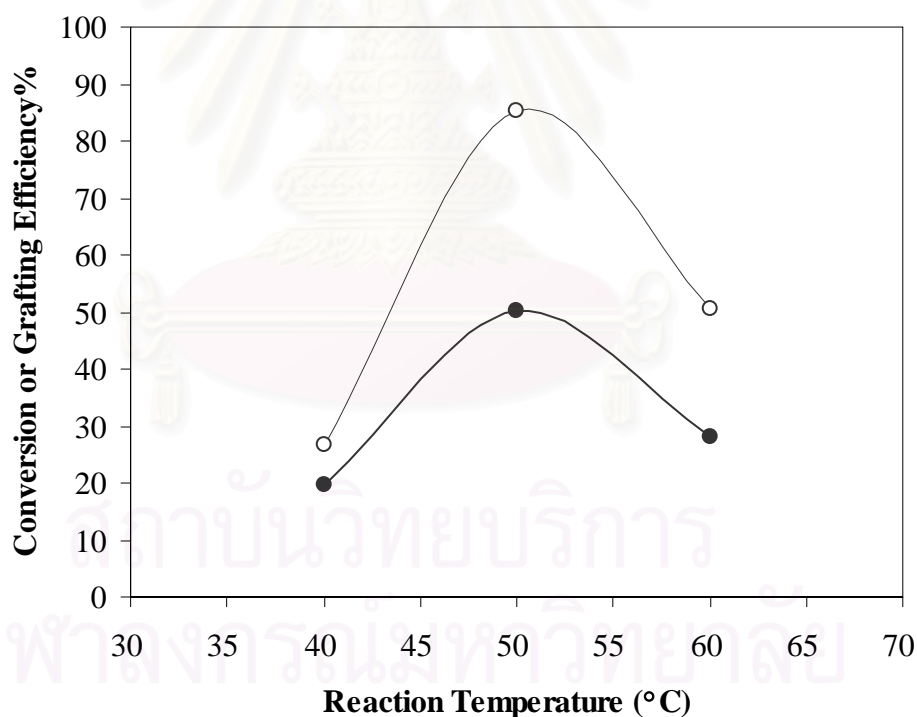
Figure 3.3   Effect of reaction temperature on percentage conversion (○) and grafting efficiency (●).

From univariate experiments of graft copolymerization of MMA onto NR, the appropriate condition, selected to prepare the graft NR for hydrogenation, is shown as follows: monomer concentration, 100 phr; initiator concentration, 1.0 phr; SDS concentration, 1.0 phr; i–propanol, 10 phr; reaction temperature, 50°C; and reaction time, 8 h.

3.3 Graft Copolymer Characterization

3.3.1 Fourier Transform Infrared Spectroscopy

The grafted NR sample prepared for characterization was carried out under a monomer–to–rubber ratio of 1.0, initiator concentration of 1.0 phr, SDS concentration of 1.0 phr, i–propanol concentration of 10 phr and a reaction temperature of 50°C. The graft copolymer consisted of 52.7% of graft NR, 23.7% free NR, and 23.6% free PMMA. Figure 3.4 shows a comparison of FTIR spectra of natural rubber, MMA-g-NR and ST-g-NR.

FTIR spectrum of NR is illustrated in Figure 3.4(a). The characteristic FTIR spectrum of NR can be attributed to C=C stretching (1,664 cm^{-1}) and olefinic C–H bending (836 cm^{-1}). For the impurities (proteins) in NR, the weak transmittance bands at 3,285 cm^{-1} and 1,530 cm^{-1} which are characteristic vibration of >N–H and >N–C=O [58] remained after the graft copolymerization reaction. FTIR spectrum of graft copolymer of MMA onto NR after Soxhlet extraction is shown in Figure 3.4(b). There are several characteristic peaks attributed to R$_2$C=CHR stretching of NR (1,664 cm^{-1}), C–H bending of NR (836 cm^{-1}), C=O (1,732 cm^{-1}) and C–O stretching of ester groups of poly(methyl methacrylate) (1,140 cm^{-1}).

The styrene-g-natural rubber (ST-g-NR) spectrum showed two intense bands at 760 and 698 cm^{-1}, which are characteristic of monosubstituted benzene rings, as shown in Figure 3.4(c). Moreover, the spectrum also displays a peak at 1,664 cm^{-1} corresponding to a C=C stretching vibration and the peaks above 3,000 cm^{-1} are characteristic of a hydrogen bonded to a sp^2–hybridized carbon. This implies that polystyrene was grafted onto natural rubber backbone.
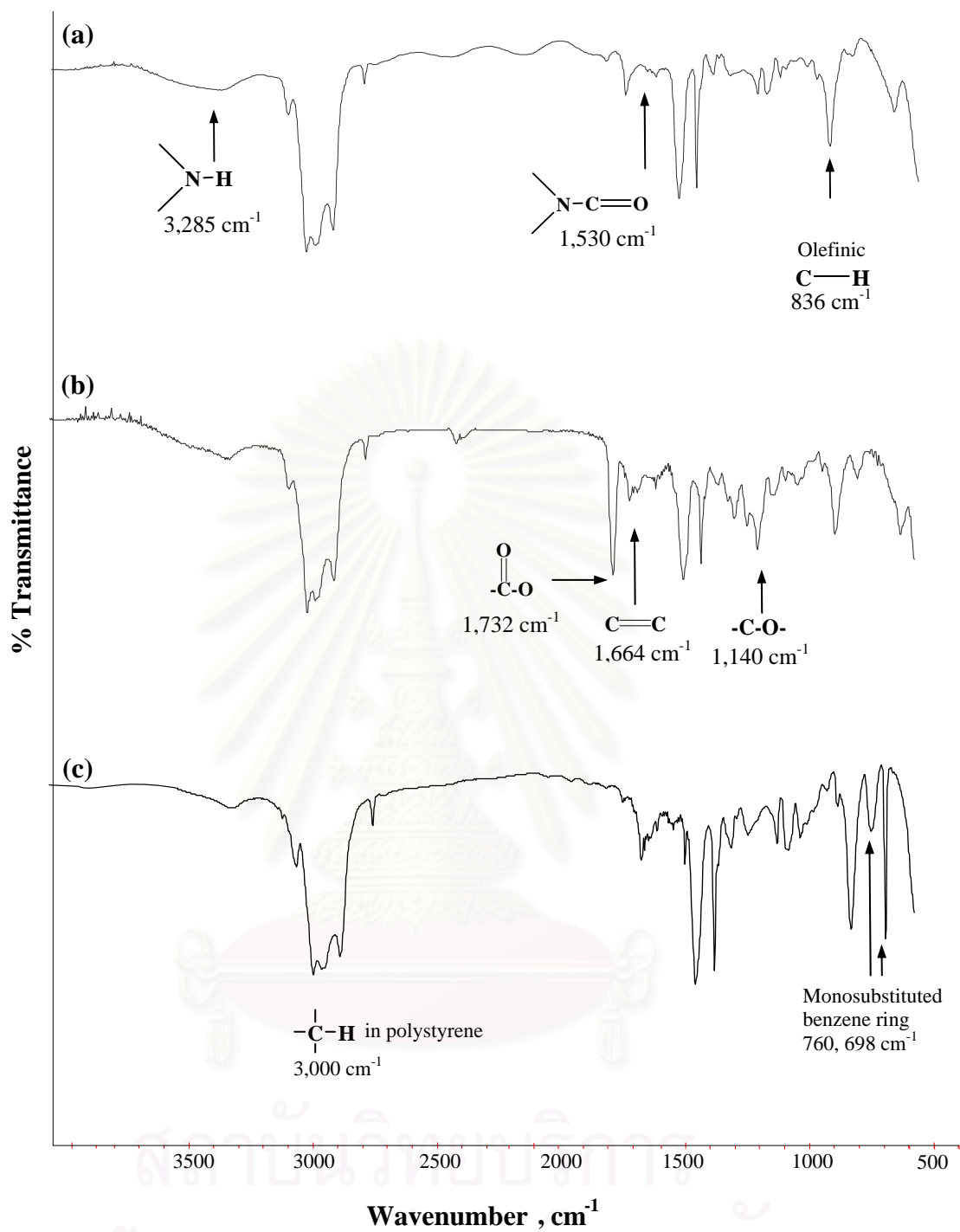
Figure 3.4 FTIR spectra of (a) Natural rubber latex, (b) MMA-*g*-NR, and (c) ST-*g*-NR.

3.3.2 Proton NMR (^{1}H–NMR)

^{1}H–NMR spectroscopy was used to investigate the MMA amount (mole%) in modified NRL. For MMA-*g*-NR, the graft copolymerization was carried out under [MMA] = 100 phr, [CHPO/TEPA] = 1.0 phr, [SDS] = 1.0 phr, [*i*–propanol] = 10 phr at a reaction temperature of 50°C for 8 h. The determination of grafted PMMA as a mole percentage was calculated by using the integration of the related peak area from NMR spectra as described in eq. (2.6). The sample for NMR characterization was purified by Soxhlet extraction to remove free NR and free polymer, respectively. By gravimetric calculation, the grafted NR consisted of 23.7% free NR, 23.6% free PMMA, and 57.2% grafted NR. The MMA conversion and grafting efficiency were 85.3% and 50.3%, respectively. A comparison of ^{1}H–NMR spectra of NR and MMA-*g*-NR is shown in Figure 3.5.

The ^{1}H–NMR spectra of NR is illustrated in Figure 3.5(a). The unsaturated olefinic proton in NR shows singlet resonance signal at 5.15 ppm. The signal at 2.10 ppm may be attributed to the methylene protons ($-CH_2-$) and the singlet resonance signal of methyl protons ($-CH_3$) appears at 1.70 ppm. The ^{1}H–NMR of MMA-*g*-NR is shown in Figure 3.5(b). The methoxy protons ($-OCH_3$) resonance of the PMMA unit appears at 3.57 ppm. These ^{1}H–NMR spectra confirm that the modified NRL contained grafted PMMA. The degree of grafting could be calculated from the peak area at 3.57 ppm and the peak area at 5.15 ppm. By NMR calculations, the mole percentage of grafting MMA in the copolymer was 28.9%.

For ST-*g*-NR, the grafted product consisted of 22 ± 2% ungrafted NR, 8 ± 2% free polystyrene, 67 ± 2% grafted NR with a grafting efficiency of 55 ± 2%. ^{1}H–NMR spectrum of ST-*g*-NR is illustrated in Figure 3.5(c). ^{1}H–NMR of grafted NR are attributed to $-CH_3$ (1.64 ppm), $-CH_2-$ (2.01 ppm), –aromatic (6.5 − 8.5 ppm), $-C=CH_2$ (5.15 ppm), and the signal of aliphatic protons of the alkane (0.9 − 1.8 ppm). From calculation, the grafted NR contained 26 ± 1 mole% of ST.
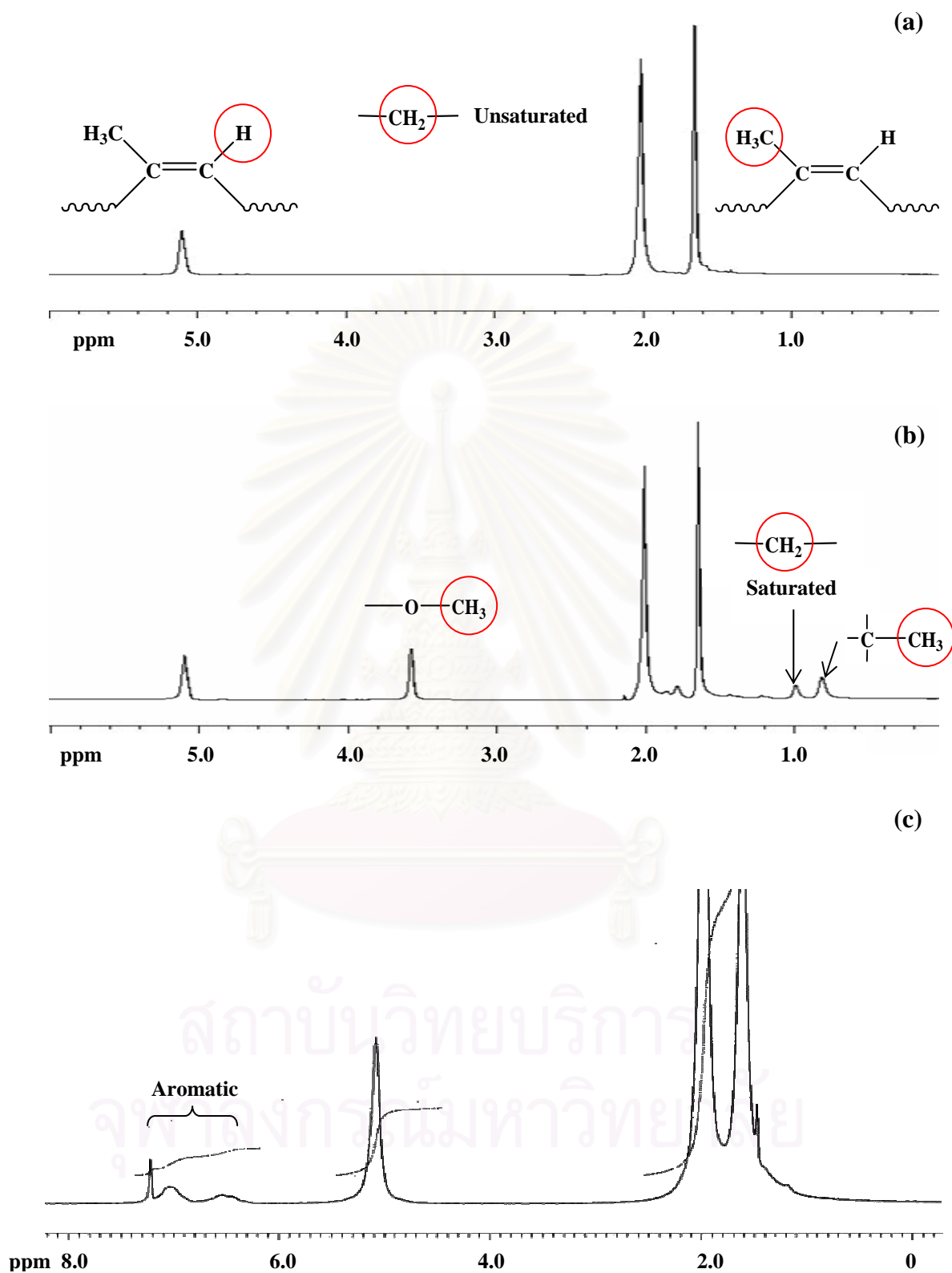
Figure 3.5 ^{1}H–NMR spectra of (a) Natural rubber and (b) MMA-*g*-NR, and (c) ST-*g*-NR.

3.3.3 Carbon NMR (^{13}C–NMR) and Distortionless Enhancement of Polarization Transfer (DEPT)

Figures 3.6 – 3.8 shows the ^{13}C–NMR spectra of NR before and after grafting with a vinyl monomer and the identification of carbon in the polymer structure. For natural rubber, the peaks at 135.3 and 125.1 ppm are related to unsaturated olefinic carbons in the NR structure as shown in Figure 3.6. For MMA-*g*-NR, the ^{13}C–NMR spectrum shows the signal of C=O and −O−CH$_3$ of the PMMA group at 177.0 − 178.0 ppm and 51.8 ppm, respectively, as shown in Figure 3.7. For ST-*g*-NR, the signals for aromatic group appeared at 127.8 ppm as shown in Figure 3.8. These results are related to the distortionless enhancement of polarization transfer (DEPT−135) which −CH and −CH$_3$ carbon appear as positive peaks, −CH$_2$− carbons as negative peaks and carbons without any attached hydrogen are nulled [59].
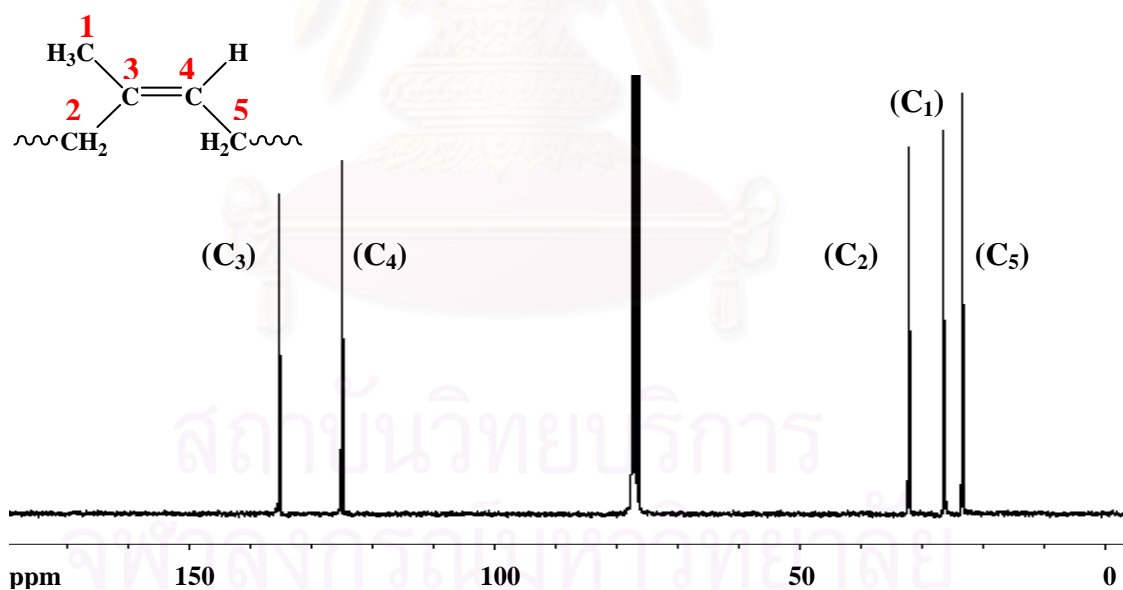
Figure 3.6 ^{13}C–NMR spectra of natural rubber.
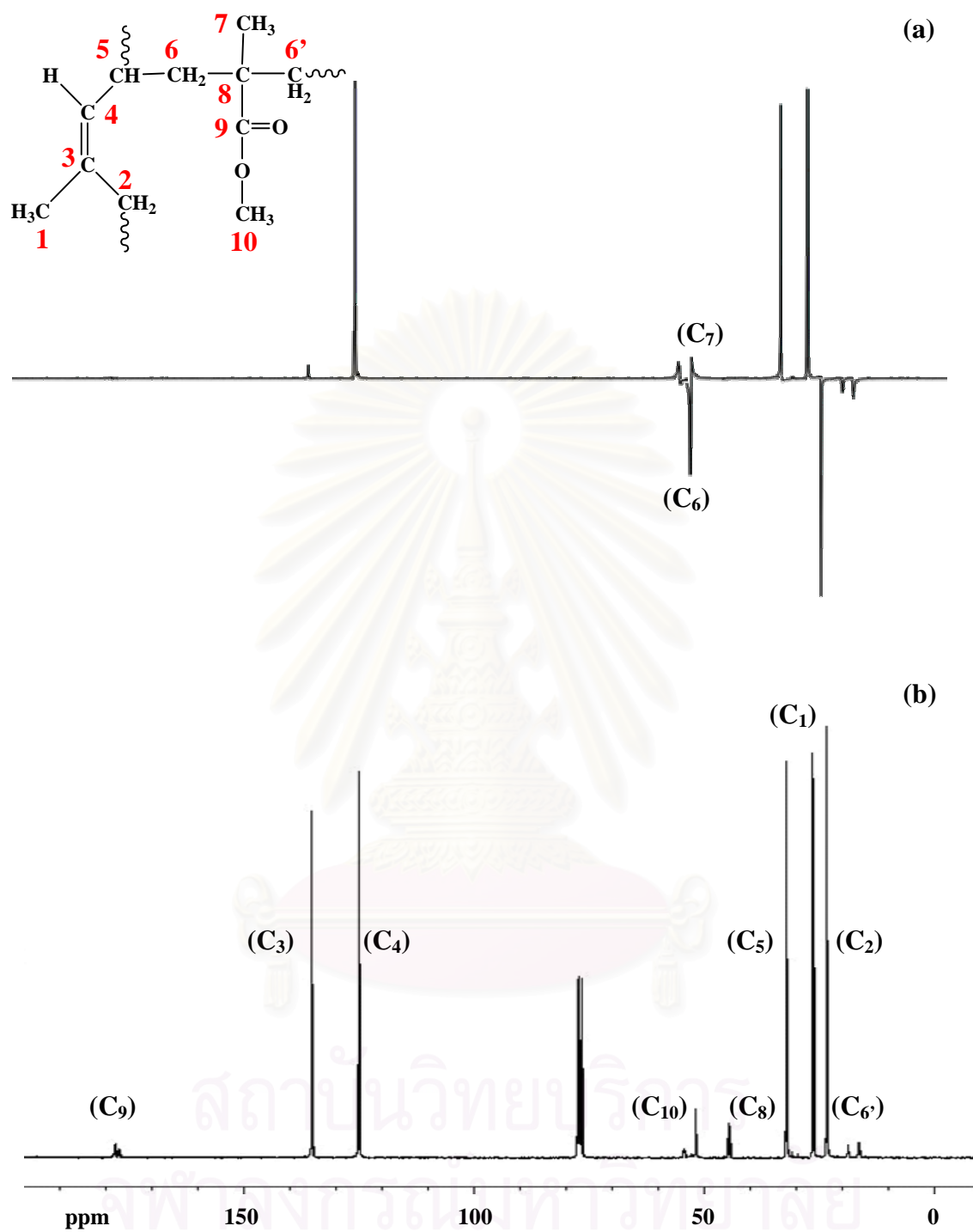
Figure 3.7 NMR spectra of MMA-*g*-NR. (a) DEPT−135 and (b) ^{13}C−NMR.
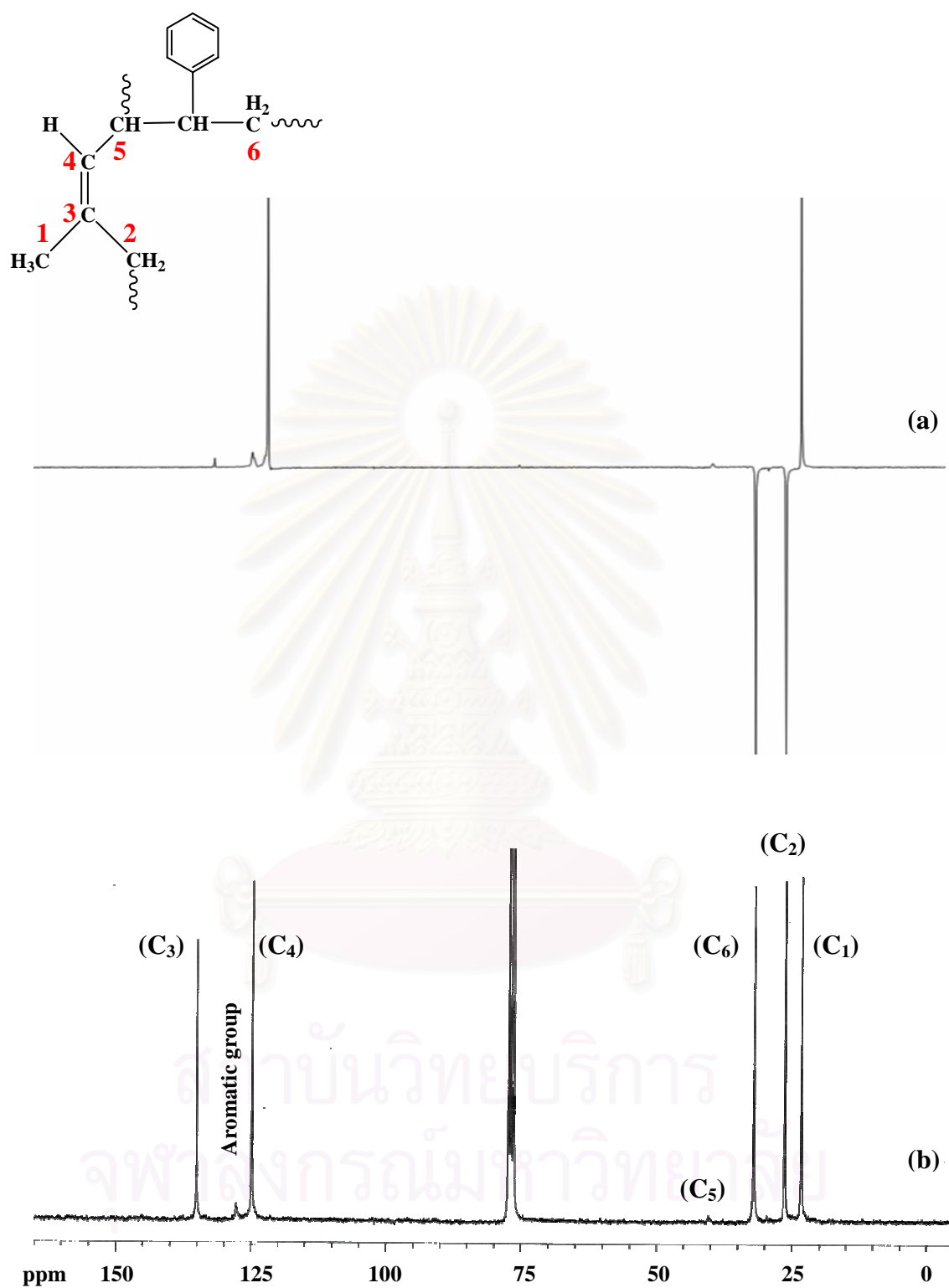
Figure 3.8 NMR spectra of ST-*g*-NR. (a) DEPT−135 and (b) ^{13}C–NMR.

CHAPTER IV

HYDROGENATION OF MMA-*g*-NATURAL RUBBER
IN THE PRESENCE OF OsHCl(CO)(O$_2$)(PCy$_3$)$_2$

One of the most important polymeric materials is natural rubber (NR) because of its outstanding flexibility, excellent heat build up properties and high mechanical strength. The unsaturated backbone in natural rubber allows various types of chemical modification to be carried out, to yield a wide range of rubber products found in today's market. Several reports have recently appeared on the subject of grafting vinyl monomers onto natural rubber. However, the disadvantage of these materials is their poor aging behavior, which is caused by the oxidation of the residual double bond within NR, resulting in deterioration of the polymer properties. Li et al. [60] investigated the thermooxidative degradation of MMA-*g*-NR. The thermooxidative degradation of the graft copolymer and the oxidative reaction of residual carbon increased with increased temperatures. Hydrogenation is a potentially useful method for improving and changing the unsaturated polymer properties toward greater stability against thermal, oxidative, and radiation−induced degradation [61, 62].

The hydrogenation of diene−based polymers and copolymers has been extensively studied during the past two decades [7]. Hydrogenation of polymers can be achieved using either non−catalytic or catalytic methods. The main method used in non−catalytic hydrogenation involves diimide reduction, however, side reactions such as chain scission, cyclization, crosslinking, and gel formation, which is very undesirable, were found to occur [9, 40]. Catalytic hydrogenation can be achieved with either heterogeneous or homogeneous catalyst systems. However, the homogeneous catalysts are more favorable than heterogeneous catalysts because of their higher selectivity and absence of microscopic diffusion problems. Moreover, the role of the homogeneous catalyst can be explained and understood at the molecular level [36]. Mahittikul et al. [23] reported natural rubber latex (NRL) hydrogenation using a homogeneous catalytic systems. It was found that OsHCl(CO(O$_2$)(PCy$_3$)$_2$ is a

much more efficient catalyst than [Ir(COD)py(PCy$_3$)]PF$_6$, Ru[CH=CH(Ph)]Cl(CO)(PCy$_3$)$_2$, and RhCl(PPh$_3$)$_3$ catalysts. The addition of a controlled amount of p−TSA demonstrated a beneficial effect on the hydrogenation rate, and 95% hydrogenation was achieved in 3 h at 150°C under P$_{H2}$ 27.6 bar. The presence of the sulfonic acid helped to prevent poisoning of the osmium catalyst by impurities present in the emulsion system. OsHCl(CO(O$_2$)(PCy$_3$)$_2$ has also been employed as an effective catalyst for the hydrogenation of acrylonitrile−butadiene copolymers (NBR) [21] and cis−1,4−polyisoprene (CPIP) [33] with up to 99% hydrogenation being attained. However, there are no reports on the hydrogenation of grafted copolymers. This modified NR can be use as compatibilizer which facilitates formation of uniform blends of normally immiscible polymers with desirable end properties.

The objective of the present work is to investigate the efficiency of the reaction involved in the quantitative hydrogenation of a graft copolymer of MMA onto NR (MMA-g-NR) in the presence of the soluble OsHCl(CO(O$_2$)(PCy$_3$)$_2$ catalyst. The effects of process variables on the hydrogenation of grafted NR were examined through a statistical analysis and univariate experiments. The effect of catalyst concentration, rubber concentration based on C=C concentration, hydrogen pressure, p−toluenesulfonic acid concentration, and reaction temperature were studied. The mechanistic aspects of these catalytic processes are discussed based on the kinetic results observed.

4.1 Preliminary Study of MMA-g-NR Hydrogenation

Using Soxhlet extraction, it was found that the grafted product consisted of 24.8% free NR, 22.7% free PMMA, and 52.5% grafted NR. The MMA conversion and grafting efficiency were 83.2% and 51.6%, respectively. From [1]H−NMR calculations, the grafted NR contains 26 − 27 mole% of MMA. The purified graft NR (MMA-g-NR) was used for MMA-g-NR hydrogenation.

A preliminary study of catalytic hydrogenation of MMA-g-NR was performed using various types of catalyst, acid, and solvent. The effects of catalyst

type are presented in Table 4.1. Ru[CH=CH(Ph)]Cl(CO)(PCy$_3$)$_2$, RhCl(PPh$_3$)$_3$, and OsHCl(CO)(O$_2$)(PCy$_3$)$_2$ were found to be active catalyst for hydrogenation of grafted natural rubber at 140°C in monochlorobenzene with acid addition. However, OsHCl(O$_2$)(PCy$_3$)$_2$ was the most efficient catalyst for MMA-*g*-NR hydrogenation. It was earlier reported for the hydrogenation of *cis*−1,4−polyisoprene [33] and natural rubber latex [23], the osmium complex was much more effective than ruthenium and rhodium complex system since the osmium complex has bulky, strong σ−donor and weak π−acceptor phosphine ligands, PCy$_3$. It exhibited high catalytic activity due to the ease of dissociation of a ligand from an 18−electron complex to produce a 16−electron species. However, the hydrogenation of NR is much more difficult because of the non−rubber components present in NR. In an effort to increase the catalyst activity for the hydrogenation reaction, the effect of acid addition on the reaction rate has been explored and will be discussed as a subsequent topic.

Table 4.1 Effect of Catalyst Types on % Hydrogenation of Grafted NR

Catalyst type	% Hydrogenation at 4 min
Ru[CH=CH(Ph)]Cl(CO)(PCy$_3$)$_2$	27.7
RhCl(PPh$_3$)$_3$	27.9
OsHCl(CO)(O$_2$)(PCy$_3$)$_2$	84.4

Condition: [Catalyst] = 100 μM, [C=C] = 150 mM, [*p*−TSA] = 2.0 mM, P_{H_2} = 27.6 bar, and T = 140°C in monochlorobenzene.

The acid and solvent play an important role in enhancing the hydrogenation rate. Three different acids and solvents were investigated for MMA-*g*-NR hydrogenation at 100 μM catalyst concentration, 100 mM rubber concentration, 2.0 mM acid concentration, 27.6 bar hydrogen pressure and a reaction temperature of 140°C. The results are presented in Table 4.2. It was found that *p*−TSA was an efficient acid promoter for MMA-*g*-NR hydrogenation in the presence of OsHCl(CO)(O$_2$)(PCy$_3$)$_2$. It can be noted that the strong acid increased the

hydrogenation rate more than the weaker acids. Sulfonic acid is more acidic than the other selected carboxylic acids. In addition, p−TSA is non−coordinating with respect to the osmium complex.

For the solvent type effect, the reaction rate increased with increasing coordinating power of the solvents in the following order: tetrahydrofuran (THF) > monochlorobenzene (MCB) > toluene. The higher the polarity of the solvent, the higher the solubility of MMA-g-NR. On the other hand, the polymer chain only swelled in the low polarity solvents. For a high polarity solvent, the polymer chain was well dissolved and it could also be easily reacted with the catalyst in solution. Thus, more polar solvents provided a higher rate of MMA-g-NR hydrogenation.

Table 4.2 Effect of Acid and Solvent Types on % Hydrogenation of Grafted NR

Acid Type	Solvent Type	% Hydrogenation
3-Chloropropionic acid	MCB	24.7 (in 4 min)
Succinic Acid	MCB	2.85 (in 10 min)
p−TSA	MCB	85.0 (in 4 min)
p−TSA	Toluene	66.8 (in 4 min)
p−TSA	THF	99.7 (in 4 min)

Condition: [Catalyst] = 100 μM, [C=C] = 100 mM, [Acid] = 2.0 mM, P_{H2} = 27.6 bar, and T = 140°C.

4.2 Kinetic Experimental Design for MMA-g-NR Hydrogenation in the presence of OsHCl(CO)(O$_2$)(PCy$_3$)$_2$

A detailed kinetic study of the hydrogenation of MMA-g-NR in the presence of OsHCl(CO)(O$_2$)(PCy$_3$)$_2$ has been conducted in an attempt to gain a better understanding of the catalytic reaction mechanism. A typical hydrogen consumption versus reaction time profile is shown in Figure 4.1. The conversion profile plot

exhibits an apparent first–order dependence on the olefinic substrate concentration, according to eq. (4.1), where k' is a pseudo first–order rate constant.

$$\frac{-d[H_2]}{dt} = \frac{-d[C=C]}{dt} = k'[C=C] \qquad (4.1)$$

Equation (4.1) can further be expressed in terms of olefin conversion according to eq. (4.2)

$$\ln(1-x) = -k't \qquad (4.2)$$

where t is the reaction time and x is the olefin conversion. Although the plots of $\ln(1-x)$ versus reaction time deviate from linearity in the later stages of the reaction, k' can still be calculated with a fair degree of confidence.
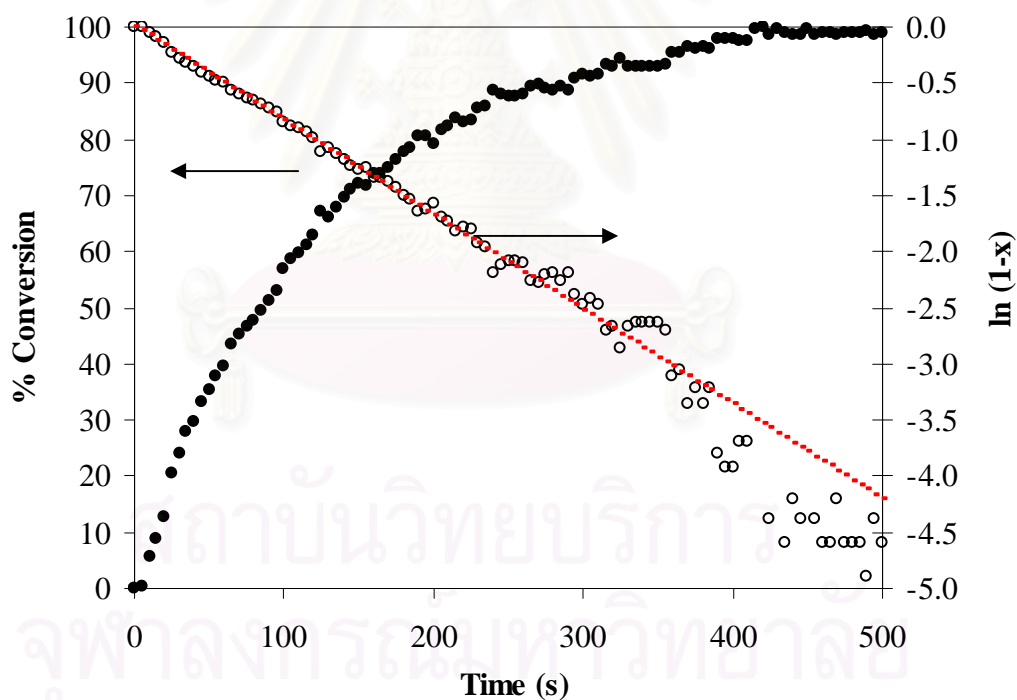
Figure 4.1   Hydrogen consumption profile for hydrogenation of MMA-*g*-NR obtained from gas–uptake apparatus: (●) Olefin conversion profiles and (○) First–order $\ln(1-x)$ vs time plot (---- Linear regression model). [Os] = 100 μM; [C=C] = 100 mM; [*p*–TSA] = 2.0 mM; P_{H2} = 27.2 bar and T = 140°C in monochlorobenzene.

For the preliminary study of the hydrogenation of MMA-*g*-NR, the main effects and the interaction effects of reaction parameters were investigated using statistical analysis [63]. The levels of the reaction parameters were arbitrarily called low level (−) and high level (+). Yates's algorithm was applied to calculate the main effects and interaction effects on the rate of hydrogenation of grafted NR derived from the hydrogen consumption experimental data.

Three principle factors, which are considered to have an effect on the hydrogenation rate of MMA-*g*-NR, are catalyst concentration ([Os]), hydrogen pressure (P_{H_2}), and acid concentration ([*p*−TSA]). The range of catalyst concentration, hydrogen pressure, and acid concentration were 100 to 145 μM, 20.4 to 40.8 bar, and 0 to 2.0 mM, respectively. The reaction was performed in monochlorobenzene at a constant reaction temperature of 140°C. The results of the factorial design experiments are presented in Table 4.3. Yate's algorithm calculation in Tables 4.4 and 4.5 indicated that [Os], P_{H_2}, [*p*−TSA], and the interaction between [Os] and [*p*−TSA] had a positive effect and strong influence on the hydrogenation rate, whereas the effect of other interactions were moderate for the system. This implies that the rate of hydrogenation increased with an increase in [Os], P_{H_2}, and [*p*−TSA]. The other binary interactions, [Os]× P_{H_2} and P_{H_2} ×[*p*−TSA], and three−factor interaction, [Os] × P_{H_2} ×[*p*−TSA], were not highly significant.

Table 4.3   Results from 2^3 Factorial Design for Hydrogenation of MMA-*g*-NR.

Expt.	[Os] (μM)	P_{H_2} (bar)	[*p*–TSA] (mM)	T (°C)	Rate Constant k' x (10^3 ; s^{-1})
1	100	20.4	0	140	0.10
2	100	20.4	0	140	0.16
3	145	20.4	0	140	0.52
4	145	20.4	0	140	0.65
5	100	40.8	0	140	1.60
6	100	40.8	0	140	1.78
7	145	40.8	0	140	2.80
8	145	40.8	0	140	2.90
9	100	20.4	2.0	140	6.24
10	100	20.4	2.0	140	6.37
11	145	20.4	2.0	140	11.62
12	145	20.4	2.0	140	11.85
13	100	40.8	2.0	140	8.50
14	100	40.8	2.0	140	8.32
15	145	40.8	2.0	140	17.53
16	145	40.8	2.0	140	17.32

T = 140^oC in monochlorobenzene.

Table 4.4   Yates's Algorithm Calculation of the 2^3 Factorial Experiments for Hydrogenation of MMA-*g*-NR.

No.	Design Matrix Variables			Algorithm						Identification
	[Os]	P_{H2}	[*p*-TSA]	Ave. k' (s^{-1})	(1)	(2)	(3)	Divisor	Estimate	
1	-	-	-	0.00013	0.00072	0.00526	0.04913	8	0.00614	Average
2	+	-	-	0.00059	0.00454	0.04388	0.01606	4	0.00402	[Os]
3	-	+	-	0.00169	0.01804	0.00162	0.01162	4	0.00291	P_{H2}
4	+	+	-	0.00285	0.02584	0.01445	0.00429	4	0.00107	[Os] × P_{H2}
5	-	-	+	0.00631	0.00046	0.00383	0.03862	4	0.00966	[*p*-TSA]
6	+	-	+	0.01174	0.00116	0.00780	0.01283	4	0.00321	[Os] × [*p*-TSA]
7	-	+	+	0.00841	0.00543	0.00071	0.00397	4	0.00099	P_{H2} × [*p*-TSA]
8	+	+	+	0.01743	0.00902	0.00359	0.00288	4	0.00072	[Os] × P_{H2} × [*p*-TSA]

Table 4.5 Calculated Effects and Standard Errors for the 2^3 Factorial Experiments for Hydrogenation of MMA-*g*-NR.

Effect	Estimate	± Standard Error
Average	0.00614	± 2.86E-05
Main Effects		
Catalyst Concentration, [Os]	0.00402	± 5.72E-05
Hydrogen Pressure, P_{H_2}	0.00291	± 5.72E-05
Acid Concentration, [*p*–TSA]	0.00966	± 5.72E-05
Two-Factor Interaction		
[Os] × P_{H_2}	0.00107	± 5.72E-05
[Os] × [*p*–TSA]	0.00321	± 5.72E-05
P_{H_2} × [*p*–TSA]	0.00099	± 5.72E-05
Three-Factor Interaction		
[Os] × P_{H_2} × [*p*–TSA]	0.00072	± 5.72E-05

4.3 Univariate Kinetic Experiments of MMA-*g*-NR Hydrogenation

Although the results of the factorial experimental design are unable to explore a wide region in the factor space, they can indicate major trends and help to determine a direction for further experiments. The factorial design is generally used for the experiments involving several factors to study only the main effect and interaction effects of factors. Thus, the univariate components augment the factorial design study by exploring how each variable influences the hydrogenation rate in isolation. The univariate experimental data are presented in Tables 4.6.

Table 4.6 Univariate of Kinetic Data of MMA-*g*-NR Hydrogenation Catalyzed by OsHCI(CO)(O$_2$)(PCy$_3$)$_2$.

Expt.	[Os] (μM)	[C=C] (mM)	P_{H_2} (bar)	Temp (°C)	[*p*−TSA] (mM)	k' x 10^3 (s^{-1})	% Hydrogenation (in 10 min)
1	30	100	20.4	140	2.0	1.48	14.3
2	50	100	20.4	140	2.0	3.66	71.8
3	100	100	20.4	140	2.0	6.31	97.5
4	145	100	20.4	140	2.0	11.7	98.0
5	30	100	27.2	140	2.0	3.26	70.1
6	50	100	27.2	140	2.0	6.07	89.3
7	100	100	27.2	140	2.0	8.61	84.3
8	145	100	27.2	140	2.0	13.4	99.7 (in 2.4 min)
9	100	100	6.8	140	2.0	4.76	89.2
10	100	100	10.2	140	2.0	6.86	93.7
11	100	100	20.4	140	2.0	7.78	97.5
12	100	100	27.2	140	2.0	8.43	94.5 (in 6.9 min)
13	100	100	40.8	140	2.0	8.41	99.9 (in 7.0 min)
14	100	100	54.4	140	2.0	8.67	95.3 (in 7.0 min)
15	100	100	68.0	140	2.0	8.78	99.2 (in 3.6 min)
16	100	100	27.2	140	0	3.23	67.1
17	100	100	27.2	140	1.0	7.87	98.5
18	100	100	27.2	140	2.0	8.80	97.7 (6.7 min)
19	100	100	27.2	140	3.5	7.45	84.9
20	100	100	27.2	140	7.0	5.25	63.4
21	100	100	27.2	120	2.0	2.5	56.45
22	100	100	27.2	130	2.0	4.4	90.79
23	100	100	27.2	140	2.0	11.6	94.2 (in 7.6 min)
24	100	100	27.2	150	2.0	13.2	98.8 (in 5.0 min)
25	100	50	27.2	140	2.0	11.8	97.1
26	100	100	27.2	140	2.0	7.67	94.8
27	100	150	27.2	140	2.0	3.70	84.1
28	100	200	27.2	140	2.0	2.82	81.3
29	100	250	27.2	140	2.0	1.93	55.4

4.3.1 Dependence on Acid Concentration

Mahittikul et al. [23] established that a strong acid enhanced the hydrogenation rate of NRL because it likely reacts with the impurities in NRL more than a weak acid. p–toluenesulfonic acid [p–TSA] is the most effective acid for increasing the hydrogenation rate of NRL in the presence of $OsHCl(CO(O_2)(PCy_3)_2$. In this investigation, the effect of acid concentration was carried out over the range of 0 to 7.0 mM. The other reaction conditions remained constant at a catalyst concentration of 100 μM, initial rubber concentration of 100 mM, and hydrogen pressure of 27.2 bar at 140°C in monochlorobenzene. It was found that p–TSA promoted the hydrogenation rate of grafted NR. From Figure 4.2, the rate of hydrogenation was increased with increasing acid concentration from 0 to 2.0 mM, at which it leveled off and then diminished at acid concentrations above 2.0 mM. At a high level of acid concentration, the hydrogenated grafted MMA-g-NR is forming a cyclized structure which has been confirmed by the ^{1}H–NMR and ^{13}C–NMR spectra (Figure 4.3).
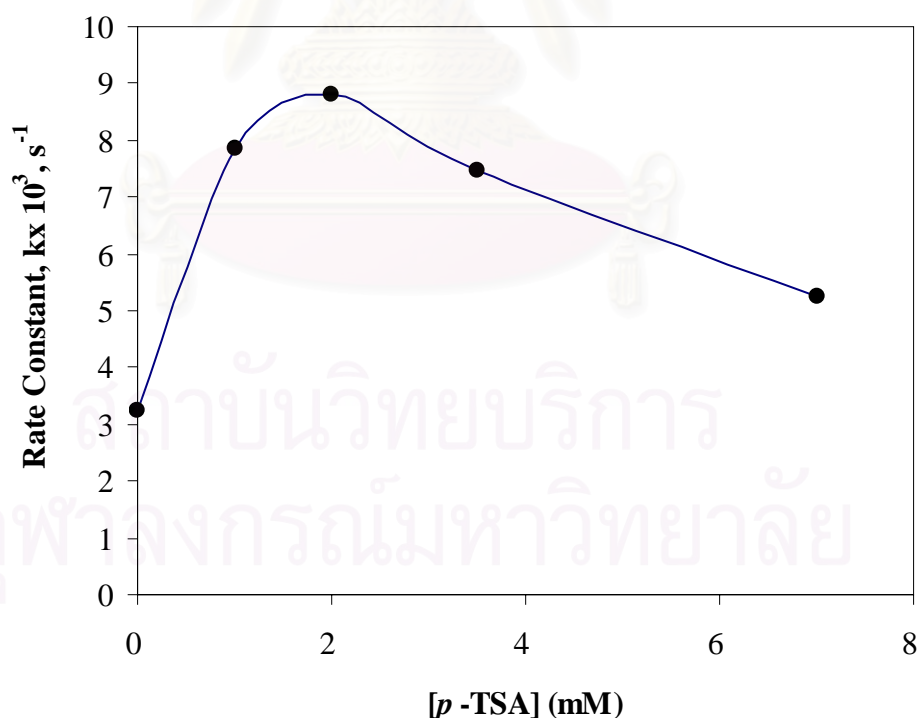
Figure 4.2   Effect of acid concentration on the rate of hydrogenation of MMA-g-NR. [Os] = 100 μM; [C=C] = 100 mM; P_{H_2} = 27.2 bar; T = 140°C in monochlorobenzene.

The cyclization of carbon–carbon double bonds in NR occurred according to a Markownikoff addition [64]. Once formed, the carbonium ion attacks the adjacent olefinic carbons which leads to the cyclic structure after deprotonation as shown in Figure 4.4. The addition of a small amount of acid demonstrated a beneficial effect on the hydrogenation of grafted NR under certain conditions. Therefore, the p–TSA concentration was kept constant at 2.0 mM for the further studies.
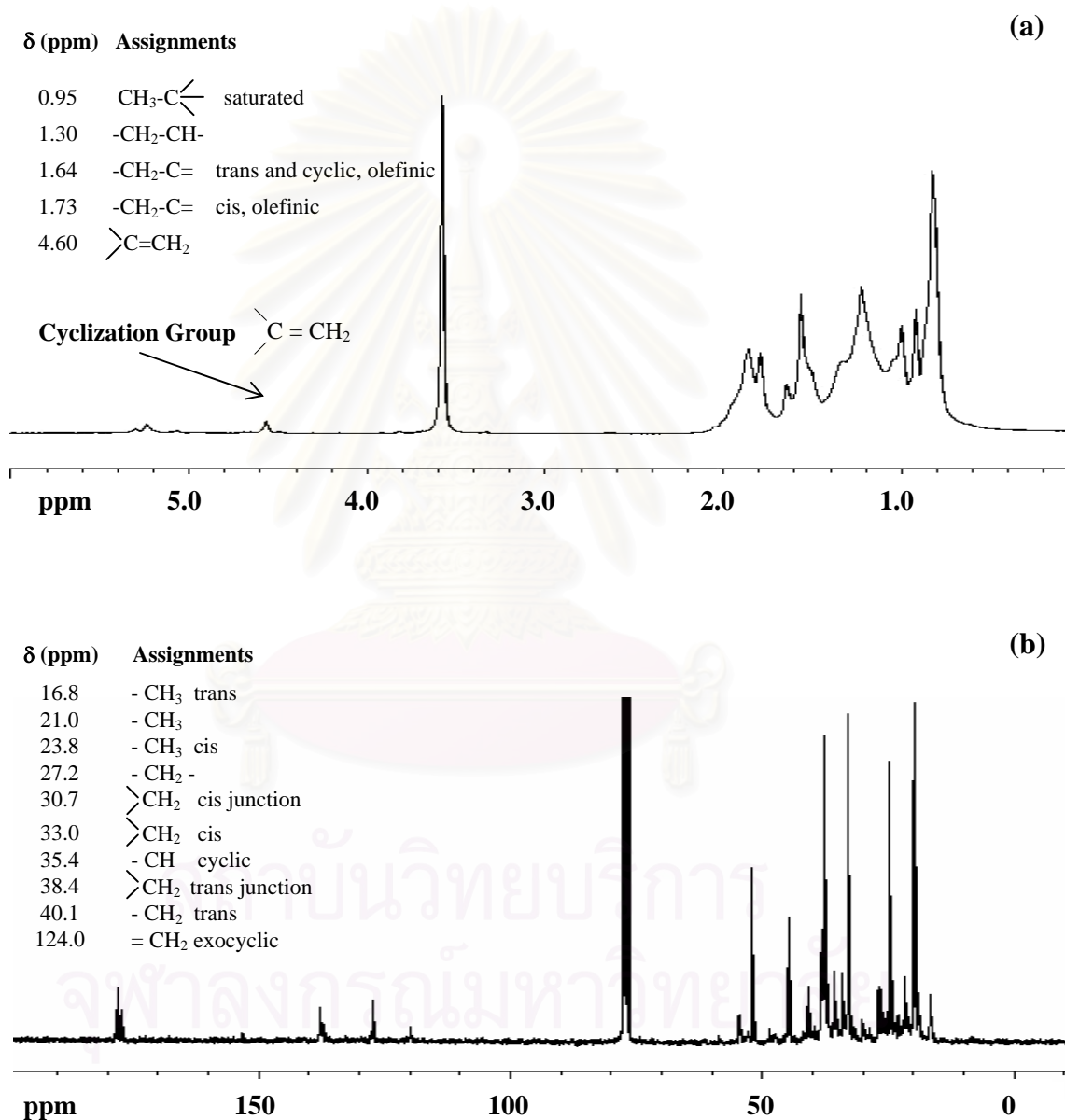
Figure 4.3   NMR spectra of cyclized hydrogenated MMA-*g*-NR. (a) ^{1}H–NMR and (b) ^{13}C–NMR.
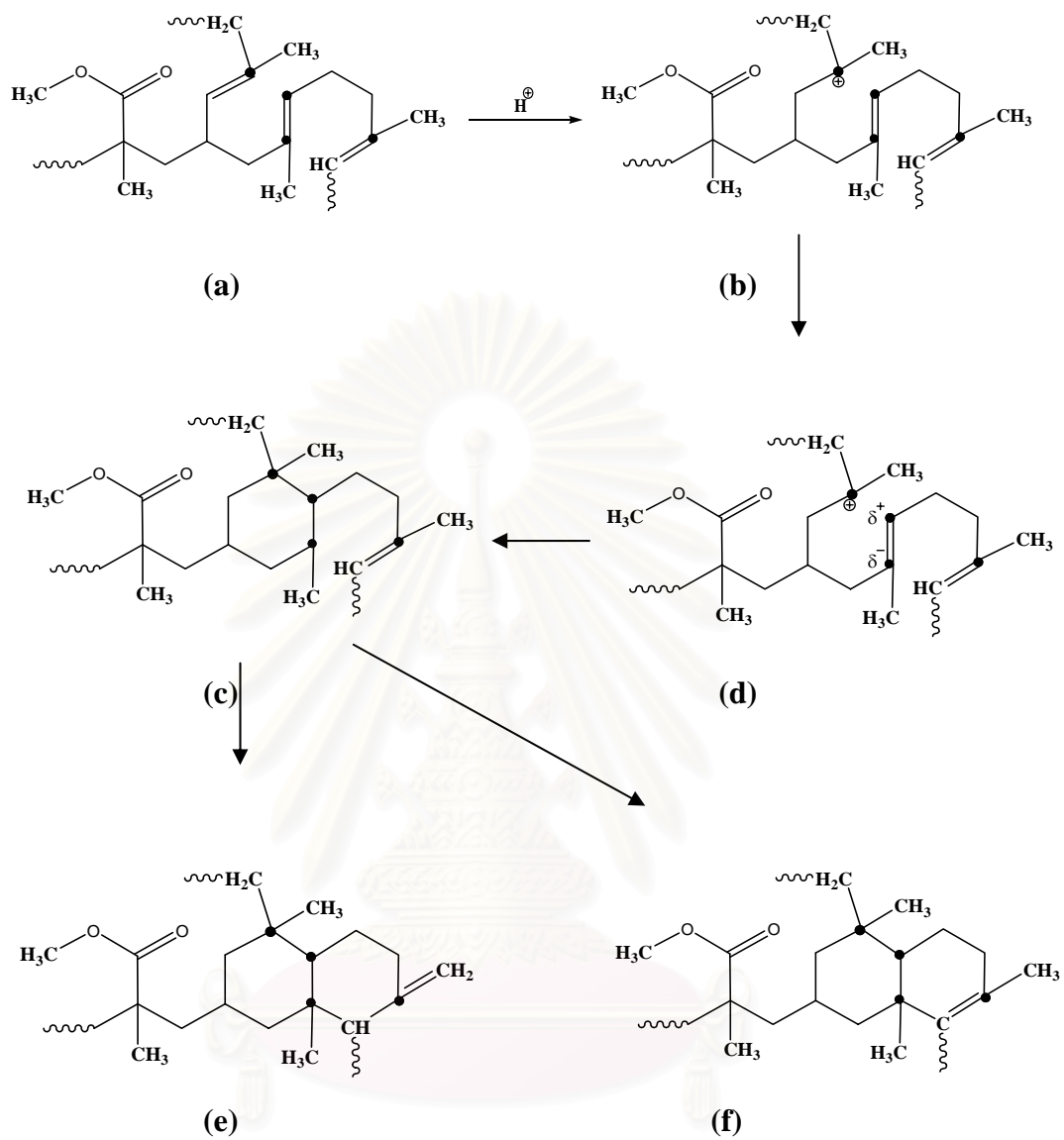
Figure 4.4 Cyclization Reaction Schematic.

4.3.2 Dependence on Catalyst Concentration

Two sets of experiments were performed to determine the effect of catalyst loading on the hydrogenation rate over the range of catalyst concentration of 50 and 150 μM at two levels of hydrogen pressure, 20.4 and 27.2 bar when the rubber concentration was 100 mM and the acid concentration was 2.0 mM at a reaction temperature of 140°C. The influence of catalyst concentration on the reaction system is shown in Figure 4.5. The plots of the hydrogenation rate constant versus catalyst concentration are linearly proportional at both hydrogen pressures. The observation indicated that the active species is linearly proportional to the catalyst precursor loading. It can be suggested that this catalyst is a mononuclear active complex. Thus, the rate of hydrogenation exhibited a first−order dependence on the catalyst concentration. This observation is consistent with the work of Parent et al. [21] for the catalytic hydrogenation of NBR in the presence of $OsHCl(CO)(O_2)(PCy_3)_2$.
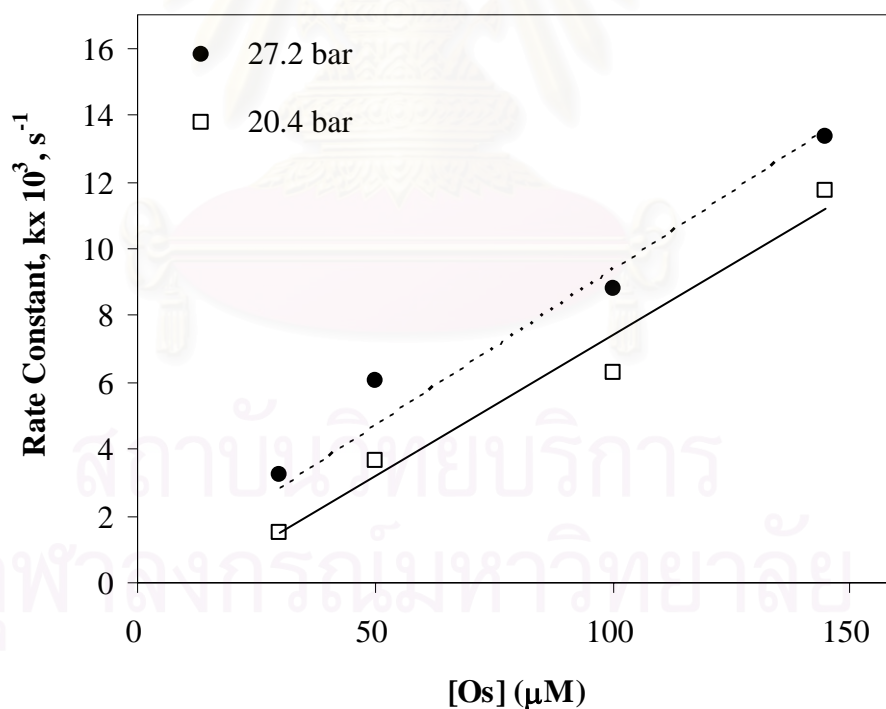
Figure 4.5 Effect of catalyst concentration on the rate of hydrogenation of MMA-*g*-NR. [C=C] = 100 mM; [*p*−TSA] = 2.0 mM; P_{H_2} = 20.4 ($\square$) and 27.2 ($\bullet$) bar and T = 140°C

4.3.3   Dependence on Rubber Concentration

The influence of the rubber concentration on the hydrogenation rate was studied over the range of 50 − 250 mM when [Os] (100 μM), P_{H_2} (20.4 bar), reaction temperature (140°C) and [p−TSA] (2.0 mM) were kept constant. The results indicated that the reaction rate decreased with an increase in rubber concentration as shown in Figure 4.6. For NR hydrogenation, the reaction rate exhibited an inverse first−order behavior with an increase in loading of rubber. Accordingly, since proteins constitute a major impurity in NR, the catalytic activity of the metal complex might be reduced by complexation with the amine contained in the protein structure [24].

For hydrogenation of MMA-g-NR, the decrease in rate can be explained by the steric effect within the polymer solution. Polymer reactivity can be sterically hindered under certain conditions when the functional group is close to the polymer chain or in a sterically hindered environment. This effect may be a consequence of the steric interaction in the bulk due to intermolecular interactions. At high rubber concentration, the grafted NR was not completely dissolved in solution and formed a highly viscous system [11]. Thus, some portion of grafted NR resulted in chain entanglement, which probably caused a reduction of hydrogen diffusivity and solubility in the polymer solution.

The reduction in MMA-g-NR hydrogenation rate can also be explained by the effect of impurities in the grafted natural rubber. It is believed that impurities such as protein in the rubber might compete with the C=C for metal coordination sites to form inactive complexes. The effect of impurities is also reported in the mechanistic interpretation section.
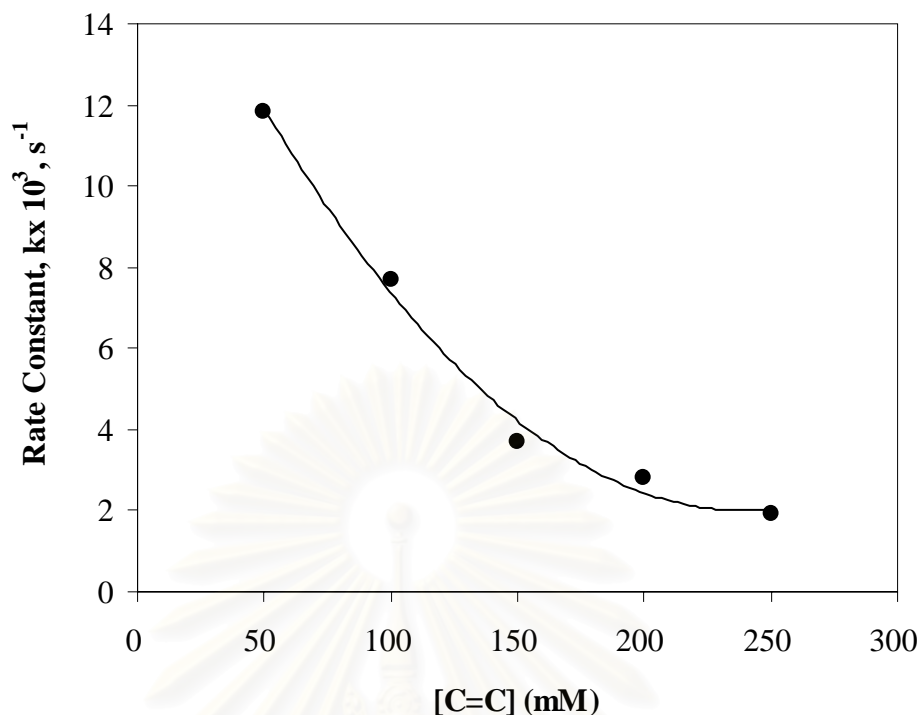
Figure 4.6   Effect of rubber concentration on the hydrogenation rate of MMA-*g*-NR. [Os] = 100 μM; [*p*–TSA] = 2.0 mM; P_{H_2} = 20.4 bar and T = 140°C in monochlorobenzene.

4.3.4   Dependence on Poly(methyl methacrylate) Concentration

A series of experiments were carried out by adding PMMA over the range of 0 − 64 mM when [Os] (100 μM), P_{H_2} (20.4 bar), initial rubber concentration (100 mM), reaction temperature (140°C) and [*p*–TSA] (2.0 mM) were kept constant. The results indicated that the hydrogenation rate increased with increasing PMMA addition from 6.9 − 17.8 mM, and then diminished, and leveled off at [PMMA] above 17.8 mM as shown in Figure 4.7. The polymer molecules are generally present in solution as random−coil conformations. With the increasing [PMMA] initially, it can be postulated that PMMA addition possibly affected the chain orientation in the polymer solution as a result of attraction and repulsion within the polymer coils. The concentration of the functional group is high within the polymer coils and zero outside as shown in Figure 4.8(a). Thus, PMMA molecules were surrounded by grafted NR chain. Over the range of 6.9 − 17.8 mM added PMMA, the hydrogenation

rate was drastically increased. However, the hydrogenation rate was decreased at above 17.8 mM added PMMA. It is believed that the GNR chains are surrounded by PMMA molecules which formed a barrier as illustrated in Figure 4.8(b).

This behavior also was observed for NR hydrogenation as shown in Figure 4.7, however, the hydrogenation rate was not drastically increased as for the grafted NR hydrogenation because of the different structure between grafted NR and NR. The grafted NR containing PMMA graft chain was more compatible with PMMA than NR. Thus, the PMMA addition demonstrated a beneficial effect on the hydrogenation of grafted rubber under certain conditions.
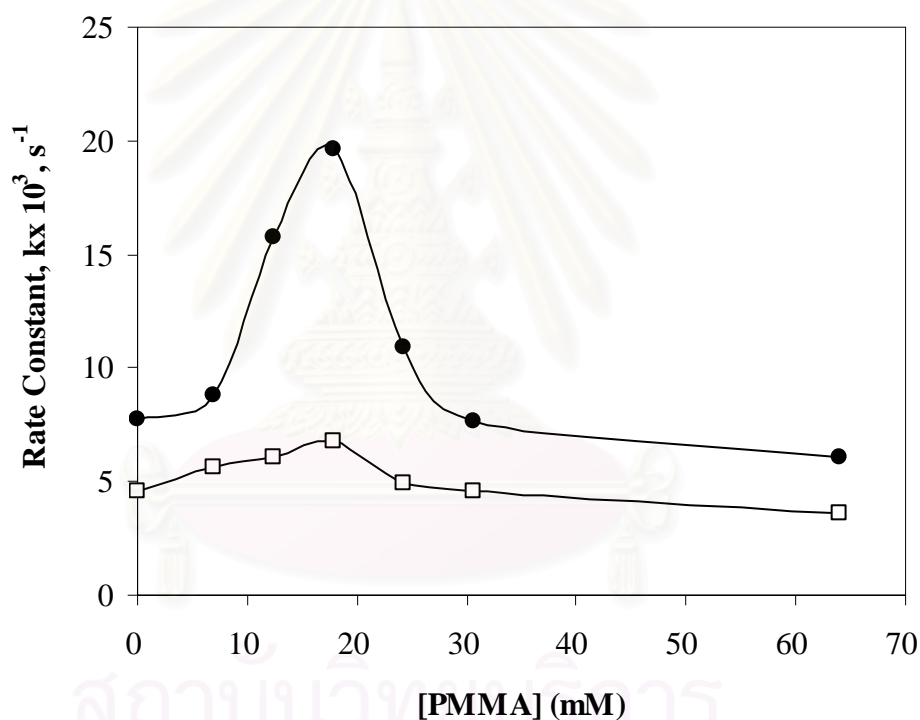
Figure 4.7 Effect of PMMA addition on the hydrogenation rate of (●) MMA-*g*-NR and (□) Natural rubber. [Os] = 100 μM; [C=C] = 100 mM; [*p*−TSA] = 2.0 mM; P_{H_2} = 20.4 bar and T = 140°C in monochlorobenzene.
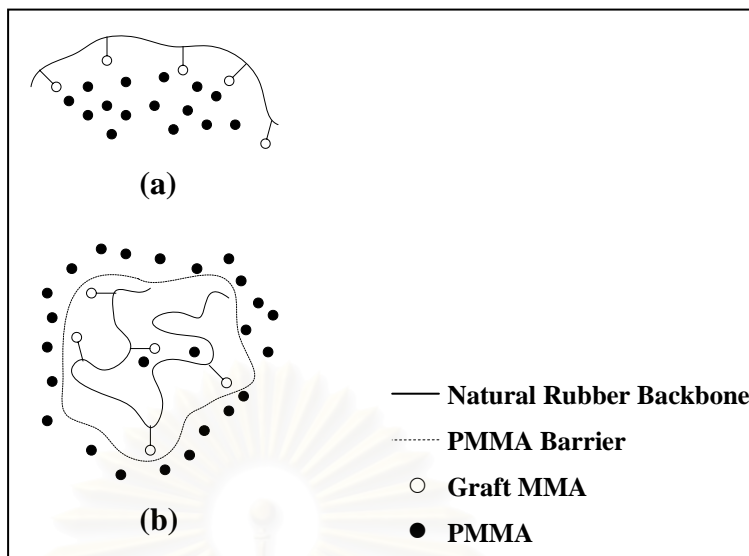
Figure 4.8 Chain orientation behaviors in polymer solution (a) PMMA surrounded by MMA-*g*-NR chain (b) MMA-*g*-NR chain surrounded by PMMA.

4.3.5 Dependence on Hydrogen Pressure

To investigate the effect of hydrogen pressure, a series of experiments were conducted in which the hydrogen pressure was varied over the range 6.8 to 68 bar with a catalyst concentration of 150 μM, rubber concentration of 100 mM, and acid concentration of 2.0 mM at 140°C in monochlorobenzene. The results shown in Figure 4.9 suggest that the hydrogenation rate of MMA-*g*-NR appears to be first−order with respect to the hydrogen pressure from 2.1 to 6.8 bar and then shifts to a zero−order dependence at a pressure higher than 20.4 bar.

These results are in agreement with those for NBR hydrogenation in the presence of the rhodium complexes, $RhCl(PPh_3)_3$ and $RhH(PPh_3)_4$ [65]. According to the literature, the hydrogenation behavior of diene−based polymers, such as NBR [21], CPIP [33] and NRL [23] catalyzed by $OsHCl(CO)(O_2)(PCy_3)_2$ exhibited a first−order dependence on hydrogen pressure, which then tended to a zero−order behavior at high hydrogen pressure. The reason for the reduction in the rate of hydrogenation of grafted NR dependence on the hydrogen pressure will be discussed in the section on the mechanistic interpretation of the kinetic data.
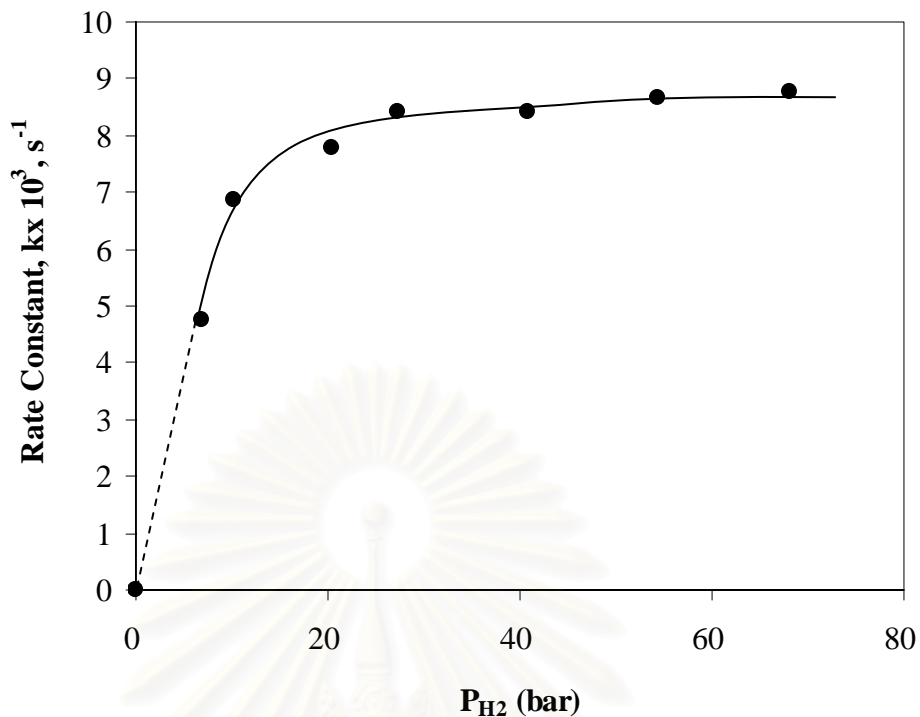
Figure 4.9 Effect of hydrogen pressure on the rate of hydrogenation of MMA-*g*-NR. [Os] = 100 μM; [C=C] = 100 mM; [*p*–TSA] = 2.0 mM; T = 140°C in monochlorobenzene.

4.3.6 Dependence on Reaction Temperature

The effect of reaction temperature on the rate of hydrogenation of grafted NR was studied over the range of 120 – 160°C with a catalyst concentration of 100 μM, rubber concentration of 100 mM and acid concentration of 2.0 mM. The hydrogen pressure was kept constant at 27.2 bar in monochlorobenzene. The apparent activation energy for the reaction was determined by using the Arrhenius law eq. (4.3) and eq. (4.4) was the Erying relationship eq. (4.5) was used to determine the activation enthalpy (ΔH^*) and entropy (ΔS^*).

$$\ln \frac{k}{T} = f\left(\frac{1}{T}\right) \tag{4.3}$$

$$k = Ae^{-E_a/RT} \tag{4.4}$$

$$\ln \frac{k}{T} = \ln \frac{k_B}{h} + \frac{\Delta S *}{R} - \frac{\Delta H *}{RT} \qquad (4.5)$$

where T is the reaction temperature, R is the universal gas constant (8.314 J mol^{-1}K^{-1}), A is the frequency factor, E_a is the apparent activation energy, k is the kinetic constant, k_B is Boltzman's constant (1.381 × 10^{-23} J/K) and h is Planck's constant (6.626 × 10^{-34} J/s).

Figure 4.10(a) shows an Arrhenius plot for the acquired data. An increase in reaction temperature resulted in increasing the rate of hydrogenation of grafted NR. The ln k' versus 1/T plot was linear and an apparent activation energy of 70.3 kJ/mole was obtained from the slope of this plot. This suggested that the experiments occurred under chemical reaction control and that a mass transfer limitation of the reaction is not a rate–determining step under the reaction conditions used in the study. Based on the corresponding Eyring's equation, the activation enthalpy and entropy were estimated as 66.9 kJ/mol and −67.7 J/mol K, respectively as shown in Figure 4.10(b).

The reaction rate increased with increasing reaction temperature and pressure for the range of investigated conditions. Thus, the osmium complex is stable and highly active over the temperature range of 120 − 150°C because this osmium complex has bulky, strong σ–donor and weak π–acceptor phosphine ligands, PCy$_3$, with Tolman's cone angle ≥ 160°C. It exhibited the high catalytic activity due to the ease of dissociation of a ligand from an 18–electron complex to produce a 16–electron species.
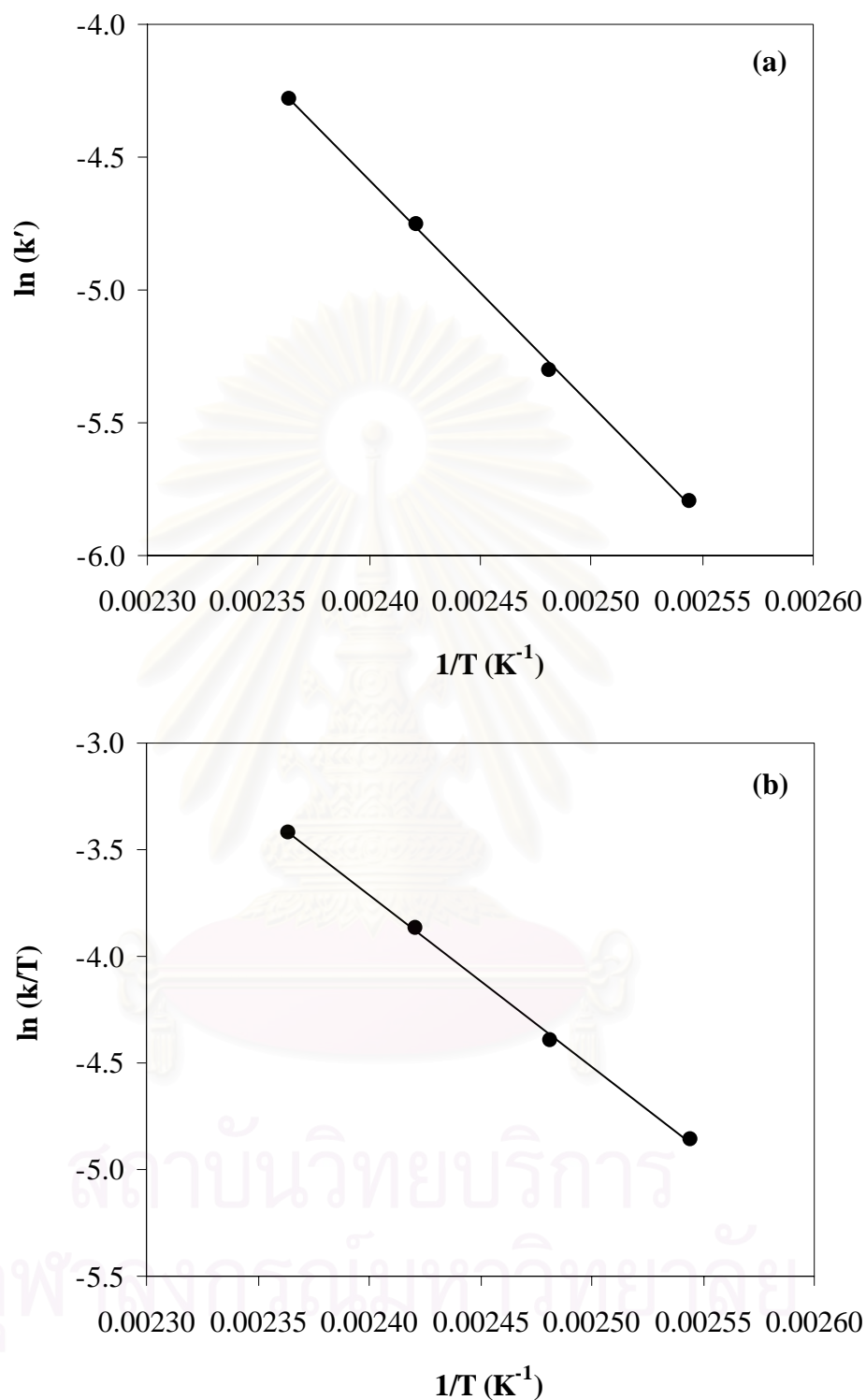
Figure 4.10 (a) Arrhenius plot and (b) Erying plot for hydrogenation of MMA-*g*-NR. [Os] = 100 μM; [C=C] = 100 mM; [*p*–TSA] = 2.0 mM; P_{H_2} = 27.2 bar; T = 140°C in monochlorobenzene.

4.4 Mechanistic Interpretation of Kinetic Data

The catalytic hydrogenation cycle of diene-based polymers in the presence of $OsHCl(CO)(O_2)(PCy_3)_2$ has been proposed in previous work [21, 23, 24, 33]. A catalytic pathway has been developed from the kinetic data and electron counting schemes. The catalytic cycle for the hydrogenation of MMA-*g*-NR in the presence of $OsHCl(CO(O_2)(PCy_3)_2$ is shown in Figure 4.11.
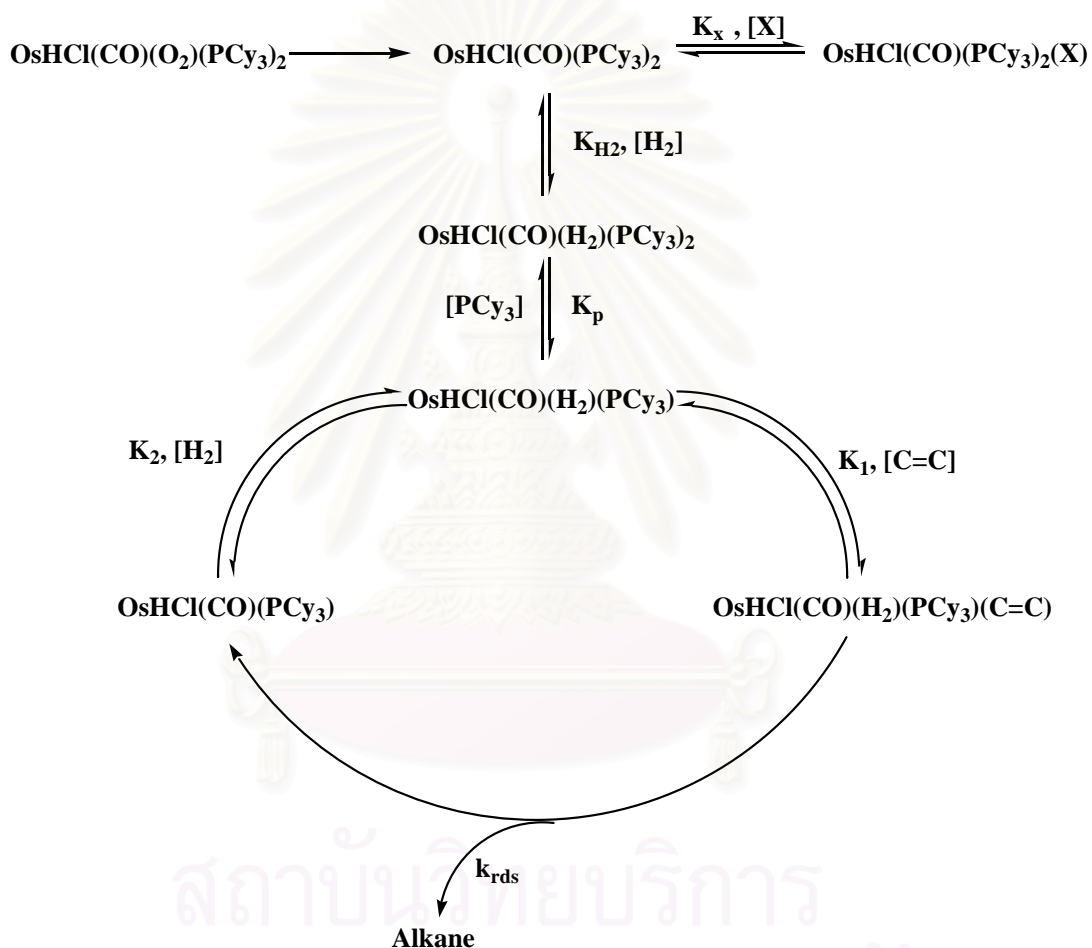
Figure 4.11 Proposed catalytic mechanism for hydrogenation of MMA-*g*-NR in the presence of $OsHCl(CO)(O_2)(PCy_3)_2$.

The $OsHCl(CO(O_2)(PCy_3)_2$ catalyst is activated by O_2 removal to produce the five–coordinate analogue, $OsHCl(CO)(PCy_3)_2$, which is the active

species. The reaction begins with the addition of H_2 to $OsHCl(CO)(O_2)(PCy_3)_2$ to give the trihydrido metal complex $OsHCl(CO)(H_2)(PCy_3)_2$, as shown by eq. (4.6).

$$OsHCl(CO)(O_2)(PCy_3)_2 + H_2 \xleftrightarrow{K_{H_2}} OsHCl(CO)(H_2)(PCy_3)_2 + O_2 \qquad (4.6)$$
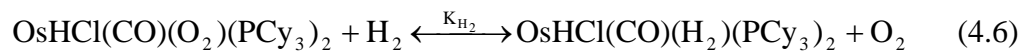
The complex formed in eq. (4.6) subsequently dissociates into a monophosphine complex, and then the complexation of a carbon−carbon double bond of the grafted NR backbone undergoes reaction with $OsHCl(CO)(H_2)(PCy_3)$ as shown in eqs. (4.7) and (4.8).

$$OsHCl(CO)(H_2)(PCy_3)_2 \xleftrightarrow{K_P} OsHCl(CO)(H_2)(PCy_3) + PCy_3 \qquad (4.7)$$

$$OsHCl(CO)(H_2)(PCy_3) + (C=C) \xleftrightarrow{K_I} OsHCl(CO)(H_2)(PCy_3)(C=C) \qquad (4.8)$$

Unlike the shift from a second−order to zero−order dependence on hydrogen pressure for the hydrogenation of NBR (Parent, 1998) or CPIP (Charmondusit, 2003) catalyzed by $OsHCl(CO)(O_2)(PCy_3)_2$, the kinetic data for the hydrogenation of MMA-*g*-NR exhibited a first−order to zero−order dependence on H_2 with increasing hydrogen pressure. It is possible that the hydrogenation of grafted NR requires only 1 molecule of H_2 to generate the active species for the hydrogenation of the grafted NR product.

Mahittikul et al. [23] and Hinchiranan et al. [24] reported on the effect of impurities in NR on the hydrogenation rate, which inhibits the catalytic activity for NR hydrogenation. It is possible that the impurities in NR might coordinate with unsaturated active species of the catalyst to reduce the hydrogenation activity. Since natural rubber contains proteins as the main impurities, these might compete with olefin for the metal coordination sites during the hydrogenation reaction. From the observed inverse behaviors with respect to the grafted natural rubber concentration, there are effective competitions between C=C and impurities. The effect of impurities (X) in natural rubber may inhibit the catalytic activity and deactivate the catalyst in MMA-*g*-NR hydrogenation. The possible pathway of impurities coordination that could inhibit the catalytic activity is shown in eq. (4.9).

$$OsHCl(CO)(PCy_3)_2 + X \xleftrightarrow{\quad K_X \quad} OsHCl(CO)(PCy_3)_2(X) \qquad (4.9)$$

An observed kinetic isotope effect investigated by Parent et al. (1998) implied that cleavage of a bond to hydrogen is involved in the rate-limiting reaction. This could result from the insertion of olefin into an Os−H bond or by a reductive elimination of an osmium−alkyl to yield the saturated product. It assumes that one of these processes is rapid relative to the rate−determining step. Accordingly, olefin hydrogenation could be governed by the rate expression as follows:

$$\frac{-d[C=C]}{dt} = k_{rds}[OsHCl(CO)(H_2)(PCy_3)(C=C)] \qquad (4.10)$$

A mass balance on the active species of osmium charged to the hydrogenation system of grafted NR is given as follows:

$[Os]_T = OsHCl(CO)(PCy_3)_2 + OsHCl(CO)(H_2)(PCy_3)_2 + OsHCl(CO)(H_2)(PCy_3) +$
$\qquad OsHCl(CO)(H_2)(PCy_3)(C=C) + OsHCl(CO)(PCy_3) + OsHCl(CO)(PCy_3)_2(X) \qquad (4.11)$

Every osmium complex species concentration term in eq. (4.11) can be expressed in terms of $[OsHCl(CO)(H_2)(PCy_3)(C=C)]$ with the equilibrium defined in Figure 4.11 which then can be substituted into eq. (4.10) to provide the resulting rate law as shown in eq. (4.13)

$$-\frac{d[C=C]}{dt} = \frac{k_{rds}K_pK_{H_2}K_1K_2[Os]_T[C=C][H_2]}{K_pK_{H_2}(1+K_2[H_2]+K_1K_2[C=C][H_2]) + K_2[PCy_3](1+K_{H_2}[H_2]+K_X[X])} \qquad (4.13)$$

The rate expression derived from the mechanism is consistent with the observed kinetic data. The rate law equation for hydrogenation of grafted NR indicates that the reaction exhibits a first−order dependence on catalyst concentration and an inverse behavior with respect to grafted natural rubber concentration due to the impurities in the grafted natural rubber. At a hydrogen pressure lower than 6.8 bar, a first−order dependence on hydrogen pressure was observed. However, the reaction

rate becomes zero–order with respect to hydrogen pressure when the hydrogen pressure is more than 20.4 bar. Above 20.4 bar, the term of $K_P K_{H2} K_2 [H_2]$ is more significant so that the rate of MMA-g-NR hydrogenation showed a reduction with respect to hydrogen pressure.

4.5   Hydrogenated MMA-g-Natural Rubber Characterization

4.5.1   Fourier Transform Infrared Spectroscopy

A comparison of FTIR spectra NR, MMA-g-NR, and hydrogenated MMA-g-NR is illustrated in Figure 4.12. The C=O stretching (1,732 cm^{-1}) and C–O stretching (1,140 cm^{-1}) appeared in the FTIR spectra for the MMA-g-NR sample. The protein impurities in the NRL are >N–H and >N–C=O and are shown via the weak transmittance bands at 3,280 cm^{-1} and 1,530 cm^{-1}, respectively [65]. The characteristic FTIR spectrum of the hydrogenated MMA-g-NR indicated that the C=C stretching (1,664 cm^{-1}) and olefinic C–H bending (836 cm^{-1}) were decreased while the intensity of the peak at 735 cm^{-1} attributed to –(CH$_2$)$_3$– increased.
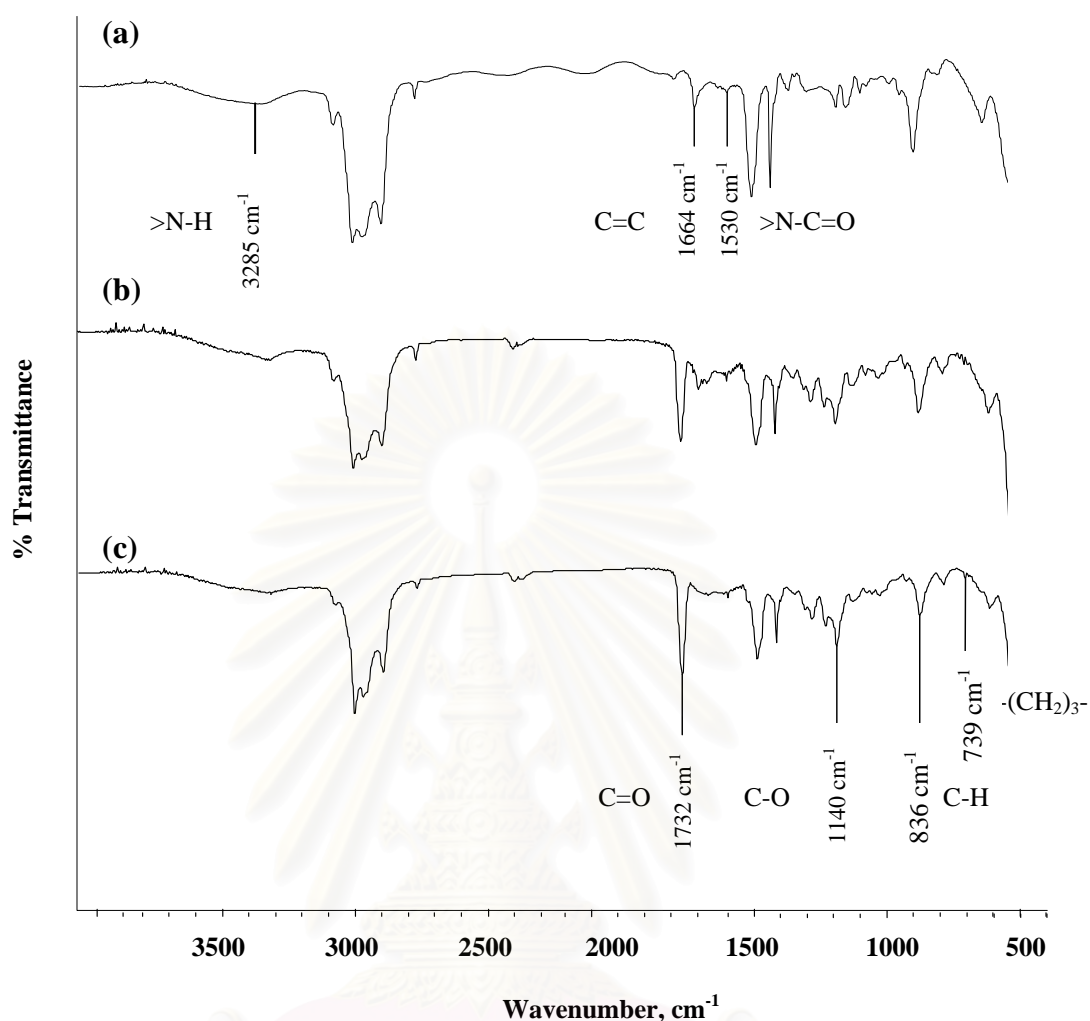
Figure 4.12 FTIR spectra of (a) NRL, (b) MMA-*g*-NR, and (c) Hydrogenated MMA-*g*-NR catalyzed by $OsHCl(CO)(O_2)(PCy_3)_2$.

4.5.2 Proton NMR (^{1}H–NMR)

^{1}H–NMR spectroscopy was also used to investigate the mole fraction of MMA in the grafted NR. From calculation, the grafted NR contained 25 – 27 mole% of MMA. A comparison between the ^{1}H–NMR spectrum of MMA-*g*-NR and hydrogenated MMA-*g*-NR is shown in Figure 4.13. ^{1}H–NMR peaks of grafted NR are attributed to $-CH_3$ (1.64 ppm), $-CH_2-$ (2.01 ppm), $-OCH_3$ (3.57 ppm), $C=CH_2$ (5.15 ppm), and the signal of aliphatic protons of the alkane (1.0 – 2.0 ppm). The hydrogenation led to the reduction in the intensity of peaks at 1.64, 2.01, and 5.15

ppm. The appearance of new peaks at 0.83 and 1.23 ppm are attributed to saturated $-CH_3$ and $-CH_2-$ of the hydrogenated graft NR, which confirms that the carbon−carbon double bonds (C=C) in grafted NR were hydrogenated.

4.5.3 Carbon NMR (^{13}C−NMR) and Distortionless Enhancement of Polarization Transfer (DEPT)

^{13}C−NMR and DEPT−135 spectra are illustrated in Figure 4.14 and Figure 4.15, respectively. The peak areas at 135.4 and 125.2 ppm decrease with an increase in the reduction of olefinic carbon double bonds and four new peaks appear at 37.5, 32.8, 24.6 and 19.9 ppm which are attributed to C_α, −CH, C_β and −CH$_3$, respectively. Signals for C=O and −O−CH$_3$ appeared at $177 - 178$ ppm and 43.2 ppm, respectively. The distortionless enhancement of polarization transfer (DEPT) is a useful method to irradiate the sample at some point during the sequence. In DEPT−135 routine, a second transmitter excites ^{1}H, and this affects the appearance of the ^{13}C spectrum in which –CH and –CH$_3$ carbon appear as positive peaks, $-CH_2-$ carbons as negative peaks and carbons without any attached hydrogen are nulled [59]. The grafted NR shows both signals of NR and MMA. This confirms the occurrence of graft copolymerization of MMA onto natural rubber and that the C=C unsaturation in the grafted NR was hydrogenated in the presence of OsHCl(CO)(O$_2$)(PCy$_3$)$_2$.
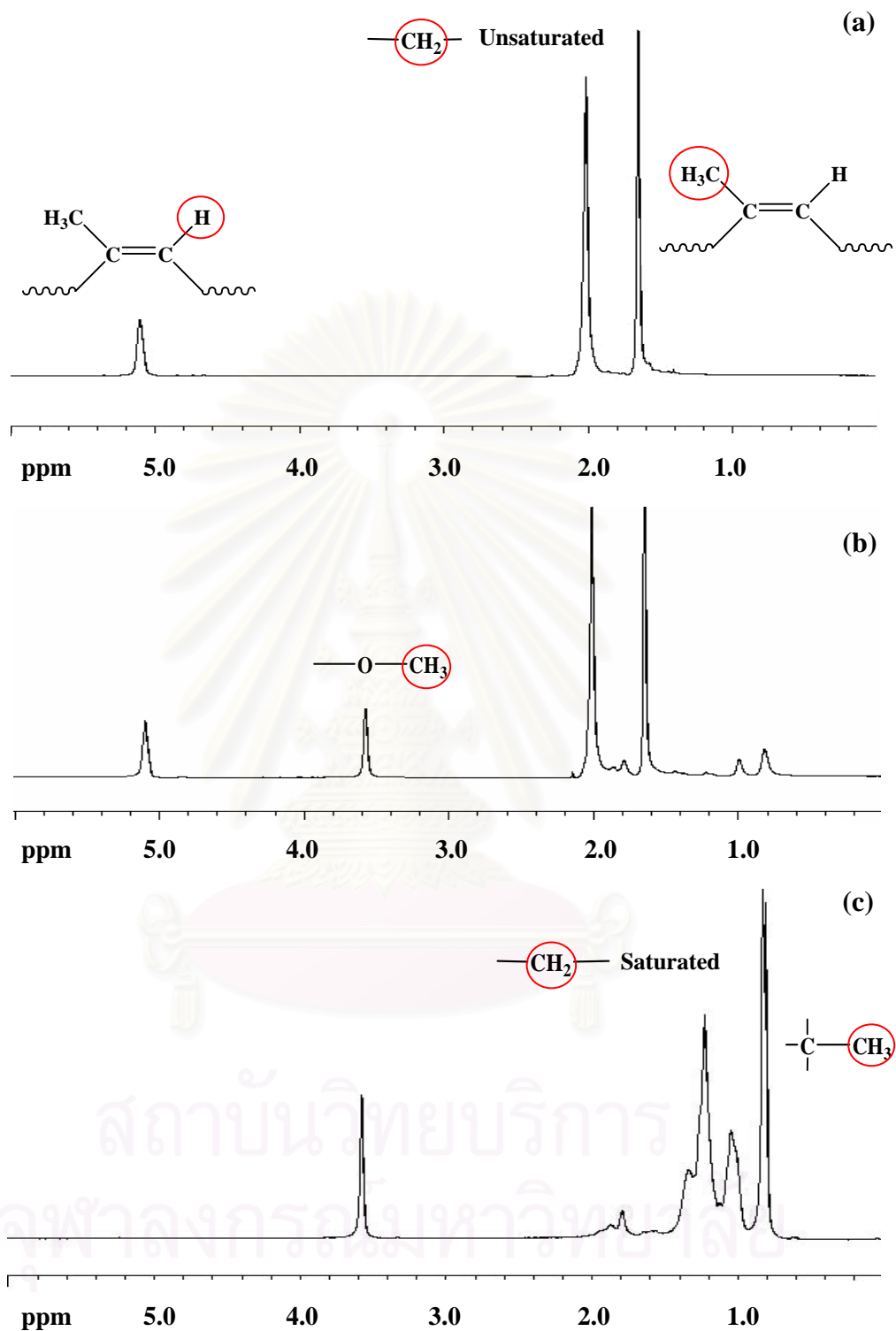
Figure 4.13 ^{1}H–NMR spectra of (a) NR (b) MMA-*g*-NR and (c) Hydrogenated MMA-*g*-NR.
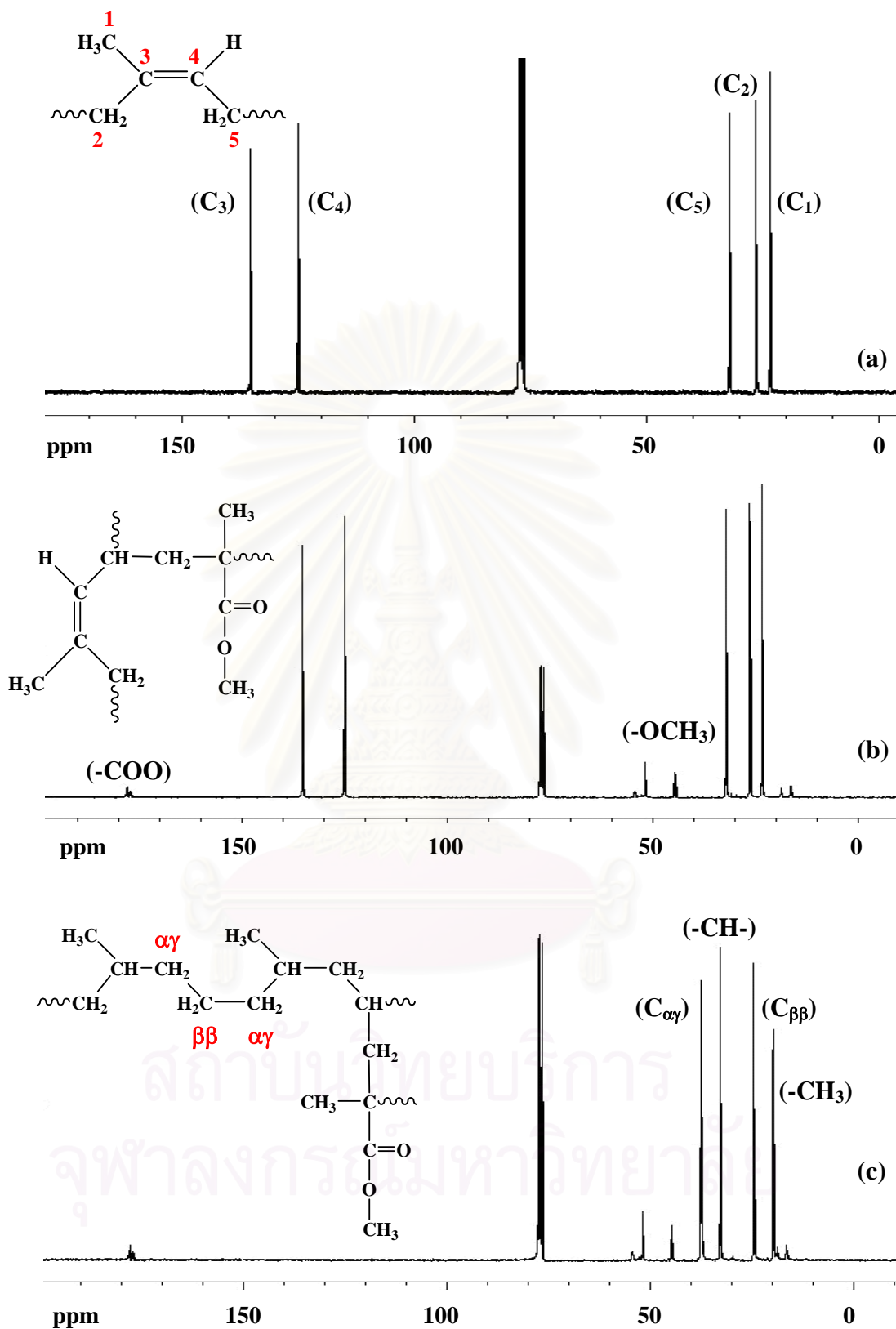
Figure 4.14 ^{13}C–NMR spectra of (a) NR (b) MMA-*g*-NR and (c) Hydrogenated MMA-*g*-NR.
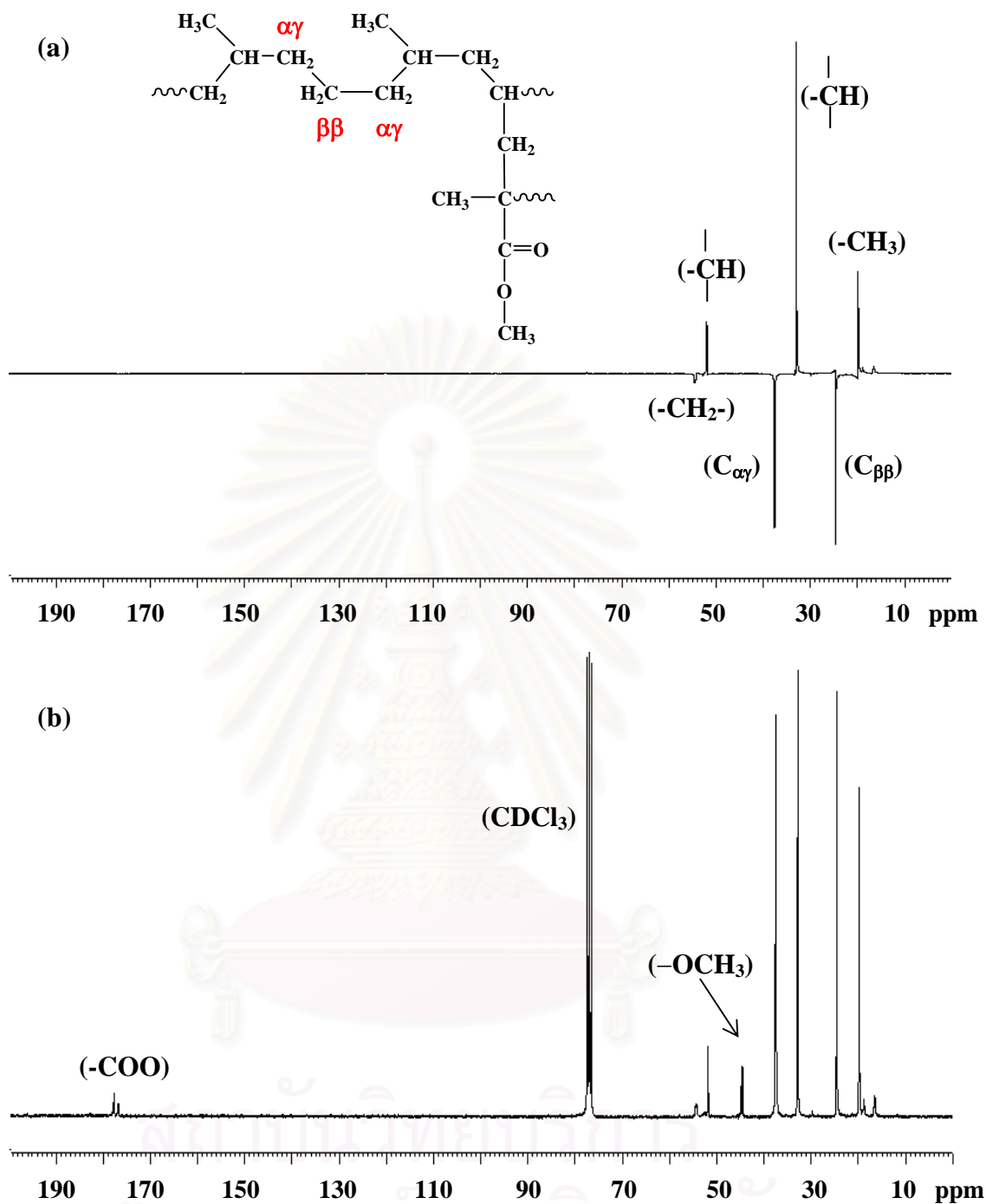
Figure 4.15 NMR spectra of MMA-*g*-NR (a) DEPT−135 and (b) ^{13}C−NMR.

CHAPTER V

HYDROGENATION OF STYRENE-*g*-NATURAL RUBBER
IN THE PRESENCE OF OsHCl(CO)(O₂)(PCy₃)₂

The modification of natural rubber (NR) via graft copolymerization can be used to prepare a product that has some better properties than that of the unmodified NR. The chemical modification of NR by grafting with vinyl monomers using various initiator systems has gained significance in modifying the rubber properties. For NR, methyl methacrylate (MMA) and styrene (ST) are the most suitable monomers when polymerized to give a high level of grafting. Synthesis of graft copolymers from NR has been carried out in solution, solid rubber and latex phases; however the most economical and practical method is possibly latex modification.

A number of reports have appeared on the grafting of vinyl monomers such as MMA or ST onto NR latex using an amine activated hydroperoxide initiator. Luankeaw [56] investigated the graft copolymerization of ST onto NR using a cumene hydroperoxide (CHPO) redox initiator. It was found that the ST-*g*-NR could be used as an impact modifier for PVC blends. Arayapranee et al. [67] studied the graft copolymerization of ST and MMA onto NRL using a cumene hydroperoxide redox initiator. It was suggested that the grafting reactions occurred mainly on the surface of latex particles. After the grafting of a vinyl monomer onto NR, the grafted NR with some residual double bond content may be degraded under exposure to sunlight and ozone. Hydrogenation is a useful method to improve weatherability and chemical resistance of copolymers because the aliphatic chains are much more resistant than their olefinic precursors toward undesirable chemical changes such as cross−linking or degradation occurring during a prolonged exposure to the atmosphere at elevated temperatures. A 5d transition metal−based complex, OsHCl(CO)(O₂)(PCy₃)₂, is the most effective homogeneous catalyst for NR hydrogenation [23, 24]. The remarkable efficiency of the osmium (II) complexes as catalysts for the selective hydrogenation of MMA-*g*-NR was reported earlier in Chapter IV.

In this chapter, the aim of the research is to study the hydrogenation of styrene-*g*-natural rubber (ST-*g*-NR), catalyzed by $OsHCl(CO)(O_2)(PCy_3)_2$. ST-*g*-NR was synthesized via emulsion polymerization using CHPO/TEPA initiator as described in Chapter III. The effect of reaction parameters on the rate of ST-*g*-NR hydrogenation such as catalyst loading, rubber concentration, hydrogen pressure, acid concentration and reaction temperature were investigated. A mechanistic interpretation of ST-*g*-NR hydrogenation was also proposed.

5.1 Preliminary Study of ST-*g*-NR Hydrogenation

Using Soxhlet extraction, it was found that the ST/NR grafted product consisted of 31.3% free NR, 13.1% free polystyrene, and 55.6% grafted NR. The styrene (ST) conversion and grafting efficiency were 63.4% and 50.7%, respectively. From NMR calculation, the grafted NR contains 24.3 mole% of styrene. The purified grafted NR (ST-*g*-NR) was used for subsequent hydrogenation.

Earlier studies reported that the catalyst type, acid type, and solvent type affected the rate of diene–based polymer hydrogenation. The initial study of ST-*g*-NR hydrogenation was performed using various types of catalyst, acid, and solvent. The results are presented in Table 5.1. $Ru[CH=CH(Ph)]Cl(CO)(PCy_3)_2$ and $OsHCl(CO)(O_2)(PCy_3)_2$ were found to be the active catalysts for hydrogenation of ST-*g*-NR at 140°C in monochlorobenzene with acid addition. However, $RhCl(PPh_3)_3$ was not an effective catalyst for ST-*g*-NR hydrogenation. It could be postulated that $RhCl(PPh_3)_3$ formed an inactive complex species within the polymer solution. Similar results have also been reported for *cis*–1,4–polyisoprene (CPIP) hydrogenation [33] and natural rubber latex hydrogenation [23]. $OsHCl(CO)(O_2)(PCy_3)_2$ was found to be the most efficient catalyst for ST-*g*-NR hydrogenation in monochlorobenzene.

Table 5.1 Effect of Catalyst Types on % Hydrogenation of ST-*g*-NR

Catalyst type	Results
Ru[CH=CH(Ph)]Cl(CO)(PCy$_3$)$_2$	45.3% hydrogenation (in 4 min)
RhCl(PPh$_3$)$_3$	No hydrogenation
OsHCl(CO)(O$_2$)(PCy$_3$)$_2$	53.8% hydrogenation (in 4 min)

Condition: [Catalyst] = 100 µM, [C=C] = 260 mM, [*p*−TSA] = 4.0 mM, P_{H_2} = 27.6 bar, and T = 140°C in monochlorobenzene.

For MMA-*g*-NR hydrogenation (Chapter IV), it was found that the acid and solvent types strongly affected the rate of hydrogenation. A series of experiments on ST-*g*-NR hydrogenation using OsHCl(CO)(O$_2$)(PCy$_3$)$_2$ were carried out, [Os] = 100 µM, P_{H_2} = 27.6 bar, [C=C] = 260 mM, and T = 140°C. The results are summarized in Table 5.2. It was found that *p*−TSA was an efficient acid for ST-*g*-NR hydrogenation in the presence of OsHCl(CO)(O$_2$)(PCy$_3$)$_2$. It can be noted that the strong acid increased the hydrogenation rate more than the weaker acids. Sulfonic acid is more acidic than the other selected carboxylic acids. In addition, *p*−TSA is non−coordinating with respect to the osmium complex. This results are in agreement with those observed for MMA-*g*-NR hydrogenation (section 4.1)

For the effect of solvent type, the reaction rate increased with an increase in coordinating power of the solvents in the following order: tetrahydrofuran (THF) > toluene (TOL) > monochlorobenzene (MCB). Similar results were observed for MMA-*g*-NR hydrogenation. The solvent has sufficient coordinating power to displace the phosphine ligand. The results show that THF is the strongest coordinating solvent. The solvent promote the dissociation of the phosphine ligand and formation of a solvated 14−electron osmium trihydride species which may lead to an increase in the catalytic activity of OsHCl(CO)(O$_2$)(PCy$_3$)$_2$.

Table 5.2 Effect of Acid and Solvent Types on % Hydrogenation of ST-*g*-NR

Acid Type	Solvent Type	% Hydrogenation
3−Chloropropionic acid	MCB	27.1% hydrogenation (in 10 min)
Succinic Acid	MCB	13.1% hydrogenation (in 10 min)
p−TSA	MCB	53.8% hydrogenation (in 4 min)
p−TSA	TOL	63.9% hydrogenation (in 4 min)
p−TSA	THF	74.3% hydrogenation (in 4 min)

Condition: [Os] = 100 μM, [C=C] = 260 mM, [Acid] = 4.0 mM, P_{H2} = 27.6 bar, and T = 140°C.

5.2 Kinetic Experimental Design for ST-*g*-NR Hydrogenation in the Presence of OsHCl(CO)(O₂)(PCy₃)₂

A kinetic study of the ST-*g*-NR hydrogenation in the presence of OsHCl(CO)(O₂)(PCy₃)₂ was performed by following the hydrogen consumption with respect to reaction time using a gas−uptake apparatus monitoring program. The conversion profile as shown in Figure 5.1 exhibited an apparent second-order reaction model with respect to olefin concentration according to eq. (5.1).

$$-\frac{d[C=C]}{dt} = k'[C=C]^2 \tag{5.1a}$$

$$\frac{1}{C} - \frac{1}{C_0} = k't \tag{5.1b}$$

where k' is a pseudo−second order rate constant. Equation (5.1b) can further be expressed in terms of olefin conversion according to eq. (5.2)

$$\frac{x}{1-x} = k't \tag{5.2}$$

where t is the reaction time and x is the olefin conversion.

Even though the plot in Figure 5.1(b) deviated from linearity in the later stage, the rate constant (k') can still be calculated with a fair degree of confidence.
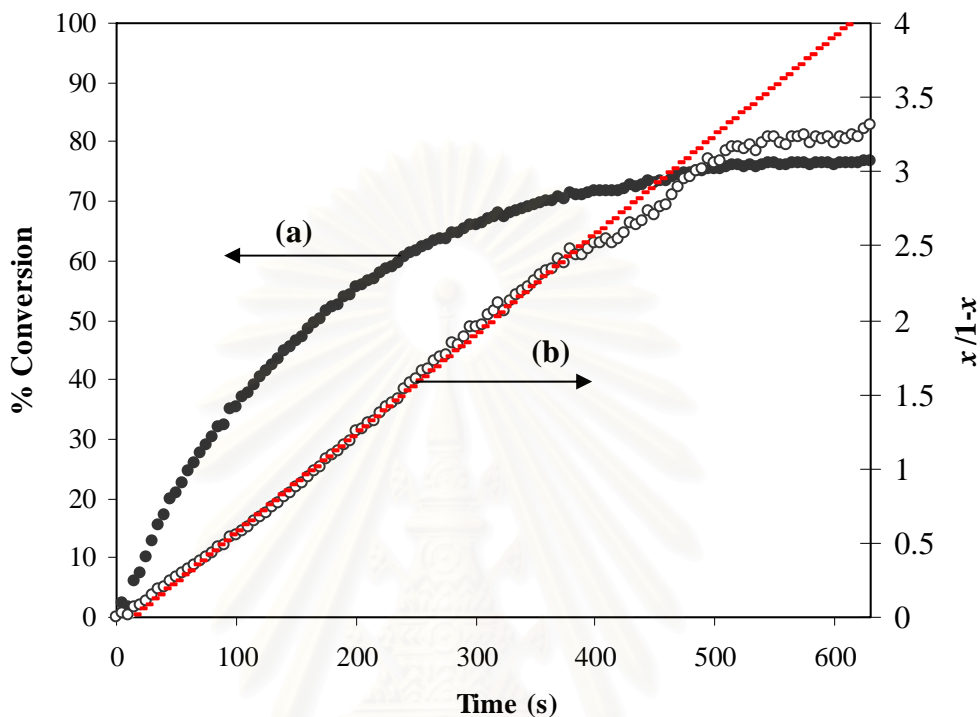
Figure 5.1   Hydrogen consumption profile for hydrogenation of ST-*g*-NR obtained from gas−uptake apparatus: (●) Olefin conversion profile and (○) Second−order $x/1-x$ vs time plot (---- Linear regression model). [Os] = 100 µM; [C=C] = 260 mM; [*p*−TSA] = 4.0 mM; P_{H_2} = 27.2 bar and T = 150°C in monochlorobenzene.

For the preliminary study of the hydrogenation of ST-*g*-NR, the main effects and interaction effects of the reaction parameters were investigated using a two−level factorial design (2^3 factorial experiment). The treatments are combinations of the levels of the factors. These levels are called `high' and `low' or `+1' and `−1', respectively. The simple factors on the degree of hydrogenation are catalyst concentration [Os], hydrogen pressure (P_{H_2}), and rubber concentration in the terms of carbon−carbon double bond concentration [C=C]. The range of catalyst concentration,

hydrogen pressure, and rubber concentration were $50 - 100$ μM, $6.8 - 40.8$ bar, and $150 - 260$ mM, respectively, as shown in Table 5.3. The reaction temperature was kept constant at 140°C. The results of the factorial experiments provided main effects and interaction effects as given by Yate's algorithm. Tables 5.4 and 5.5 summarize the results from the Yate's algorithm and the calculation of effects and standard error for 2^3 factorial design experiments. The results indicated that the main effects ([Os], P_{H2}, and [C=C]) and interaction effects ([Os] $\times$ P_{H_2}, [Os] $\times$ [C=C], P_{H_2} $\times$ [C=C], [Os] $\times$ P_{H_2} $\times$[C=C]) were significant for ST-g-NR hydrogenation. The [Os] and P_{H2} effects had a positive effect which implied that the level of hydrogenation increased with an increase in the [Os] and P_{H_2}. On the other hand, [C=C] showed a negative effect which indicated that the level of hydrogenation decreased with an increase in the [C=C].

Table 5.3 Results from 2^3 Factorial Design for Hydrogenation of ST-g-NR.

Expt.	[Os] (μM)	P_{H_2} (bar)	[C=C] (mM)	T (°C)	Rate Constant ($M^{-1}s^{-1}$)
1	50	6.8	150	140	0.0102
2	50	6.8	150	140	0.0096
3	100	6.8	150	140	0.0135
4	100	6.8	150	140	0.0121
5	50	40.8	150	140	0.0236
6	50	40.8	150	140	0.0240
7	100	40.8	150	140	0.2483
8	100	40.8	150	140	0.2303
9	50	6.8	260	140	0.0029
10	50	6.8	260	140	0.0036
11	100	6.8	260	140	0.0137
12	100	6.8	260	140	0.0125
13	50	40.8	260	140	0.0214
14	50	40.8	260	140	0.0209
15	100	40.8	260	140	0.0268
16	100	40.8	260	140	0.0259

Condition: [p−TSA] = 4.0 mM and solvent = monochlorobenzene.

Table 5.4   Yates's Algorithm Calculation of the 2^3 Factorial Experiments for Hydrogenation of ST-*g*-NR.

No.	Design Matrix Variables			Ave. k'	Algorithm					Identification
	[Os]	P_{H2}	[C=C]		(1)	(2)	(3)	Divisor	Estimate	
1	-	-	-	0.0099	0.0227	0.2858	0.3496	8	0.0437	Average
2	+	-	-	0.0128	0.2631	0.0639	0.2334	4	0.0583	[Os]
3	-	+	-	0.0238	0.0164	0.2184	0.2716	4	0.0679	P_{H2}
4	+	+	-	0.2393	0.0475	0.0150	0.2079	4	0.0520	[Os]×P_{H2}
5	-	-	+	0.0033	0.0029	0.2404	-0.2219	4	-0.0555	[C=C]
6	+	-	+	0.0131	0.2155	0.0311	-0.2034	4	-0.0508	[Os]×[C=C]
7	-	+	+	0.0212	0.0099	0.2126	-0.2093	4	-0.0523	P_{H2}×[C=C]
8	+	+	+	0.0263	0.0052	-0.0047	-0.2173	4	-0.0543	[Os]×P_{H2}×[C=C]

Table 5.5   Calculated Effects and Standard Errors for the 2^3 Factorial Experiments for Hydrogenation of ST-*g*-NR.

Effect	Estimate	± Standard Error
Average	0.04370	± 1.13E-03
Main Effects		
Catalyst Concentration, [Os]	0.05834	± 5.13E-06
Hydrogen Pressure, P_{H_2}	0.06789	± 5.13E-06
Rubber Concentration, [C=C]	-0.05548	± 5.13E-06
Two-Factor Interaction		
[Os]× P_{H_2}	0.05197	± 5.13E-06
[Os]×[C=C]	-0.05084	± 5.13E-06
P_{H_2} ×[C=C]	-0.05232	± 5.13E-06
Three-Factor Interaction		
[Os]× P_{H_2} × [C=C]	-0.05432	± 5.13E-06

5.3 Univariate Kinetic Experiments for ST-*g*-NR Hydrogenation

ST-*g*-NR hydrogenation in the presence of OsHCl(CO)(O$_2$)(PCy$_3$)$_2$ was performed under various conditions. The effect of parameters on ST-*g*-NR hydrogenation was investigated by varying the amount of acid addition, catalyst concentration, rubber concentration, polystyrene addition, hydrogen pressure, and reaction temperature. The univariate experimental data are summarized in Tables 5.6.

Table 5.6   Univariate Kinetic Data for ST-*g*-NR Hydrogenation Catalyzed by OsHCl(CO)(O$_2$)(PCy$_3$)$_2$.

No.	[Os] (mM)	[C=C] (mM)	P$_{H2}$ (bar)	Temp (°C)	[*p*–TSA] (mM)	%HYD (in 10 min.)	k' x 10^3 (M^{-1}s^{-1})
1	50	260	27.2	140	4.0	20.8	4.0
2	80	260	27.2	140	4.0	52.5	10.6
3	100	260	27.2	140	4.0	72.5 (in 8 min)	19.8
4	145	260	27.2	140	4.0	92.6	58.3
5	50	260	40.8	140	4.0	40.5	5.1
6	80	260	40.8	140	4.0	53..4	15.9
7	100	260	40.8	140	4.0	70.6	26.8
8	145	260	40.8	140	4.0	93.5	62.9
9	100	260	6.8	140	4.0	25.6	4.3
10	100	260	13.6	140	4.0	55.98	13.5
11	100	260	27.2	140	4.0	72.5 (in 8 min)	19.8
12	100	260	40.8	140	4.0	70.6	27.8
13	100	260	47.6	140	4.0	71.2	28.8
14	100	260	54.4	140	4.0	74.9	31.4
15	100	260	61.2	140	4.0	72.0 (in 6 min)	31.9
16	100	260	27.2	140	4.0	77.3 (in 5 min)	50.1
17	100	150	27.2	140	4.0	64.1 (in 5 min)	46.7
18	100	260	27.2	140	4.0	72.5 (in 8 min)	19.8
19	100	350	27.2	140	4.0	57.8	11.9
20	100	450	27.2	140	4.0	29.8	7.7
21	100	260	27.2	140	0	7.4	2.9
22	100	260	27.2	140	2.0	63.6	16.6
23	100	260	27.2	140	4.0	72.5 (in 8 min)	19.8
24	100	260	27.2	140	6.0	51.7	11.5
25	100	260	27.2	140	8.0	32.4	5.5
26	100	260	27.2	120	4.0	34.9	5.3
27	100	260	27.2	120	4.0	33.7	5.0
28	100	260	27.2	130	4.0	47.7	6.9
29	100	260	27.2	130	4.0	64.0	7.3
30	100	260	27.2	140	4.0	72.5 (in 8 min)	17.1
31	100	260	27.2	140	4.0	69.7	22.4
32	100	260	27.2	150	4.0	94.4	67.0
33	100	260	27.2	150	4.0	94.0	65.9

5.3.1 Dependence on Acid Concentration

Acid has been observed to enhance the rate of hydrogenation of diene−based polymers in the presence of ruthenium and osmium catalysts. Guo and Rempel [68] reported that carboxylic acids enhanced the catalytic activity of $RuCl(CO)(CH=CH(Ph))(PCy_3)_2$ for the hydrogenation of a NBR emulsion. It was suggested that the carboxylic acid was an effective acid in preventing the catalyst poisoning. Hinchiranan et al. [24] reported that for NR hydrogenation, the addition of a small amount of acids, 3−chloropropionic acid (3−CPA) or p−toluenesulfonic acid (p−TSA), could assist in helping to prevent the poisoning of $OsHCl(CO)(O_2)(PCy_3)_2$ by the impurities present in NR. Mahittikul et al. [23] also found that the presence of sulfonic acid in natural rubber latex (NRL) hydrogenation prevented the poisoning of the osmium catalyst. It is possible that the acid neutralized the impurities in the NRL.

In this work, the role of acids, 3−chloropropionic acid (3−CPA), p−toluenesulfonic acid (p−TSA), and succinic acid (SA) on ST-g-NR hydrogenation were studied (section 5.1). It was found that p−TSA is an efficient acid promoting ST-g-NR hydrogenation in the presence of $OsHCl(CO)(O_2)(PCy_3)_2$. For the effect of p−TSA concentration, the reaction conditions were 100 μM [Os], 260 mM [C=C] in monochlorobenzene, 27.6 bar hydrogen pressure and a temperature of 140°C. Figure 5.2 indicated that the rate of hydrogenation increased with an increase in p−TSA concentration and decreased at an acid concentration above 4.0 mM. At high acid concentration, p−TSA results in a higher concentration of an anion ($PTSO_4^{2-}$) which may decrease the catalytic activity by forming an inactive species.

The hydrogenated ST-g-NR materials prepared at low and high acid concentration were characterized using ^{1}H−NMR. From Figure 5.3, the spectra of the hydrogenated ST-g-NR samples were similar with the exception that the two absorption bands at 4.68 ppm (exocyclic olefinic carbon, $>C=CH_2$) and 2.60 ppm (aromatic $-CH_3$ of p−TSA). At high level of acid addition, the cyclization of C=C in natural rubber backbone occurred. This is in agreement with the work on MMA-g-NR hydrogenation (section 4.3.1). It can be concluded that the addition of an appropriate acid concentration increased the rate of hydrogenation.
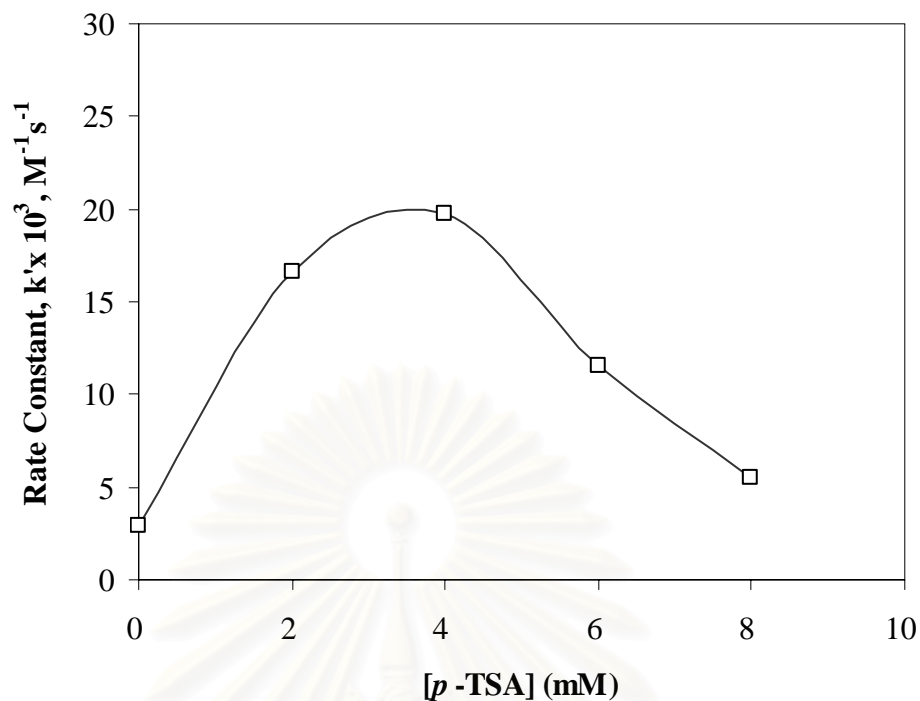
Figure 5.2 Effect of acid concentration on the rate of hydrogenation of ST-*g*-NR. [Os] = 100 μM; [C=C] = 260 mM; P_{H_2} = 27.2 bar; T = 140°C in monochlorobenzene.
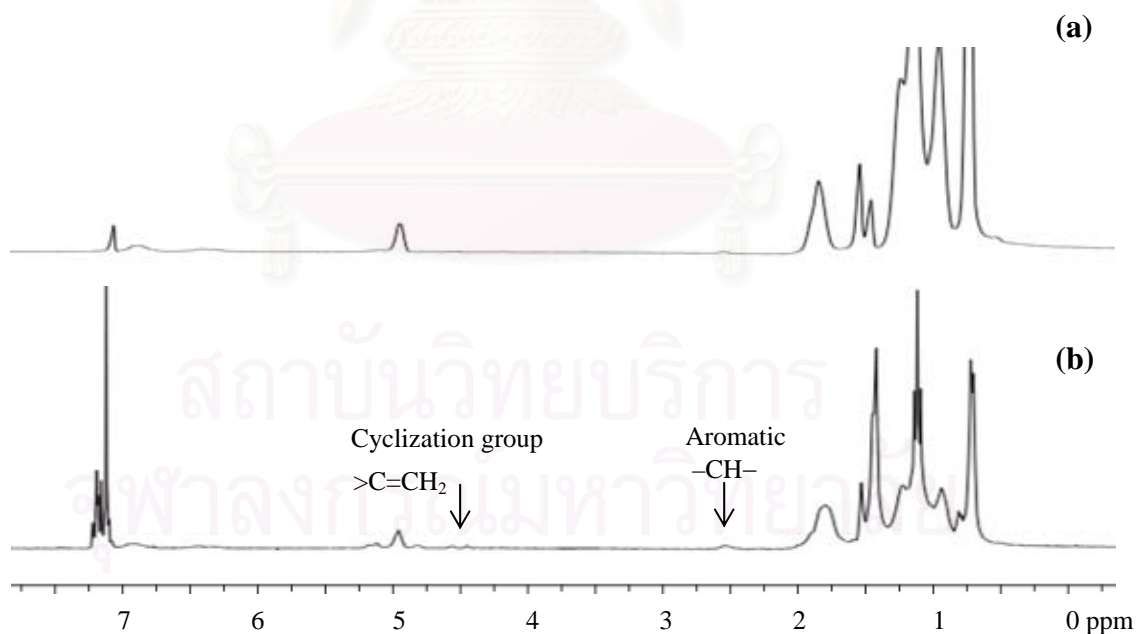
Figure 5.3 ^{1}H−NMR spectra of (a) hydrogenated ST-*g*-NR (64.0% hydrogenation, [*p*−TSA] = 2.0 mM) and (b) hydrogenated ST-*g*-NR (52.1% hydrogenation, [*p*−TSA] = 6.0 mM).

5.3.2 Dependence on Catalyst Concentration

The influence of catalyst concentration on the rate of ST-*g*-NR hydrogenation was studied over the range of 50 to 145 µM at two levels of hydrogen pressure, 27.2 and 40.8 bar and 140°C, whereas the rubber concentration was 260 mM and the acid concentration was 4.0 mM in monochlorobenzene. The results are illustrated in Figure 5.4. It was found that the rate constant was linearly dependent on catalyst concentration at both hydrogen pressure levels. These results are consistent with the work of Andriollo et al. [69] for phenylacetylene hydrogenation using OsHCl(CO)(PR$_3$)$_2$ [PR$_3$ = PMe$-t-$Bu$_2$ and P$-i-$Pr$_3$] catalyst and Parent et al. [22] for acrylonitrile $-$ butadiene copolymer hydrogenation using OsHCl(CO)(O$_2$)(PCy$_3$)$_2$. The rate of ST-*g*-NR hydrogenation was first$-$order with respect to catalyst concentration. Furthermore, the plot exhibited a positive interception on the [Os] $-$ axis which suggested that some of the active species of osmium was deactivated during the reaction, due to the presence of impurities in the ST-*g*-NR.
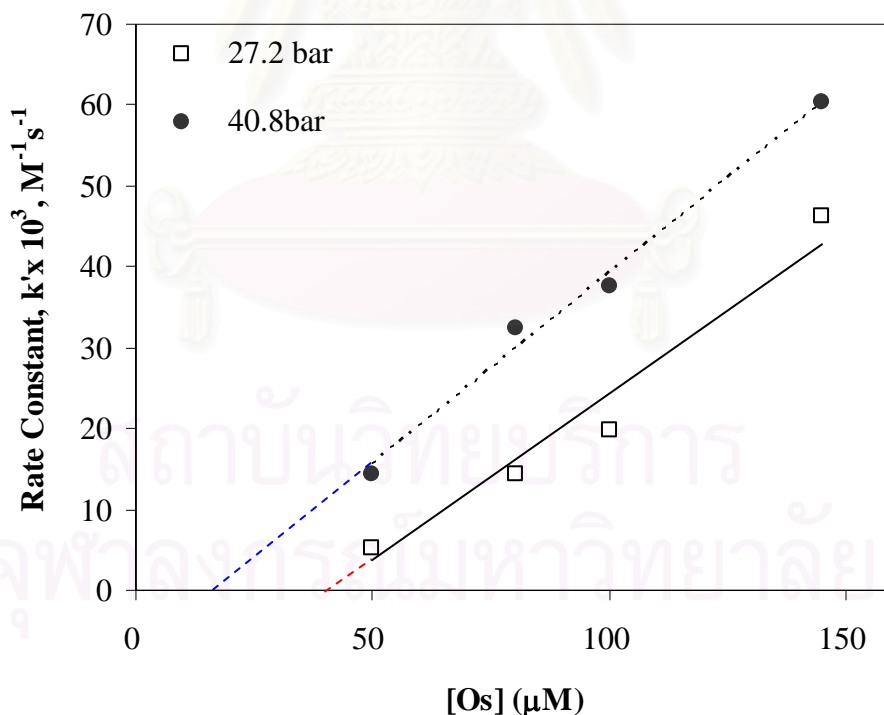
Figure 5.4   Effect of catalyst concentration on the rate of ST-*g*-NR hydrogenation. [C=C] = 260 mM; [*p*$-$TSA] = 4.0 mM; P$_{H_2}$ = 20.4 (□) and 27.2 (●) bar and T = 140°C in monochlorobenzene.

5.3.3 Dependence on Rubber Concentration

To investigate the effect of rubber concentration on the rate of ST-*g*-NR hydrogenation, the range of rubber concentration based on double bond concentration was varied between 100 to 450 mM for which the catalyst concentration (100 μM), *p*−TSA concentration (4.0 mM), hydrogen pressure (27.2 bar), and reaction temperature (140°C) were kept constant. The results are shown in Figure 5.5. It can be seen that the rate of ST-*g*-NR hydrogenation decreased with an increase in rubber concentration. This characteristic is consistent with the result of MMA-*g*-NR hydrogenation (section 4.3.3). Since proteins constitute a major impurity in NR, the catalytic activity of the osmium complex might be reduced by complexation with the amine contained in the protein structure. The decrease in rate can also be explained by the steric effect within the polymer solution. This effect may be a consequence of a steric interaction in the bulk due to intermolecular interactions.
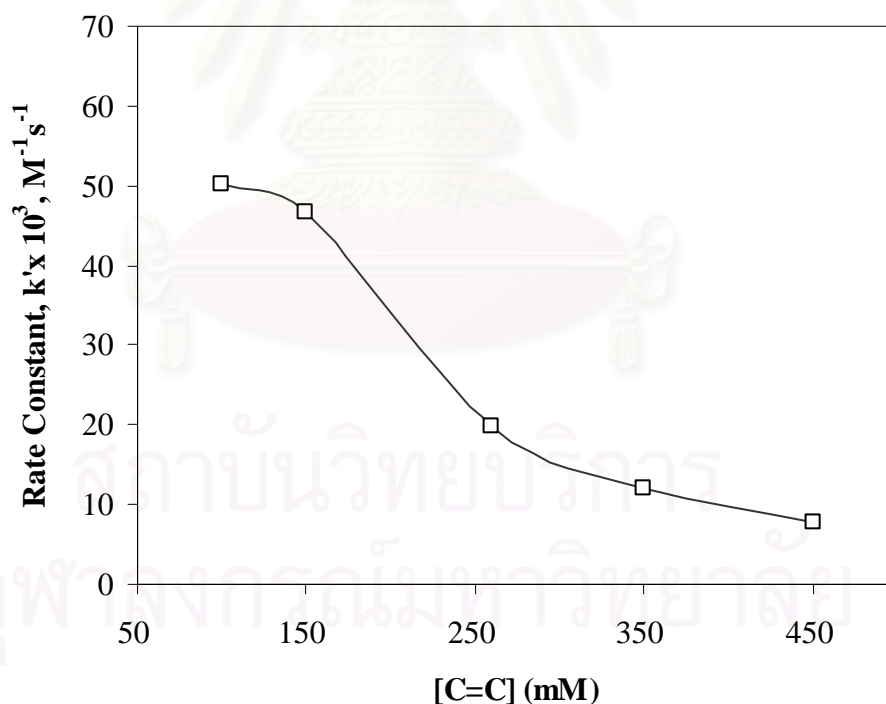
Figure 5.5 Effect of rubber concentration on the rate of ST-*g*-NR hydrogenation. [Os] = 100 μM; [*p*−TSA] = 4.0 mM; P_{H_2} = 27.2 bar and T = 140°C in monochlorobenzene.

5.3.4 Dependence on Polystyrene Concentration

A series of experiments were carried out by adding polystyrene (PS) over the range of 0 – 50 mM when [Os] (100 µM), P_{H2} (27.2 bar), reaction temperature (140°C) and [p–TSA] (4.0 mM) were kept constant. The results indicated that the hydrogenation rate increased with increasing PS concentration, [PS], up to 4.05 mM, and then diminished, and leveled off at [PS] above 4.05 mM as shown in Figure 5.6. over the range of 4.0 to 99.0 mM, it can be postulated that PS addition possibly affected the chain orientation in the polymer solution as a result of attraction and repulsion within the polymer coils. A similar result was also observed for the MMA-g-NR hydrogenation (section 4.3.4). It was suggested that the concentration of the functional group was high within the polymer coils and zero outside and the grafted NR chains were surrounded by additional polymer molecules which formed a barrier (see Figure 4.8). Thus, the PS addition demonstrated a beneficial effect on the ST-g-NR hydrogenation under certain conditions.
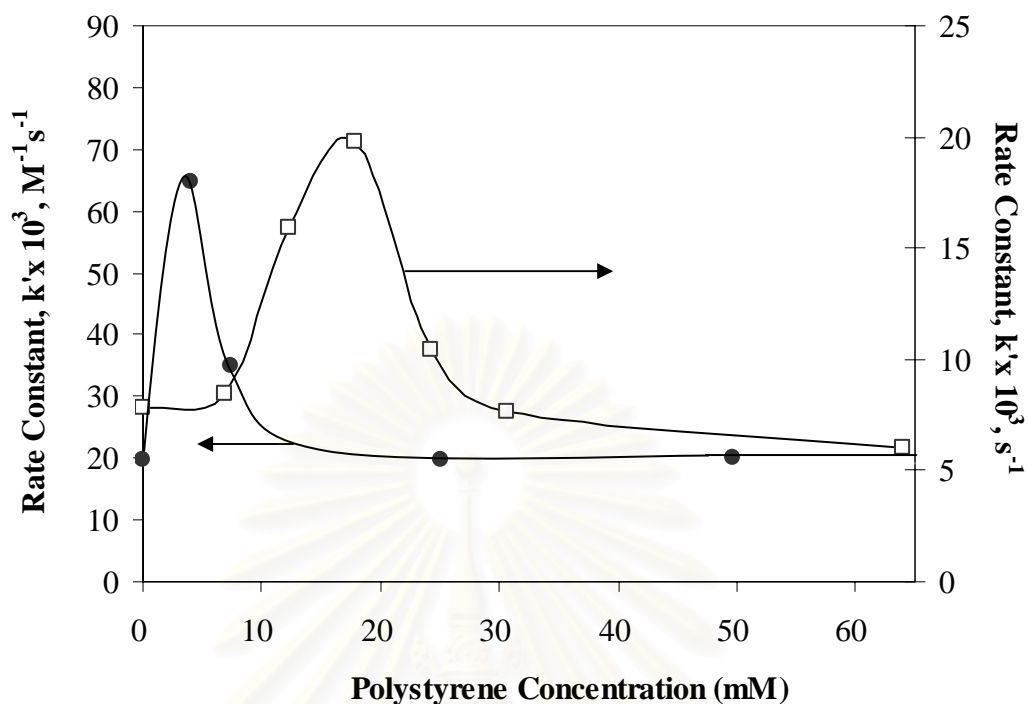
Figure 5.6 Effect of polystyrene addition on the rate of ST-*g*-NR hydrogenation compared with MMA-*g*-NR hydrogenation (section 4.3.4). For ST-*g*-NR (●): [Os] = 100 μM; [C=C] = 260 mM; [*p*−TSA] = 4.0 mM; [PS] = 0 − 50 mM; P_{H_2} = 27.2 bar and T = 140°C in monochlorobenzene. For MMA-*g*-NR (□): [Os] = 100 μM; [C=C] = 260 mM; [*p*−TSA] = 2.0 mM; [PMMA] = 0 − 60 mM; P_{H_2} = 27.2 bar and T = 140°C in monochlorobenzene.

5.3.5 Dependence on Hydrogen Pressure

A series of experiments were conducted over the hydrogen pressure range of 6.8 − 68.0 bar at 140°C in monochlorobenzene. The catalyst concentration of 100 μM, rubber concentration of 260 mM, and p−TSA concentration of 4.0 mM were kept constant. The hydrogenation rate exhibited a first−order shift to zero−order with respect to hydrogen pressure as shown in Figure 5.7. For NR hydrogenation, the shift curve of the reaction order at a high level of hydrogen pressure was different in that the reaction rate constant decreased when the hydrogen pressure was higher than 41.4 bar [24]. This may be explained in terms of the rate constant from the rate law equation. For ST-g-NR hydrogenation, the first−order shift to zero−order will be discussed later in the mechanistic aspects section.
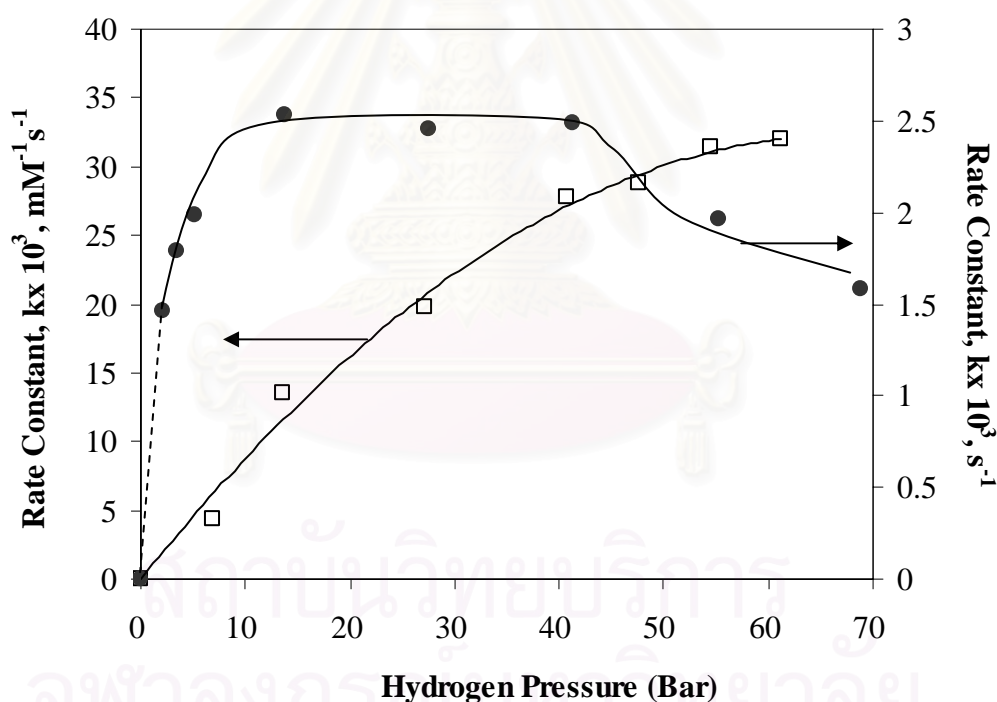
Figure 5.7 Effect of hydrogen pressure on the rate of ST-g-NR hydrogenation compared with NR hydrogenation (Hinchiranan et al. [24]). For ST-g-NR (□): [Os] = 100 μM; [C=C] = 260 mM; [p−TSA] = 2.0 mM; T = 140°C in monochlorobenzene. For NR (●): [Os] = 100 μM; [C=C] = 260 mM; T = 140°C in monochlorobenzene.

5.3.6   Dependence on Reaction Temperature

The effect of reaction temperature on the rate of ST-*g*-NR hydrogenation was studied over the range of 50 to 145°C. The reaction conditions were kept constant at 100 μM [Os], 260 mM [C=C] and 4.0 mM [*p*–TSA] at 27.6 bar hydrogen pressure. The apparent activation energy, enthalpy, and entropy for the reaction were determined by using the Arrhenius law and Erying relationship (eq. 4.3. – 4.5). An Arrhenius plot is illustrated in Figure 5.8(a) and the apparent activation energy was 106.5 kJ/mol. This provided evidence that the experiments were performed without any mass–transfer limitation. The activation energy of ST-*g*-NR hydrogenation was higher than that of MMA-*g*-NR hydrogenation (70.3 kJ/mol) but lower than that of NR hydrogenation (122.8 kJ/mol). The difference in activation energy was due to the different chemical structure of NR, MMA-*g*-NR and ST-*g*-NR. Based on the corresponding Eyring's equation, the activation enthalpy and entropy were estimated as 58.1 kJ/mol and −82.2 J/mol K, respectively as deduced from Figure 5.8(b).

It is well known that the thermodynamic state of the polymer system does affect the chain conformation of the polymer. The activation energy is the minimum energy required for a chemical reaction to occur. This energy required to convert the reactants into the activated complex (or transition state) where bonds are in the process of forming and breaking. Therefore, the effect of the differences in chain conformation has to be considered.
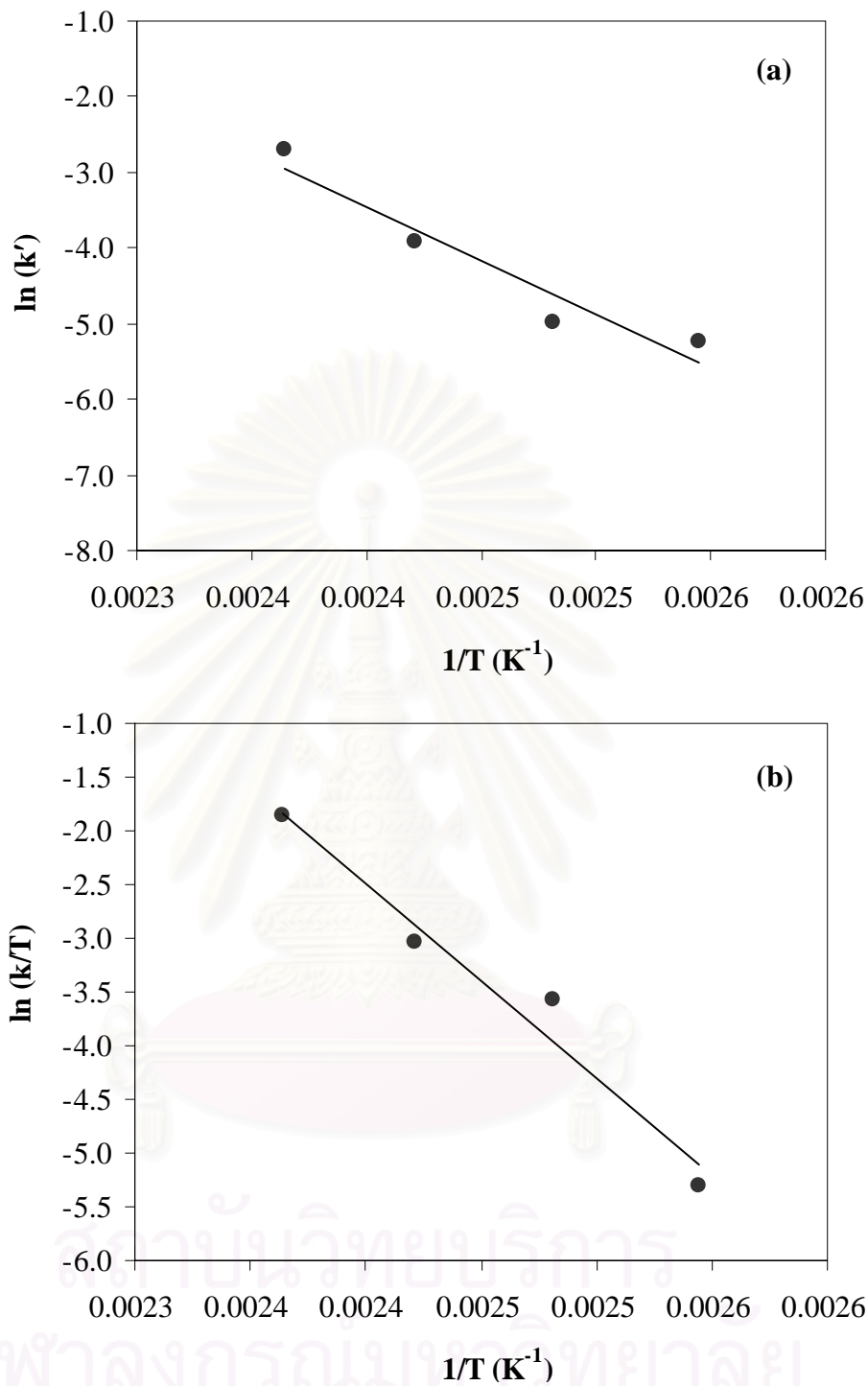
Figure 5.8 (a) Arrhenius plot and (b) Erying plot for ST-*g*-NR hydrogenation. [Os] = 100 μM; [C=C] = 260 mM; [*p*−TSA] = 4.0 mM; P_{H_2} = 27.2 bar; T = 140°C in monochlorobenzene.

5.4 Mechanistic Interpretation of Kinetic Data

The catalytic pathway of olefinic hydrogenation in the presence of OsHCl(CO)(O$_2$)(PCy$_3$)$_2$ and its analogues has been investigated. Unlike the first−order dependence on the olefinic substrate concentration in conversion profile plot of MMA-*g*-NR hydrogenation (Section 4.2), the conversion profile plot of ST-*g*-NR hydrogenation exhibits a second−order dependence on the olefinic substrate concentration. A possible reason for the second−order dependence on [C=C] may be attributed to a substituent effect as shown in Figure 5.9.
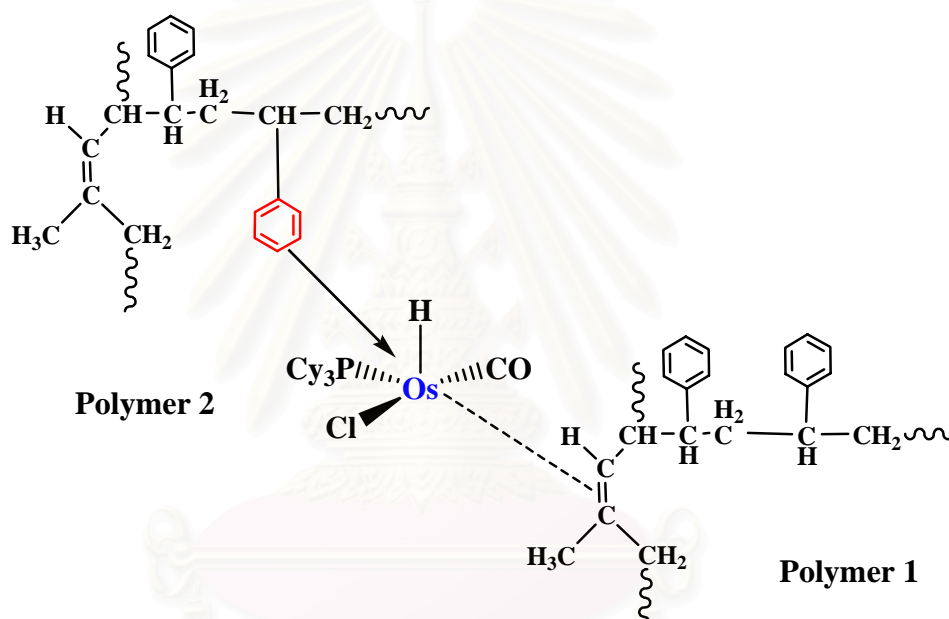
Figure 5.9 Substituent effect for ST-g-NR hydrogenation.

For an electron withdrawing group effect such as −CN, −COOCH$_3$, the substituent decreases the electron density on the C=C [11]. Thus, π−back bonding is not very strong. It can be concluded that electron withdrawing groups inhibited the electrophile attack as shown below:
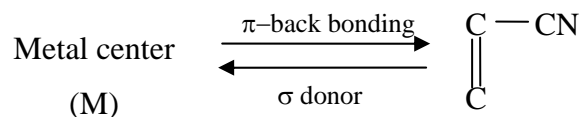
For the –phenyl substituent (electron donating group), it may provide stronger π–back bonding than for an electron withdrawing group. It can be concluded that the phenyl substituent may promote the electrophilic attack whereas the carbonyl substitute inhibited the interaction. The proposed catalytic mechanism of ST-*g*-NR hydrogenation in the presence of $OsHCl(CO(O_2)(PCy_3)_2$ is shown in Figure 5.10.

P = Polymer
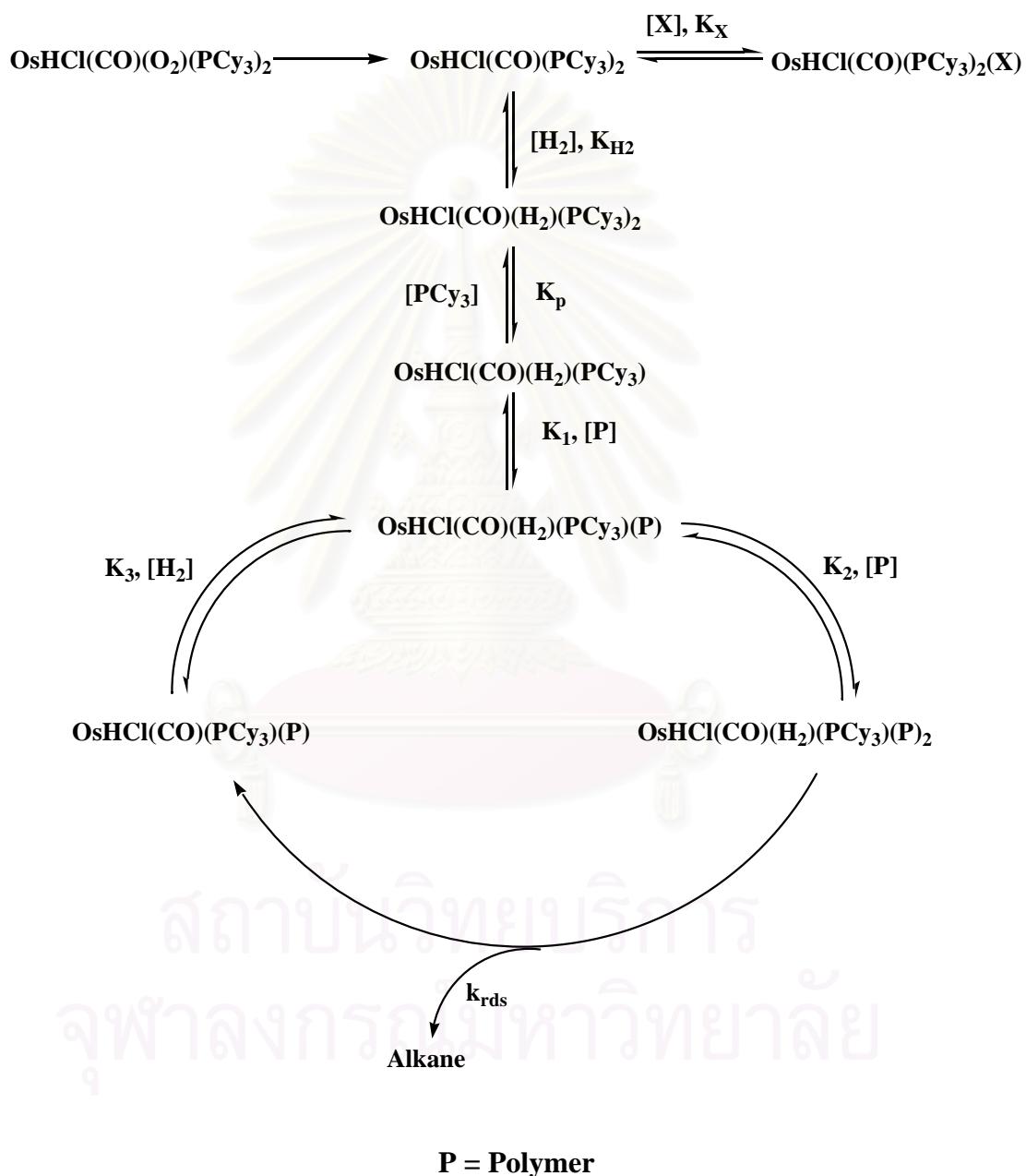
Figure 5.10   Proposed catalytic mechanism for ST-*g*-NR hydrogenation in the presence of $OsHCl(CO)(O_2)(PCy_3)_2$.

The OsHCl(CO(O$_2$)(PCy$_3$)$_2$ catalyst is activated by O$_2$ removal to produce the five–coordinate analogue, OsHCl(CO)(PCy$_3$)$_2$, which is the active species. The reaction begins with the addition of H$_2$ to OsHCl(CO)(O$_2$)(PCy$_3$)$_2$ to give the trihydrido metal complex OsHCl(CO)(H$_2$)(PCy$_3$)$_2$, as shown by eq. (5.3).

$$OsHCl(CO)(O_2)(PCy_3)_2 + H_2 \xleftrightarrow{\text{K}_{\text{H}_2}} OsHCl(CO)(H_2)(PCy_3)_2 + O_2 \qquad (5.3)$$
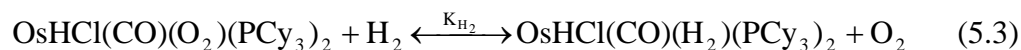
The complex formed in eq. (5.3) subsequently dissociates into a monophosphine complex, then interacts with styryl ring in the polymer grafted chain, followed by second equilibrium in which the olefin entity of another polymer interact with the catalyst as shown in eqs. (5.4) to (5.6).

$$OsHCl(CO)(H_2)(PCy_3)_2 \xleftrightarrow{\text{Kp}} OsHCl(CO)(H_2)(PCy_3) + PCy_3 \qquad (5.4)$$

$$OsHCl(CO)(H_2)(PCy_3) + (P) \xleftrightarrow{\text{K}_1} OsHCl(CO)(H_2)(PCy_3)(P) \qquad (5.5)$$

$$OsHCl(CO)(H_2)(PCy_3)(P) + (P) \xleftrightarrow{\text{K}_2} OsHCl(CO)(H_2)(PCy_3)(P)_2 \qquad (5.6)$$
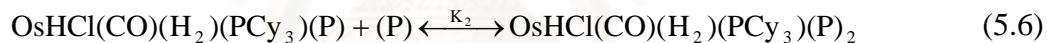
where OsHCl(CO)(H$_2$)(PCy$_3$) represents the catalytic active site, constituted by a transition metal hydride; P represents the double bonds or styryl units of the ST-*g*-NR; OsHCl(CO)(H$_2$)(PCy$_3$)(P)$_2$ corresponds to the activated complex.

The effect of impurities (X) in natural rubber may inhibit the catalytic activity and deactivate the catalyst in ST-*g*-NR hydrogenation. The possible pathway of impurities coordination that could inhibit the catalytic activity is shown in eq. (5.7).

$$OsHCl(CO)(PCy_3)_2 + X \xleftrightarrow{\text{K}_X} OsHCl(CO)(PCy_3)_2(X) \qquad (5.7)$$

Assuming that the complexity of this process can be described by the substituent effect of the styryl ring and the C=C entity within the grafted copolymer as mentioned above, the product from eq. (5.6) is illustrated in Figure 5.9. This

complex contains the styryl and olefin ligands. It can be followed by a rate–determining step to provide the hydrogenated product as shown in eq. (5.8).

$$-\frac{d[C=C]}{dt} = k_{rds}[OsHCl(CO)(H_2)(PCy_3)(P)_2] \qquad (5.8)$$
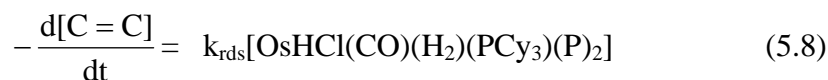
Subsequently, the second hydrogen molecule reacts with $OsHCl(CO)(PCy_3)(P)$ to from the stable 18–electron catalytic species, $OsHCl(CO)(H_2)(PCy_3)(P)$, as shown in eq. (5.9).

$$OsHCl(CO)(PCy_3)(P) + H_2 \xleftrightarrow{\ K_3\ } OsHCl(CO)(H_2)(PCy_3)(P) \qquad (5.9)$$

A material balance on the osmium complex in the catalytic reaction scheme given by eq. (5.10) is a function of the total amount of osmium ($[Os]_T$).

$$[Os]_T = [OsHCl(CO)(PCy_3)_2]+[OsHCl(CO)(H_2)(PCy_3)_2]+[OsHCl(CO)(H_2)(PCy_3)]$$
$$+[OsHCl(CO)(H_2)(PCy_3)(P)]+[OsHCl(CO)(H_2)(PCy_3)(P)_2]+[OsHCl(CO)(PCy_3)(P)]$$
$$+[OsHCl(CO)(PCy_3)_2(X)] \qquad (5.10)$$

All the osmium complex species concentration terms in eq. (5.11) can be converted in term of $OsHCl(CO)(H_2)(PCy_3)(P)_2$ using equilibrium defined in Figure 5.10 which can be substituted into eq. (5.8) to provide the resulting rate law as shown in eq. (5.11). Derivation of the expression is shown in Appendix C.

$$-\frac{d[P]}{dt} = \frac{k_{rds}K_P K_H K_1 K_2 K_3 [H_2][P]^2[Os]_T}{K_3[PCy_3](1+K_H[H_2]+K_X[X])+K_P K_H K_1[P](1+K_3[H_2]+K_2 K_3[H_2][P])+K_P K_H K_3[H_2]} \qquad (5.11)$$

Therefore, the reaction rate equation corresponds to a second–order reaction rate model with respect to the concentration of the double bonds of the polymer. It indicates that the reaction exhibited a first–order dependence on osmium concentration and exhibited a first–order dependence at low hydrogen pressure. The shift to a zero–order dependence on hydrogen at high hydrogen pressure is due to the term of $K_P K_H K_1 K_2 K_3 [H_2][P]^2$ in eq. (5.11). The effect of impurities (X) in grafted natural rubber is an important factor for reduction in the rate of hydrogenation.

5.5 Hydrogenated Styrene-*g*-Natural Rubber Characterization

5.5.1 Fourier Transform Infrared Spectroscopy

From gravimetric calculations, the grafted product consisted of 20 – 25% ungrafted NR, 7 – 10% free PS, 65 – 70% grafted NR. The FTIR spectra of NR, ST-*g*-NR and hydrogenated ST-*g*-NR are shown in Figure 5.11. The FTIR spectrum of ST-*g*-NR showed two intense bands at 760 and 698 cm^{-1}, which are characteristic of the benzene ring. Moreover, the spectrum also displays a peak at 1,664 cm^{-1} corresponding to its C=C stretching vibration. The peaks above 3,000 cm^{-1} are characteristic of a hydrogen bonded to a *sp^2*–hybridized carbon. The FTIR spectrum of the hydrogenated ST-*g*-NR with an 82.3% degree of hydrogenation showed a reduction of the peak at 1,664 cm^{-1}, whereas the peaks of the monosubstituted benzene remained at 760 and 698 cm^{-1}. This indicates that the carbon double bonds were hydrogenated without affecting the aromatic group of styrene.

(a)

>N-H

3285.2 cm⁻¹

C=C   **1664.1 cm⁻¹**   **1530.3 cm⁻¹**   >N-C=O

(b)

Monosubstituted
benzene

760.3 cm⁻¹   **698.5 cm⁻¹**

(c)

% Transmittance

836.4 cm⁻¹   C-H

3500   3000   2500   2000   1500   1000   500

Wavenumber, cm⁻¹
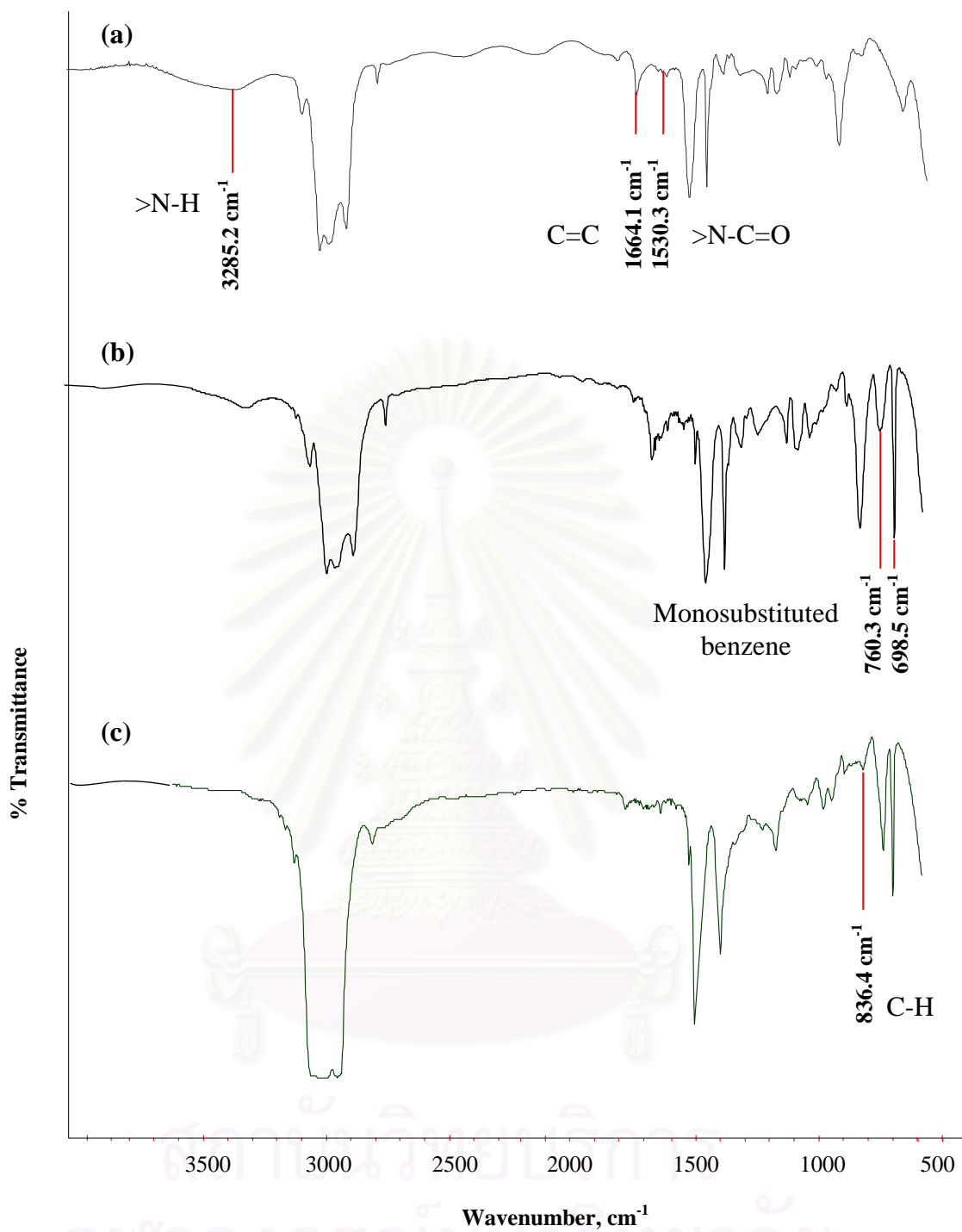
Figure 5.11   FTIR spectra of (a) NRL, (b) ST-*g*-NR and (c) hydrogenated ST-*g*-NR

(82.3% hydrogenation).

5.5.2   Proton NMR (^{1}H–NMR)

^{1}H–NMR spectroscopy can be employed to determine the mole fraction of styrene (ST) in the grafted NR. From calculation, ST-g-NR contained 25.3 mole% of ST. The ^{1}H–NMR spectra of ST-g-NR and hydrogenated ST-g-NR are shown in Figure 5.12. ^{1}H–NMR peaks are attributed to –CH$_3$ (1.64 ppm), –CH$_2$– (2.01 ppm), –aryl protons (6.5 – 8.0 ppm), –C=CH$_2$ (5.15 ppm), and the signal of aliphatic protons of the alkane (0.9 – 1.8 ppm). The peak intensity at 1.64, 2.01, and 5.15 ppm decreased with an increase in the degree of hydrogenation, whereas the peaks of aryl protons in ST-g-NR graft chains remained in the range of 6.5 – 8.0 ppm. It can be concluded that the residual C=C in the natural rubber backbone was hydrogenated without affecting the aromatic ring of the polystyrene graft chain.

5.5.3   Carbon NMR (^{13}C–NMR) and Distortionless Enhancement of Polarization Transfer (DEPT).

The ^{13}C–NMR spectra of ST-g-NR and hydrogenated ST-g-NR are illustrated in Figures 5.13. For the ^{13}C–NMR spectrum of natural rubber, the peaks at 125.1 and 135.3 ppm refer to olefinic carbons (C=C) in the natural rubber backbone. For the ^{13}C–NMR spectrum of ST-g-NR, new absorptions in the range of 127 – 129 ppm were found and attributed to carbons in the aromatic group. After hydrogenation, the ^{13}C-NMR spectrum of hydrogenated ST-g-NR exhibited four new peaks at 37.4, 32.7, 24.3, and 19.6 ppm which are attributed to the typical alkane region. The reduction in olefinic carbons (C=C) peaks indicated that the C=C in the natural rubber backbone was hydrogenated. For ST-g-NR and hydrogenated ST-g-NR, the peaks of the aromatic carbons remained at the same absorption bands. It can be concluded that the OsHCl(CO)(O$_2$)(PCy$_3$)$_2$ resulted in the selective hydrogenation of C=C in the rubber backbone without affecting the monosubstituted benzene group.

The DEPT–135 spectrum of hydrogenated ST-g-NR is used to distinguish –CH$_3$, –CH$_2$–, –CH, and quaternary carbons. The proposed chemical structure of hydrogenated ST-g-NR is illustrated in Figure 5.14.
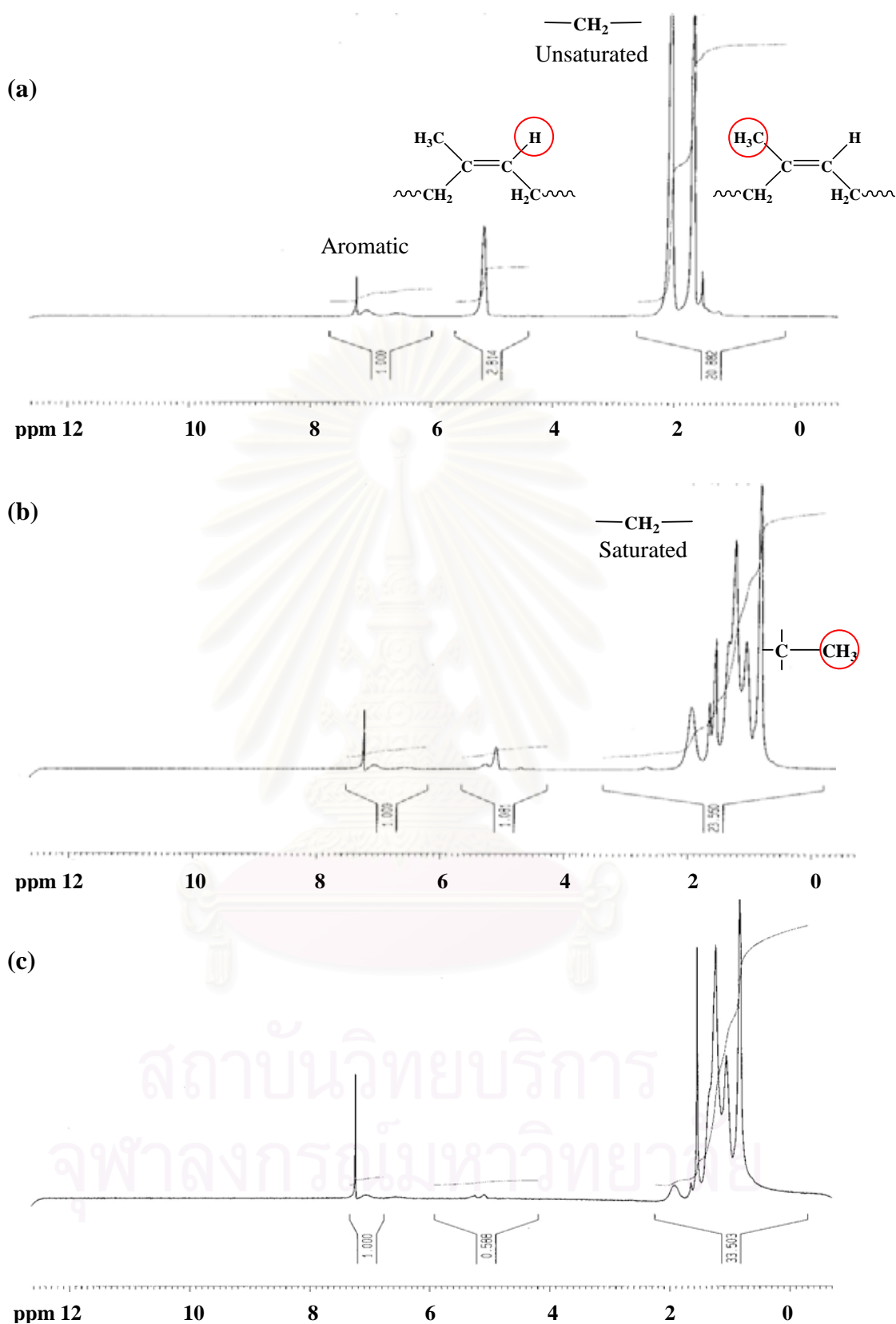
Figure 5.12 ^{1}H–NMR spectra of (a) ST-*g*-NR, (b) hydrogenated ST-*g*-NR (50%

hydrogenation), and (c) hydrogenated ST-*g*-NR (80% hydrogenation).
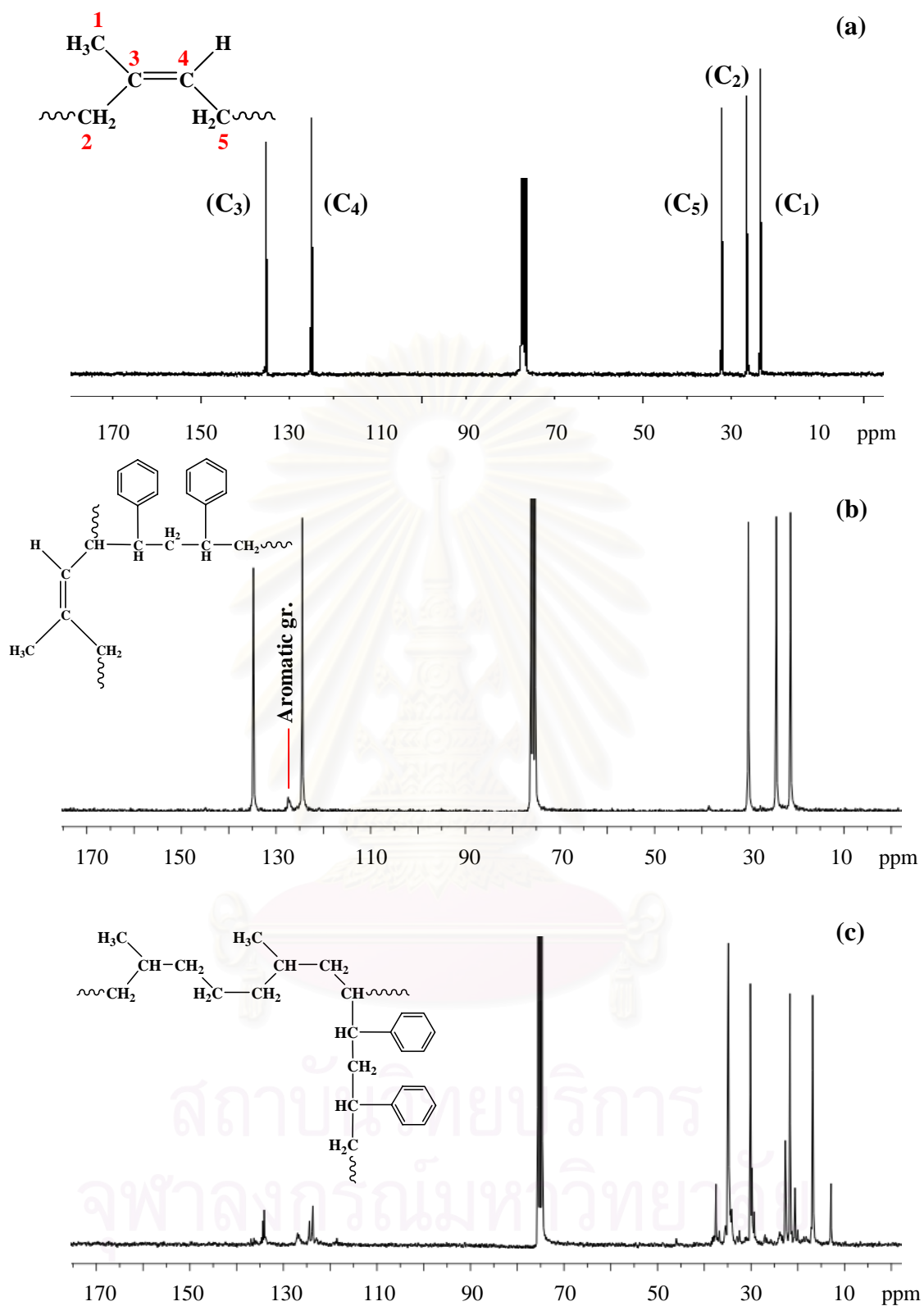
Figure 5.13 ^{13}C–NMR spectra of (a) NR, (b) ST-*g*-NR and (c) hydrogenated ST-*g*-NR (80% hydrogenation).
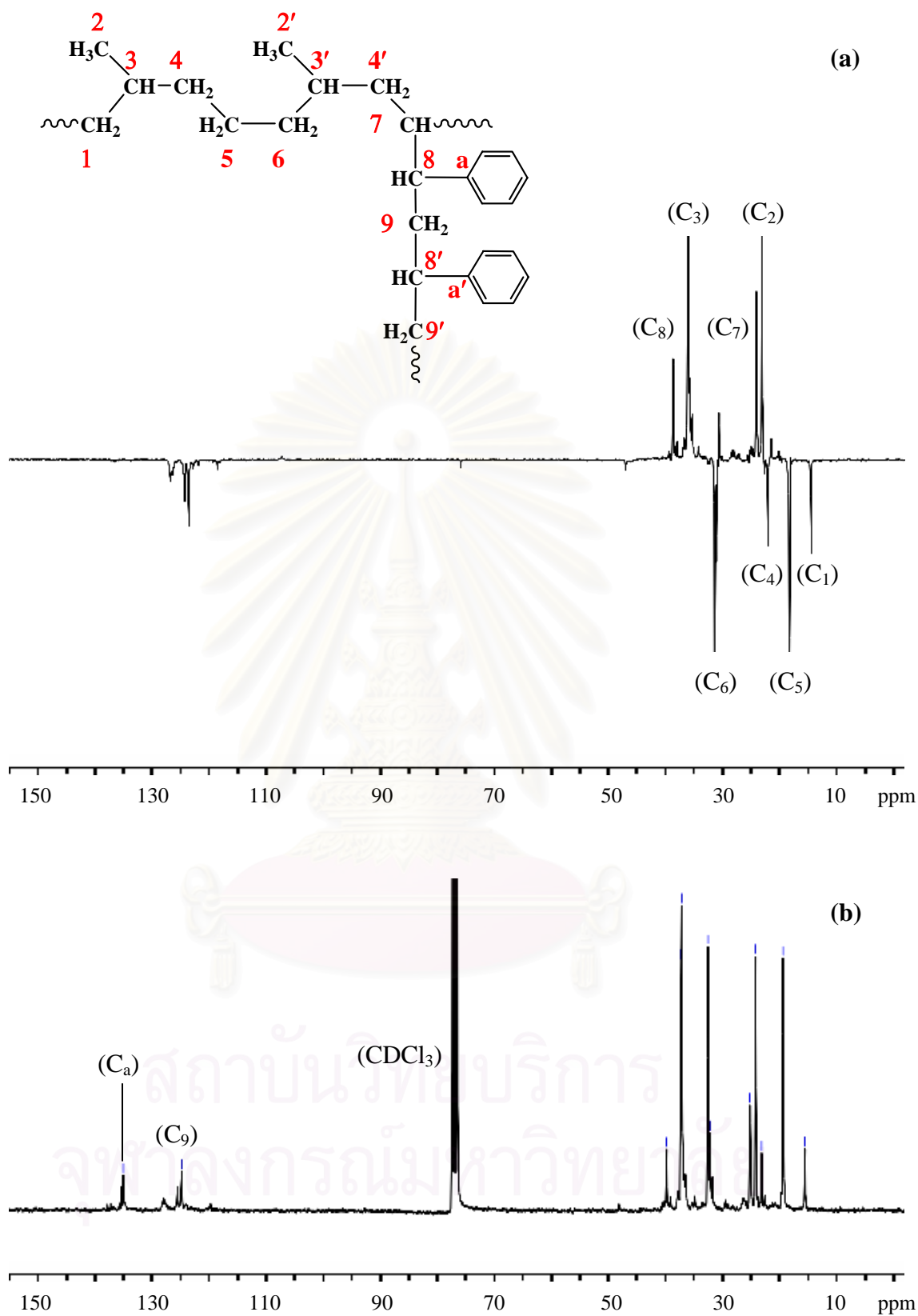
Figure 5.14 NMR spectra of hydrogenated ST-*g*-NR (80% hydrogenation): (a) DEPT−135 spectra and (b) ^{13}C−NMR spectra.

CHAPTER VI

PROPERTIES OF GRAFTED NATURAL RUBBER AND
HYDROGENATED GRAFTED NATURAL RUBBER

In polymer synthesis and its application, the molecular weight and thermal properties of the modified polymer are of prime importance. The modified diene polymer by graft copolymerization leads to the introduction of a functional group onto the polymer backbone. One of the subsequent modifications for the grafted product is the hydrogenation of residual C=C which change the unsaturated rubber backbone toward greater stability against thermal and oxidative degradation. A study of molecular weight and thermal properties is required to understand the performance of the materials for commercial utilization.

This chapter focuses on the investigation of molecular weight and thermal properties of grafted NR (GNR) and hydrogenated grafted NR (HGNR). Molecular weight and molecular weight distribution of modified NR were also determined. The thermal properties of grafted NR and hydrogenated grafted NR were investigated by differential scanning calorimetry (DSC) and thermogravimetric analysis (TGA). DSC provided the low temperature properties of the grafted NR and the hydrogenated grafted NR (glass transition temperature, T_g). The thermal degradation of the samples was obtained from TGA.

6.1 Graft Copolymerization and Hydrogenation of Natural Rubber

For the graft copolymerization of methyl methacrylate (MMA) onto natural rubber using a redox initiator, the gross products consisted of free NR, poly(methyl methacrylate), and graft copolymer (MMA-*g*-NR). On the other hand, the graft copolymerization of styrene (ST) onto NR yielded the gross product containing free NR, polystyrene, and graft copolymer (ST-*g*-NR). Free NR, poly(methyl methacrylate) and polystyrene were extracted from the gross product by extraction with petroleum ether, acetone, and methyl ethyl ketone, respectively, as described in Chapter III.

In Chapter IV and V, the hydrogenation of MMA-*g*-NR and ST-*g*-NR using the homogeneous catalyst, $OsHCl(CO)(O_2)(PCy_3)_2$ was reported. Although a high degree of hydrogenation was achieved in a short period of reaction time (< 10 min), the homogeneous catalyst still remained in the rubber and was difficult to be separated. The color of hydrogenated rubbers, hydrogenated MMA-*g*-NR and hydrogenated ST-*g*-NR, was white. The appearance and color of NR, grafted NR, and hydrogenated grafted NR are also shown in Figure 6.1.

(a) **(b)** **(c)**

(d) **(e)**
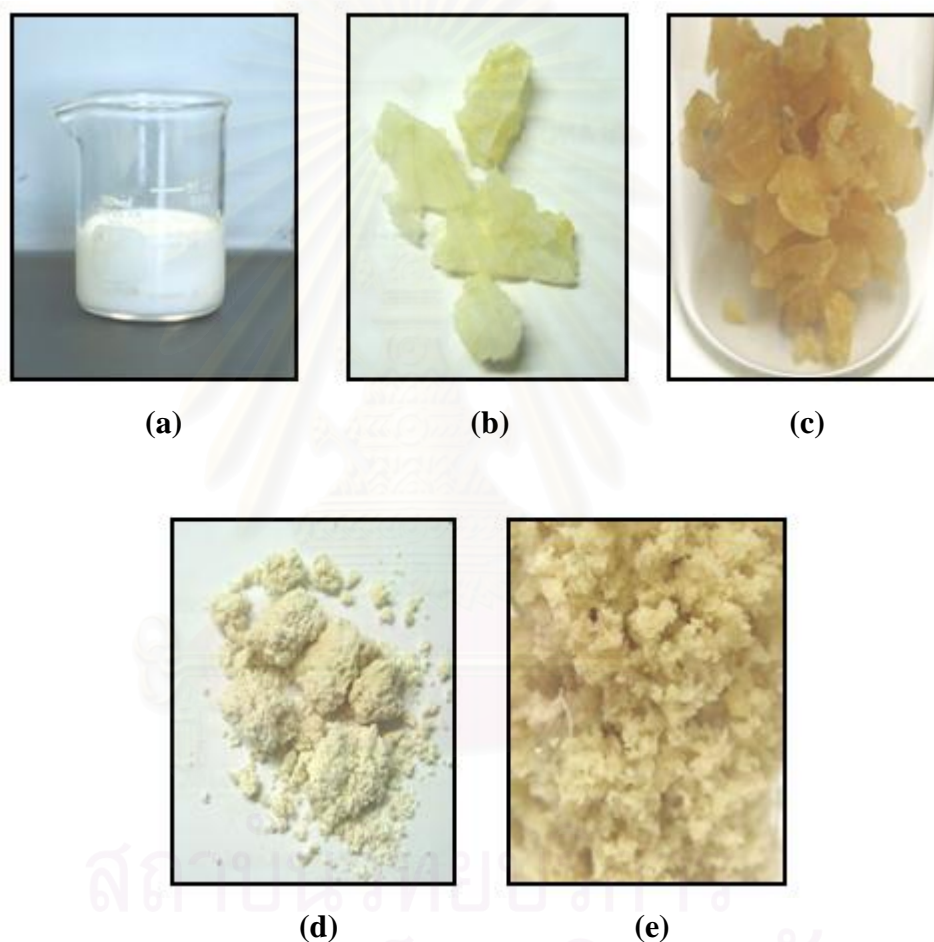
Figure 6.1   Appearance of samples (captured by CCD camera): (a) natural rubber latex, (b) MMA-*g*-NR (25.2% mole MMA), (c) ST-*g*-NR (25.4% mole ST), (d) hydrogenated MMA-*g*-NR (98.4% hydrogenation), and (e) hydrogenated ST-*g*-NR (85.6% hydrogenation).

6.2 Molecular Weight and Molecular Weight Distribution of Modified Natural Rubber

Molecular weight and molecular weight distribution are fundamental characteristics of a polymer material. Gel permeation chromatography (GPC) is a useful separation method for polymers and provides a measure of relative molecular weight [70]. With the exception of proteins and a very few other macromolecules, most polymers exhibit some forms of heterogeneity. The heterogeneity involves a distribution of chemical composition, including statistical, alternating, block, and graft copolymers. The other type of heterogeneity relates to functionality, particular end groups. Most synthetic and natural polymers form random coils and many polymers are branched. Generally, rubber from *Hevea brasiliensis* has a high molecular weight with a broad molecular weight distribution [71]. The gel fraction of the natural rubber latex as the aggregate of phospholipids is in a micellar form (a natural surfactant). When the hydrophobic initiator (CHPO/TEPA) was added, the aggregate state of NR was disturbed slightly because of the same hydrophobic nature and some polymerization could take place to increase the gel content [20]. Gel content increased after the graft copolymerization reaction because some portions of NR formed insoluble crosslinked polymer, which could not be dissolved in either toluene or chloroform for molecular weight determination. Chain scission of any molecule also results in the formation of unstable molecules. The M_n and M_w values of non-crosslinked polymers in the soluble fraction are lower than that of NR because of chain scission or degradation of the polymer [72].

Weight–averaged molecular weight (M_w), number–averaged molecular weight (M_n), and polydispersity index (M_w/M_n or PDI) of NR, grafted NR (MMA-*g*-NR and ST-*g*-NR), and hydrogenated grafted NR obtained from gel permeation chromatography (GPC) are shown in Table 6.1. The M_n, M_w, and PDI of highly hydrogenated MMA-*g*-NR (98% hydrogenation) were lower than that of NR and MMA-*g*-NR samples. This result indicated that the molecular weight of hydrogenated MMA-*g*-NR decreased due to the high reaction temperature of the hydrogenation system. Consequently, the molecular weight distribution of hydrogenated MMA-*g*-NR became nearly unimodal while NR and MMA-*g*-NR had originally a bimodal

molecular weight distribution as illustrated in Figure 6.2. At high acid concentration, ([p–TSA] = 7.0 mM), the gel content and molecular weight of hydrogenated MMA-g-NR were the lowest but the polydispersity index was not greatly changed. It is possible that the high amount of acid concentration possibly caused the chain scission or chain degradation of the polymer chain.

For graft copolymerization of styrene onto natural rubber, the uncrosslinked polymers, ST-g-NR in the soluble fraction had a lower molecular weight, M_w, than NR. After hydrogenation, the gel content of hydrogenated ST-g-NR was decreased due to the crosslink gel in the graft copolymer. The molecular weight, M_w, of hydrogenated ST-g-NR was decreased whereas the degree of hydrogenation did not have any significant effect on M_w. It might be explained that the polymer chain length was changed due to the hydrogenation condition at high temperature (140°C). It can be implied that the hydrogenated grafted copolymer may have formed a branching polymer and retained a high molecular weight. A similar result was also observed for NR hydrogenation in the presence of a Ru complex [38], and an Os complex [24]. This indicated that the highly saturated structure has more resistance to thermal degradation than the unsaturated form.

Table 6.1 Molecular Weight and Molecular Weight Distribution of Rubber Samples

Rubber sample	Hydrogenation (%)	Gel (%)	$M_n \times 10^{-5}$	$M_w \times 10^{-5}$	PDI
NR	-	40.7	3.75	11.60	3.09
MMA-*g*-NR	-	60.9	2.74	7.21	2.63
Hydrogenated MMA-*g*-NR [a]	76.0	55.3	1.54	3.07	1.99
	98.4	53.9	1.26	3.72	2.95
Hydrogenated MMA-*g*-NR [b]	99.5	45.7	0.84	2.26	2.69
ST-*g*-NR	-	70.1	3.58	5.04	1.41
Hydrogenated ST-*g*-NR [c]	56.2	68.0	3.46	5.25	1.48
	98.7	60.4	3.32	4.51	1.36

[a] [Os] = 100 μM, [C=C] = 100 mM, [*p*–TSA] = 2.0 mM, P_{H2} = 27.2 bar, and T = 140°C in monochlorobenzene.

[b] [Os] = 100 μM, [C=C] = 100 mM, [*p*–TSA] = 7.0 mM, P_{H2} = 27.2 bar, and T = 140°C in monochlorobenzene.

[c] [Os] = 100 μM, [C=C] = 260 mM, [*p*–TSA] = 4.0 mM, P_{H2} = 27.2 bar, and T = 140°C in monochlorobenzene.

(a)

Natural Rubber

MMA-*g*-NR

Hydrogenated MMA-*g*-NR

Slice Log MW

(b)

Natural Rubber

ST-*g*-NR

Hydrogenated ST-*g*-NR

Slice Log MW

(c)

Hydrogenated MMA-*g*-NR (15.3%)

Hydrogenated MMA-*g*-NR (76.0%)

Hydrogenated MMA-*g*-NR (99.5%)

Slice Log MW
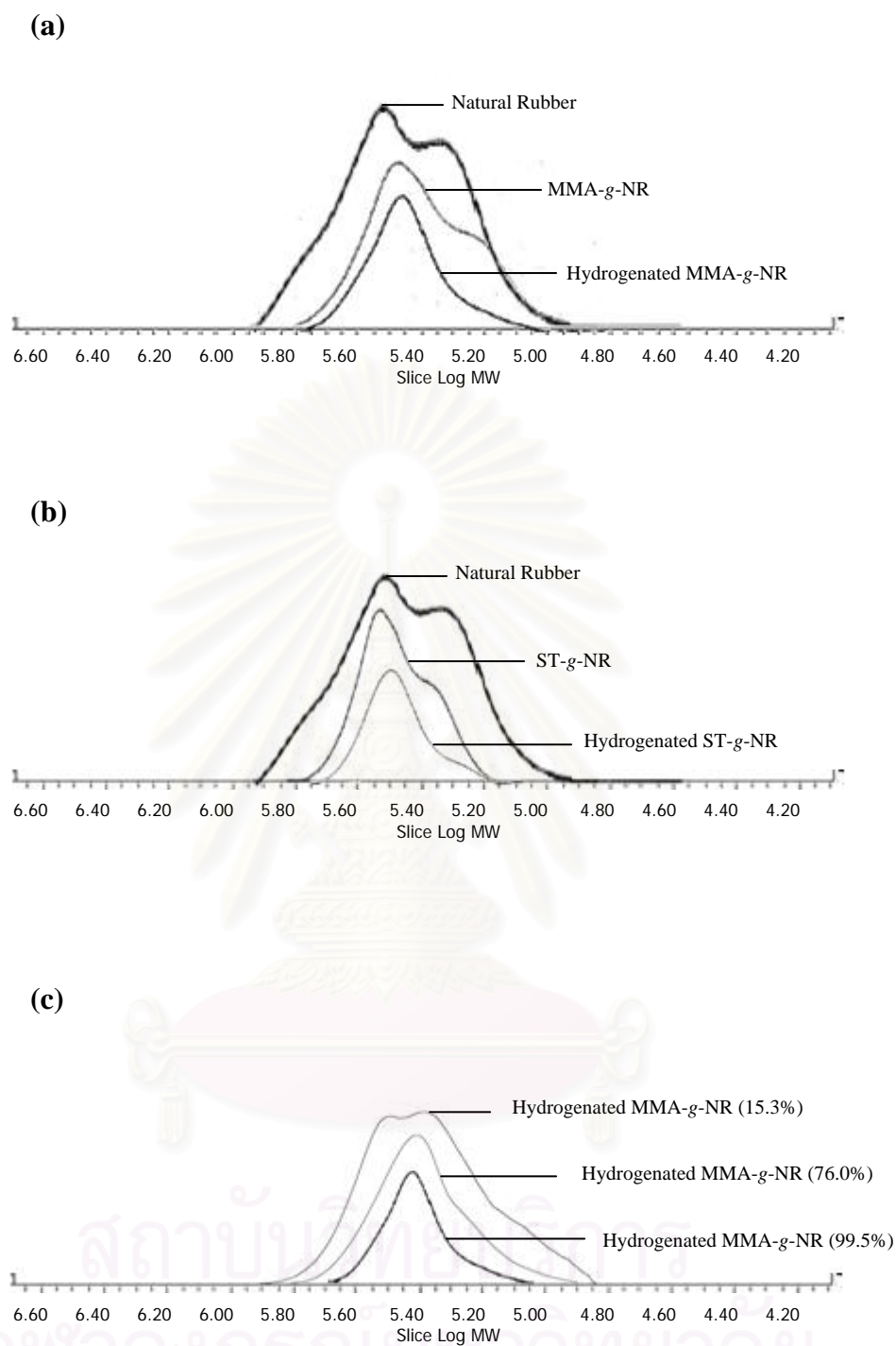
Figure 6.2   GPC chromatograms of natural rubber samples before and after modification: (a) NR grafted with MMA and (b) NR grafted with ST and (c) hydrogenated MMA-*g*-NR (15.3%, 76.0% and 99.5% hydrogenation).

6.3 Glass Transition Temperature and Decomposition Temperature

Thermal analysis is used to investigate the thermal properties of the polymer as a function of temperature. These experiments were carried out using a differential scanning calorimeter (DSC) and a thermal gravimetric analysis (TGA) apparatus to obtain the glass transition temperature (T_g), initial decomposition temperature (T_{id}), and maximum decomposition temperature (T_{max}). Glass transition temperature (T_g) is the transition related to the motion in the amorphous section of polymer. It is determined from the mid point of the base line shift of the DSC thermogram. TGA of the samples was conducted under a nitrogen atmosphere. T_{id} was determined from the intersection of two tangents at the onset of the decomposition temperature. T_{max} was obtained from the maximum peak of the derivative of the TGA curves. T_g, T_{id} and T_{max} of NR, grafted NR and hydrogenated grafted NR are presented in Table 6.2.

Graft copolymers consisted of rubber as backbone with a graft chain. It should exhibit two widely separated glass transition temperatures. From the DSC thermogram of the grafted rubber, a two step base–line shift was exhibited. For natural rubber, the lower glass transition temperature is −62.3°C and the upper glass transition temperature is 95 − 110°C for PMMA and 90 − 100°C for polystyrene (Figure 6.3). For hydrogenated samples (hydrogenated MMA-*g*-NR and hydrogenated ST-*g*-NR) at various degrees of hydrogenation (Figures 6.4 and 6.5), the glass transition temperature of NR backbone was slightly increased with an increase in the level of hydrogenation. The glass transition temperature of the hydrogenated grafted natural rubber was also compared with *cis*−1,4−polyisoprene (CPIP) and ethylene−propylene rubber (EPDM: Nordel 4640). It can be concluded that the T_g of the amorphous rubber phase was increased by up to 20°C which is close to the T_g of EPDM. It is possible that the amorphous segments in the hydrogenated grafted NR were changed into crystalline units. The results suggest that the hydrogenated grafted NR has a higher degree of crystallinity within the polymer structure than grafted NR. However, DSC curves in Figure 6.4 and 6.5 also showed the changes over temperature range of 77 − 83°C. This is due to the motion of the low-molecular weight components of a polymer with a broad-weight distribution.

Table 6.2 Glass Transition Temperature and Decomposition Temperature of Rubber Samples

Rubber sample	Hydrogenation (%)	T_g (°C)	T_{id} (°C)	T_{max} (°C)
CPIP	-	-59.0	359.2	384.0
NR	-	-62.3	357.2	380.9
EPDM [a]	-	-43.3	455.1	473.4
MMA-*g*-NR [b]	-	-62.8	364.0	391.9
Hydrogenated MMA-*g*-NR [c]	76.0	-59.9	371.4	451.0
	98.4	-59.2	373.8	469.9
ST-*g*-NR [d]	-	-61.9	331.0	391.2
Hydrogenated ST-*g*-NR [e]	56.2	-60.1	366.5	454.9
	98.7	-58.5	380.4	453.0

[a] Ethylene−propylene copolymer (EPDM) has the ratio of ethylene/propylene as 55/45 and molecular weight 160,000 with medium molecular weight distribution.

[b] Graft copolymer of methyl methacrylate onto natural rubber with approximately 25% mole of MMA.

[c] [Os] = 100 μM, [C=C] = 100 mM, [*p*−TSA] = 2.0 mM, P_{H2} = 27.2 bar, and T = 140°C in monochlorobenzene.

[d] Graft copolymer of styrene onto natural rubber with approximately 25% mole of PS.

[e] [Os] = 100 μM, [C=C] = 260 mM, [*p*−TSA] = 4.0 mM, P_{H2} = 27.2 bar, and T = 140°C in monochlorobenzene .
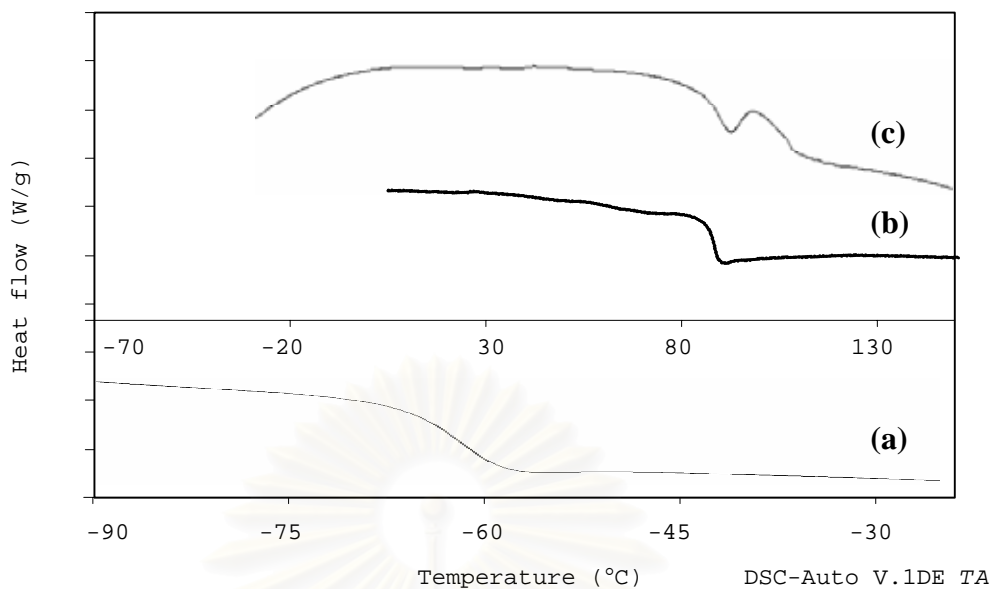
Figure 6.3   DSC thermograms of polymer samples: (a) natural rubber, (b) polystyrene and (c) poly(methyl methacrylate).
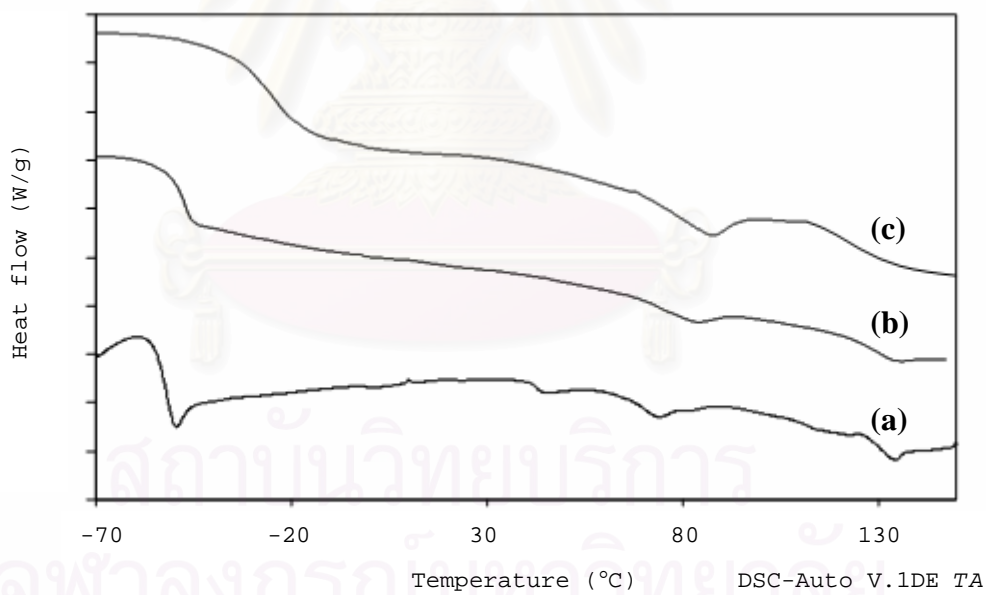
Figure 6.4   DSC thermograms of rubber samples: (a) MMA-*g*-NR, (b) hydrogenated MMA-*g*-NR (76.0% hydrogenation) and (c) hydrogenated MMA-*g*-NR (98.4% hydrogenation).
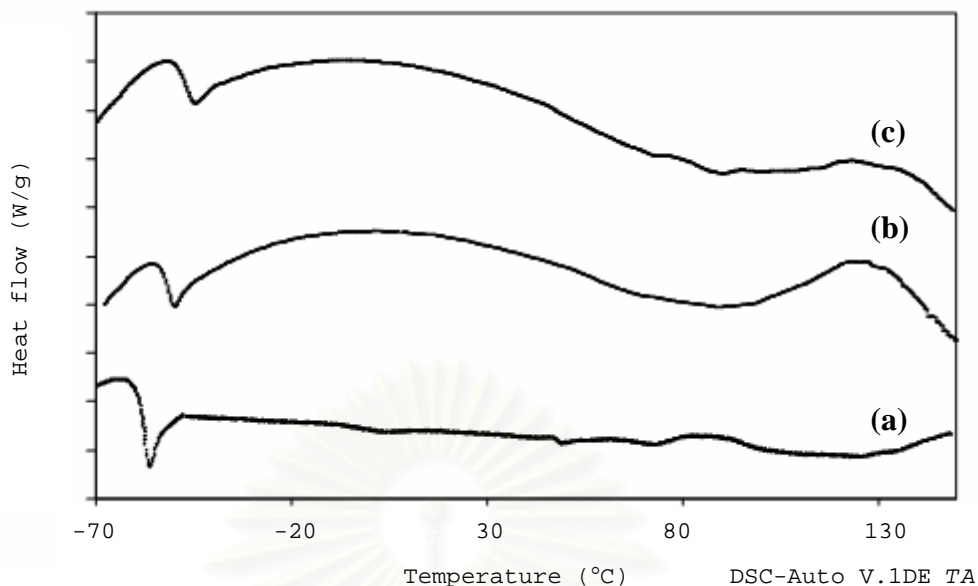
Figure 6.5   DSC thermograms of rubber samples: (a) ST-*g*-NR, (b) hydrogenated ST-*g*-NR (56.2% hydrogenation) and (c) hydrogenated ST-*g*-NR (98.7% hydrogenation).

From the TGA thermograms (Figures 6.6 and 6.7), the weight loss occurred between 330 – 460°C due to the loss of volatile matter contained within the polymer. The results indicated that the thermal degradation of grafted NR, MMA-*g*-NR and ST-*g*-NR, under a nitrogen atmosphere is a one-step reaction because the TGA curves of the samples show only a one-step change and provide a smooth weight loss curve. These results are similar to the thermal properties behavior of MMA-*g*-NR, reported by Peng et al. [73]. T_{id} and T_{max} of hydrogenated graft NR samples increased with an increase in the reduction of the amount of carbon–carbon double bonds. Therefore, the hydrogenation can improve the thermal stability of grafted NR by converting the weak π bond within the grafted NR backbone to the stronger C–H σ bond [31].
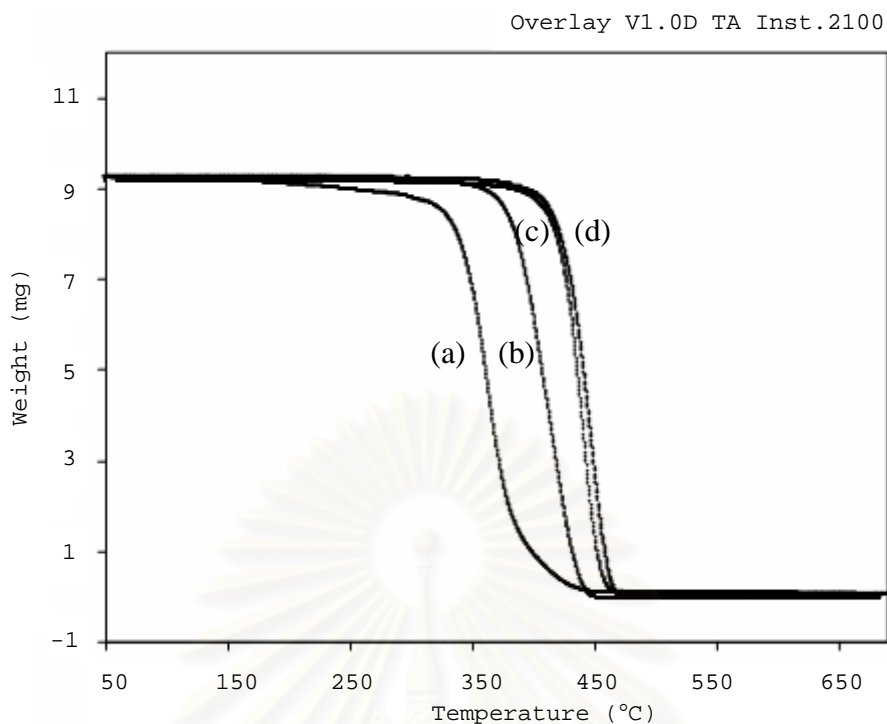
Figure 6.6 TGA thermograms of rubber samples: (a) NR, (b) MMA-*g*-NR, (c) hydrogenated MMA-*g*-NR (76.0% hydrogenation) and (d) hydrogenated MMA-*g*-NR (98.4% hydrogenation).
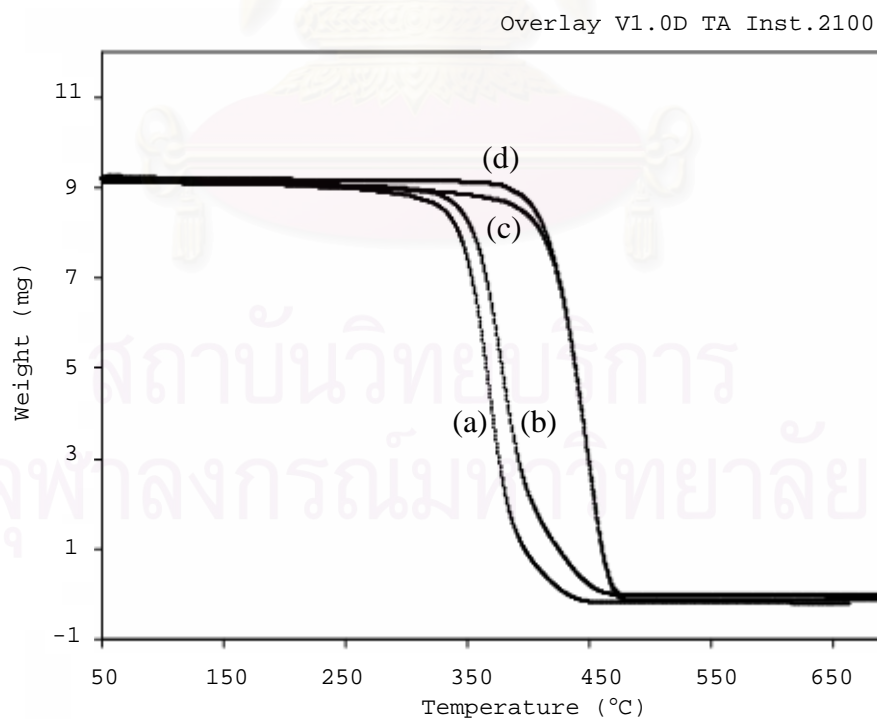
Figure 6.7 TGA thermograms of rubber samples: (a) NR, (b) ST-*g*-NR, (c) hydrogenated ST-*g*-NR (56.2% hydrogenation) and (d) hydrogenated ST-*g*-NR (98.7% hydrogenation).

CHAPTER VII

PROPERTIES OF THERMOPLASTIC AND ELASTOMER
BLENDS

Polymer blends are a popular form of new thermoplastic engineering materials and constitute a rapidly changing field. A thermoplastic elastomer (TPE) is a blend of rubber and thermoplastic and most probably the fastest growing sector in the polymer market. The stiffness of the rubber is increased with the incorporation of plastic into the rubber matrix. Usually TPEs and rubber modified thermoplastics are of multi−phase polymer systems consisting of hard and soft domains which can be copolymers [74]. The microphase separation into domains of an appropriate molecular architecture leads to materials possessing unique and technologically useful physical properties. The rubber phase is partially cross−linked and thereby produces a morphology involving microphase separation responsible for the unique properties of the material. In many rubber or plastic blends, the homogeneity is assessed from the position of the glass transition temperature, T_g, of the blend where a compatibilized blend will show a single T_g within the two T_g's of the components [75].

According to the modification of natural rubber latex (NRL) by graft copolymerization, the chemical structure of natural rubber has been changed. For MMA-g-NR and ST-g-NR graft copolymer, the chemical structure consisted of the MMA graft chain and ST graft chain, respectively. After hydrogenation of grafted natural rubber, the chemical structure of the NR backbone was converted from the unsaturated structure to a saturated form, providing an alternating ethylene−propylene copolymer. The hydrogenated grafted NR can be used as a compatibilizer for thermoplastic/elastomer blending.

Non−reactive compatibilization is the classical approach to compatibilize immiscible polymer blends. A well−selected copolymer bearing two distinct segments, typically a block or graft copolymer, will be located preferentially at the interfaces. In this chapter, the compatibility of ethylene−propylene rubber

(EPDM) and plastic (PMMA or PS) in blends by adding hydrogenated grafted NR were investigated. The effect of compatibilizer and blend ratio on the mechanical and morphological properties of the blends was also studied.

7.1 Mechanical Properties of Thermoplastic/Elastomer Blends

The mechanical properties of thermoplastic/elastomer blends with compatibilizer addition are required to understand its performance for commercial utilization. It is well known that brittle thermoplastics such as poly(methyl methacrylate) (PMMA) and polystyrene (PS) can be toughened by the addition of a rubber phase. Ethylene–propylene–diene monomer or ethylene–propylene rubber (EPDM) has outstanding resistance to heat, light, oxygen, and ozone attributed to its non–conjugated diene polymer. Blending of PMMA/EPDM and PS/EPDM result in brittle/ductile combination. These blends may not result in a toughened plastic because of the immiscibility of two components. However, an introduction of graft copolymer as a compatibilizer leads to improving the interfacial tension between the two phases of the polymers. The hydrogenated MMA-*g*-NR (HGMMA) and hydrogenated ST-*g*-NR (HGST) was used as compatibilizer in PMMA/EPDM and PS/EPDM blend, respectively. The effect of compatibilizer content on mechanical properties of the blend such as tensile strength, % elongation, hardness and impact energy was investigated.

7.1.1 PMMA/EPDM/ Hydrogenated MMA-*g*-NR

Figure 7.1 shows the effect of blend ratios on mechanical properties of PMMA/EPDM blends without compatibilizer. The tensile strength decreased with an increase in rubber content as shown in Figure 7.1(a). The maximum tensile strength of PMMA/EPDM was exhibited at a PMMA/EPDM ratio of 95/5 (w/w). This implies that the high EPDM content (10 − 30 part, based on total weight of the blend) provided an immiscible blend with phase separation. From Figure 7.1(b), the elongation at break increased with an increase in EPDM content and then decreased when EPDM content was over 10 part. At a high EPDM content, the decreased in elongation was due to immiscibility of the blends. From Figure 7.1(c), hardness

decreased with an increase in EPDM content. The lower hardness indicated that the blended samples are of a nature soft due to the high rubber content. For the impact strength of PMMA/EPDM blend, Figure 7.1 (d) showed that the high loading of EPDM might cause poor mechanical properties due to an increase in immiscibility of the thermoplastic and rubber blend.

Copolymers have been widely used as compatibilizing agents in polymer blends due to the functionality of the different parts of the molecule that can physically and/or chemically interact with the different components of the blend. The hydrogenated grafted NR could be used as compatibilizer in PMMA/EPDM blend. The effect of hydrogenated MMA-*g*-NR (HGMMA) content on tensile strength of PMMA/EPDM blends (80/20 and 95/5) was investigated. From Figure 7.2 (a), the tensile strength of the samples slightly decreased and then increased with an increase in HGMMA content. At low HGMMA content, the reduction of tensile strength was due to the immiscibility of the polymer phases. The blends with high HGMMA content resulted an increase in tensile strength. The addition of HGMMA could promote the homogeneity of the blend and provide greater compatibility.

Elongation at break of PMMA/EPDM blends (80/20 and 95/5) with HGMMA addition (2 – 10 part) were slightly increased with an increase in HGMMA content as illustrated in Figure 7.2 (b). The elongation of the blend at ratio of 80/20 exhibited higher elongation at break than that of the blend at ratio of 95/5. This is due to the effect of the rubber content in the blends, which caused the higher elongation at break. As mentioned above, the addition of HGMMA gave more homogeneity of the PMMA/EPDM blends. Thus, the elongation at break of the blends at high HGMMA content was improved.

Hardness testing is used to measure the indentation of a polymer under a compression load. The hardness of the PMMA/EPDM blends containing HGMMA (2 – 10 part) decreased with an increase in rubber content (Figure 7.2 (c)). The hardness of PMMA/EPDM blends at ratio of 95/5 was also found to be higher than that of blends at ratio of 80/20. It can be concluded that a high rubber content in

thermoplastic/elastomer blends exhibited a soft polymer characteristic compared with hard characteristic of PMMA as the pure component.

Impact strength is one of the many quantities used to characterize the strength of material. The impact test method measures the energy required to break a notched specimen. The influence of HGMMA content on the impact energy of PMMA/EPDM blend is shown in Figure 7.2 (d). The notched Charpy impact strength of the blends continues to increase with the HGMMA content. This implies that the brittle PMMA polymer was toughened by EPDM rubber in the presence of the HGMMA compatibilizer. It can be concluded that the impact behavior of PMMA/EPDM blends can be improved considerably by HGMMA addition.
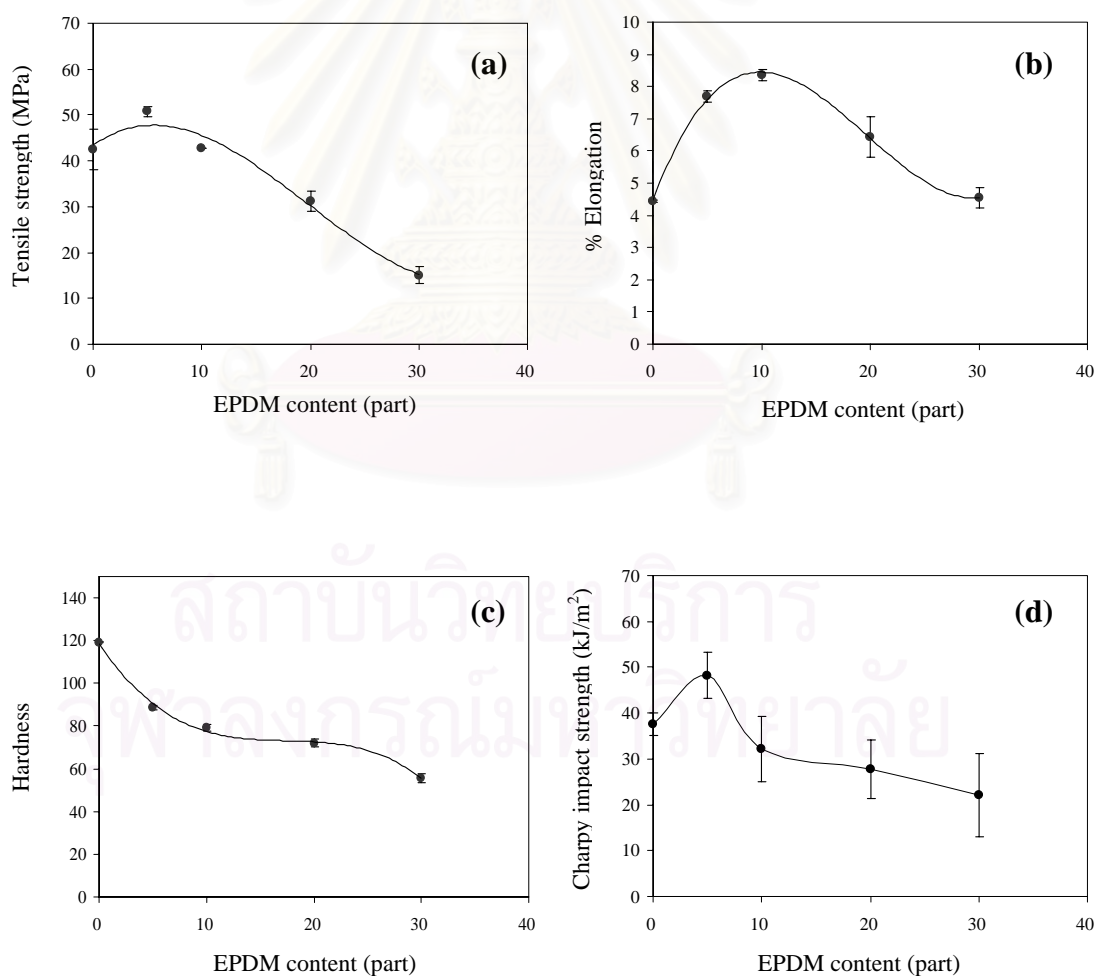
Figure 7.1 Mechanical properties of PMMA/EPDM blend.
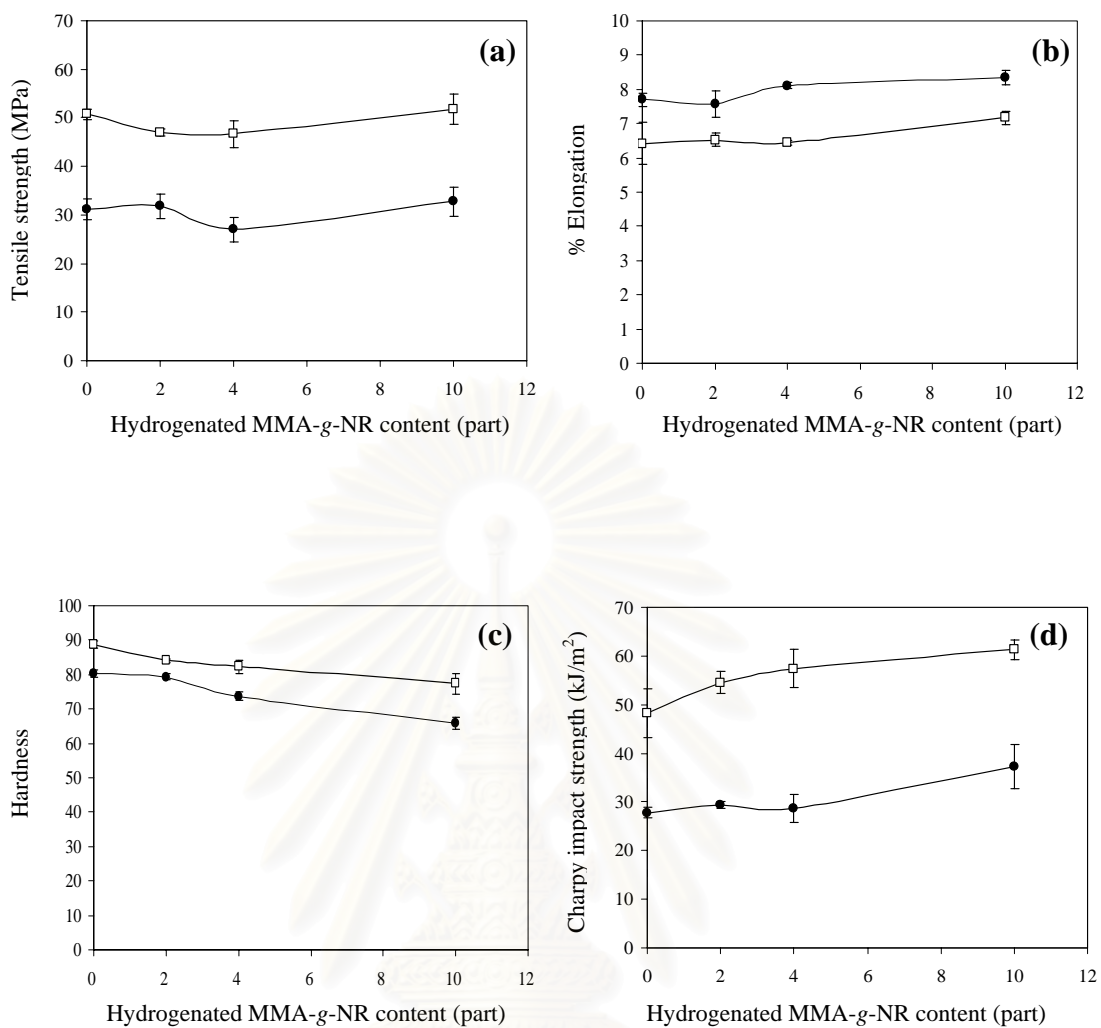
Figure 7.2 Effect of hydrogenated MMA-*g*-NR content on the mechanical properties of PMMA/EPDM blends at ratios of 80/20(●); and 95/5(□).

7.1.2 Polystyrene/Ethylene Propylene Rubber/Hydrogenated ST-*g*-NR

The results of tensile strength, elongation, hardness and impact strength for PS/EPDM and PS/EPDM/hydrogenated ST-*g*-NR (HGST) blends are illustrated in Figure 7.3 and Figure 7.4, respectively. For PS/EPDM blends, although PS and EPDM are immiscible and incompatible over the whole composition range, the PS/EPDM binary blends exhibited modified mechanical properties between PS and EPDM, which showed higher tensile strength at the blend ratio of 90/10 (Figure 7.3 (a)). However, the modified structure became worse and was finally broken with a continuous increase of EPDM content, which resulted in a higher incompatibility of EPDM and the hard segments of PS. As illustrated in Figure 7.3 (b), the elongation of both PS/EPDM blends tends to increase with increasing EPDM content up to 40 part. It can be concluded that the EPDM–rich blends containing EPDM content above 10 part exhibited a higher elongation than the PS homopolymer. From Figure 7.3 (c), the hardness of the PS/EPDM blend decreased with an increase in EPDM content. From Figure 7.3 (d), the impact strength of PS/EPDM blends increased with an increase in EPDM content. This is due to the incompatibility between PS and EPDM at high EPDM content. It is clearly shown that the interfacial adhesion is an important factor in rubber toughening.

To investigate the compatibility of a PS/EPDM blend, the hydrogenated ST-*g*-NR (HGST) as a compatibilizer was employed in the PS/EPDM blend at weight ratio of 80/20 and 90/10. The tensile strength of the PS/EPDM/HGST blends with different HGST levels are shown in Figure 7.4 (a). With the incorporation of the rubber phase in the thermoplastic matrix, tensile strength of PS/EPDM blends decreased with increasing EPDM content. Here, the PS/EPDM/HGST exhibited better adhesion than that of the PS/EPDM blends is observed due to the presence of HGST content at the interface of two phases, which is the contributing factor for the improvement of tensile strength.

From Figure7.4 (b), the elongation at break of PS/EPDM/HGST blends slightly decreased with an increase in HGST content. It is noted that the

addition of HGST (2 − 10 part) to the PS/EPDM blends (70/30 and 90/10 blend ratios) did not significantly affect for the elongation at break. Figure 7.4 (c) showed that the hardness of ternary blends (PS/EPDM/HGST) decreased with an increasing rubber content. Figure 7.4 (d) presents the relationship between the impact strength of PS/EPDM blends and the HGST content. With the addition of 2 −10 part of HGST, the PS/EPDM/HGST ternary blends presented higher impact properties than the uncompatibilized PS/EPDM blends. It is evident that the interfacial adhesion between PS and EPDM can be significantly improved by the HGST addition. Hence, as the impact strength increased, the strength of PS/EPDM increased due to the interaction of the HGST.
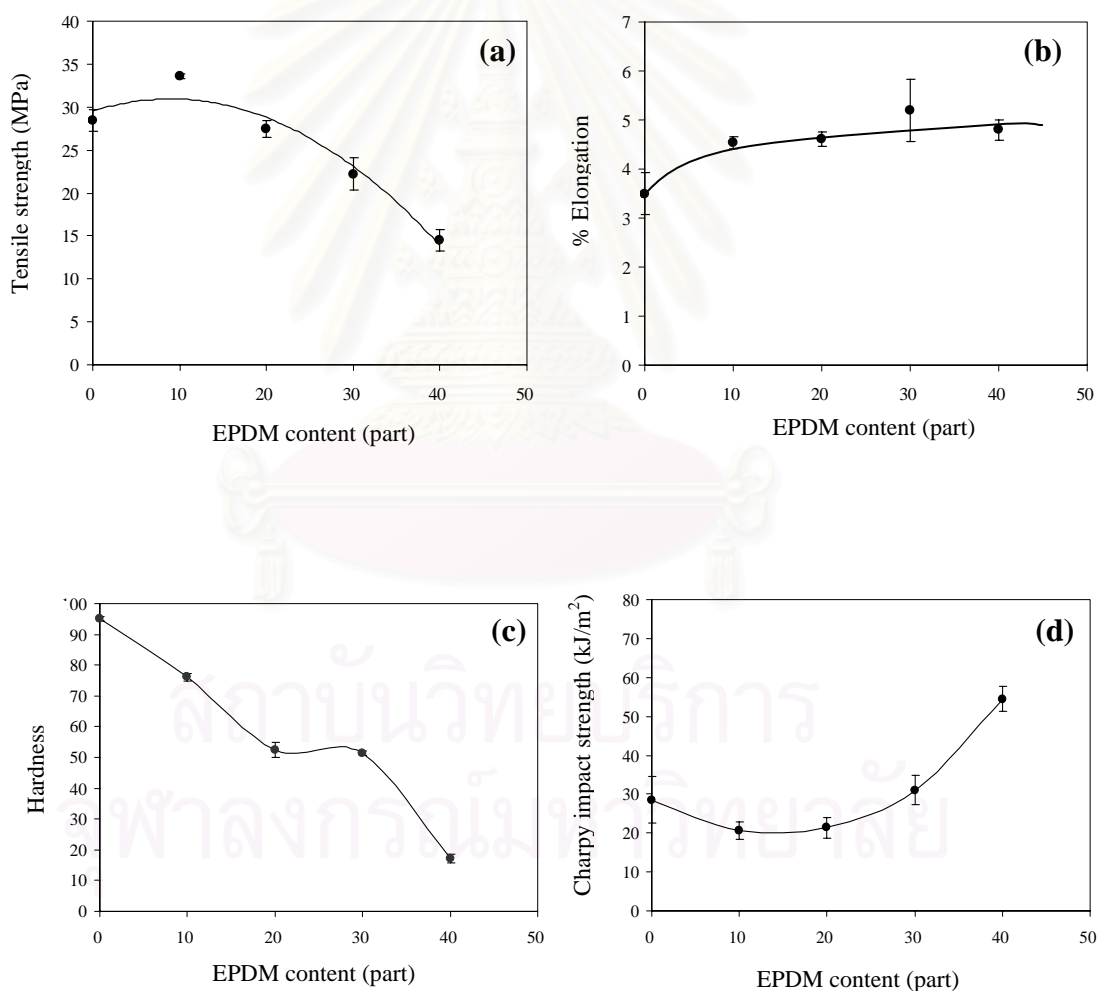
Figure 7.3 Mechanical properties of PS/EPDM blend.
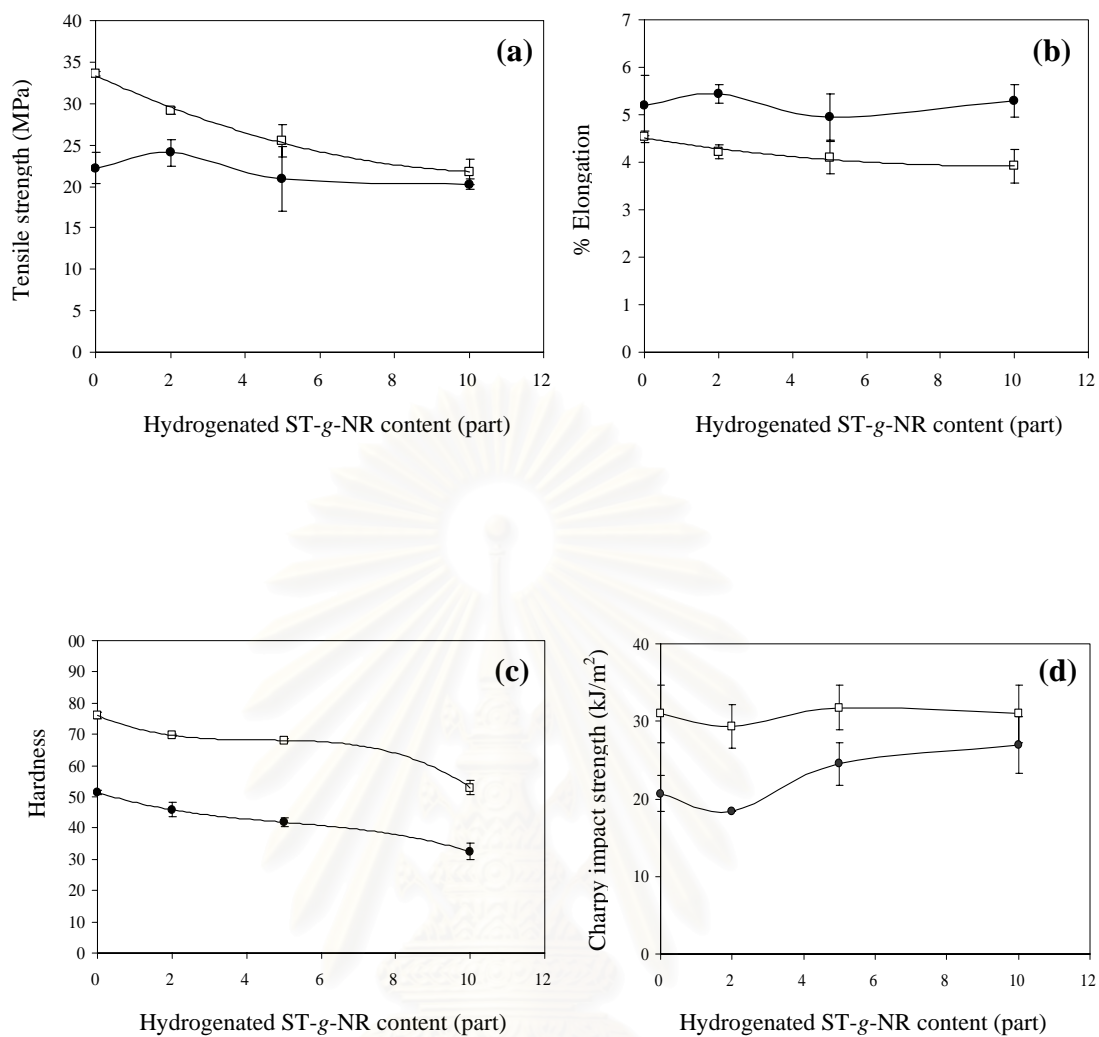
Figure 7.4 Effect of ST-*g*-NR and hydrogenated ST-*g*-NR content on the mechanical properties of PS/EPDM blends at ratios of 70/30 (●); and 90/10 (□).

7.2 Morphological Study

The properties of the blend depend not only on the mechanical behavior of the interface, but also on the size of the respective polymer phases. It is known that the size of dispersed particles has a dramatic effect on deformation behavior in ductile dispersed phase/brittle matrix systems. Therefore, the scanning electron microscopy (SEM) technique was employed to investigate the morphology of the PMMA/EPDM blends. Figures 7.5 − 7.9 clearly indicated the surface morphology of various blends compared with pure poly(methyl methacrylate) (PMMA) and pure polystyrene (PS). The fracture surfaces of pure PMMA and PS showed a rigid and glassy surface (Figure 7.5). For PMMA/EPDM blend, the fracture surfaces exhibited two phases of morphology as shown in Figures 7.6 (a) and 7.7 (a) for the PMMA/EPDM ratio of 80/20 and 95/5, respectively. The morphology of the blends showed two phases with irregular domain sizes and shapes. This could be explained by the immiscible blends of PMMA and EPDM. The immiscible polymers formed coarse mixtures with comparatively large domain sizes (up to 10 μm). Therefore, this system requires a compatibilizer during the blending process to reduce the interfacial tension between the different phases of the polymers. At high interfacial tension, the morphology of the blends showed a large size of the dispersed rubber phase. The morphology of fracture surface observations of the PS/EPDM blends (70/30, Figure 7.8 (a) and 90/10, Figure 7.9 (a)) are similar with the PMMA/EPDM blends.

Morphology of PMMA/EPDM blends with the addition of hydrogenated MMA-*g*-NR (HGMMA) are presented in Figures 7.6 (b) − (d) and 7.7 (b) − (d). It can be seen that the average size of the dispersed phase particles decreased by the addition of HGMMA (2 − 10 parts). It was also observed that the dispersed particles showed more spherical shape and smaller uniform size (< 0.1 − 2 μm) when the amount of added HGMMA was increased. It can be seen that HGMMA acted as compatibilizer for the PMMA/EPDM blends. This is a result in that the HGMMA contains a methacrylate group which is similar to PMMA and contains an alternate ethylene−propylene part which is similar to EPDM. Each segment will penetrate into the phase, which has a specific affinity. This would reduce the interfacial tension, enhance the interfacial adhesion, promote dispersion of the

dispersed phase in the matrix, and stabilize the morphology of the blend. The increase in impact energy of the compatibilized blends is in agreement with this expectation.

The morphology study of PS/EPDM blends with the addition of hydrogenated ST-*g*-NR (HGST) is presented in Figures 7.8 (b) − (d) and 7.9 (b) − (d). It was found that the blend morphology contained both irregular shapes and spherical shapes. The addition of HGST promoted the phase dispersion in the blends. The chemical structure of HGST contains a styrenic group that is similar to PS and contains an alternate ethylene–propylene part in the rubber backbone that is similar to EPDM. This similar result is also observed for PMMA/EPDM blends with the addition of hydrogenated MMA-*g*-NR as mentioned above.

It can be concluded that the addition of a suitable compatibilizer into an immiscible polymer blend enhanced the interfacial adhesion between the two phases. The decrease in the particle size increased the interfacial surface between the rubber particles and the PMMA or PS matrix. These surface interactions help to bind the different phases together or to increase the adhesion of component particles in the matrix. A modified polymer with various functional groups attached could behave like a copolymer where the different functional groups act as interaction points leading to a chemical or physical interaction between the incompatible components of the blend.
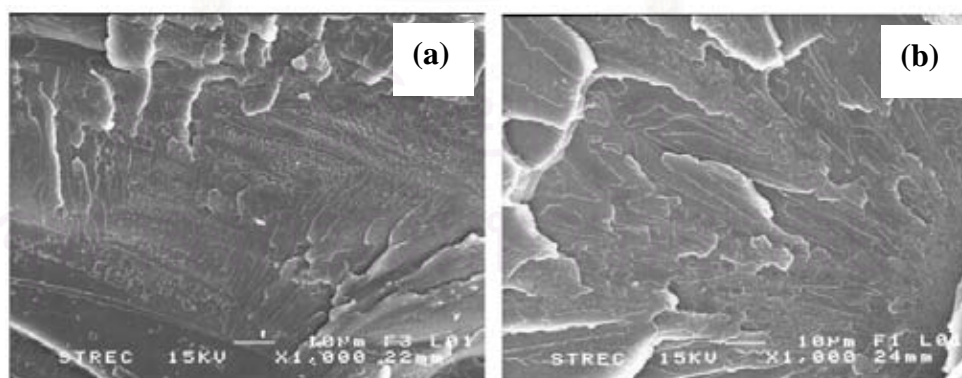
Figure 7.5   Scanning electron micrographs of tensile fracture surfaces of
(a) PMMA and (b) PS (magnification×1000).
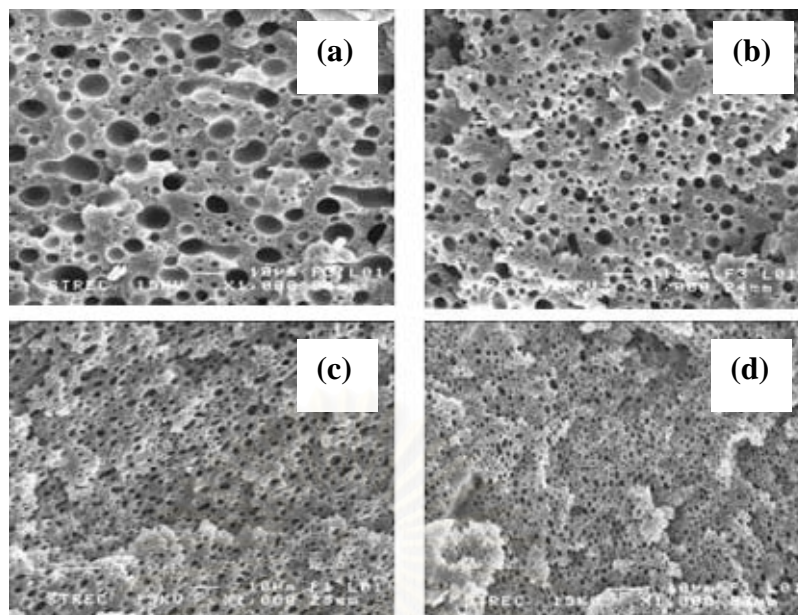
Figure 7.6 Scanning electron micrographs of tensile fracture surfaces of PMMA/EPDM (80/20) blends containing various hydrogenated MMA-*g*-NR contents: (a) 0, (b) 2, (c) 4 and (d) 10 parts (magnification×1000).
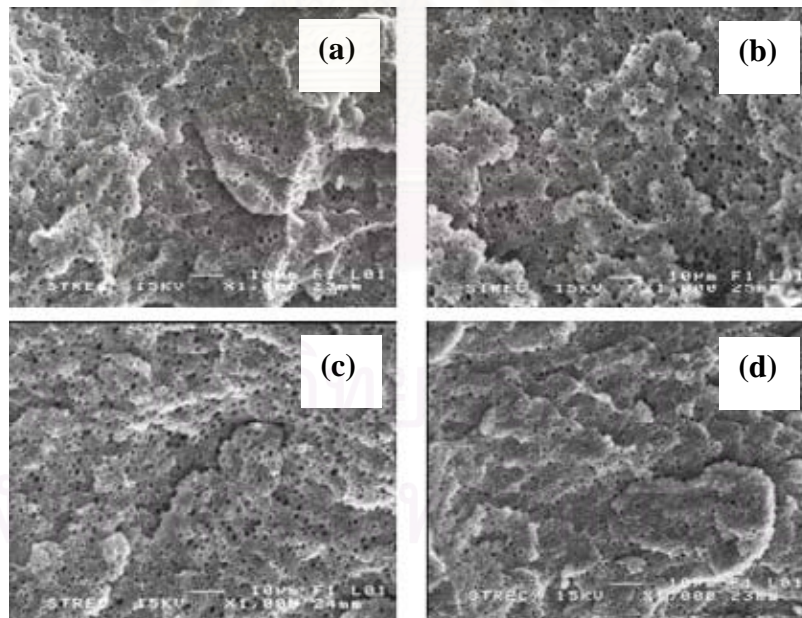
Figure 7.7 Scanning electron micrographs of tensile fracture surfaces of PMMA/EPDM (95/5) blends containing various hydrogenated MMA-*g*-NR contents: (a) 0, (b) 2, (c) 4 and (d) 10 parts (magnification×1000).
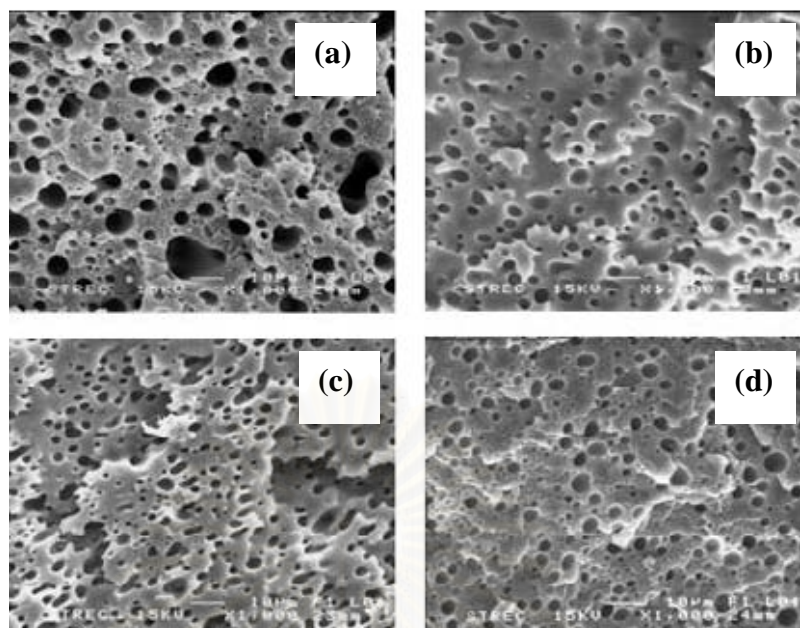
Figure 7.8 Scanning electron micrographs of tensile fracture surfaces of PS/EPDM (70/30) blends containing various hydrogenated ST-*g*-NR contents: (a) 0, (b) 2, (c) 5 and (d) 10 parts (magnification×1000).
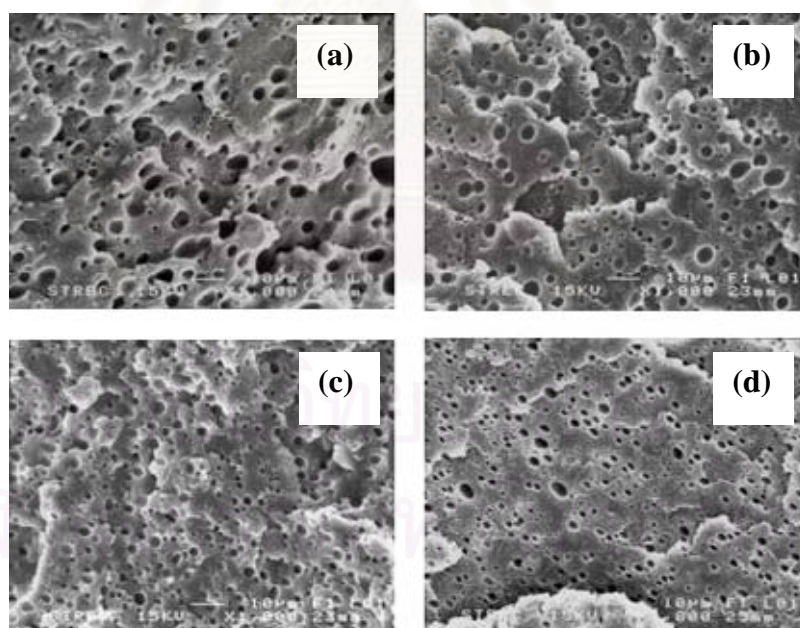
Figure 7.9 Scanning electron micrographs of tensile fracture surfaces of PS/EPDM (90/10) blends containing various hydrogenated ST-*g*-NR contents: (a) 0, (b) 2, (c) 5 and (d) 10 parts (magnification×1000).

7.3   Thermal Properties of Thermoplastic/Elastomer Blends

The glass transition temperature (T_g) of the blend plays an important role in differentiating the blend as phase-separated or as a single–phase system. It was used to study the miscibility of PMMA/EPDM/HGMMA and PS/EPDM/HGST blends. T_g of PMMA (T_g = 90 – 110°C) and PS (T_g = 90 – 100°C) were largely different from EPDM (T_g = −43.3°C). Figure 7.9 and 7.10 show the glass transition temperature of PMMA/EPDM/HGMMA and PS/EPDM/HGST blends at various compatibilizer content (2 – 10 part).The T_g results are summarized in Table 7.1.

It was found that all polymer blends exhibited two glass transition temperatures (T_{g1} and T_{g2}). The lower glass transition temperatures are expected for EPDM and the upper glass transition temperatures are expected for PMMA or PS in the blends. The addition of compatibilizer (HGMMA or HGST) slightly reduced the shift between the two glass transition temperatures. These shifts can be referred to the changes in blend composition. It could be postulated that the ternary blends were partially miscible and the phase interaction between thermoplastic and elastomer increased with an increase in compatibilizer content. For high EPDM content, the results indicated that the blends exhibited phase separation even in the presence of the compatibilizer. These results are in agreement with the decrease in mechanical properties of PMMA/EPDM/HGMMA and PS/EPDM/HGST blends.

Table 7.1 Glass Transition Temperature Evaluated from DSC thermograms.

Blend composition	T_{g1} (°C)	T_{g2} (°C)
PMMA/EPDM/HGMMA		
80/20/0	-44.6	111.4
80/20/2	-47.3	111.6
80/20/4	-48.7	107.8
80/20/10	-48.0	109.3
95/5/0	-49.6	98.7
95/5/2	-48.5	97.6
95/5/4	-46.9	86.5
95/5/10	-47.4	86.9
PS/EPDM/HGST		
70/30/0	-47.6	104.5
70/30/2	-45.0	100.4
70/30/5	-48.0	101.0
70/30/10	-49.7	100.2
90/10/0	-50.5	105.2
90/10/2	-47.0	100.1
90/10/5	-48.3	102.3
90/10/10	-49.6	104.0
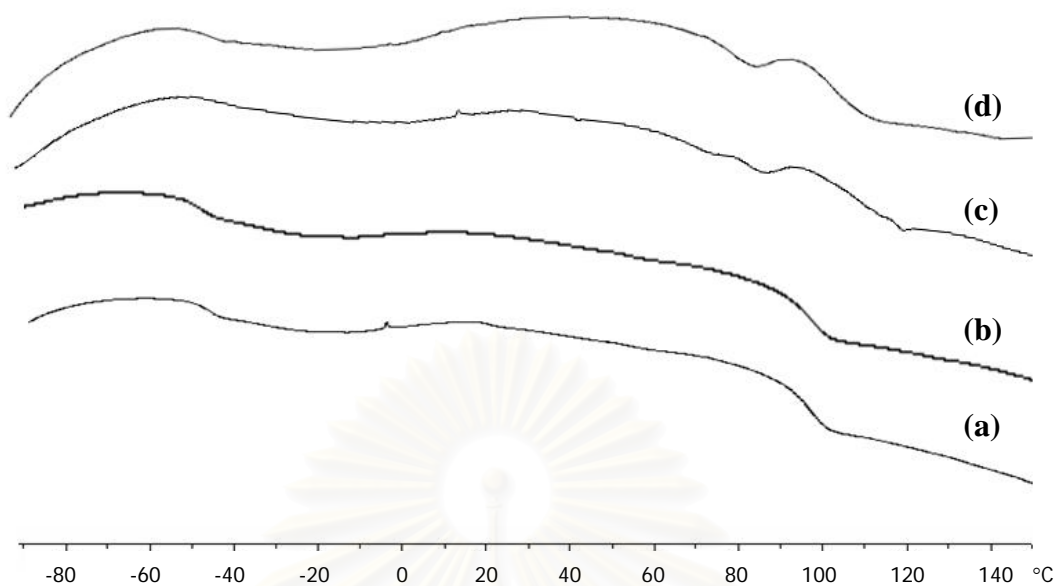
Figure 7.10 DSC thermograms of PMMA/EPDM/HGMMA blends: (a) 95/5/0, (b) 95/5/2, (c) 95/5/4 and (d) 95/5/10.
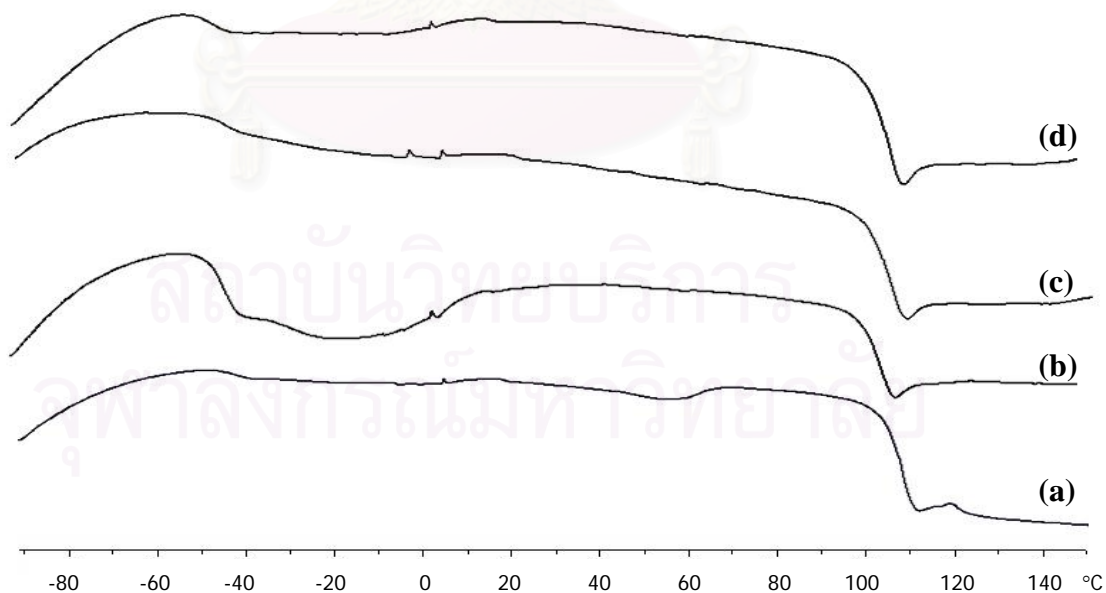
Figure 7.11 DSC thermograms of PS/EPDM/HGST blends: (a) 90/10/0, (b) 90/10/2, (c) 90/10/5 and (d) 90/10/10.

7.4 Dynamic Mechanical Properties of Thermoplastic/Elastomer Blends

The storage modulus (E′), loss modulus (E″) and tan δ of PMMA/EPDM blends with and without compatibilizers is shown in Figure 7.11. The T_g values (peak temperature of tan δ curves) of all samples are summarized in Table 7.2. Considering the immiscibility of PMMA and EPDM, the blends exhibited two glass- transitions temperature (T_g) corresponding to those of the parent polymers as shown in Figure 7.11 (b). The low glass transition at about −50°C referred to the T_g of EPDM and high glass transition at about 100°C referred to the T_g of PMMA in the blends. The presence of two peaks in the blends confirmed that the blends consisted of two phases. Two T_g's of the PMMA/EPDM/HGMMA blends were slightly shifted towards that of the ideally miscible blend. It can be postulated that the blends are partially miscible.

The E′ response represents the change in stiffness of the sample with regards to temperature, while the E″ curve reflects the damping or energy absorbing characteristics. The loss transition at about 50°C was a pre−melting transition and was believed to be due to the movement of small crystallites. The tan δ values slightly decreased with an increase in HGMMA content and the tan δ peaks were also slightly shifted. This could be implied that the compatibility of PMMA/EPDM blends increased in the presence of HGMMA.

Table 7.2 Tan δ and glass transition temperature of PMMA/EPDM/HGMMA blends

Blend composition	Glass Transition Temperature (°C)		Tan δ	
	T_{g1}	T_{g2}	1	2
80/20/0	-47.1	99.0	0.05	1.20
80/20/2	-46.5	99.1	0.06	1.00
80/20/4	-46.0	98.8	0.08	0.90
80/20/10	-47.2	97.0	0.08	0.95
95/5/0	-46.9	98.7	0.06	1.25
95/5/2	-47.0	97.6	0.07	1.17
95/5/4	-46.5	97.5	0.07	1.20
95/5/10	-46.0	96.3	0.08	1.05
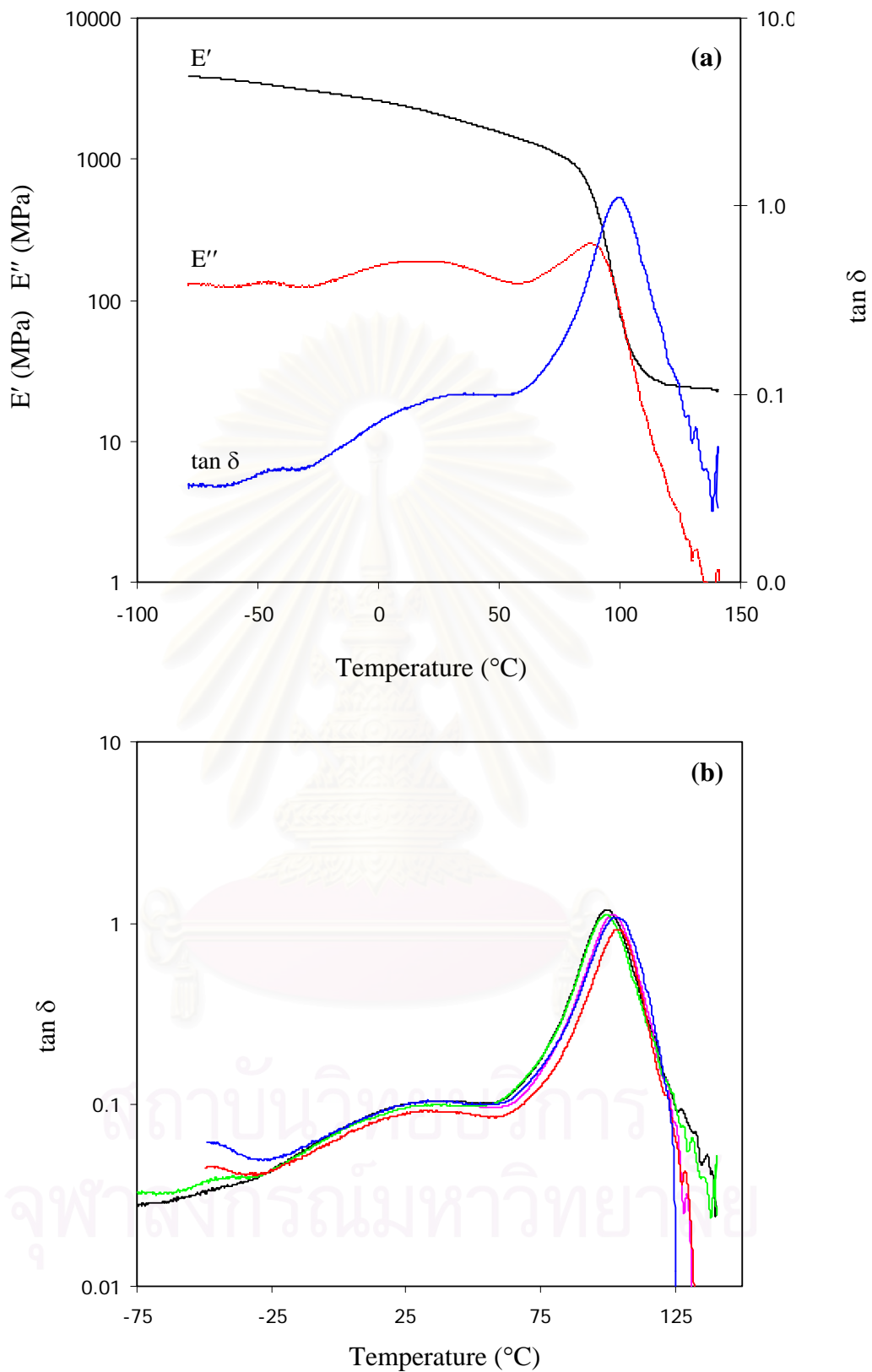
Figure 7.12 Dynamic mechanical analysis: (a) tan δ and storage modulus of PMMA/EPDM (95/5) and (b) tan δ of PMMA/EPDM (95/5) with HGMMA (2 – 10 part).

CHAPTER VIII

CONCLUSIONS AND RECOMMENDATIONS

8.1 Conclusion

8.1.1 Graft Copolymerization of Vinyl Monomers onto Natural Rubber Using Cumene Hydroperoxide/Tetraethylene Pentamine as Initiator

Methyl methacrylate and styrene are the most suitable monomers for graft copolymerization onto natural rubber using an amine activated hydroperoxide. The results from a statistical analysis indicated that initiator concentration, [INT], and reaction temperature, T, showed a negative influence on the grafting efficiency, whereas monomer−to−rubber ratio, M/R, exhibited a positive result. This implies that the grafting efficiency increased with an increase in M/R ratio. In contrast, the grafting efficiency decreased with an increase in [INT] and T. The two−factor interactions, [INT] × M/R, [INT] × T, and M/R × T, and the three−factor interaction, [INT] × M/R × T were not highly significant. From univariate experiments of graft copolymerization of MMA onto NR, the appropriate condition for preparing the graft NR for hydrogenation, is as follows: monomer concentration of 100 phr, initiator concentration of 1.0 phr, SDS concentration of 1.0 phr, i−propanol of 10 phr, reaction temperature of 50°C, and reaction time of 8 h.

8.1.2 Hydrogenation of MMA-g-Natural Rubber in the Presence of OsHCl(CO)(O$_2$)(PCy$_3$)$_2$

The purified MMA-g-NR was hydrogenated by using a homogeneous osmium catalyst, OsHCl(CO)(O$_2$)(PCy$_3$)$_2$. The detailed kinetic investigation of the hydrogenation was carried out by monitoring the amount of hydrogen consumption versus time using a gas−uptake apparatus. The kinetic results for the hydrogenation of graft natural rubber indicated that the rate of hydrogenation exhibited a first−order dependence on the catalyst concentration. A first−order to zero−order dependence on

increasing hydrogen pressure was found. The addition of a small amount of acid promoted the hydrogenation rate of MMA-*g*-NR. The hydrogenation was observed to be inverse–first order with respect to rubber concentration. The addition of a small amount of poly(methyl methacrylate) demonstrated a beneficial effect on the hydrogenation. It possibly affected the chain orientation in the polymer solution as a result of attraction and repulsion within the polymer coils. The hydrogenation rate was dependent on the reaction temperature and the apparent activation energy over the range of 120 – 160°C was found to be 70.3 kJ/mol which indicated that the hydrogenation reaction was free of any mass transfer control.

8.1.3 Hydrogenation of ST-*g*-Natural Rubber in the Presence of OsHCl(CO)(O$_2$)(PCy$_3$)$_2$

A 5d transition metal–based, OsHCl(CO)(O$_2$)(PCy$_3$)$_2$ was an effective catalyst for ST-*g*-NR hydrogenation in monochlorobenzene. The kinetic results indicated that the hydrogenation exhibited a first–order dependence on the catalyst concentration. The hydrogenation exhibited a first–order dependence on hydrogen pressure and then decreased toward a zero–order dependence at higher hydrogen pressure. The hydrogenation was also observed to exhibited a second order dependence on [C=C]. The rate of hydrogenation was found to decrease with an increase in rubber concentration. The addition of a small amount of acid provided a beneficial effect on the hydrogenation rate of the grafted natural rubber. The hydrogenation rate of ST-*g*-NR was dependent on the reaction temperature and the apparent activation energy over the range of 120 – 160°C was found to be 106.5 kJ/mol.

8.1.4 Properties of Grafted Natural Rubber and Hydrogenated Grafted Natural Rubber

The M$_n$, M$_w$, and PDI of hydrogenated MMA-*g*-NR (98% hydrogenation) were lower than that of the NR and MMA-*g*-NR samples. The molecular weight of hydrogenated MMA-*g*-NR decreased due to the high reaction temperature of the hydrogenation system. Consequently, the molecular weight

distribution of hydrogenated MMA-*g*-NR became nearly unimodal while the molecular weight distribution of NR and MMA-*g*-NR was originally bimodal. For graft copolymerization of styrene onto natural rubber, the uncrosslinked polymers, ST-*g*-NR in the soluble fraction had lower molecular weight than NR. After hydrogenation, the gel content of hydrogenated ST-*g*-NR was decreased. The molecular weight, M_w, of hydrogenated ST-*g*-NR was lower than that of ST-*g*-NR and not change with degree of hydrogenation. From thermal analysis results, the hydrogenation could improve the thermal stability of grafted NR by converting the weak π bond within the grafted NR backbone to the stronger C–H σ bond.

8.1.5 Properties of Thermoplastic and Elastomer Blends

Hydrogenated MMA-*g*-NR (HGMMA) and hydrogenated ST-*g*-NR (HGST) could be used as compatibilizers for thermoplastic and elastomer blends. The mechanical properties of the blend such as tensile strength, % elongation, hardness and impact energy were also investigated. The results showed that the addition of HGMMA in PMMA/EPDM and HGST in PS/EPDM blends at appropriate content could improve the mechanical properties of the blends. The addition of a suitable compatibilizer to an immiscible polymer blend enhances the interfacial adhesion between the two phases. The decrease in the particle size increased the interfacial surface between the rubber particles and PMMA or PS matrix.

8.2 Recommendations

A further study of the hydrogenation of grafted natural rubber should be concerned with the following aspects:

1. Hydrogenation of ST-*g*-NR in the presence of Ru complex

Since the Ru[CH=CH(Ph)](Cl)(CO)(PCy$_3$)$_2$ was an efficient catalyst for the hydrogenation of ST-*g*-NR, additional work on the activity and selectivity of Ru complex for the ST-*g*-NR hydrogenation would be informative and interesting. In

particular, the kinetic dependence on rubber concentration would be of interest given the behavior of the osmium analogue studied in the present thesis.

2. Hydrogenation in latex form

Product from graft copolymerization is in an emulsion form. The hydrogenation of graft copolymers in latex form is an interesting pathway and the amount of solvent used in the hydrogenation process should be reduced.

3. Improvement of the hydrogenation process

By applying a different method and apparatus for the graft copolymerization and hydrogenation reaction, the possibility continuous process should be further studied to reduce the cost of the operation.

4. Thermoplastic and elastomer blending

There are the other strategies for compatibilizing immiscible polymers. The reactive compatibilization should also be further studied. This method can be used to improve the effective for using grafted NR as a compatibilizer to control the interfaces and the morphology of the immiscible polymer blends.

REFERENCES

[1]   United Nations Statistics Division. <u>World Rubber Exports</u> [online]. Available from: http://www.intracen.org/tradstat/sitc3-3d/ep231.htm   [2007, October 19].

[2]   d' Auzac, J., Jacob, J. L., and Chrestin, H. <u>Physiology of Rubber Tree Latex: The Laticiferous Cell and Latex−A Model of Cytoplasm.</u> Florida: CRC Press, Inc., 1989.

[3]   Tanaka, Y. Structural characterization of natural polyisoprenes: Solve the mystery rubber based on structural study. <u>Rubber Chem. Tech.</u> 74 (2001): 355 − 375.

[4]   Resing, W. Production, processing and properties. <u>Natural Rubber−1st Quarter.</u> 17 (2000): 2 − 3.

[5]   Kovuttikulrangsie, S. and Sakdapipanich, J. T. The molecular weight (MW) and molecular weight distribution (MWD) of NR from different age and clone *Hevea* trees. <u>Songklanakarin J. Sci. Technol.</u> 27(2) (2005) : 337 − 342.

[6]   Venharr, G. Natural latex as a colloidal system. <u>Rubber Chem. Tech</u>. 32 (1959): 1627 − 1659.

[7]   McManus, N. T. and Rempel, G. L. Chemical modification of polymers: Catalytic hydrogenation and related reactions. <u>Rev. Macromol. Chem. Phys.</u> C35(2) (1995): 239 − 285.

[8]   Ebewele, R. O. <u>Polymer Science and Technology.</u> Florida: CRC Press LLC, 1996.

[9]   Schulz, D. N. and Turner, S. R. Recent advances in the chemical modification of unsaturated polymers, <u>Rubber Chem. Tech.</u> 55 (1982): 809 – 859.

[10]   Gelling, I. R. and Porter, M. <u>Natural Rubber Science and Technology.</u> Roberts, A. D. Edition, Oxford: University Press, 1988, 359.

[11]   Odian, G. <u>Principles of Polymerization.</u> 4th Edition, New Jersey: Interscience, 2004.

[12]   Calvin, E. S. <u>Polymerization Processes</u>. New York: Interscience, 1977: 228 – 246.

[13]   Braun, D., Cherdron, H., Rehahn, M. Ritter, H., and Voit, B. <u>Polymer Synthesis: Theory and Pratice. Fundamentals, methods, experiments.</u> 4th Edition, New York: Springer-Verlag, 2005.

[14]   Lovell, P. A. and El−Aasser, M. S. <u>Emulsion Polymerization and Emulsion Polymers</u>. England: Interscience, 1997.

[15]   Sudol, E. D., Daniels, E., and El−Aasser, M. S. <u>Polymer Latexes: Preparation, Characterization, and Applications. Chapter 1: Overview of Emulsion Polymerization: Stepping Toward Prediction.</u> ACS symposium series. Washington: ACS, 1992: 1 – 11.

[16]   Hashim, A. S., Ong, S. K. and Jessy, R.S. A general review of recent developments on chemical modification of NR. <u>Rubber</u>. 28 (2002): 3 – 9.

[17]   Charmondusit, K., Kiatkamjornwong, S. and Prasassarakich, P. Grafting of methyl methacrylate and styrene onto natural rubber. <u>J. Sci. Chula. Univ.</u> 23(2) (1998): 168 – 181.

[18]   Arayapranee, W. <u>Grafting of Styrene and Methyl Methacrylate onto Natural Rubber in Batch Emulsion Process.</u> Doctoral dissertation, Department of Chemical Technology, Faculty of Science, Chulalongkorn University, 2000.

[19]   Arayapranee, W., Prasassarakich, P., and Rempel, G. L. Synthesis of graft copolymers from natural rubber using cumene hydroperoxide redox initiators. <u>J. Appl. Polym. Sci.</u> 83 (2002): 2993 – 3001.

[20]   Kochthongrasamee, T., Prasassarakich, P. and Kaitkamjornwong, S. Effects of redox initiator on graft copolymerization of methyl methacrylate onto natural rubber. <u>J. Appl. Polym. Sci.</u> 101 (2006): 2587 – 2601.

[21]   Parent, J. S., McManus, N. T., and Rempel, G. L. OsHCl(CO)(O2)(PCy$_3$)$_2$-Catalyzed hydrogenation of acrylonitrile–butadiene copolymers. <u>Ind. Eng. Chem. Res.</u> 37 (1998): 4253 – 4261.

[22]   Parent, J. S., McManus, N. T., and Rempel, G. L., Selectivity of the OsHCl(CO)(O$_2$)(PCy$_3$)$_2$ catalyzed hydrogenation of nitrile–butadiene rubber. <u>J. Appl. Polym. Sci.</u> 79 (2001): 1618 – 1626.

[23]   Mahittikul, A., Prasassarakich, P., and Rempel, G. L. Hydrogenation of natural rubber latex in the presence of OsHCl(CO)(O$_2$)(PCy$_3$)$_2$. <u>J. Appl. Polym. Sci.</u> 100 (2006): 640 – 655.

[24]   Hinchiranan, N., Charmondusit, K., Prasassarakich, P., and Rempel, G. L. Hydrogenation of natural rubber in the presence of OsHCl(CO)(O$_2$)(PCy$_3$)$_2$: Kinetics and Mechanism. <u>J. Appl. Polym. Sci.</u> 100 (2006): 4499 – 4514.

[25]   Moers, F. G. A new hydridocarbonyl complexes of osmium (II). <u>J. Chem. Soc., Chem. Commun.</u> (1971): 79.

[26]   Esteruelas,   M.   A.,   Werner,   H.   Five−   and   six−coordinate hydrido(carbonyl)−ruthenium(II)   and   −osmium(II)   complexes containing triisopropylphosphine as ligand. J. Organometallic Chem. 303 (1986): 221 − 231.

[27]   Esteruelas, M. A., Sola, E., Oro, L. A., Meyer, U. and Werner, H. Coordination of H_2 and O_2 to [OsHCl(CO)(PiPr$_3$)$_2$]: A catalytically active M(η^2−H$_2$) complex. Chem. Int. Ed. Engl. 27 (1998): 1563 − 1564.

[28]   Moers,   F.   G.   Ruthenium   (II)   and   osmium   (II)   complexes   of tricyclohexylphosphine. J. Coord. Chem. 13 (1984): 215 − 219.

[29]   Parent, J. S., McManus, N. T., Rempel, G. L., Power, W. P., and Marder, T. B. Ligand exchange processes of OsHCl(CO)(L)(PR$_3$)$_2$ (L=vacant, H$_2$, R′CN, O$_2$; R=Cy, i−Pr). J. Mol. Cat. A: Chem. 135(3) (1998): 285 − 293.

[30]   Mao, T., −F and Rempel, G. L. Catalytic hydrogenation of acrylonitrile− butadiene copolymers by a series of osmium complexes. J. Mol. Cat. A: Chem. 153 (2000): 63 − 73.

[31]   Charmondusit, K. Hydrogenation of cis−1,4−poly(isoprene) and Natural Rubber   Catalyzed   by   OsHCl(CO)(O$_2$)(PCy$_3$)$_2$ and [Ir(COD)py(PCy$_3$)]PF$_6$. Doctoral dissertation, Department of Chemical Technology, Faculty of Science, Chulalongkorn University, 2002.

[32]   Charmondusit, K., Prasassarakich, P., McManus, N. T., and Rempel, G. L. Hydrogenation   of cis−1,4−poly(isoprene)   catalyzed   by OsHCl(CO)(O$_2$)(PCy$_3$)$_2$. J. Appl. Polym. Sci. 89 (2003): 142 − 152.

[33]   Hinchiranan, N. <u>Hydrogenation of Natural Rubber Catalyzed by OsHCl(CO)(O$_2$)(PCy$_3$)$_2$ and   Ir(cod)(PCy$_3$)(py)PF$_6$.</u>   Doctoral dissertation, Department of Chemical Technology, Faculty of Science, Chulalongkorn University, 2004.

[34]   Mahittikul, A. <u>Structure and Properties of Hydrogenated Natural Rubber Latex Using OsHCl(CO)(O$_2$)(PCy$_3$)$_2$ as a Catalyst and Diimide Reduction.</u> Doctoral dissertation, Department of Chemical Technology, Faculty of Science, Chulalongkorn University, 2005.

[35]   Hashim, A. S., Ong, S. K. and Jessy, R. S. A general review of recent developments on chemical modification of natural rubber. <u>Rubber</u>. 28 (2002): 3 – 9.

[36]   Bhaduri, S. and Mukesh, D. <u>Homogeneous Catalysis Mechanisms and Industrial Applications</u>. New York: John Wiley & Sons, 2000: 8.

[37]   Tangthongkul, R. <u>Hydrogenation of Synthetic Rubber cis–1,4–Polyisoprene and Natural Rubber Catalyzed by Ruthenium (II) Complex.</u> Doctoral dissertation, Department of Chemical Technology, Faculty of Science, Chulalongkorn University, 2003.

[38]   Tangthongkul, R., Prasassarakich, P., and Rempel, G. L. Hydrogenation of natural rubber with Ru[CH=CH(Ph)]Cl(CO)(PCy$_3$)$_2$ as a catalyst. <u>J. Appl. Polym. Sci.</u> 97 (2005): 2399 – 2406.

[39]   Hinchiranan, N., Charmondusit, K., Prasassarakich, P., and Rempel, G. L. Hydrogenation of synthetic cis–1,4–polyisoprene and natural rubber catalyzed by [Ir(COD)py(PCy$_3$)]PF$_6$. <u>J. Appl. Polym. Sci.</u> 100 (2006): 4219 – 4233.

[40]   Nang, T. D., Katabe, Y., and Minoura, Y. Diimide reduction of cis–1,4–polyisoprene with p–toluenesulphonylhydrazide. <u>Polymer</u>. 17 (1976): 117-120.

[41]   Wideman, L. G. Process for hydrogenation of carbon−carbon double bonds in an unsaturated polymer in latex form. U.S. Patent 4,452,950 (1984).

[42]   Samran, J., Phinyacheep, P., Daneil, P. and Kittipoom, S. Hydrogenation of unsaturated rubbers using diimide as a reducing agent. J. Appl. Poly. Sci. 95 (2005): 16 − 27.

[43]   Mahittikul, A., Prasassarakich, P., and Rempel, G. L. Diimide hydrogenation of natural rubber latex. J. Appl. Polym. Sci. 103 (2006): 2885 − 2895.

[44]   Mahittikul, A., Prasassarakich, P., and Rempel, G. L. Diimide hydrogenation of natural rubber latex. J. Appl. Polym. Sci. 105 (2007): 1188 − 1199.

[45]   Baker, W. E. and Hu, G. –H. Reactive Polymer Blending: Introduction. Hyun, K. S. Edition, München: Hanser, 2001.

[46]   Elias, H. –G. An Introduction to Plastics. 2nd Completely Revised Edition, Weinheim: Wiley-VCH, 2003.

[47]   Liu, N. C. and Huang, H. Reactive Polymer Blending: Types of Reactive Polymers Used in Blending. Hyun, K. S. Edition, München: Hanser, 2001: 14 − 31.

[48]   Utracki, L. A. Polymer Alloys and Blends. Munich New York: Hanser, 1989.

[49]   Sundararaj, U. and Macosko, C. W. Drop breakup and coalescence in polymer blends: The effects of concentration and compatibilization. Macromolecules. 28 (1995): 2647 − 2657.

[50]   Oommen, Z. and Thomas, S. Mechanical properties and failure mode of thermoplastic elastomers from natural rubber/poly(methyl methacrylate)/natural rubber-g-poly(methyl methacrylate) blends. J. Appl. Polym. Sci. 65 (1997): 1245 − 1255.

[51] Thiraphattaraphun, L., Kiatkamjornwong, S., Prasassarakich, P., and Damronglerd, S. Natural rubber-*g*-methyl methacrylate/poly(methyl methacrylate) blends. J. Appl. Polym. Sci. 81 (2001): 428 – 439.

[52] Suriyachi, P. and Kiatkamjornwong, S. Natural rubber-*g*-glycidyl methacrylate/styrene as a compatibilizer in natural rubber/PMMA blends. Rubber Chem. Tech. 77 (2004): 914 – 930.

[53] Macosko, C. W., Guégan, P., Khandpur, K., Nakayama, A., Maréchal, P., and Inoue, T. Compatibilizers for melt blending: Premade block copolymers Macromol. 29 (1996): 5590 – 5598.

[54] Oliveira, P. C., Oliveira, A. M., Garcia, A., Barboza, J. C. S., Zavaglia, C. A. C., and Santos, A. M. Modification of natural rubber: A study by ^{1}H NMR to assess the degree of graftization of polyDMAEMA or polyMMA onto rubber particles under latex form in the presence of a redox couple initiator. Eur. Polym. J. 41 (2005): 1883 – 1892.

[55] Mohammadi, N. A. and Remple, G. L. Control, data acquisition and analysis of catalytic gas-liquid mini slurry reactors using a personal computer. Comput. Chem. Eng. 11 (1987): 27 – 35.

[56] Andrews, E. H. and Turner, D. T. The distribution of polymethyl Methacrylate formed in natural rubber latex: An electron microscopical study. J. Appl. Polym. Sci. 3 (1960): 366 – 367.

[57] Luankeaw, W. Synthesis of Natural Rubber Grafted Styrene as Impact Modifier for Poly(vinyl chloride). Master thesis, Department of Chemical Technology, Faculty of Science, Chulalongkorn University, 2002.

[58] Aik–Hwee, E., Tanaka, Y. and Seng–Neon, G. FTIR studies on amino groups in purified *Hevea* rubber. J. Nat. Rubber. Res. 7(2) (1992):152 – 155.

[59]   Carey, F. A. <u>Organic Chemistry: Spectroscopy.</u> 4th Edition, Boston: McGraw Hill, 2000.

[60]   Li, S. –D., Wang, C., Xu, K., and Peng, Z. Thermooxidative degradation of methyl methacrylate-graft-natural rubber. <u>J. Appl. Polym. Sci.</u> 90 (2003): 1227 – 1232.

[61]   Singha, N. K., De, P. P., and Sivaram, S. Homogeneous catalytic hydrogenation of natural rubber using RhCl(PPh$_3$)$_3$. <u>J. Poly. Sci.</u> 66 (1997): 1647 – 1652.

[62]   Sarkar, M. D., Mukunda, P. G., De, P. P., and Bhowmick, A. K. Degradation of hydrogenated styrene-butadiene rubber at high temperature. <u>Rubber Chem. Tech.</u> 70 (1997): 855 – 870.

[63]   Montgomery, D. C. <u>Design and Analysis of Experiments.</u> 5th Edition. New York: John Wiley & Sons, 2000.

[64]   Patterson, D. J. and Koenig, J. L. Solid-state ^{13}C NMR characterization of irradiation−cross−linked natural rubber. <u>Appl. Spectro.</u> 41 (1987): 441 – 446.

[65]   Parent, J. S., McManus, N. T., and Rempel, G. L. RhCl(PPh$_3$)$_3$ and RhH(PPh$_3$)$_4$ Catalyzed hydrogenation of acrylonitrile-butadiene copolymers. <u>Ind. Eng. Chem. Res.</u> 35 (1996): 4417 – 4423.

[66]   Lu, F. J. and Hsu, S. L. A vibrational spectroscopic analysis of the structure of NR. <u>Rubber Chem. Tech.</u> 60 (1987): 647 – 658.

[67]   Arayapranee, W., Prasassarakich, P., and Rempel, G. L. Process variables and their effects on grafting reactions of styrene and methyl methacrylate onto natural rubber. <u>J. Appl. Polym. Sci.</u> 89 (2003): 63 – 74.

[68] Guo, X. Y. and Rempel, G. L. Catalytic hydrogenation of nitrile-butadiene copolymer emulsion. J. Appl. Polym. Sci. 65 (1997): 667 – 675.

[69] Andriollo, A., Esteruelas, M. A., Mayer, U., Oro, A. L. Delgado, R. A., Sola, E., Valero, C. And Werner, H. Kinetic and mechanistic investigation of the sequential hydrogenation of phenylacetylene catalyzed by OsHCl(CO)(PR$_3$)$_2$ [PR$_3$ = PMe-t-Bu$_2$ and P-i-Pr$_3$]. J. Am. Chem. Soc. 111 (1989): 7431 – 7434.

[70] Sandler, S. R., Karo, W. Bonesteel, J. A. and Pearce, E. M. Polymer Synthesis and Characterization. A Laboratory Manual. (San Diago: Academic Press, 1998), pp. 108 – 130, 140 – 147.

[71] Tanaka, Y. Structure and biosynthesis mechanism of natural polyisoprene. Prog. Polym. Sci. 14 (1989): 339 – 371.

[72] Fukushima, Y., Kawahara, S. and Tanaka, Y. Synthesis of graft copolymers from highly deproteinized natural rubber. J. Rubber Res., 1 (1998): 154 – 166.

[73] Peng, Z., Li, S.-D., Huang, M.–F., Xu, K., Wang, C., Li, P.–W., and Chen, X.–G. Thermogravimetric analysis of methyl methacrylate-graft-natural rubber. J. Appl. Polym. Sci. 85 (2002): 2952 – 2955.

[74] Elias, H. –G. An Introduction to Plastics. Second, Completely Revised Edition, Weinheim: Wiley-VCH GmbH & Co. KGaA, 2003.

[75] Ravikumar, H. B., Ranganathaiah, C., Kumaraswamy, G. N., Urs, M. V. D., Jagannath, J. H., Bawa, A. S., and Thomas, S. Differential scanning calorimetric and free volume study of reactive compatibilization by EPM-g-MA of poly(trimethylene terephthalate)/EPDM blends. J. Appl. Polym. Sci. 100 (2006): 740 – 747.

APPENDICES

Appendix A

Overall Compositions of Rubbers

Table A-1 Properties of Natural Rubber Latex Concentrated (Thai Rubber Latex; 2005)

Properties	Test Results
Total solids content, %	61.79
Dry rubber content, %	60.12
Non rubber solids, %	1.67
Ammonia content (on total weight), %	0.69
Ammonia content (on water phase), %	1.81
pH value	10.32
KOH number	0.6020
Volatile fatty acid number (VFA)	0.0288
Mechanical stability at 55% TS. Sec	900
Specific gravity at 25 ^{0}C	0.9461
Magnesium content, ppm	33.75
Viscosity (60% TS, spindle no. 1.60 rpm), cps	76
Coagulum content (80 mesh), ppm	28

All tests are performed according to relevant ISO 2004–1997(E) specification.

Table A-2 Properties of Ethylene–Propylene–Diene Copolymer (Nordel 4640)

Properties	Test Results
Mooney Viscosity, ML(1+4) at 125°C, MU	39
Ethylene, %	55
ENB*	4.9
Molecular weight	160,000
Density, g/cm^3	0.86
Crystallinity, mass%	4
Crytallinity temperature, °C	-10
Total Volatiles, %	0.1
Yellowness Index	2

*ENB = Ethylidenenorbene

Table A-3 Properties of Poly(methyl methacrylate) (AcrypetTM)

Properties	Test Results
Methyl methacrylate–methyl acrylate copolymer, %	99.0
Softening point, °C	85
Autoignition Temperature, °C	421
Specific gravity	1.19

Table A-4 Properties of Polystyrene (PS Resin)

Properties	Test Results
Melt Index, g/min	0.6 – 0.9
Softening point, °C	107
Weight average molecular weight	~230,000

Appendix B

Calculations

1.   Graft Copolymerization Calculations

The grafted copolymers are characterized according to the following equation:

$$\text{Total Conversion (\%)} = \frac{\text{Weight of monomer consumed}}{\text{Weight of monomer charged}} \times 100 \qquad \text{(B1-1)}$$

$$\text{Grafting efficiency (\%)} = \frac{\text{Weight of monomer grafted}}{\text{Total weight of monomer polymerized}} \times 100 \qquad \text{(B1-2)}$$

$$\text{Free Natural Rubber (\%)} = \frac{\text{Weight of free natural rubber}}{\text{Weight of gross polymer}} \times 100 \qquad \text{(B1-3)}$$

$$\text{Free Homopolymer (\%)} = \frac{\text{Weight of free homopolymer}}{\text{Weight of gross polymer}} \times 100 \qquad \text{(B1-4)}$$

$$\text{Graft Copolymer (\%)} = \frac{\text{Weight of grafted natural rubber}}{\text{Weight of graft copolymer}} \times 100 \qquad \text{(B1-5)}$$

2.   Degree of Grafting by $^{1}\text{H}-$NMR Calculation

For MMA-*g*-NR, the degree of grafting PMMA onto NR backbone was calculated from the results of average molar composition for each copolymer according to the following equations:

$$S_0 = 1y \rightarrow y = S_0 \qquad \text{(B2-1)}$$

$$S_1 = 3x \rightarrow x = S_1/3 \qquad \text{(B2-2)}$$

$$M = \left[\frac{S_1/3}{(S_0 + S_1/3)} \right] \times 100 \qquad \text{(B2-3)}$$

where y = unsaturated olefinic protons in NR backbone ($-C=C-H$); x = methoxy protons in PMMA graft chain ($-OCH_3$); S_0 = integrated peak area of the unsaturated olefinic protons at 5.15 ppm, S_1 = integrated peak area value of the methoxy protons at 3.16 ppm and M = mole % of PMMA in graft MMA-*g*-NR.

$$
\begin{array}{lll}
S_0 & = 1.00 & \rightarrow \quad y = 1.00 \\
S_1 & = 1.00 & \rightarrow \quad x = 1.00/3
\end{array}
$$

Mole % of PMMA in MMA-*g*-NR:

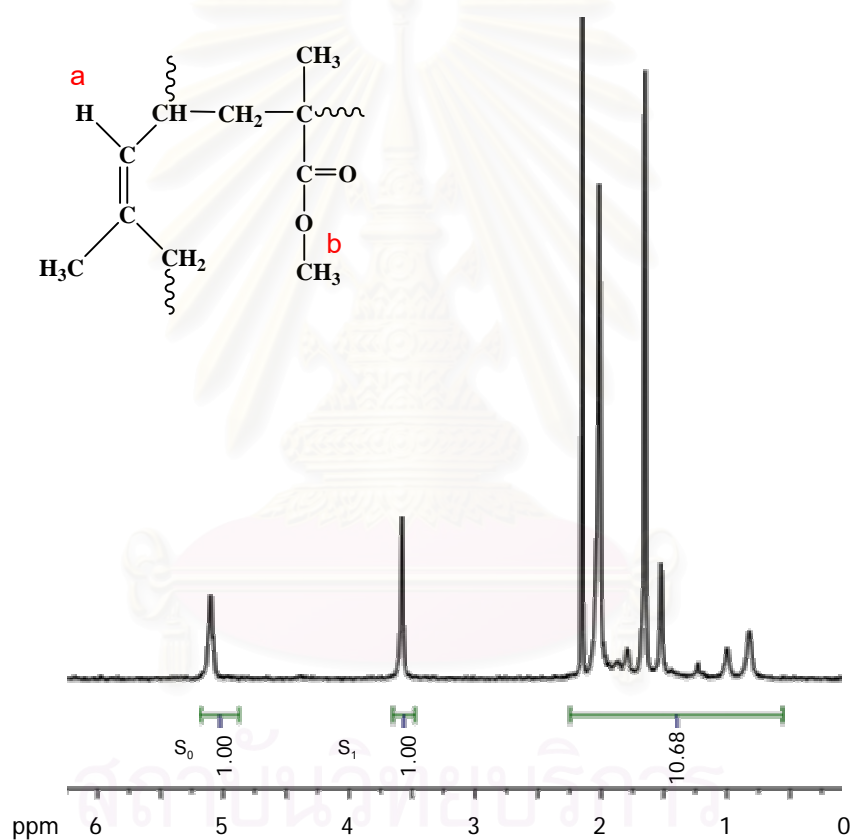$$M = \left[\frac{1.00/3}{(1.00 + 1.00/3)} \right] \times 100 = 25.0\% \qquad \text{(B2-4)}$$

For ST-*g*-NR, the degree of grafting PS onto NR backbone was calculated form the results of average molar composition for each copolymer were according to the following equations:

$$S_0 = 1y \rightarrow y = S_0 \tag{B2-5}$$

$$S_1 = 5x \rightarrow x = S_1/5 \tag{B2-6}$$

$$M = \left[\frac{S_1/5}{(S_0 + S_1/5)} \right] \times 100 \tag{B2-7}$$

where y = unsaturated olefinic protons in NR backbone ($-C=C-H$); x = aromatic protons in PS graft chain ($-$aromatic); S_0 = integrated peak area of the unsaturated olefinic protons at 5.15 ppm, S_1 = integrated peak area value of the aromatic protons in the range of 6.5 $-$ 8.5 ppm and M = mole % of PS in graft MMA-*g*-NR.
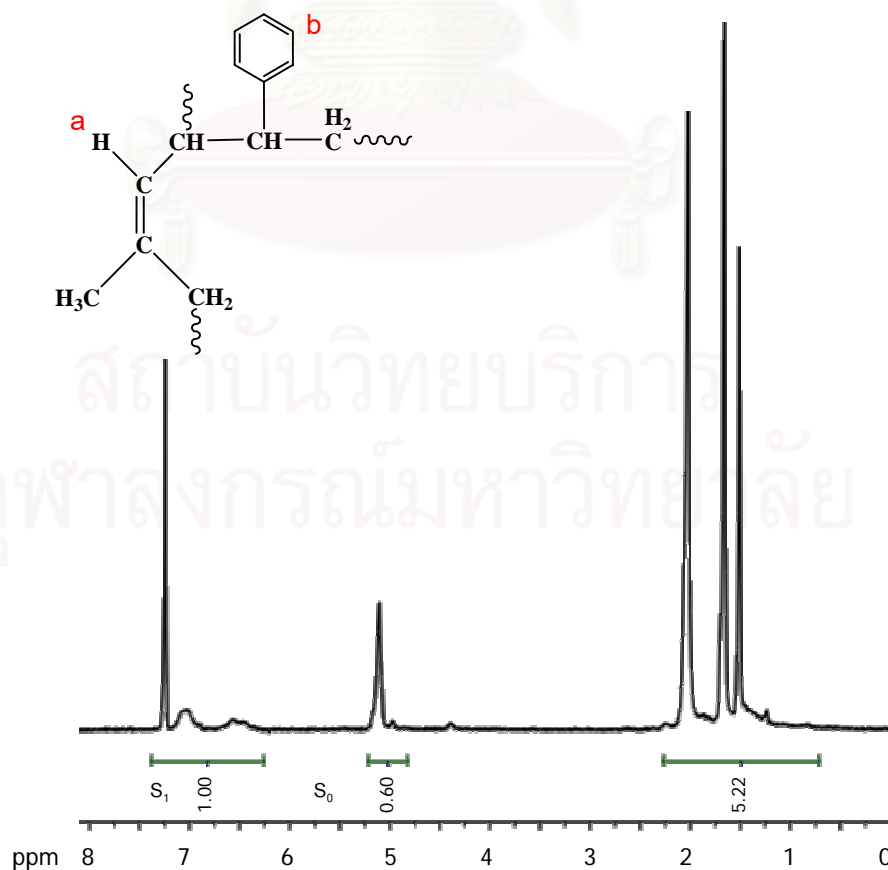
$$S_0 \quad = 0.60 \qquad \rightarrow \qquad y = 0.60$$

$$S_1 \quad = 1.00 \qquad \rightarrow \qquad x = 1.00/5$$

Mole % of PS in the ST-*g*-NR:

$$M \quad = \quad \left[\frac{1.00/5}{(0.60 + 1.00/5)}\right] \times 100 = 25.0\% \qquad (B2\text{-}8)$$

3. Percentage of Hydrogenation of MMA-*g*-NR

Species 1 → Hydrogenation → **Species 2**
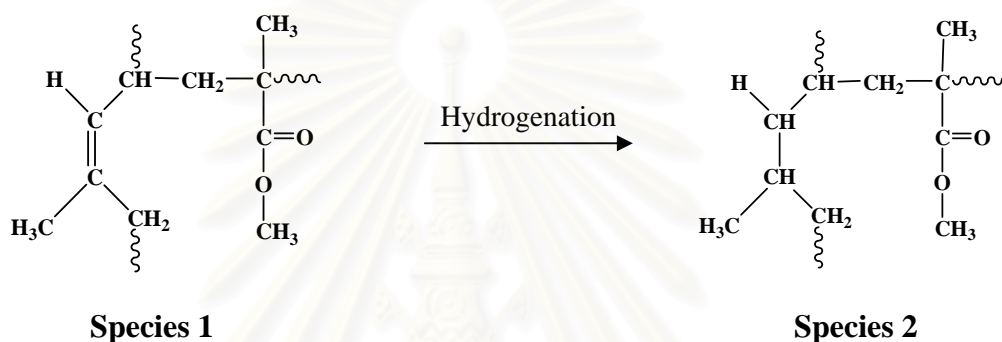
Proton of isoprene repeating unit except =CH in species 1 = 6 protons

Proton of methyl methacrylate unit except –OCH$_3$ in species 1 = 5 protons

Proton of ethylene-propylene segment in species 2 = 9 protons
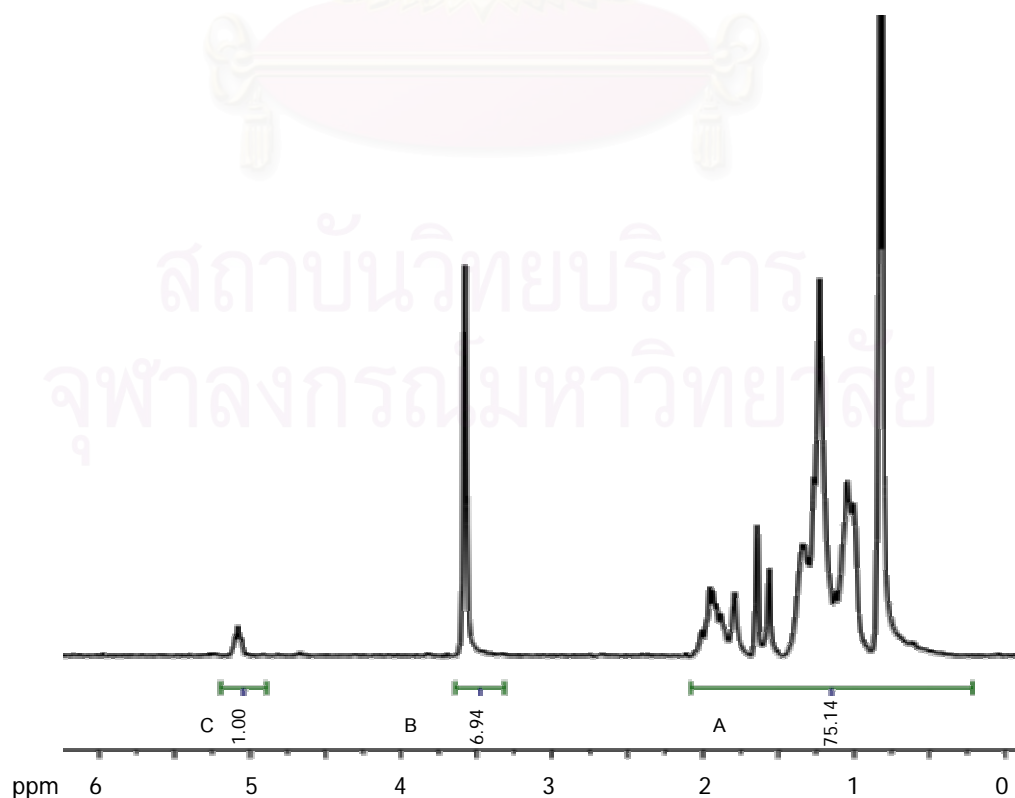
A = Peak area in the range of 0.5 to 2.0 ppm

B = Peak area at 3.5 ppm

C = Peak area at 5.2 ppm

D = Peak area of saturated $-CH_2-$ and $-CH_3$

$$A = 5B + 6C + 9D$$

$$D = \frac{A - 5B - 6C}{9} \qquad \text{(B3-1)}$$

Total peak area = Peak area of saturated $-CH_2-$ and $-CH_3$

+ Peak area at 5.2 ppm

$$= D + C$$

$$= \frac{A - 5B - 6C}{9} + C$$

$$= \frac{A - 5B + 3C}{9} \qquad \text{(B3-2)}$$

$$\% \text{ Hydrogenation} = \left[\frac{\text{Peak area of saturated} - CH_2 - \text{and} - CH_3}{\text{Total peak area}} \right] \times 100$$

$$= \frac{\left(\dfrac{A - 5B - 6C}{9} \right)}{\left(\dfrac{A - 5B + 3C}{9} \right)} \times 100$$

$$= \left(\frac{A - 5B - 6C}{A - 5B + 3C} \right) \times 100 \qquad \text{(B3-3)}$$

For example: A = 75.14, B = 6.94 and C = 1.00

$$\% \text{ Hydrogenation} = \frac{75.14 - 5(6.94) - 6(1.00)}{75.14 - 5(6.94) + 3(1.00)} \times 100 \qquad \text{(B3-4)}$$

$$= 79.3 \ \%$$

4.   Percentage of Hydrogenation of ST-*g*-NR
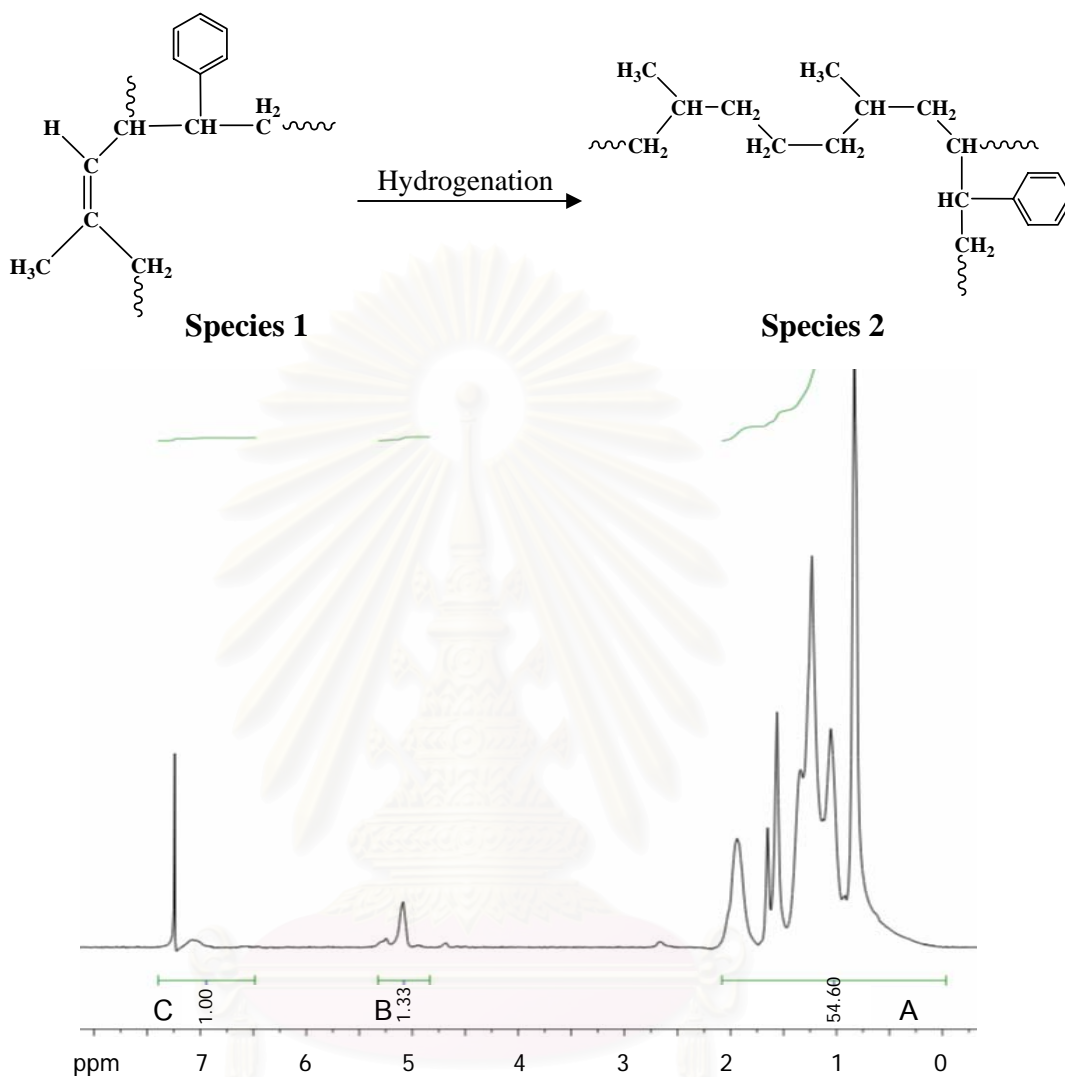
Species 1   **Species 2**

Proton of isoprene repeating unit except =CH in species 1 = 6 protons

Proton of styrenic unit except ─aromatic in species 1 = 2 protons

Proton of ethylene-propylene segment in species 2 = 9 protons

A = Peak area except at 3.5 and 5.2 ppm

B = Peak area at 5.2 ppm

C = Peak area at 6.5 to 8.5 ppm

D = Peak area of saturated –CH_2─ and -CH_3

$$A \quad = \quad 6B + 2C + 9D$$

$$D \quad = \quad \frac{A - 6B - 2C}{9} \tag{B4-1}$$

$$\text{Total peak area} \quad = \quad \text{Peak area of saturated } –CH_2– \text{ and } –CH_3$$

$$+ \text{ Peak area at 5.2 ppm}$$

$$= \quad D + B$$

$$= \quad \frac{A - 6B - 2C}{9} + B$$

$$= \quad \frac{A + 3B - 2C}{9} \tag{B4-2}$$

$$\% \text{ Hydrogenation} \quad = \quad \left[\frac{\text{Peak area of saturated } - CH_2 - \text{ and } - CH_3}{\text{Total peak area}} \right] \times 100$$

$$= \quad \frac{\left(\dfrac{A - 6B - 2C}{9} \right)}{\left(\dfrac{A + 3B - 2C}{9} \right)} \times 100$$

$$= \quad \left(\frac{A - 6B - 2C}{A + 3B - 2C} \right) \times 100 \tag{B4-3}$$

For example: A = 54.60, B = 1.33 and C = 1.00

$$\% \text{ Hydrogenation} \quad = \quad \frac{54.60 - 6(1.33) - 2(1.00)}{54.60 + 3(1.33) - 2(1.00)} \times 100 \tag{B4-4}$$

$$= \quad 78.8\%$$

Appendix C

Derivation of the Rate Law from the Proposed Kinetic Model

1.   Hydrogenation of MMA-*g*-NR catalyzed by OsHCl(CO)(O₂)(PCy₃)₂
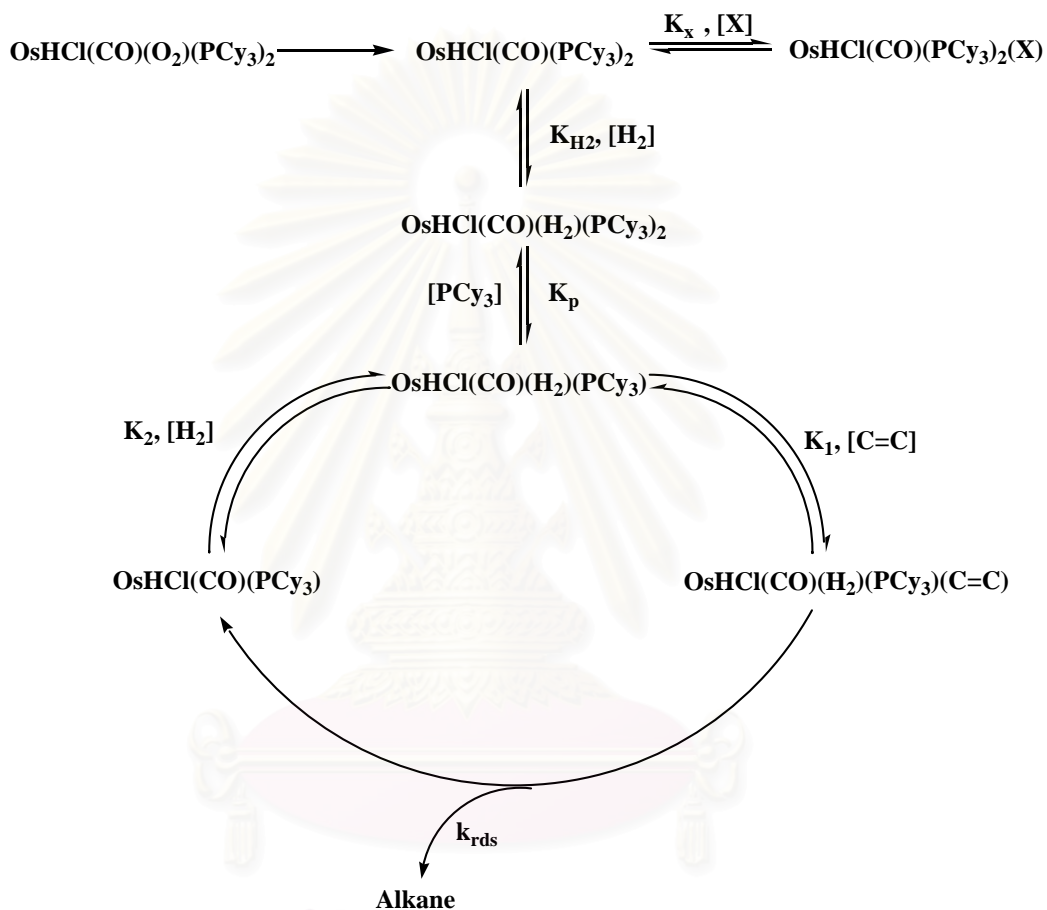
Using the steady state assumption for reaction intermediates, the following equilibrium define the concentration of each catalytic species related the rate determining step.

$$-\frac{d[C=C]}{dt} = k_{rds}[OsHCl(CO)(H_2)(C=C)(PCy_3)] \tag{C1-1}$$

$$[OsHCl(CO)(H_2)(PCy_3)] = \frac{[OsHCl(CO)(H_2)(PCy_3)(C=C)]}{K_1[C=C]} \tag{C1-2}$$

$$[OsHCl(CO)(H_2)(PCy_3)_2] = \frac{[OsHCl(CO)(H_2)(PCy_3)(C=C)][PCy_3]}{K_p K_1 [C=C]} \quad (C1\text{-}3)$$

$$[OsHCl(CO)(PCy_3)_2] = \frac{[OsHCl(CO)(H_2)(PCy_3)(C=C)][PCy_3]}{K_p K_{H_2} K_1 [C=C][H_2]} \quad (C1\text{-}4)$$

$$[OsHCl(CO)(PCy_3)] = \frac{[OsHCl(CO)(H_2)(PCy_3)(C=C)]}{K_1 K_2 [C=C][H_2]} \quad (C1\text{-}5)$$

$$[OsHCl(CO)(PCy_3)_2(X)] = \frac{K_x[OsHCl(CO)(H_2)(PCy_3)(C=C)][PCy_3][X]}{K_p K_{H_2} K_1 [C=C][H_2]} \quad (C1\text{-}6)$$

A material balance on the osmium charged to the system yields:

$$[Os]_T = OsHCl(CO)(PCy_3)_2 + OsHCl(CO)(H_2)(PCy_3)_2 + OsHCl(CO)(H_2)(PCy_3) +$$
$$OsHCl(CO)(H_2)(PCy_3)(C=C) + OsHCl(CO)(PCy_3) + OsHCl(CO)(PCy_3)_2(X) \quad (C1\text{-}7)$$

The osmium species in eq. (C1-7) are substituted by eq. (C1-2) to eq. (C1-6) and then subsequently substituted into eq. (C1-1) to provide the resulting rate law as shown in eq. (C1-8).

$$-\frac{d[C=C]}{dt} = \frac{k_{rds} K_p K_{H_2} K_1 K_2 [Os]_T [C=C][H_2]}{K_p K_{H_2}(1 + K_2[H_2] + K_1 K_2 [C=C][H_2]) + K_2 [PCy_3](1 + K_{H_2}[H_2] + K_X[X])} \quad (C1\text{-}8)$$

2. Hydrogenation of ST-*g*-NR catalyzed by OsHCl(CO)(O$_2$)(PCy$_3$)$_2$
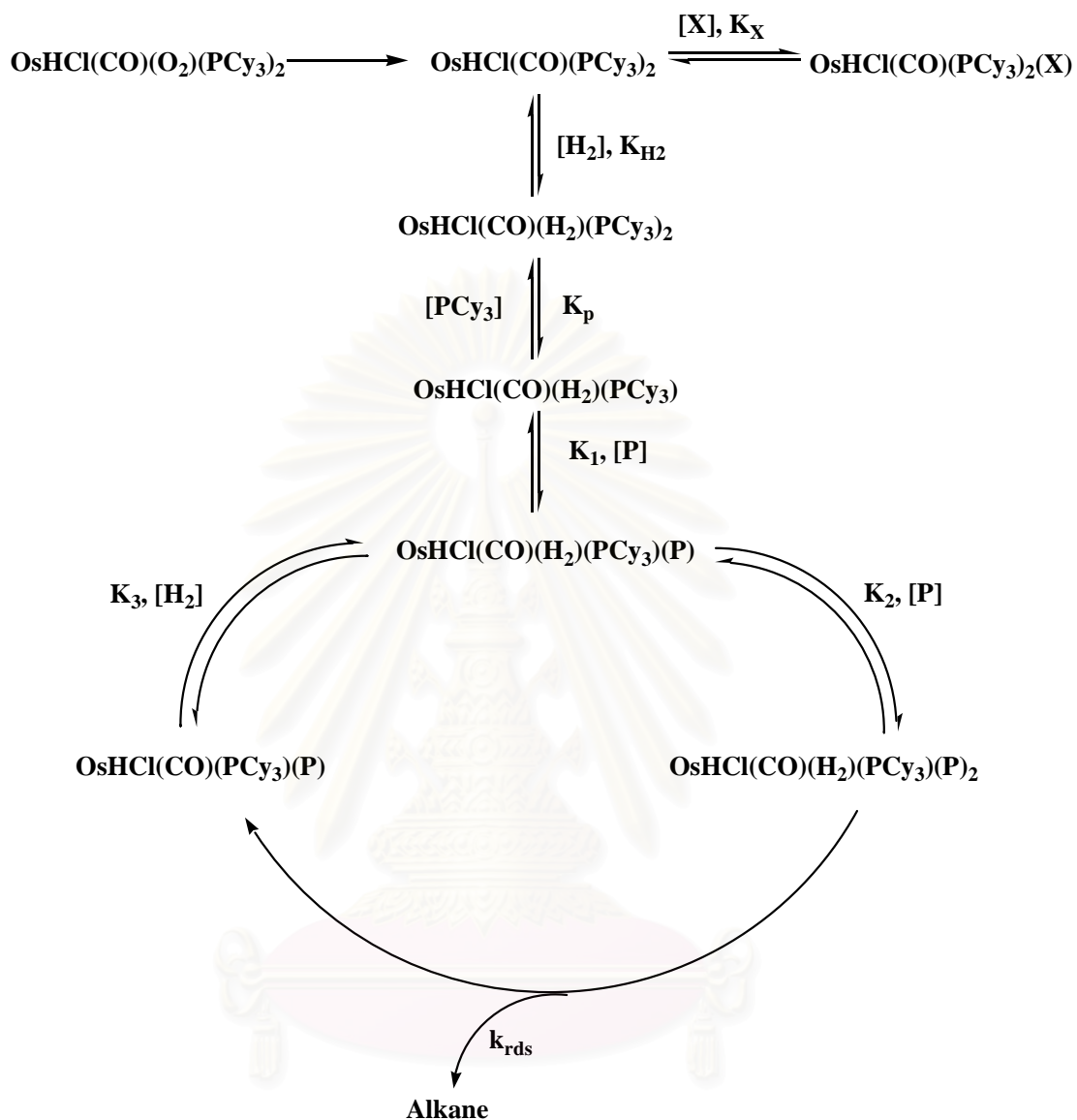
P = Polymer

$$-\frac{d[C=C]}{dt} = k_{rds}[OsHCl(CO)(H_2)(PCy_3)(P)_2] \qquad (C2\text{-}1)$$

$$[OsHCl(CO)(H_2)(PCy_3)(P)] = \frac{\left[OsHCl(CO)(H_2)(PCy_3)(P)_2\right]}{K_2[P]} \qquad (C2\text{-}2)$$

$$[\text{OsHCl(CO)(H}_2)(\text{PCy}_3)] = \frac{\left[\text{OsHCl(CO)(H}_2)(\text{PCy}_3)(\text{P})_2\right]}{K_1K_2[\text{P}]^2} \quad (\text{C2-3})$$

$$[\text{OsHCl(CO)(H}_2)(\text{PCy}_3)_2] = \frac{[\text{OsHCl(CO)(H}_2)(\text{PCy}_3)(\text{P})_2][\text{PCy}_3]}{K_PK_1K_2[\text{P}]^2} \quad (\text{C2-4})$$

$$[\text{OsHCl(CO)(PCy}_3)_2] = \frac{[\text{OsHCl(CO)(H}_2)(\text{PCy}_3)(\text{P})_2][\text{PCy}_3]}{K_PK_{H_2}K_1K_2[\text{H}_2][\text{P}]^2} \quad (\text{C2-5})$$

$$[\text{OsHCl(CO)(PCy}_3)(\text{P})] = \frac{[\text{OsHCl(CO)(H}_2)(\text{PCy}_3)(\text{P})_2]}{K_2K_3[\text{H}_2][\text{P}]} \quad (\text{C2-6})$$

$$[\text{OsHCl(CO)(PCy}_3)_2(\text{X})] = \frac{K_X[\text{OsHCl(CO)(H}_2)(\text{PCy}_3)(\text{P})_2][\text{PCy}_3][\text{X}]}{K_PK_{H_2}K_1K_2[\text{H}_2][\text{P}]^2} \quad (\text{C2-7})$$

A material balance on the osmium charged to the system yields:

$[\text{Os}]_T$ = [OsHCl(CO)(PCy$_3$)$_2$]+[OsHCl(CO)(H$_2$)(PCy$_3$)$_2$]+[OsHCl(CO)(H$_2$)(PCy$_3$)]

+[OsHCl(CO)(H$_2$)(PCy$_3$)(P)]+[OsHCl(CO)(H$_2$)(PCy$_3$)(P)$_2$]+[OsHCl(CO)(PCy$_3$)(P)]

+[OsHCl(CO)(PCy$_3$)$_2$(X)] (C2-8)

The osmium species in eq. (C2-8) are substituted by eq. (C2-2) to eq. (C2-7), then subsequently substituted into eq. (C2-1) to provide the resulting rate law as shown in eq. (C2-9).

$$-\frac{d[\text{P}]}{dt} = \frac{k_{rds}K_PK_HK_1K_2K_3[\text{H}_2][\text{P}]^2[\text{Os}]_T}{K_3[\text{PCy}_3](1+K_H[\text{H}_2]+K_X[\text{X}])+K_PK_HK_1[\text{P}](1+K_3[\text{H}_2]+K_2K_3[\text{H}_2][\text{P}])+K_PK_HK_3[\text{H}_2]} \quad (\text{C2-9})$$

Appendix D

Mechanical Properties of Thermoplastic/Elastomer Blends

Table D-1 Tensile Strength of PMMA/EPDM/HGMMA blends

	PMMA	PMMA/EPDM				PMMA/EPDM/Hydrogenated MMA-*g*-NR					
		95/5	90/10	80/20	70/30	80/20/2	80/20/4	80/20/10	95/5/2	95/5/4	95/5/10
Tensile	42.02	51.97	42.75	33.65	14.96	35.20	28.28	35.84	47.59	48.69	55.42
Strength	40.17	50.47	42.71	30.09	18.66	31.86	28.56	34.69	47.36	46.65	53.62
(MPa)	45.06	51.75	42.80	29.64	16.94	31.14	24.08	32.84	47.45	50.06	51.98
Means	42.42	51.40	42.75	31.13	16.85	32.73	26.97	34.46	47.47	48.47	53.67
S.D.	2.47	0.81	0.04	2.20	1.85	2.17	2.51	1.51	0.11	1.72	1.72

Table D-2 Ultimate Elongation of PMMA/EPDM/HGMMA blends

	PMMA	PMMA/EPDM				PMMA/EPDM/Hydrogenated MMA-*g*-NR					
		95/5	90/10	80/20	70/30	80/20/2	80/20/4	80/20/10	95/5/2	95/5/4	95/5/10
Ultimate	4.47	7.49	8.56	6.79	4.72	6.31	6.43	7.19	7.45	8.01	8.30
Elongation	4.41	7.80	8.32	6.78	4.17	6.68	6.40	6.97	7.23	8.11	8.16
(%)	4.43	7.81	8.20	5.70	4.75	6.59	6.52	7.36	7.99	8.20	8.57
Means	4.44	7.70	8.36	6.42	4.55	6.53	6.45	7.17	7.56	8.11	8.34
S.D.	0.03	0.18	0.18	0.63	0.33	0.20	0.06	0.19	0.39	0.10	0.21

Table D-3 Hardness of PMMA/EPDM/HGMMA blends

	PMMA	PMMA/EPDM				PMMA/EPDM/Hydrogenated MMA-*g*-NR					
		95/5	90/10	80/20	70/30	80/20/2	80/20/4	80/20/10	95/5/2	95/5/4	95/5/10
Hardness	119.30	90.00	81.50	81.10	53.20	79.30	75.10	65.10	83.90	82.90	79.99
	119.30	88.70	79.90	80.40	56.50	80.20	72.70	67.70	84.60	83.80	78.04
	119.20	87.90	80.80	79.30	57.00	78.60	73.40	64.40	83.70	80.20	74.07
	118.00	89.30	81.00	78.30	50.30	77.00	70.00	63.00	83.00	78.50	70.00
	120.00	88.00	78.20	79.20	52.30	76.50	68.70	65.40	80.40	79.10	75.40
Means	119.16	88.78	80.28	79.66	53.86	78.32	71.98	65.12	83.12	80.90	75.50
S.D.	0.72	0.89	1.30	1.10	2.84	1.55	2.60	1.71	1.62	2.34	3.84

Table D-4 Impact Strength of PMMA/EPDM/HGMMA blends

	PMMA	PMMA/EPDM				PMMA/EPDM/Hydrogenated MMA-*g*-NR					
		95/5	90/10	80/20	70/30	80/20/2	80/20/4	80/20/10	95/5/2	95/5/4	95/5/10
Impact	37.59	53.39	35.06	35.06	18.39	30.11	26.58	32.38	52.96	53.70	62.95
(kJ/m^2)	40.15	48.03	25.31	25.31	35.06	32.57	32.38	38.39	53.51	59.26	62.32
	35.06	43.22	22.95	22.95	20.67	25.31	27.15	41.15	56.73	53.70	59.46
Means	37.60	48.21	27.77	27.77	24.71	29.33	28.70	37.31	54.40	55.55	61.58
S.D.	2.54	5.09	6.42	6.42	9.04	3.69	3.20	4.49	2.04	3.21	1.86

Table D-5 Tensile Strength of PS/EPDM/HGST blends

| | PS | PS/EPDM | | | | PS/EPDM/Hydrogenated ST-*g*-NR | | | | | |
		90/10	80/20	70/30	60/40	70/30/2	70/30/5	70/30/10	90/10/2	90/10/5	90/10/10
Tensile strength (MPa)	29.50	33.84	28.56	24.35	13.36	22.41	16.36	20.34	29.31	25.06	20.45
	27.00	33.67	26.54	20.98	15.84	24.27	22.84	20.77	29.35	27.66	21.22
	28.79	33.25	27.26	21.32	14.41	25.52	23.55	19.56	28.64	23.91	20.57
Means	28.43	33.58	27.45	22.22	14.54	24.07	20.91	20.22	29.10	25.54	20.75
S.D.	1.29	0.30	1.03	1.86	1.25	1.56	3.96	0.61	0.40	1.92	0.41

Table D-6 Ultimate Elongation of PS/EPDM/HGST blends

| | PS | PS/EPDM | | | | PS/EPDM/Hydrogenated ST-*g*-NR | | | | | |
		90/10	80/20	70/30	60/40	70/30/2	70/30/5	70/30/10	90/10/2	90/10/5	90/10/10
Ultimate Elongation (%)	3.98	4.44	4.77	5.24	4.77	5.52	4.40	5.02	4.17	3.70	3.74
	3.27	4.66	4.48	5.81	4.59	5.21	5.10	5.66	4.13	4.37	4.33
	3.22	4.51	4.56	4.53	5.02	5.58	5.34	5.20	4.39	4.21	3.69
Means	3.49	4.53	4.61	5.19	4.79	5.44	4.94	5.29	4.23	4.09	3.92
S.D.	0.43	0.11	0.15	0.64	0.22	0.20	0.49	0.33	0.14	0.35	0.36

Table D-7 Hardness of PS/EPDM/HGST blends

| | PS | PS/EPDM | | | | PS/EPDM/Hydrogenated ST-*g*-NR | | | | | |
		90/10	80/20	70/30	60/40	70/30/2	70/30/5	70/30/10	90/10/2	90/10/5	90/10/10
Hardness	95.00	75.00	53.40	52.50	17.10	45.60	42.10	35.60	69.50	68.80	55.90
	94.90	77.40	53.60	51.30	16.00	48.50	40.00	29.40	69.50	68.10	51.50
	96.30	75.00	54.30	50.80	18.50	46.50	42.30	34.10	69.60	68.00	54.20
	94.40	75.90	52.20	51.60	18.70	42.20	44.00	32.90	69.70	68.30	50.10
	94.80	77.20	48.30	51.30	15.30	46.50	40.90	30.20	70.20	67.30	53.20
Means	95.08	76.10	52.36	51.50	17.12	45.86	41.86	32.44	69.70	68.10	52.98
S.D.	0.72	1.16	2.39	0.63	1.50	2.30	1.52	2.61	0.29	0.54	2.27

Table D-8 Impact Strength of PS/EPDM/HGST blends

| | PS | PS/EPDM | | | | PS/EPDM/Hydrogenated ST-*g*-NR | | | | | |
		90/10	80/20	70/30	60/40	70/30/2	70/30/5	70/30/10	90/10/2	90/10/5	90/10/10
Impact (kJ/m^2)	22.95	18.39	22.95	27.69	50.78	27.69	35.06	30.11	18.39	22.95	30.11
	27.69	20.67	22.95	30.11	56.29	32.57	30.11	35.06	18.39	27.69	22.95
	35.06	22.95	18.39	35.06	56.29	27.69	30.11	27.69	18.39	22.95	27.69
Means	28.57	20.67	21.43	30.95	54.45	29.32	31.76	30.95	18.39	24.53	26.92
S.D.	6.10	2.28	2.63	3.76	3.18	2.82	2.86	3.76	0.00	2.73	3.64

VITA

Miss Suwadee Kongparakul was born on May 16, 1981 in Bangkok, Thailand. She received her B.Sc. (Second class honors) degree in Chemical Engineering from Chulalongkorn University. Suwadee joined the department of Chemical Technology at Chulalongkorn University as a doctoral student in 2003. She has received the Royal Golden Jubilee Scholarship from Thailand Research Fund for her Ph.D. study. Suwadee also served as a teaching assistant for undergraduate courses "Process and Dynamic Control" and "Chemical Process and Plant Design". While in graduate school, Suwadee spent one year (2005) and three months (2007) doing research in "Applied Catalysis Laboratory" at University of Waterloo, ON, Canada. Her paper entitled "Effect of Grafted Methyl Methacrylate on the Catalytic Hydrogenation of Natural Rubber" has been accepted for publication in "European Polymer Journal". She also presented her work at 1 conference in Singapore, 1 conference in USA and 1 conference in Thailand.